

Changes in energy fluxes during NPQ in LHCII and PSII-LHCII

Francesco Saccon

Submitted in partial fulfillment of the requirements of the Degree of Doctor of
Philosophy

School of Biological and Chemical Sciences
Queen Mary University
United Kingdom

January 2020



Declaration

I, Francesco Saccon, confirm that the research included within this thesis is my own work or that where it has been carried out in collaboration with, or supported by others, that this is duly acknowledged below and my contribution indicated. Previously published material is also acknowledged below. I attest that I have exercised reasonable care to ensure that the work is original, and does not to the best of my knowledge break any UK law, infringe any third partys copyright or other Intellectual Property Right, or contain any confidential material. I accept that the College has the right to use plagiarism detection software to check the electronic version of the thesis. I confirm that this thesis has not been previously submitted for the award of a degree by this or any other university. The copyright of this thesis rests with the author and no quotation from it or information derived from it may be published without the prior written consent of the author.

Signature:

Date:

22 January 2020

Support of work by others

Chapter 3 is the outcome of a collaboration between current and past members of Prof. Alexander Ruban's laboratory. Dr. Vasco Giovagnetti, Dr. Petra Ungerer, Dr. Alexandra Burgess, Dr. Mahendra Shukla and Mr. Sam Wilson were involved in performing the experiments and in the critical discussion of the results.

The single molecule microscopy experiments described in Chapter 4 were performed by Dr. Marijonas Tutkus in Prof. Leonas Valkunas' laboratory at Vilnius University.

The transient absorption spectroscopy experiments described in Chapter 5 were performed using Prof. Tomáš Polívka's setup at University of South Bohemia, in collaboration with Dr. Milan Durchan.

The time-resolved fluorescence experiments described in Chapter 5 were performed by Dr. Jevgenij Chmeliov in Prof. Leonas Valkunas' laboratory at Vilnius University.

Outreach of the work

Scientific publications

1. Chmeliov, J.; Gelzinis, A.; Franckevičius, M.; Tutkus, M.; Saccon, F.; Ruban, A. V.; Valkunas, L. (2019) Aggregation-Related Nonphotochemical Quenching in the Photosynthetic Membrane. *Journal of Physical Chemistry Letters*, **10** (23), 7340-7346.
<https://doi.org/10.1021/acs.jpcllett.9b03100>
2. Saccon, F.; Durchan, M.; Kaňa, R.; Prášil, O.; Ruban, A. V.; Polívka, T. (2019) Spectroscopic Properties of Violaxanthin and Lutein Triplet States in LHCII are Independent of Carotenoid Composition. *Journal of Physical Chemistry B*, **123** (44), 9312-9320.
<https://doi.org/10.1021/acs.jpcb.9b06293>
3. Townsend, A. J.*; Saccon, F.*; Giovagnetti, V.; Wilson, S.; Ungerer, P.; Ruban, A. V. (2018) The Causes of Altered Chlorophyll Fluorescence Quenching Induction in the Arabidopsis Mutant Lacking All Minor Antenna Complexes. *Biochimica et Biophysica Acta - Bioenergetics*, **1859** (9), 666-675.
<https://doi.org/10.1016/j.bbabi.2018.03.005>
(*equal contribution)
4. Tutkus, M.; Saccon, F.; Chmeliov, J.; Venckus, O.; Ciplys, I.; Ruban, A. V.; Valkunas, L. (2019) Single-Molecule Microscopy Studies of LHCII Enriched in Vio or Zea. *Biochimica et Biophysica Acta - Bioenergetics*, **1860** (6), 499-507.
<https://doi.org/10.1016/j.bbabi.2019.05.002>

International meetings where the work was presented

Oral presentations

- December 2019: Biochemical Society Christmas Bioenergetics meeting, London
- August 2019: European Society for Photobiology Congress, Barcelona
- February 2018: SE2B “Nanoscale Dynamics of the Thylakoid Pigment-Protein Complexes”, Naantali
- March 2017: First meeting of the SE2B network, Hattersheim

Poster presentations

- October 2019: SE2B “Biophysics of Photosynthesis: from molecules to the field”, Rome
- August 2018: European Bioenergetics Conference, Budapest
- September 2017: European conference for spectroscopy of biological molecules, Amsterdam
- September 2017: European Society for Photobiology Congress, Pisa

Additional work in collaboration with the students of the Marie-Curie network SE2B

- Creation of a YouTube educational channel for high school and university students, to explain general concepts of photosynthesis and our research projects. https://www.youtube.com/channel/UCH0ms3oQjfpeGWnDM6ufr-A?view_as=subscriber
- Organisation of the last international conference of the Marie-Curie network SE2B: “Energy to Biomass Optimisation of light energy conversion in plants and microalgae Conference”, Porto, February 2020.

Acknowledgements

Firstly, I thank my mentor, Prof. Alexander Ruban, who tirelessly fed me with passion and inspiration. Thanks to him I achieved goals I considered impossible and grew as a mature scientist. I am indebted to him for this.

I thank the laboratory members, Petra, Vasco, Sam, Mahendra, Lili and Alex, for the friendship we created over the years, and for always being kind and helpful to me.

Thanks to Dr. Chris Duffy, who remarkably never lost patience when explaining physics concepts to me. Thanks also to the collaborators, Prof. Tomáš Polívka, Dr. Radek Kaňa, Dr. Erica Belgio, Dr. Milan Durchan, Dr. Juan Manuel Artés and Dr. Marijonas Tutkus for being keen on our projects and for teaching me a lot of new techniques.

I thank the SBCS 4th floor people and especially office 4.36, for sharing with me ideas, knowledge, ordinary life, politics, gossip, coffee breaks, a lot of sweets and many nights out.

Thanks to the European Union and the people involved in the SE2B PhD network for encouraging the exchange of ideas across borders and putting up this exciting international program.

A huge acknowledgement goes to my family, that have always been supportive and encouraging towards my work and proud of the outcome.

From the bottom of my heart, I want to thank Dori for always believing in me and pushing me constantly to pursue my dreams.



This project has received funding from the European Union's Horizon 2020 research and innovation programme under the Marie Skłodowska-Curie grant agreement No 675006.

Abstract

The non-photochemical quenching of excess energy (NPQ) is a fast molecular adaptation of photosynthetic organisms to variations of sunlight intensities. In plants, the energy-dependent quenching (qE) is the main NPQ component, which promptly protects the thylakoid membrane components by dissipating the excess energy absorbed. While the *trigger* of this physiological process is known to be thylakoid ΔpH , the *site* in the membrane, the structural *changes* involved and the nature of the *quencher* pigment are still a subject of debate. In this thesis, I addressed these gaps in our knowledge of qE. The results presented here show that neither minor light harvesting antenna complexes nor reaction cores are sites of qE, which instead takes place entirely in major LHCII trimers. The nature of the change from a light-harvesting to a dissipative state in LHCII and its dependence on the binding of xanthophyll-cycle carotenoids was investigated. Zeaxanthin was found to exert no effect on the quenching dynamics of single LHCII trimers, disproving its role as a quencher. However, it controls the kinetics of the transition to the quenched state by favouring LHCII aggregation. To determine the nature of the quencher species, transient absorption spectroscopy was applied to isolated LHCII. A mechanism was identified whereby chlorophylls donate energy to a carotenoid species, likely a lutein, leading to quick energy dissipation. Overall, this work reveals the self-regulatory nature of photosynthetic light harvesting, showing that in principle only trimeric LHCII and the proton gradient are sufficient to enable qE *in vivo*. The protein PsbS and zeaxanthin exert an allosteric regulation of the process, that, by tuning the degree of antennae sensitivity to the amplitude of the proton gradient, assures a fine control of light harvesting.

Contents

Declaration	I
Acknowledgements	IV
Abstract	V
List of Abbreviations	X
List of Figures	XII
List of Tables	XVI
Chapter 1: Introduction	1
1.1 Energy and life: the light phase of photosynthesis	1
1.2 Principle of sunlight energy harvesting	3
1.2.1 Pigments	3
1.2.2 Tuning energy transfer between pigments	8
1.2.3 Functional architecture of photosystems	11
1.3 Molecular responses to light intensity fluctuations in plants	15
1.3.1 The requirement for regulation	15
1.3.2 Long-term acclimation	19
1.3.3 Carotenoid triplets	20
1.3.4 Fast adaptations to low light	21
1.3.5 Non-photochemical quenching of chlorophyll fluorescence . . .	23
1.4 Aims of the thesis	43
Chapter 2: Methodologies and approaches	45
2.1 Plant material and growth conditions	45
2.2 Isolation of mesophyll cells and sub-cellular membranes	46

CONTENTS

2.2.1	Isolation of protoplasts	47
2.2.2	Isolation of chloroplasts	47
2.2.3	Isolation of thylakoids	48
2.2.4	Zeaxanthin enrichment of leaf and thylakoid material	49
2.3	Pigment analysis	50
2.3.1	Chlorophyll quantification	50
2.3.2	Carotenoid quantification	50
2.4	Protein purification and analysis	51
2.4.1	Sucrose density gradient ultracentrifugation	51
2.4.2	Iso-electric focussing	53
2.4.3	Immobilisation of LHCII in polyacrylamide gels	54
2.4.4	SDS-polyacrylamide gel electrophoresis	54
2.5	Fluorescence spectroscopy	55
2.5.1	Principles of chlorophyll fluorescence spectroscopy and pulse-amplitude modulated (PAM) fluorimetry	55
2.5.2	Imaging PAM	57
2.5.3	Electron transport rates	57
2.5.4	Fast fluorescence induction	58
2.5.5	Measurements of ΔpH across the thylakoids and its modulation using chemicals	59
2.5.6	Low temperature steady-state fluorescence	60
2.5.7	Time-resolved fluorescence	61
2.5.8	Single molecule fluorescence microscopy	64
2.6	Absorption measurements	66
2.6.1	Steady-state absorption	67
2.6.2	Absorption changes related to NPQ	67
2.6.3	Transient absorption spectroscopy	68
Chapter 3: Identification of the qE site		72
3.1	The origin of altered NPQ induction in the NoM mutant	73
3.1.1	Minor antennae mediate the functional connectivity of of LHCs in PSII	73

3.1.2	The fast NPQ development in <i>NoM</i> is independent of the presence of reaction centres and zeaxanthin	79
3.1.3	The origin of the transient fluorescence recovery during illumination in <i>NoM</i>	83
3.1.4	Discussion	87
3.2	Fast photoprotection (qE) in plants lacking minor antennae and RCs	92
3.2.1	Making the thylakoid membranes enriched only in major LHCII	93
3.2.2	qE is formed in the absence of minor antennae and reaction centres	96
3.2.3	Zea and PsbS exert an allosteric control of qE	100
3.2.4	LHCII aggregation: tuning the activity of LHCII to regulate light harvesting	103
3.2.5	Discussion	107
Chapter 4: Investigation of the conformational change of LHCII associated with qE		110
4.1	Isolation of LHCII enriched in xanthophyll cycle Cars	110
4.2	The dissipative conformational change in LHCII	114
4.3	Fluorescence blinking of single LHCII trimers	117
4.4	Conclusions	123
Chapter 5: Identification of the qE quencher		126
5.1	<i>In vitro</i>	128
5.1.1	Induction of efficient energy dissipation in isolated LHCII in the absence of protein aggregation	128
5.1.2	A new spectroscopic marker appears upon incorporation of LHCII in gels	131
5.1.3	The new marker is associated with a Car dark excited state and correlates to the quenching of Chl excitation	133
5.1.4	Induction of the quenched conformation is independent of Car composition	139
5.1.5	The internal Car pockets in LHCII shape the functional properties of the xanthophylls bound	149

CONTENTS

5.1.6	Discussion	152
5.2	<i>In vivo</i>	155
5.2.1	NPQ induction in the absence of reaction centre proteins . . .	156
5.2.2	Stabilisation of a strongly quenched state in chloroplasts leads to a redistribution of the fluorescence spectral components . .	157
5.2.3	Red and FR emitting states are not involved in energy quenching	162
5.2.4	The deeply quenched state of chloroplasts bears marked si- milarities with <i>in vitro</i> LHCII aggregates	164
5.2.5	Discussion	165
Chapter 6: Conclusions		168
6.1	Plasticity in the regulation of light harvesting: the duality of LHCII purpose	168
6.2	Physiological significance of qE control	169
6.3	Improving solar energy utilisation in a dynamic environment	172
6.4	The future of qE research.	176
Bibliography		178

List of Abbreviations

- ΔA , difference absorption
- ΔpH , light-dependent thylakoid pH gradient
- 9-aa, 9-aminoacrydine
- AL, actinic light
- APS, ammonium persulfate
- Car(s), carotenoid(s)
- Chl(s), chlorophyll(s)
- DAD, diaminodurene
- DCMU, 3-(3,4-dichlorophenyl)-1,1-dimethylurea
- EDTA, ethylenedinitrilotetraacetic acid
- ESA, excited state absorption
- ETR, electron transport rate
- F700, fluorescence emission at 700 nm
- FR, far red
- F_m' , maximal chlorophyll fluorescence with closed reaction centres, during actinic light exposure
- F_m , maximal chlorophyll fluorescence with closed reaction centres
- F_o , minimal chlorophyll fluorescence with open reaction centres
- GSB, ground state bleach
- HEPES, 4-(2-hydroxyethyl)piperazine-1-ethanesulfonic acid

- HOMO, highest occupied molecular orbital
- IEF, iso-electric focussing
- LHC(s), light harvesting complex(es)
- LHCI, light harvesting complex of photosystem I
- LHCII, major light harvesting complex of photosystem II
- LUMO, lowest unoccupied molecular orbital
- Lut, lutein
- MES, 4-morpholineethanesulfonic acid
- NPQ, non-photochemical quenching of chlorophyll fluorescence
- Neo, neoxanthin
- PLA2, phospholipase A2
- PSI, photosystem I
- PSII, photosystem II
- Pheo, pheophytin
- PsbS, photosystem II subunit S
- qE, energy-dependent non-photochemical quenching of chlorophyll fluorescence
- RC(s), photosystem reaction centre(s)
- SD, standard deviation of the mean
- SE, standard error of the mean
- SM, single molecule
- TA, transient absorption
- TEMED, N,N,N',N'-tetramethylethylenediamine
- TIRF, total internal reflection fluorescence
- TRF, time-resolved fluorescence
- Vio, violaxanthin
- Zea, zeaxanthin
- pK, proton antenna association constant

List of Figures

1.1	The Z-scheme of photosynthesis	2
1.2	Structure and energetics of the pigments involved in light harvesting in plants	5
1.3	The structural organisation of PSII, PSI and LHCII	12
1.4	The requirements for light harvesting regulation in plants . .	17
1.5	The qE scenario	43
2.1	Principles of chlorophyll fluorescence spectroscopy and pulse amplitude modulated (PAM) measurements	56
2.2	Principles of TIRF exploited in single molecule (SM) fluorescence microscopy	65
2.3	Principles of transient absorption (TA) spectroscopy	69
3.1	<i>NoM</i> plants exhibit disrupted growth rates.	74
3.2	Electron transport rates (ETR) are affected in <i>NoM</i> mutants. .	74
3.3	The functional antenna size in mutants lacking minor antennae is increased.	75
3.4	A large pool of weakly coupled LHCII is present in <i>NoM</i> thylakoid membranes.	76
3.5	Minor antennae control the dynamics of quinone reduction at the PSII acceptor side.	77
3.6	Δ pH generation and maintenance are compromised in the <i>NoM</i> mutant.	78
3.7	The altered Chl fluorescence quenching induction in the <i>NoM</i> mutant.	80

3.8	The fast quenching phase is independent of RCs, minor antennae and Zea.	81
3.9	Fo fluorescence dynamics indicate antenna rearrangements during quenching induction.	81
3.10	Transient highly fluorescent state of LHCII during light induction in <i>NoM</i>	84
3.11	No changes in functional antenna cross section occur during Chl fluorescence induction in <i>NoM</i>	85
3.12	Zea formation is delayed during <i>NoM</i> induction	86
3.13	The altered Chl fluorescence induction in plants exposed to limiting light intensities	88
3.14	Features of NPQ induction phases in <i>Arabidopsis</i> plants lacking minor antenna complexes	89
3.15	Lincomycin-treated <i>NoM</i> plants have thylakoids greatly enriched in LHCII	94
3.16	Absorption profiles attest a selective enrichment of LHCII in <i>NoM</i> + lincomycin plants	95
3.17	qE is formed in plants lacking minor antennae and RCs . . .	97
3.18	The qE recovery kinetics are accelerated in the plants lacking minor antenna complexes	98
3.19	Microscopy assessment of the intactness of cellular and sub-cellular preparations from <i>Arabidopsis</i>	99
3.20	The pH dependence of quenching in lincomycin-treated <i>NoM</i> mutants	100
3.21	Zea controls the kinetics and maximum amplitude of qE . . .	101
3.22	Zea retention in the thylakoids causes partial quenching in the dark	102
3.23	Enhancing Δ pH causes a restoration of qE in the absence of PsbS	104
3.24	PsbS presence alters the pH sensitivity of LHCII for the activation of qE	105

3.25	Photoprotective quenching in LHCII-enriched thylakoid membranes exhibits the fluorescence markers of antenna aggregation	106
4.1	LHCII has a peripheral Car binding site involved in the xanthophyll cycle operation	111
4.2	Isolation of LHCII enriched in Vio or Zea	112
4.3	Induction of the photoprotective conformation in LHCII . . .	115
4.4	Zea doesn't induce changes in the fluorescence intensity profiles of single LHCII trimers	119
4.5	The duration of LHCII conformational states is not significantly altered by xanthophyll cycle Cars	120
4.6	Zea marginally affects the switch of LHCII complexes between different conformational states under NPQ conditions	122
5.1	Trapping of LHCII trimers into polyacrylamide gels	129
5.2	LHCII in gels exhibit a negligible degree of singlet-singlet annihilation during TA measurements	130
5.3	A new spectroscopic marker appears upon incorporation of LHCII in gels	132
5.4	The newly found Car signal differs from Car S ₁ state	133
5.5	The new Car excited state correlates with the de-excitation of Chls	134
5.6	Derived kinetics of the "quencher" signal indicate the possible contribution of neoxanthin	136
5.7	Direct Chl excitation is not needed to populate the new Car state	137
5.8	Structural changes of LHCII cause alterations of the spectroscopic properties of the bound Cars and Chls	138
5.9	Genetic alteration of Car biosynthesis pathways changes the xanthophyll composition of LHCII complexes	140
5.10	Enzymatic removal of phosphatidylglycerol causes monomerization of LHCII	141

5.11	Lutein replacement does not hinder the dissipative switch in LHCII	142
5.12	Absorption spectroscopy reveals dramatic changes in the Lut 1 site upon quenching induction	143
5.13	Low-energy forms of Chls are mostly affected by the LHCII conformational change	145
5.14	Fluorescence spectroscopy reveals changes in the terminal emitting Chls that are independent of Car composition . . .	147
5.15	Spectra of the quencher from WT and <i>npq1lut2</i> LHCII share marked similarities	148
5.16	Vio can replace Lut in the internal Car binding pockets in LHCII	150
5.17	Lut and Vio triplets in LHCII are spectroscopically identical	151
5.18	Model of the dissipative switch in LHCII	154
5.19	PsbS enhances NPQ in isolated chloroplasts from lincomycin-treated <i>Arabidopsis</i> plants	156
5.20	The time- and temperature-resolved fluorescence spectra of chloroplasts from lincomycin-treated plants	158
5.21	Lincomycin treatment strongly diminishes the fluorescence emission contribution from RC complexes of PSI	159
5.22	Red and FR emitting forms decay significantly slower than the 680 nm emitting state	161
5.23	TFR data can be analytically described by a two-(emitting)-state model	163
5.24	The spectral decomposition of L17 chloroplasts under NPQ conditions and LHCII aggregates exhibit similar profiles . . .	164
5.25	NPQ shifts the conformational equilibrium of LHCII in the thylakoid membrane	166
6.1	Outcome of the thesis	170
6.2	Re-engineering the NPQ switch	174

List of Tables

3.1	Pigment composition of <i>Arabidopsis</i> WT, <i>NoM</i> and <i>NoM</i> + lincomycin plants	96
4.1	Pigment composition of Vio- and Zea- enriched LHCII	113
4.2	Bi-exponential description of the fluorescence decay kinetics in Vio- and Zea-enriched LHCII trimers before and after quenching induction	116
5.1	Pigment composition of the LHCII samples used in the study	139

‘Nothing in life is to be feared, it is only to be understood.’

MARIE SKŁODOWSKA CURIE

Chapter 1

Introduction

1.1 Energy and life: the light phase of photosynthesis

Obtaining an exhaustive definition of “*life*” is not a trivial task. It can even be paradoxical, in that there is a blunt transition between animate and inanimate matter. Perhaps what can be envisaged as a common trait of all life forms is their apparent violation of the second law of thermodynamics that states that all isolated systems evolve towards a minimum of entropy (Schrödinger, 1944; Monod, 1971). Living organisms exert processes that relentlessly maintain order in their structures by actively consuming *energy*. That plants are alive is rather undoubted. Similarly to animals, plants move, crawl, grow and reproduce. However, the growth of plants has remained a mystery for centuries, until it was understood that their *energy* source is located 150 millions km away from Earth and is generated from the Sun, the star at the centre of our solar system. Plants have the remarkable capacity to harvest swift photons of sunlight and trap their energy in stable chemical forms used for their growth.

Oxygenic photosynthesis fuels energy into the biosphere and is responsible for the survival of virtually all life forms. The process is carried out in two phases, occurring in separate parts of the chloroplast. The “light” phase involves the harvest of sunlight energy and its stabilisation into NADPH and ATP. In these reactions, water is oxidised and oxygen is released. The “dark” phase leads to the conversion of

carbon dioxide into carbohydrates, necessary to sustain the growth of the organism. The overall reaction is endergonic since it requires an external energy input, offered by photons of sunlight.

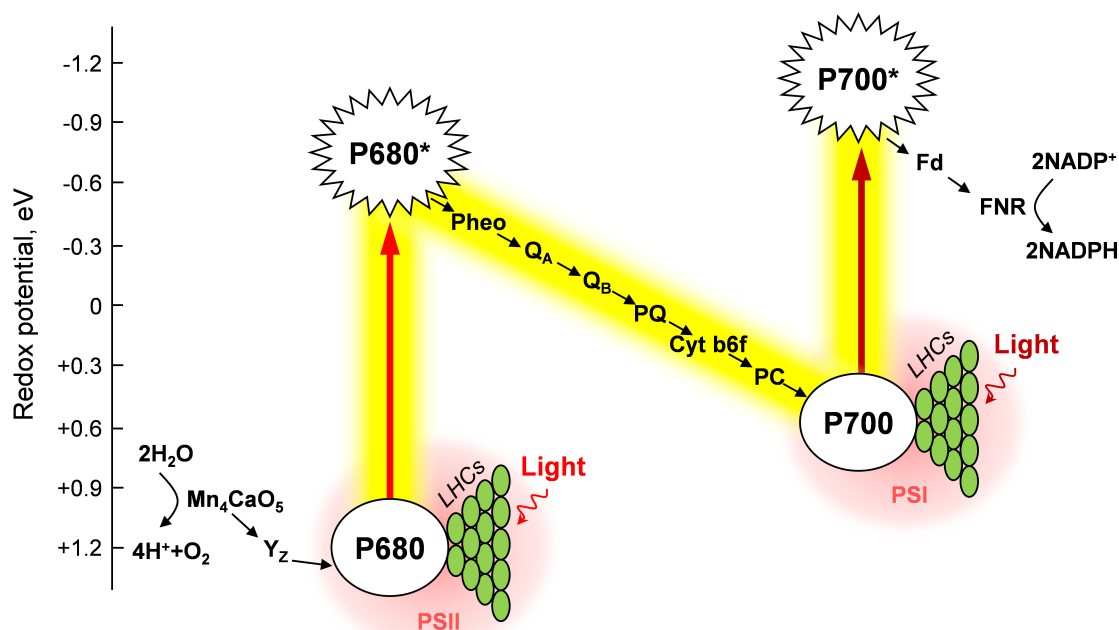


Figure 1.1: **The Z-scheme of photosynthesis.** Schematic representation of the linear electron transport during the “light” phase of photosynthesis. The main redox species involved are shown with their approximate redox potentials. PSII, photosystem II; PSI, photosystem I; LHCs, light harvesting complexes; P680/P680*, relaxed/excited special chlorophyll pair in PSII reaction centre; P700/P700*, relaxed/excited special chlorophyll pair in PSI reaction centre; Mn_4CaO_5 , manganese-calcium-oxygen complex; Y_Z , tyrosine Z; Pheo, pheophytin; Q_A , quinone A; Q_B , quinone B; PQ, plastoquinone; Cyt b_6f , cytochrome b_6f ; PC, plastocyanin; Fd, ferredoxin; $\text{NADP}^+/\text{NADPH}$ oxidised/reduced nicotinamide adenine dinucleotide phosphate; FNR, Ferredoxin- NADP^+ reductase.

In the “light” reactions, two thylakoid membrane-bound reaction centres, photosystem II (PSII) and photosystem I (PSI), mediate the capture of photons and drive the electron transport chain and the stabilisation of a trans-thylakoid ΔpH gradient. The series of electron reactions involved are classically described using a characteristic Z-scheme (Figure 1.1), drawn on a scale of redox potential, where vertical transitions mark uphill reactions that require the absorption of a photon, followed by downhill reactions of electron transfer from stronger to weaker reducing agents.

An “antenna” system of pigment-binding light harvesting complexes is used to harvest the energy of photons and deliver excitation energy to PSII centres. Charge separation then occurs in a specialised chlorophyll pair (P680). The electron generated is channelled to a pheophytin (Pheo, a chlorophyll without the central magnesium atom) and subsequently to two bound quinone molecules (Q_A and Q_B). The latter is loosely bound and, after accepting electrons and binding protons, it diffuses to the cytochrome b_6f complex in the form of plastoquinone (PQ), resulting in the reduction of a small copper protein, plastocyanin (PC). The absorption of an additional photon by PSI and associated light harvesting complexes is used to oxidize P700, a special chlorophyll pair located at the centre of PSI. The electron removed from P700 by this oxidation event migrates along the electron transport chain to eventually reduce ferredoxin (Fd), the final electron acceptor of PSI. Among many downstream targets of Fd, the main electron acceptor is $NADP^+$. This is used, in a reaction catalysed by the ferredoxin- $NADP^+$ reductase (FNR), to form NADPH, which is then used in the following “dark” phase reactions. In PSII, after electron transfer to Pheo and then Q_A , a strongly oxidising species, $P680^+$ (~ 1.2 eV), is formed. This chemical form is used in a series of reactions to oxidize water, whose tendency to donate electrons is normally very low due to its positive redox potential. $P680^+$ is reduced by a nearby tyrosine residue (Y_Z). The latter in turn oxidises a luminal Mn_4CaO_5 cluster. This cluster is the catalytic centre for water splitting: after four oxidation events, two water molecules are split into $4 H^+$ and 1 O_2 molecule.

1.2 Principle of sunlight energy harvesting

1.2.1 Pigments

Chlorophylls

Photosynthesis relies on the capture of light from a dilute source (the sun) and its storage into redox potential. Therefore, the choice of a pigment is based on its capacity to absorb in a spectral region where radiation is available, and where quanta of light contain enough energy to move electrons from a high-potential electron

donor to a low-potential electron acceptor. Chlorophylls (Chls, Chl for singular) are nature’s pick for the light harvesting processes (Björn *et al.*, 2009).

The chemical structure of Chl is presented in Figure 1.2a. The portion that gives bright green colour to Chl is a squarish porphyrin-like structure, composed of four pyrrole rings (tetrapyrrole). The four nitrogen atoms of the pyrroles coordinate a central magnesium atom. The hydrophobic tail is a isoprenoid tail since it is formed by the condensation of four 5-C isoprene units. Chl *a* and *b* are identical, except for the presence of a formyl-group instead of a methyl group attached to C7 of the tetrapyrrole ring in the latter. This moiety shifts the absorption maximum of Chl *b* to shorter wavelengths (Figure 1.2c). Two regions of absorption transitions are visible in the absorption spectra (Figure 1.2c). The red-most transitions correspond to the excitation to the first excited state (S_1). The blue-most region, instead, comprises transitions to the second excited state (S_2) and is often called the Soret region. Two absorption peaks are present in each region for each Chl, which are called Q_X and Q_Y reflecting the direction of the transition dipole moments in the tetrapyrrole ring. However, Q_Y is predominant and the term is normally used to identify the red absorption band (in contrast with the Soret band identifying the blue absorption band).

Several exclusive features underline the importance of Chl for light harvesting (Björn *et al.*, 2009):

- They are very stable compounds, in particular when bound to proteins. H-bonds are formed between Chls and amino acids, together with coordination bonds with the central Mg atom. The phytol chain anchors them stably to the protein scaffold;
- They are fairly large and contain a wide array of conjugated carbon double bonds. This ensures the presence of a spread “ π -electron box”, which confers absorption properties in the visible light range (Figure 1.2c);
- Their π -electron system is asymmetric, which causes the occurrence of multiple absorption transitions and increases the spectrum of captured photons (Figure 1.2c);
- They possess large values of molar extinction ($\sim 10^5$) and cross-section ($\sim 4 \text{ \AA}^2$) making them efficient light-harvesters;

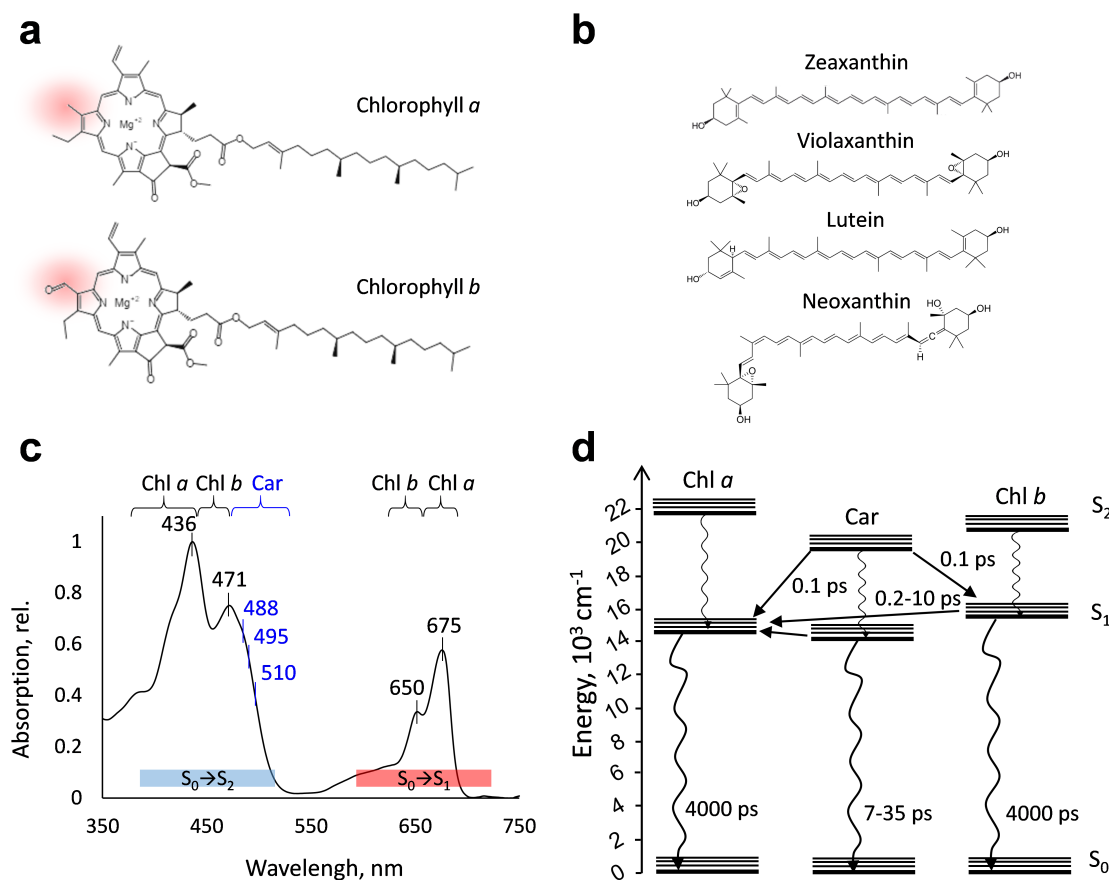


Figure 1.2: **Structure and energetics of the pigments involved in light harvesting in plants.** Chemical structure of chlorophylls (Chls, **a**) and carotenoids (Cars, **b**) bound to light-harvesting complexes. The red glow in **a** highlights the difference between Chl *a* and Chl *b*, due to substitution of a methyl- with a formyl- group in position C7 in the latter. **c** Absorption spectra of the major light harvesting complex of photosystem II (LHCII). Peaks corresponding to the major absorption transitions of Chl and Car are displayed in black and blue, respectively. S_0 to S_2 and S_0 to S_1 transitions are marked by blue and red rectangles, respectively. **d** Energy levels (horizontal bars), energy migration pathways (straight arrows) and internal conversion routes (wavy arrows) between pigments involved in light harvesting in plants. Migration/decay rates are expressed in picoseconds (ps).

- They present a long-lived first excited state. Their intrinsic lifetime is 15 ns and becomes 0.3-2 ns *in vivo*, which is still far longer than the time required for charge separation in the reaction centre (up to 10 ps). This means that the excitation dwells long enough on the molecule to guarantee charge separation when the conditions are favourable (*i.e.* open reaction centres);

- Their lower excited state is high enough (1.77 eV) to assure a low rate of radiation-less de-excitation (internal conversion to the ground state S_0);
- They are capable of losing or gaining electrons, making them effective in storing excitation energy into redox potential;
- The latter process occurs only when the environment favours the charge separation (*i.e.* in the reaction centres where tyrosine Z (Y_Z in Figure 1.1) acts as a high potential redox co-factor). Chls bound to antenna complexes do not eject electrons.

Chl *a* is ubiquitous and by far the most abundant Chl in nature, being found in all oxygenic phototrophic organisms. It is surprising, given the degree of variability of natural habitats, that a single Chl type has become the dominant one. In part, its ubiquity is reflected in the early evolution of this chemical form, compared to other Chls (Larkum, 2006). But the uniqueness of Chl *a* resides likely (1) in their strong absorption in red regions of the spectrum and (2) in their unique ability to lose electrons in reaction centres and drive photochemistry while being redox-inactive when bound to antenna proteins and act as light harvesters (Björn *et al.*, 2009). Recently, the dogma of Chl *a* as essential in charge separation processes, reflected in the “red limit” of photosynthesis, has been challenged (Nürnberg *et al.*, 2018). Far red (FR)-absorbing Chl *d* and Chl *f* were found to drive photochemistry when bound to the reaction centres of FR-adapted cyanobacteria species (Nürnberg *et al.*, 2018).

Carotenoids

To further increase the spectrum of useful sun radiation, nature exploited another set of molecules absorbing blue-green colours, the carotenoids (Cars, Car for singular). Cars are long isoprenoid molecules. They are generally less abundant than Chls and in plant thylakoids are found in a Chl/Car ratio of 3.5-4 (Dall’Osto *et al.*, 2017). However in some organisms, such as diatoms, the Chl/Car ratio can be even 1 (Büchel, 2015). The most represented class of Cars are xanthophylls, which possess oxygenated cyclic end rings (Figure 1.2b). This feature makes them, to different extents, more hydrophylic. In some molecules, such as rhodopin glucoside, the amphiphilic trait is so accentuated that they can behave like detergents (Ruban,

2009a). Since Cars belong to the C_{2h} symmetry group (two-fold symmetry on an horizontal plane due to their planar polyenic structure), the ground state (S_0) and the first excited state (S_1) have the same symmetry label (Ag^-). The selection rules of quantum mechanics forbid the transition between two states with the same symmetry label, therefore the $S_0 \rightarrow S_1$ transition is optically dark (Figure 1.2c) (Schulten and Karplus, 1972). This means that the only Car state involved in light harvesting is the S_2 state. Being strongly dipole allowed, $S_0 \rightarrow S_2$ is highly absorptive and possesses extinction coefficients ϵ in the order of $10^5 \text{ M}^{-1} \text{ cm}^{-1}$ (Figure 1.2c) (Polívka and Frank, 2010).

The number of carbon double bonds in their polyene-like structure, called conjugation length (N), determines the extent of the delocalised π -electron system and defines their excited-state transition energies (thereby defining also their colour). The energies of the $S_0 \rightarrow S_1$ and $S_0 \rightarrow S_2$ transitions decrease for increasing N values. Therefore, the 0-0 band (transition between lowest vibrational levels of two states) of the $S_0 \rightarrow S_2$ transition of violaxanthin ($N=9$) in methanol occurs at 467 nm, while that of zeaxanthin ($N=11$) occurs at 476 nm. Cars, however, are very sensitive to structural distortions. The properties related to the N value are affected by the structural constraints that the Car is subject to in the protein environment. Therefore, as an example, a lutein molecule that is found in the major light harvesting complex of plants (LHCII) is in a distorted configuration, which causes an increase of the effective N and therefore a marked red-shift in the absorption spectrum, by as much as 15 nm (Ruban *et al.*, 2000). Besides the modulation of the transition energies, the effective N value also exerts a control on the excited state dynamics. A high N corresponds to faster decay rates from S_1 to S_0 . On the contrary, low N results in slower decay rates. Thus, for example, in solution violaxanthin S_1 has a lifetime of ~ 23 ps while zeaxanthin is ~ 8 ps (Frank *et al.*, 1997). It is interesting to note that the lifetime of the lowest excited state is roughly two orders of magnitude shorter than the one of Chls (tens vs thousands of ps). The binding to a protein also exerts a strong modulation of the S_1 dynamics. Among the most dramatic effects, it was shown that the reconstitution of LHCII apoproteins with different xanthophylls results in very similar Car S_1 lifetimes, irrespective of the chemical nature of the xanthophyll bound (Polívka *et al.*, 2002). A similar effect was observed in antenna complexes isolated from mutants of xanthophyll biosynthetic pathways,

which accumulate different sets of Cars (Fuciman *et al.*, 2012).

Cars bound to the photosynthetic complexes in plants present a conserved distribution pattern: xanthophylls (*i.e.* neoxanthin, Neo; violaxanthin, Vio; lutein, Lut; zeaxanthin, Zea) are generally bound to the outer antenna complexes of photosystems I and II. Non-oxygenated carotenoids (*i.e.* β -carotene), by contrast, are present in the inner antenna complexes and reaction centres of both photosystems (Bassi *et al.*, 1993). The generally lower Cars abundance with respect to Chls, their forbidden $S_0 \rightarrow S_1$ transition (Figure 1.2c) and the extremely fast relaxation of Car S_2 and S_1 to the ground state (Figure 1.2d) could suggest a seemingly marginal role for them as light harvesters in plants. However, Cars have actually been found to play a vast number of essential roles in the membranes. In fact, their absence often causes severe or even lethal phenotype to the photosynthetic organisms (Sistrom *et al.*, 1956; Shuvalov and Parson, 1981; Siefermann-Harms, 1987). A common motif in all characterised Cars bound to photosynthetic complexes is that their π -electron-conjugated chain is buried into the hydrophobic domain of the protein and usually form close van der Waals contacts with a Chl. This feature underlines their importance both as light harvesters, ensuring fast energy migration between them and Chl (Figure 1.2d) (van Grondelle *et al.*, 1994), and as protectors of the main Chl pigments. The latter trait was indeed revealed in many studies, showing that Cars can safely dissipate the excess energy accumulated by Chls as singlet or triplet excited states and avoid damage of membrane components (Dall’Osto *et al.*, 2014b). Cars also exerts antioxidant functions, by quenching the energy of singlet oxygen (Havaux *et al.*, 2007). A remarkable feature of Cars resides in their structural role, as they are often needed for the correct folding of pigment-binding protein complexes (Dall’Osto *et al.*, 2006).

1.2.2 Tuning energy transfer between pigments

When two pigments are in close association, energy transfer (or migration) can occur between them. A donor molecule (D) transfers excitation energy to an acceptor molecule (A), provided some requirements are met. The process requires Coulombic interactions between molecules, therefore, besides short distances, an overlap in donor emission spectrum and acceptor absorption spectrum is needed. The theori-

sation of this energy transfer process was achieved by Förster in 1946 (see Forster (2012) and references therein).

The rate of resonant energy transfer (k_T) between a donor and an acceptor molecule is defined by the equation (Forster, 2012; Ruban, 2012):

$$k_T = k_f \left(\frac{R_0}{R} \right)^6$$

where k_f is the fluorescence rate constant of the donor, R_0 is the distance between the molecules at which the efficiency of energy transfer is 50% of the maximum and R is the actual distance. The sixth-power dependence of the energy transfer rate indicates a steep decrease in the efficiency of this process as the distance between pigments increases. R_0 depends upon various parameters, such as the mutual orientation of the molecules, the fluorescence yield of the donor, the refraction index of the medium and the energy overlap integral (which describes the overlap between the fluorescence emission spectrum of the donor and the absorption spectrum of the acceptor).

An additional mechanism of energy transfer has been proposed to occur in the pigment-congested light-harvesting complexes and does not involve resonance excitation energy transfer. A Dexter type of energy transfer involves electron exchange processes was first described in inorganic phosphor (luminescent) crystals (Dexter, 1953). It involves the electron transfer from the LUMO of an excited-state molecule to the LUMO of another molecule in its ground state. The latter, in turn, transfers one electron from its HOMO to the HOMO of the other molecule. In this way the excitation energy is transferred without formation of radicals. The rate of the Dexter mechanism (k_T) can be defined by the equation (Ruban, 2012):

$$k_T \simeq J e^{\frac{2R}{L}}$$

where J is the energy overlap integral (that depends on the distance between molecules and their transition dipole moments), R is the distance between donor and acceptor and L is the sum of their van der Waals radii. Unlike the sixth-power dependence of the Forster mechanisms, the rate of Dexter energy transfer decreases exponentially with the distance between pigments. This mechanism is very fast to

occur compared to Forster's. The likelihood of this mechanism is high when the molecules are so close together that they effectively share molecular orbitals. Due to the very close proximity of some xanthophylls to Chl in light harvesting systems, their very short excited-state lifetime and their optically-forbidden S_1 state, a Dexter mechanism was proposed to be the main energy transfer mechanism, although still no consensus has been reached on the matter (van Grondelle *et al.*, 1994). The Dexter type of energy transfer is crucial for triplet-triplet energy transfer processes (see "Carotenoid triplets").

While the described mechanisms of excitation energy transfer require simply two molecules (*i.e.* donor and acceptor), *in vivo* complexity is added by the presence of excitonic interactions, that are formed when the excitation is shared simultaneously between two or more chromophores (van Amerongen *et al.*, 2000). When two pigments are in close contact and become excitonically coupled, they behave like a single excitation unit. Here, quantum coherence is promoted and the excitation is simultaneously delocalised in both pigments instead of being preferentially localised in one of them. Interactions with the environment (solvent, protein) exert the opposite effect of localising the excitation energy, leading to incoherence in energy transfers. While these perturbations can generally exert a strong negative effect on coherent processes, the latter can become predominant in light harvesting complexes where pigments are in close proximity with each other (Fassioli *et al.*, 2014). Coherence is usefully exploited in nature since it significantly increases the rates of energy migrations between pigments and overcomes the need for large downhill energy gaps, since the pigments involved in the excitonic interactions can be almost iso-energetic (Malý and Van Grondelle, 2018). Coherent excitons are therefore a way to minimise energy losses in photosynthesis. An outstanding example of electronic coherence is the LH2 complex of purple bacteria, that presents rings of strongly coupled Chl forming large delocalised excitons (Cogdell *et al.*, 2006; Scholes *et al.*, 2011).

In LHCII, after excitation of a Car or a Chl molecule, very fast energy migration occurs (Figure 1.2d), on a femto- to picosecond time scale (Croce and Van Amerongen, 2011). Cars can donate their energy to both Chl *b* and Chl *a* molecules, either from their S_2 state, or after internal conversion from their S_1 state (Gradinaru *et al.*, 2000; Croce *et al.*, 2001). From Chl *b*, energy migrates to Chl *a* with an average rate constant of 350 fs at room temperature (Connelly *et al.*,

1997; van Amerongen and van Grondelle, 2001). Modelling based on the crystal structure of LHCII (Liu *et al.*, 2004) allowed the mapping of Chl clusters involved in excitonic interactions, revealing the presence of one cluster of low-energy Chl *a* molecules (Chl *a* 610, 611 and 612 following nomenclature of Liu *et al.* (2004)) that are likely involved in inter-complex energy hopping (Novoderezhkin *et al.*, 2005).

1.2.3 Functional architecture of photosystems

The concept of the photosynthetic unit

The pioneering work of Emerson and Arnold, using brief flashes of light to probe photosynthesis, led to the discovery that not all Chl molecules are involved in the formation of chemical products. In fact, one molecule of O₂ is produced for every 2500 Chls (Blankenship, 2002). Thus, the concept of a “photosynthetic unit” was introduced, in which only one Chl (later found to be a pair of Chls) is photochemically active and is surrounded by accessory Chl pigments. The concept of the photosynthetic unit was born even before a theory of energy migration between pigments was formulated, but was vastly confirmed by the following biochemical works (*e.g.* Malkin *et al.* (1981), Peter and Thornber (1991), Belgio *et al.* (2014)). The experiments of Duysens in the 1950s, shed light on the functional organisation of Chl in the thylakoid membranes and showed that these are present in two clusters (called photosystem I, PSI, and photosystem II, PSII) that work in series during photosynthesis (Duysens, 1989). Both PSI and PSII are formed by reaction centre complexes (or reaction cores, RCs), where excitation energy is stabilised by charge separation, and peripheral antenna complexes, whose pigments are optimised for energy harvesting and migration.

The first structural insights of the PSII supercomplexes revealed the dimeric association of the RCs, each of them binding one copy of the minor antennae CP24, CP26, CP29 and major LHCII trimer (Figure 1.3a) (Boekema *et al.*, 2006). Minor antenna complexes bridge RCs and major LHCII and are necessary for the correct assembly of the supercomplex (Kovács *et al.*, 2006). Through mild fractionation of thylakoid membranes with detergent, it was demonstrated that the number of LHCII per RC dimer is ~ 8 , raising the uncertainty of their binding sites (Boekema *et al.*, 1999a,b). Based on the frequency of their isolation with RCs, they were clas-

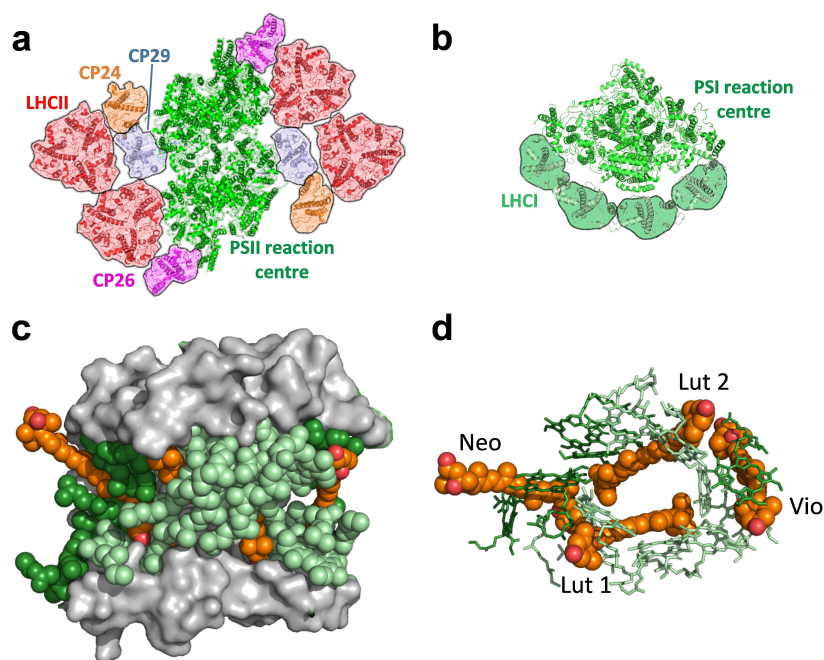


Figure 1.3: **The structural organisation of PSII, PSI and LHCII.** **a** Arrangement of reaction centres (RCs) and antenna complexes in the photosystem II (PSII) dimeric supercomplex. The structure is taken from pdb entry 5xnm (Su *et al.*, 2017). **b** Structure of the monomeric photosystem I (PSI) binding four LHCI. The structure is taken from pdb entry 5l8r (Mazor *et al.*, 2017). **c** Side view of a LHCII monomer. The protein is visualised in surface mode (grey) while pigments are shown in space filling model using the following colour code: Chl *a*, pale green; Chl *b*, dark green; Car, orange. **d** Top view of the pigments in a LHCII monomer. The LHCII structure is taken from pdb entry 1rwt (Liu *et al.*, 2004). All structures are displayed using the software PyMol.

sified as strongly (S), moderately (M) and loosely (L) bound LHCII. Recently, cryo electron microscopy led to high resolution PSII structures and the determination of the structure of $C_2S_2M_2$ (Figure 1.3a) and $C_2S_2M_2L_2$ supercomplexes, ($C=RCs$) (Wei *et al.*, 2016; Su *et al.*, 2017; Burton-Smith *et al.*, 2019). In one monomer of the $C_2S_2M_2$ supercomplex, there are 28 protein subunits that overall coordinate 157 Chls, 44 Cars, 2 Pheo and several other cofactors and lipids (Su *et al.*, 2017).

The PSI-light harvesting complexes I (LHCI) supercomplex consists of 16 protein subunits, which bind 192 light-harvesting pigments (Figure 1.3b) (Mazor *et al.*, 2017). Of these, 156 are Chls and 32 are Cars (Mazor *et al.*, 2015). The structure reveals also the presence of several lipid molecules and other prosthetic groups. The first resolution of the structure of plant PSI supercomplex showed that it occurs in

monomeric form (Ben-Shem *et al.*, 2003), in contrast to cyanobacteria, where it was isolated in trimeric or tetrameric form (Boekema *et al.*, 1987). 4 LHCI complexes are attached, formed by the polypeptides Lhca 1,2,3,4. Contrarily to PSII, PSI RC proteins coordinate the majority of pigments in the supercomplex (95 Chl and 22 Car). The adaptive process of state transitions (see “Fast adaptations to low light”) involves the redistribution of collected sunlight energy between the two photosystems and occurs via detachment of LHCII from PSII and binding to PSI (Bellafore *et al.*, 2005). Recently, the structure of PSI binding one LHCII trimer was solved, providing structural evidence of this mechanism (Pan *et al.*, 2018).

The architecture of the thylakoid membranes in plants is such that a separation of PSII and PSI components and ATP synthases is achieved by dividing the membranes in appressed and non-appressed regions (Anderson and Boardman, 1966; Wietrzynski *et al.*, 2019). Steric hindrance of PSI and ATPase causes their segregation to non-appressed regions. Instead, PSII and related light harvesting complexes are found in appressed regions, the latter being critically involved in membrane stacking (Ruban and Johnson, 2015). This so-called “lateral heterogeneity” is of great functional significance in keeping PSII and PSI reactions separate and avoiding wasteful effects such as the “spillover” of excitation energy from PSII to PSI that bypasses charge separation in the former.

Reaction centre of PSII

The homodimeric PSII RC is a large (700 kDa) complex comprising several membrane-spanning polypeptides. The main components are the subunits D1 and D2, which bind the cofactors involved in electron transfer and water oxidation reactions, and the inner antenna complexes CP43 and CP47, that bind several Chl molecules and serve a light harvesting purpose (Shen, 2015). In addition, there are 13 subunits of low molecular weight (<10 kDa), mainly bound at the periphery of the complex. P680 identifies the cluster of RC Chls bound to D1 and D2.

Light harvesting complexes (LHCs) of PSII

Higher plants have six LHC proteins associated with PSII (Lhcb1-6), with Lhcb1-3 forming the major trimeric antenna (LHCII) while Lhcb4, 5 and 6 form monomeric

complexes (CP29, CP26 and CP24, respectively) (Peter and Thornber, 1991; Jansson, 1999). These proteins share a high structural homology which results in well conserved pigment binding sites (Liu *et al.*, 2004; Pan *et al.*, 2011). In the early 1990s, the first structure of the major LHCII complex became available (Kühlbrandt and Wang, 1991), but it was only in the early 2000s that a sufficiently high structural resolution was achieved (*e.g.* enough to unambiguously distinguish between Chl *a* and Chl *b* molecules) (Liu *et al.*, 2004). One LHCII monomer is formed by three trans-membrane α helices (A,B and C) and two shorter ones on the luminal side, almost parallel to the membrane plane (D and E). The luminal loop between helices C and E have been suggested to have a regulatory function and control the function of LHCII in response to lumen acidification (occurring during high light exposure).

One monomer binds 14 Chl molecules in total (8 Chls *a* and 6 Chls *b*). In addition, 4 xanthophylls are present. One Neo is bound to a selective cleft in a peripheral site called N1 (Croce *et al.*, 1999b). Its peculiar 9-*cis* conformation (Figure 1.2b) essentially anchors it to the LHCII scaffold and makes it hardly separable from the complex (Ruban *et al.*, 1999). By contrast, on the other site of the monomer a Vio molecule is found, which binds weakly to a peripheral site called V1 (Liu *et al.*, 2004). It has been proposed, in virtue of these characteristics, that in this place a major regulatory event takes place, with the conversion of Vio to Zea during high light exposure (Ruban *et al.*, 1999). Central to the LHCII structures are two Lut molecules, strongly anchored to the protein scaffold in the sites L1 and L2. The Lut in the L1 site has been proposed to be crucial in regulatory processes (Ruban *et al.*, 2007; Mozzo *et al.*, 2008). Several amino acids are important for the coordination of pigments (Croce *et al.*, 1999a) and confer a certain specificity to the different binding sites. The protein scaffold acts as a “programmed solvent” (Scholes *et al.*, 2011) to accurately separate the pigments, thus ensuring a fine tuning of excitation energy migration. On the contrary, in the absence of physical restraints acting on pigments, most of the Chl fluorescence would be quenched at Chl concentrations found in LHCs (up to 1 M) (Beddard and Porter, 1976). Interestingly, Chls are found in two distinct layers in LHCII, one close to the stromal side of the thylakoid and the other to the luminal one. All chromophores are found in a belt-like arrangement surrounding the LHCII monomer and are deeply buried in

the bilayer (Figure 1.3c,d). This arrangement ensures energetic connectivity both inter- and intra-monomers and is vaguely reminiscent of the circular positioning of (bacterio)Chl in the LH2 of purple bacteria (Cogdell *et al.*, 2006). Besides Lut 2, essential for the trimerisation of the LHCII complex is a phosphatidylglycerol molecule, which interacts with the N-terminal region of the protein (Sakurai *et al.*, 2003). The occurrence of LHCII as trimers, contrarily to CP24, CP26 and CP29 that are found as monomers, prompted researchers to investigate the significance of this trait for light harvesting. Trimerisation was found to stabilise the protein and prevent it from unfolding (Wentworth *et al.*, 2003; van Oort *et al.*, 2007). The local lipid environment of LHCII trimers is also playing a relevant role in stabilising the correct protein conformation (Seiwert *et al.*, 2017). In addition, trimers exhibit a larger degree of cooperativity in the transition from light harvesting to dissipative, quenched states, resulting from a smaller entropy value. Therefore, trimerisation is functionally meaningful, as it results in a more “tunable” system to cope with light fluctuations.

1.3 Molecular responses to light intensity fluctuations in plants

1.3.1 The requirement for regulation

Photosynthetic organisms colonise almost all habitats on our planet. As for plants, 30 % of the whole land surface is covered by forests, which contribute 50% of the total plant productivity <https://earthobservatory.nasa.gov/features/ForestCarbon>. From tropical to boreal forests, a remarkable property of plants is to adapt to the most diverse and occasionally impervious environmental conditions. Unlike animals, plants are sessile organisms which require feedback mechanisms and extensive molecular signalling networks to adapt and acclimate to their habitat. It is crucial for plants to retain a high plasticity of their photosynthetic apparatus to cope with daily and seasonal variations in the quality and intensity of sunlight.

Photosynthesis under light starvation

The range of light intensities to which plants are exposed (photosynthetic photon flux density) can be several orders of magnitude wide. Full sunlight can be as bright as $2300 \mu\text{mol photons m}^{-2} \text{ s}^{-1}$ while an overcast day as dim as $15 \mu\text{mol photons m}^{-2} \text{ s}^{-1}$. Under dense canopies, only a tiny fraction of this light reaches shaded leaves.

The photosynthetic apparatus evolved under dim environments and specialised to get the best energy output from a very dilute source. Therefore, only a small portion of the chlorophylls in the thylakoids is photochemically competent and can drive redox reactions to store chemical energy (Blankenship, 2002). The vast majority of the pigments in the membranes are accessory chromophores that enhance the absorption cross-section of the system, increasing the gamma of wavelengths harvested and maximising the numbers of photons captured. Generally, plants perform well under low/moderate light conditions, which do not saturate the photosynthetic reactions. The biggest challenge for these organisms is to maintain the correct balance of energy input between the two photosystems that work in series, to minimise the energy losses. Hence, state transitions take place that tune the cross-section of each photosystem in a process involving the lateral mobility of some light harvesting complexes (Ruban and Johnson, 2009). Under dense canopies, the energy input becomes often too low to sustain the growth of the organism. Some plant species are “shade-tolerant” and have acclimated well to these conditions (Johnson *et al.*, 1993). In most cases, however, a feedback response, triggered by the perception of elevated FR intensities by the phytochrome receptors, cause the so-called “shade-avoidance” response, involving the elongation of plant stems to reach brighter areas and overgrow neighbours (Gilbert *et al.*, 2001).

Photosynthesis under saturating light

The most limiting conditions to which plants are exposed is under elevated light intensities. The extensive arrays of antenna complexes feeding each RC cause an excessive amount of photons to be absorbed, more than the energy stabilised via charge separation (Figure 1.4a). This discrepancy originates from the inherently slower electron transport processes, occurring in micro/milliseconds, compared to the energy capture and transfer, that occur from femtoseconds up to nanoseconds.

This overflow of excitation energy to the cores causes a quick saturation of the photosynthetic electron transport chain and the subsistence of potentially dangerous Chl excited states. If not promptly dissipated, Chl triplets can be accumulated via inter-system crossing from the first singlet excited state, which can react with molecular oxygen to form singlet oxygen radicals (Figure 1.4b). These molecular species are extremely reactive and can damage the photosynthetic components by oxidising lipids and proteins.

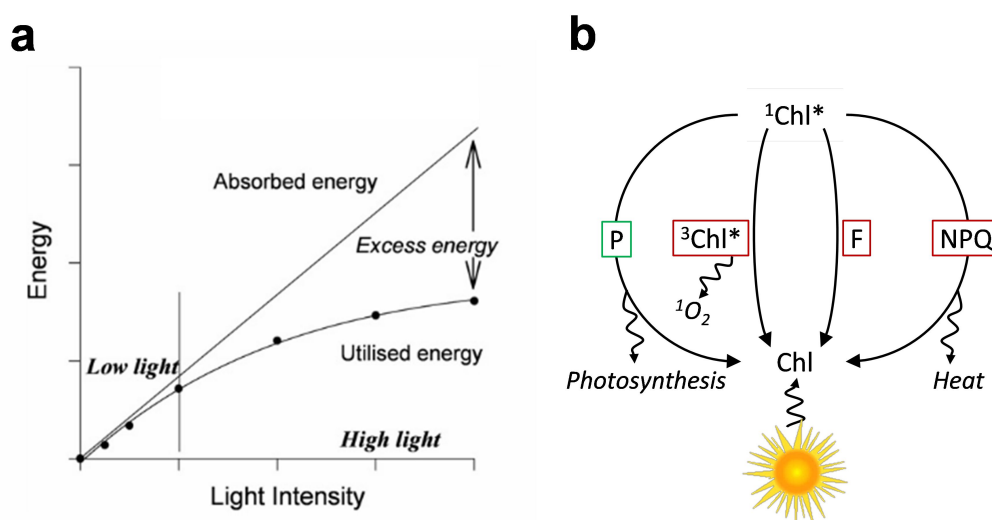


Figure 1.4: **The requirements for light harvesting regulation in plants.** **a** Relationship between energy utilised in photosynthetic processes and light intensity. Taken from Ruban *et al.* (2012). **b** The fates of light energy absorbed by Chls. P, photochemistry; $^3\text{Chl}^*$, chlorophyll triplet state; $^1\text{O}_2$, singlet oxygen; F, fluorescence; NPQ, non-photochemical quenching. Re-adapted from Demmig-Adams and Adams (2000).

Another factor that limits photosynthesis and contributes to the build-up of unused excitation energy is the rate of the dark phase reactions. The activity of the enzyme RuBisCO is not constant, but it is rather light dependent and controlled by another enzyme called RuBisCO activase. Especially during fluctuating light, the utilisation of sunlight energy is substantially lessened by the delayed activation of CO_2 assimilation (Taylor and Long, 2017).

The D1 component is the most susceptible component of PSII since it is subject

to a lot of excitation pressure coming downhill from the antenna complexes. Damage or inactivation of D1 leads effectively to a stop of light harvesting reactions, leading to a phenomenon called photoinhibition. At that point, the protein must be targeted for degradation and be replaced by a newly translated one, in a process that is both time and energy consuming (Li *et al.*, 2018). While photoinhibition was suggested to be potentially a means of photoprotection, by preventing damage to PSI (Tikkanen *et al.*, 2014), it is generally disfavoured due to the poor reversibility of the process. Instead, plants developed conserved mechanisms of fast photoprotection, that preserve the economics of photosynthesis by protecting the molecular components from high light damage at a very little metabolic cost (Pinnola and Bassi, 2018). Non-photochemical quenching of chlorophyll excited states (NPQ) is one such conserved mechanism, that is activated on a second to minute time scale (Figure 1.4b). It is feedback-controlled by the amplitude of trans-thylakoid ΔpH driven by photosynthetic reactions. When photosynthetic electron flow activity is high, due to the overflow of excitation energy from collected photons, ΔpH becomes pronounced. The LHCs sense it and switch their mode of operation to become ineffective in photon harvesting, thereby reducing excitation energy pressure to the RCs (Ruban, 2016). The rearrangements and conformational changes in the light harvesting system brings about the formation of a quenching pigment interaction, whereby excitation energy from Chl is transferred to a quencher that dissipates it quickly through heat. The whole process is effective in reducing the accumulation of potentially harmful chlorophyll triplet species and avoiding lipid and protein peroxidation (Havaux and Niyogi, 1999).

When this layer of photoprotection fails, or is yet to become active, a constitutive form of photoprotection is present, which does not require activation. The energy of Chl triplets can be transferred to Car molecules, whose triplets do not react with molecular oxygen. From here, once again, the energy is released harmlessly by internal conversion to the ground state (heat release). This mechanism is extremely conserved across a wide variety of photosynthetic organisms and is of vital importance for their growth (Di Valentin and Carbonera, 2017; Khoroshyy *et al.*, 2018). Cars perform an additional function, which is widely known and exploited for health and well-being purposes. They can act as direct reactive oxygen species scavengers and impede oxidative damage to protein and lipids. Neoxanthin was shown to have

a specific anti-oxidant capacity in plants since, in its absence, plants were shown to be more sensitive to damage by singlet oxygen (Dall'Osto *et al.*, 2014b). Also, the accumulation of zeaxanthin in the thylakoid membranes was shown to be important for this photoprotective mechanism (Havaux *et al.*, 2007; Johnson *et al.*, 2007).

1.3.2 Long-term acclimation

Plants grown in shaded habitats are not capable of performing photosynthesis at high rates, but they perform efficiently under low light conditions. On the contrary, plants grown in highly irradiated environments are under-performing if they are placed in the shade, but present high photosynthetic rates when exposed to bright light (Boardman, 1977). Some shade species, such as the tropical *Alocasia macrorrhiza*, exhibit an incredible tolerance to low photon fluxes, a trait called “shade tolerance”, as mentioned before (Björkman *et al.*, 1972; Johnson *et al.*, 1993). The ability of plants to adjust their chloroplasts’ photosynthetic apparatus at the level of cells and organelles to the light habitat is called acclimation (Walters, 2005). Acclimation is a long-term process, since the re-programming of the plant organs requires transcriptional, translational and post-translational responses that take place in days or weeks (Ruban, 2009b). One needs to distinguish between developmental and dynamical acclimation. The former comprises profound adjustments that involve changes of root and leaf morphology and depends on the ecological niche that the plant occupies. These changes are very slow, taking weeks and months and are therefore strictly interlinked with the plants’ ontogenetic phases. Photosynthetic acclimation, however, is a dynamical acclimation response. It follows the variations of light intensity and quality occurring in that environment (*e.g.* sinusoidal pattern of irradiance during the day, changes in the angles of incident light, sunflecks leading to sudden “bursts” of photons, etc.). Acclimation is a mechanism evolved to preserve the economics of photosynthesis and avoid resource misuse (Björkman *et al.*, 1972). Therefore, sun plants under-express the antenna constituents, favouring instead the accumulation of cytochrome *b₆f*, ATP synthase and RuBisCO, involved in CO₂ assimilation. By contrast, shade plants exhibit large photosystem cross-sections, reflected in the lower Chl *a/b* ratio, and a downregulation of electron transport and Calvin-Benson cycle enzymes, whose presence in great amount would be redundant

under low irradiances. It is also well documented that plants can adjust the relative proportions of photosystems I and II depending on the light quality, to keep an adequate stoichiometry and guarantee the correct output of NADPH and ATP (Walters and Horton, 1994). Not only do the proteins associated with light harvesting and electron transport change during acclimation, but some components that exclusively act in photoprotective responses, such as the PsbS protein and the xanthophyll cycle carotenoids also change (Ballottari *et al.*, 2007; Rungrat *et al.*, 2019). The photosynthetic and photoprotective performances can be largely affected by acclimation to different light regimes, as demonstrated for example in plants exposed to fluctuating light regimes (Jahns and Junge, 1992; Yin and Johnson, 2000).

It is likely that a variety of mechanisms are acting in the perception of light and signal transduction during acclimative responses. This conclusion can be drawn from the observations that exposure to low and high light induces different responses (Bailey *et al.*, 2001) and that, although photoreceptors may not be directly involved, acclimation activates a common network of transducing signals (Walters *et al.*, 1999; Walters, 2005). Despite the open questions about light perception and the induction of responses, it is known that acclimation is effective in increasing plant fitness under dynamic light environments (Athanasίου *et al.*, 2010).

1.3.3 Carotenoid triplets

As mentioned above, a pivotal role for Cars resides in their ability to accept energy from Chl triplet states. The lowest-energy excited state of Chl *a* is long lived and can undergo intersystem crossing to form a triplet state. Subsequently, triplet-triplet energy transfer could occur between Chl and Car. This takes place at much faster rates than Chl triplet accumulation, which is limited by the decay time of Chl singlet excited states (~ 4 ns in isolated LHCII, Figure 1.2b) (Schödel *et al.*, 1998). As Car triplets are low-lying and possess less energy than singlet oxygen, they are non-reactive and quickly and safely decay by internal conversion to the ground state (Siefermann-Harms, 1987). Triplet-triplet energy transfer usually occurs through a Dexter-type energy transfer, which requires close van der Waals contacts between the molecules involved. It is not by chance therefore that crucial Cars involved in this type of energy transfer are situated in close proximity to Chls. In the native

thylakoid membranes, several Car triplet species have been identified, an important fraction of which associated with LHCII (Santabarbara *et al.*, 2002, 2005). β -carotene has an essential photoprotective role in quenching triplet states forming in RC proteins (Santabarbara *et al.*, 2005). Car triplets have been extensively studied in major LHCII monomers and oligomers (Nechushtai *et al.*, 1988; van der Vos *et al.*, 1991; Peterman *et al.*, 1995, 1997; Naqvi *et al.*, 1997; Schödel *et al.*, 1998; Lampoura *et al.*, 2002; Dall'Osto *et al.*, 2006; Mozzo *et al.*, 2008; Di Valentin *et al.*, 2009; Gall *et al.*, 2011; Salvadori *et al.*, 2012). Neo is likely not to participate in triplet formation, since it is in close contact with Chl b molecules for which ultrafast transfer of energy to Chl a molecules compete effectively with triplet formation (Peterman *et al.*, 1997; Mozzo *et al.*, 2008). On the same line, it was found that Vio isn't involved in triplet formation (Lampoura *et al.*, 2002; Mozzo *et al.*, 2008). Vio was found not to be strongly bound to the LHCII scaffold and is not strongly coupled to other pigments (Caffarri *et al.*, 2001; Duffy and Ruban, 2012). Only Lut, found in the inner Chl *a* enriched pockets, are involved in Chl triplet quenching. The Lut occupying the L1 site is the main site of chlorophyll triplet quenching (Mozzo *et al.*, 2008; Di Valentin *et al.*, 2009). It forms close contacts with the Chl *a* 610, 611, 612 cluster, where at equilibrium excitation energy is more likely to dwell (Novoderezhkin *et al.*, 2005). Lut in LHCII are able to quench about 95% of chlorophyll triplets at room temperature (Nechushtai *et al.*, 1988; Peterman *et al.*, 1995). The importance of this photoprotective mechanism is undeniable, as observed in organisms where it is impaired, where the sensitivity to oxidative stress is highly enhanced (Sistrom *et al.*, 1956). Unquenched Chl triplets were specifically associated with a decline in PSII efficiency, either due to direct damage to light harvesting components or to the delay induced in the repair of PSII core proteins (Murata *et al.*, 2007).

1.3.4 Fast adaptations to low light

Contrarily to acclimation responses, that take place in hours or days, adaptations to light quality and quantity are much faster and occur after seconds or minutes of light exposure. They generally involve post-translational modifications and do not require intricate transduction networks to be initiated. A well-documented adap-

tation to low/moderate light involves the so-called state transitions. PSII and PSI work in series in the photosynthetic electron transport chain and both contain Chl-binding complexes forming the antenna complement. However, PSI absorbs mainly FR light in contrast to PSII, since it contains red-shifted Chl *a* molecules and binds less Chl *b*. To avoid imbalances in the energy input to both systems, a temporary lateral redistribution of some antenna complexes occurs that selectively increase the absorption-cross section of one photosystem at the expenses of the other. This process is effective within minutes of light exposure and under sub-saturating intensities. State transitions were discovered independently by Bonaventura and Myers (Bonaventura and Myers, 1969) and Murata (Murata, 1969), who reported small changes in chlorophyll fluorescence and O₂ yields following variations of light intensity and wavelength. Considerable progress in the molecular details of this process was made by Bennett and Horton groups at the end of the 1970s. It was demonstrated that the control of excitation transfer is achieved via the phosphorylation of LHCs associated with photosystem II (Bennett, 1977, 1979) and that the redox state of the plastoquinone pool is critical in determining the activity of the kinase involved in the phosphorylation (Horton and Black, 1980; Allen *et al.*, 1981; Horton *et al.*, 1981). The identity of the kinase was later determined from a forward genetics approach and it was named STN7 in higher plants (Depege, 2003; Bellafigliore *et al.*, 2005). Importantly, cytochrome *b₆f* was also found to be involved in state transitions (Bennett *et al.*, 1988). The reversible nature of LHC's phosphorylation implies the existence of phosphatases that quickly remove phosphate groups during darkness or FR illumination, when the PQ pool is oxidised and the STN7 kinase is not active (Bennett, 1980; Shapiguzov *et al.*, 2010). The fraction of LHCs involved in state transitions is the outer ring of loose LHCII trimers (Ruban, 2009b). Since PSII and PSI are inhomogenously distributed, with PSII being found in grana thylakoids and PSI in stroma lamellae and grana margins, a considerable remodelling of the thylakoid membranes and supercomplexes occurs during state transitions. LHCII, together with cytochrome *b₆f*, relocate to the grana margins to associate with PSI, in a process involving several phosphorylation events (Vallon *et al.*, 1991; Iwai *et al.*, 2008; Tikkanen *et al.*, 2008). In algae, unlike plants, thermal dissipation of excess energy is an acclimative response, rather than a quick adaptation to fluctuating light. By contrast, it has been proposed that state transitions constitute the

major photoprotective mechanism in these organisms (Ünlü *et al.*, 2014), although recent reports questioned this hypothesis (Nawrocki *et al.*, 2016). In plants, state transitions are active under sub-saturating light intensities and don't provide photoprotection from high light, rather being limited to a redistribution of excitation between the photosystems (Lemeille and Rochaix, 2010).

1.3.5 Non-photochemical quenching of chlorophyll fluorescence

As previously introduced, high light exposure is a stressful condition for plants, that must protect their photosynthetic components from the production of harmful reactive oxygen species. Acting on a fast time scale, NPQ is a safety valve that controls the excitation pressure on the PSII core and represent a conserved process in different photosynthetic organisms (Niyogi and Truong, 2013; Goss and Lepetit, 2015; Giovagnetti and Ruban, 2018).

The downregulation of PSII efficiency

The occurrence of changes in the fluorescence yield on illuminated leaves or chloroplasts is well known since the 1930s and goes under the name of the “Kautsky effect” (Krause, 1991). Chlorophyll fluorescence varies between a basal fluorescence level, achieved under very low illumination (F_0) and a maximal fluorescence level (F_m) reached upon light exposure of moderate/high intensity. The yields of oxygen evolution and variable fluorescence ($F_v = F_m - F_0$) are inversely proportional, that is, when variable fluorescence is large, oxygen evolution is small, whilst when oxygen evolution is large, variable fluorescence is small. Duysens and Sweers (see *e.g.* Duysens (1989)) were the first to propose the existence of a “quencher”, Q of the chlorophyll fluorescence of PSII that would be responsible for the observed quenching of F_v . Nowadays, we know that the identity of this quencher species is a quinone molecule, and that the redox state of the quinone pool of PSII, controls the yield of photochemical fluorescence quenching (qP). However, not all changes in the fluorescence yield are associated with photochemical processes, as described for example by Weis and Berry (1987), who showed the non-linearity of the photosynthesis yield (measured as the yield of CO_2 fixation) with qP. Conversely, large non-photochemical quenching

processes (qN) are observed, especially when plants or algae are irradiated with high intensities. At the end of the 1960s, three groups independently described a form of non-photochemical quenching (NPQ) of chlorophyll fluorescence dependent on the energisation of the thylakoid membranes (*i.e.* formation of ΔpH) (Papageorgiou and Govindjee, 1968; Murata, 1969; Wraight and Crofts, 1970). Wraight and Crofts (1970), in particular, envisaged a protective nature of NPQ and wrote “It is evident, therefore, that in the absence of a protective mechanism, coupled chloroplasts could be severely damaged by intense light” and “The energy-dependent quenching, as with other quenching phenomena, must occur by an increase in the rate of non-radiative dissipation of the chlorophyll excited singlet state. It is most probable that the actual pathway is that of thermal degradation”. Until that point, it was clear that the photochemical efficiency of PSII was not constant, but could be controlled, in a mechanism that is ΔpH dependent.

qE: reversible control of excitation energy pressure on PSII

Krause was the first to observe the occurrence of thylakoid membrane restructuring during NPQ when he measured absorbance changes at 535 nm linked to ΔpH formation and fluorescence quenching (Krause, 1973). Briantais and co-workers first determined the quantitative relationship between ΔpH and NPQ, which led to the definition of qE to define the fluorescence quenching associated “high-energy” structural state of the thylakoids (Briantais *et al.*, 1979). The development of modulated fluorimetry and the saturating pulse analysis led to the separation of different components of NPQ, initially based on the kinetics of the process (Horton and Hague, 1988). qE was therefore distinguished by qI, photoinhibitory quenching and qT, quenching associated with state transitions. qE was identified as the fraction of NPQ that is readily reversible and constitutes the main component of the whole process in plants. Together with the processes associated with qP, it was soon recognised the importance of qE to control the redox state of PSII, regulating the excitation energy pressure and therefore preventing damage from over-excitation (Weis and Berry, 1987). In those years, it was demonstrated that qE is important for the economics of the photosynthetic membranes, because its impairment with uncouplers leads to an enhancement of photoinhibitory damage, caused by exposure

to high light (Krause and Behrend, 1986). These results prompted considerable efforts by the scientific community to resolve the site and mechanism of qE.

The site of qE

Although ΔpH appears to trigger the qE response and the associated membrane changes (535 nm), it is not linearly correlated with fluorescence quenching, suggesting that it acts merely on the ignition of the process, but the quenching requires additional factors to be obtained (Horton *et al.*, 1991). The site and the rearrangements in the thylakoids related to the onset of qE have been subject to intense debates. At the end of the 1980s, a dominating hypothesis for the site of qE was the suggestion that the RC proteins were able to quench the excess energy alone, thus modulating their efficiency, while antenna proteins purely performed a light harvesting function (Weis and Berry, 1987; Krieger *et al.*, 1992; Krieger and Weis, 1993). Several explanations were put forward in support of a RC-mediated quenching mechanism. From the first experiments on qE, it was proposed that RCs convert to an inactive form by the direct effect of the acidification of the lumen (Weis and Berry, 1987). Alternatively, it was proposed that new electron transfer pathways arise around PSII, possibly involving cytochrome *b₆f* or other redox mediators, which established a futile electron cycle around PSII by reacting with its oxidised form (Neubauer and Schreiber, 1987). A role for a dissipative charge recombination to take place after charge separation in the special chlorophyll pair, under conditions of donor-side limitations, was also speculated (Schreiber and Neubauer, 1990). Donor-side limitations (inhibition of the oxygen-evolving complex) were shown to take place at a pH lower than 5.5 and to be accompanied by a release of Ca^{2+} in the lumen, proposed to be the physiological mechanism underlying the transient PSII inactivation (Krieger *et al.*, 1992). According to this last model, the release of calcium ions raised the potential of the acceptor side, thereby promoting useless charge recombination in the RC. However, little experimental support was achieved to prove that RCs are the site of energy-dependent quenching of excess energy. Most of the evidence came from experiments involving artificially lowering pH in isolated thylakoid membranes. This produced results partially contradicting leaf measurements, and were often inferred from indirect measurements of CO_2 assimilation and

oxygen production, weakly linked to the qE process itself. It is not clear whether the evidence supporting RC inactivation are indicative of a physiological mechanism taking place in the thylakoids or simply an inhibitory phenomenon of PSII under stress (Ruban, 2018).

By contrast, a large body of evidence suggests that the site of qE control is in the light-harvesting complexes of PSII (Ruban, 2012):

- qE is not only quenching the maximal chlorophyll fluorescence when RCs are closed (F_m), but also quenches substantially the fluorescence when RCs are open (F_o) (Genty *et al.*, 1992; Farooq *et al.*, 2018);
- Direct measurements of heat emission suggest that the qE process is completed within 1.4 μ s after illumination, much faster than the rates of charge separation and recombination for the proposed quenching mechanisms in the RCs (Mullineaux *et al.*, 1994);
- It is evident, from spectral decomposition of the quenching response, that qE and qP processes quench different bands of PSII. The former quenches bands peaking at 680 nm and 700 nm, consistent with PSII antenna components, while the latter quenches bands at 685 nm and 693 nm, belonging to the core complexes CP43 and CP47 (Ruban and Horton, 1994).
- The kinetics of fluorescence decay, measured with time-resolved techniques, are consistent with quenching taking place in antenna (Genty *et al.*, 1992; Chmeliov *et al.*, 2016, 2019);
- qE depends upon the presence of xanthophylls that are exclusively bound to antenna components (Niyogi *et al.*, 1998; Pogson *et al.*, 1998; Niyogi *et al.*, 2001);
- PsbS, a protein essential for qE *in vivo*, was not found in PSII supercomplexes but rather randomly localised within the antenna system (Nield *et al.*, 2000). Moreover, it interacts selectively with LHCII rather than RCs under NPQ conditions (Teardo *et al.*, 2007; Sacharz *et al.*, 2017).
- Several studies show the similarities in the behaviour of isolated LHCs and intact photosynthetic systems. For example, qE and isolated LHCII responds in the same way to a number of agents such as DCCD (Wentworth *et al.*, 2001),

antimycin A (Ruban *et al.*, 1994a), tertiary amines (Ruban and Horton, 1992) and cross-linkers (Iliescu *et al.*, 2008; Johnson and Ruban, 2009). qE and *in vitro* LHCII quenching respond to pH (Petrou *et al.*, 2014), Mg^{2+} (Ruban *et al.*, 1994a) and xanthophyll cycle Cars (Ruban and Horton, 1999). Aggregates of light harvesting complexes bear the same qE fingerprints associated with qE *in vivo*, such as distortion of Neo (Ruban *et al.*, 2007), appearance of red-shifted Chl species (Ruban *et al.*, 1991; Horton *et al.*, 1991) and absorption/scattering changes (Ruban and Horton, 1992).

- Antibiotic treatments that substantially decrease the accumulation of RCs (*e.g.* lincomycin) do not impair the capacity to form qE (Gáspár *et al.*, 2006; Belgio *et al.*, 2012). On the contrary, mutants lacking antenna components possess reduced qE amplitudes (Andersson *et al.*, 2003);

The first proposal of qE taking place in the antenna came from the antenna aggregation model proposed by Horton and colleagues (Horton *et al.*, 1991). This hypothesis suggested for the first time that the rearrangement of the thylakoid membranes occurring during qE involve the tuning of the light harvesting function via allosteric regulation. A number of studies are consistent with this model (Ruban *et al.*, 2007; Johnson *et al.*, 2011b; Chmeliov *et al.*, 2016). Although it is now accepted that the largest portion of qE takes place in the antenna, it is still controversial whether both minor and major LHCS are playing a role in qE or whether the process is entirely located in one species. These uncertainties are due to their high structural and functional homology, which makes it virtually impossible to distinguish their spectroscopic signatures *in vivo*. When extracted from the thylakoid membranes with detergents, both major and minor antennae can be subject to aggregation, which is accompanied with fluorescence quenching (Holleboom *et al.*, 2015). The pH sensitivity was shown to be similar between each species, as all complexes were shown to bind DCCD, resulting in the suppression of qE (Ruban *et al.*, 1992; Walters *et al.*, 1994, 1996). Moreover, the thylakoids exhibit an extreme plasticity and can easily compensate the loss of a particular polypeptide with the overexpression of another (Ruban *et al.*, 2003; Havaux *et al.*, 2007; Damkjær *et al.*, 2009). qE is therefore often present, even when crucial components of the light harvesting system are missing (Andersson *et al.*, 2003). For this reason, a genetic approach didn't offer a clear-cut

picture on the matter, as envisaged. Interpretable results have not been obtained on mutants knockout or knockdown for minor antenna complexes (Andersson *et al.*, 2001; Kovács *et al.*, 2006; de Bianchi *et al.*, 2008; van Oort *et al.*, 2010; de Bianchi *et al.*, 2011; Miloslavina *et al.*, 2011).

Conversely, the absence of a single polypeptide species forming the major LHCII trimers was found to variably affect the qE process (Damkjær *et al.*, 2009; Pietrzykowska *et al.*, 2014). Absence of the Lhcb2 and Lhcb3 components didn't attenuate the qE capacity. By contrast, the absence of Lhcb1 caused a 35% decrease in qE amplitudes (Pietrzykowska *et al.*, 2014). These different quenching capacities, however, were linked to a marked plasticity of the thylakoid membranes, where the overexpression of another antenna constituent could partially restore the function of a missing one. This was proven for the double knockdown mutant of Lhcb1 and Lhcb2, where Lhcb5 and Lhcb3 complexes were found to associate in heterotrimeric interactions (Ruban *et al.*, 2006). Recently, an *Arabidopsis* mutant lacking the Lhcb1 and Lhcb2 polypeptides, the main constituents of the major LHCII trimer, was characterised (Nicol *et al.*, 2019). The approach used, consisting of gene silencing using artificial micro-RNAs, differed from the antisense knockdown of the same genes performed in a previous work (Andersson *et al.*, 2003). A key novelty was the lack of a significant upregulation of other antenna components, unlike in the antisense mutants, where all minor antenna components accumulated at increased amounts (Andersson *et al.*, 2003; Ruban *et al.*, 2006). A greater decrease in NPQ was observed in the mutants compared to the previous work (60% against 28%), a large part of the quenching belonging to the reversible qE process. This work clearly showed that a large part of qE takes place in the major LHCII. However, it doesn't prove the origin of the remaining reversible quenching since, although very reduced, a fraction of trimeric complexes is still present in the thylakoids of the mutant, which could contribute to the residual qE. Unlike for minor antennae, a mutant lacking all major antenna constituents has so far never been created.

Role of PsbS

The pigment-binding light-harvesting complexes alone are not sufficient to describe the occurrence of NPQ *in vivo*. The photosystem II subunit S (PsbS) was discov-

ered to play an essential role in plants during NPQ and specifically qE (Funk *et al.*, 1995; Li *et al.*, 2000). The 22 kDa protein is a member of the LHC superfamily, but presents 4 trans-membrane α helices instead of 3, as found instead in LHCII and minor antenna complexes (Fan *et al.*, 2015). The 21 phenylalanine residues in its structure confers a marked hydrophobic character. Hydrophobic forces are largely the glue that holds together two PsbS monomers in a dimeric association (Fan *et al.*, 2015). Despite sharing homology with the other Chl *a/b* enriched antenna proteins, purified PsbS was shown not to bind any pigments, nor to incorporate them in reconstitution experiments (Dominici *et al.*, 2002; Bonente *et al.*, 2008). Moreover, the amino acids that coordinate pigment binding in other antenna complexes are absent in PsbS. Therefore, the initial excitement of having found the site of the quencher faded since a pigment needs to be involved in the dissipation of the excess excitation energy of chlorophylls bound to antenna complexes. In addition, the crystal structure didn't show strongly associated pigments (Fan *et al.*, 2015). In particular, it revealed the compactness of the whole structure, where no pigment cleft is detectable. The four trans-membrane helices are in close proximity with each other and steric hindrance impedes the stable binding of pigments. Moreover, the purified protein exhibits a flat circular dichroism spectrum in the red region, where chlorophylls bound to the protein scaffold normally present very distinctive signature peaks (Fan *et al.*, 2015). However, some labile interactions with pigments could still be possible *in vivo*. The occurrence of a transient interaction between the high light-induced carotenoid Zea and the PsbS protein was proposed and could be central in qE dynamics (Aspinall-O'Dea *et al.*, 2002; Li *et al.*, 2004; Park *et al.*, 2018). Reconstitution of PsbS with Zea was shown to be possible and to bring an absorption change at 535 nm that is associated with qE *in vivo* (Aspinall-O'Dea *et al.*, 2002). The driving force for this association could consist of hydrophobic interactions, between LHC-like proteins (PsbS) and the most hydrophobic of antenna-associated xanthophylls (Zea). However, the aggregation of Zea rather than its binding to PsbS has been shown to cause the observed absorption changes at 535 nm (Ruban *et al.*, 1993a; Bonente *et al.*, 2008). Thus, the formation of a PsbS-Zea quenching complex remains an unlikely scenario. There is evidence revealing the distinct roles of PsbS and the Zea during qE (Johnson *et al.*, 2009; Crouchman *et al.*, 2006; Sylak-Glassman *et al.*, 2014).

In order to discover the function of a new protein it is necessary to see where it localises and what are the interaction partners, if any. The marked hydrophobic character of PsbS underlines the ability of the protein to interact with almost every component of PSII (Dominici *et al.*, 2002; Teardo *et al.*, 2007). When isolated, PsbS tends to aggregate (Caffarri *et al.*, 2009). Given these characteristics, PsbS has proven to be a difficult protein to isolate via detergent solubilisation. Curiously, PsbS has never been visualised within PSII supercomplexes (Nield *et al.*, 2000; Caffarri *et al.*, 2009; Pagliano *et al.*, 2014; Wei *et al.*, 2016; Nosek *et al.*, 2017; Su *et al.*, 2017). In some studies, the protein has been found to co-migrate during isolation with supercomplexes (Caffarri *et al.*, 2009; Wei *et al.*, 2016), but its distribution didn't follow linearly that of other RC subunits and it wasn't resolved in the electron density maps of isolated supercomplexes, suggesting simply co-migration rather than binding. In addition, the overexpression of PsbS, which leads to a marked qE increase, isn't accompanied by a proportional increase in the amount of other PSII subunits, suggesting that it functions independently (Li *et al.*, 2002). Since the stoichiometry of PsbS has never been thoroughly investigated (Funk *et al.*, 1995), it remains an open possibility that PsbS is present in sub-stoichiometric quantities and therefore PSII is rather "insensitive" to changes in its expression pattern. A recently identified cleft in the cryo-EM structure of the C2S2M2 supercomplex, was suggested to offer a possible binding site for PsbS *in vivo* (Su *et al.*, 2017). In this scenario, a weak but functional interaction could arise between PsbS, CP24, CP29 and the core antenna CP47 (Su *et al.*, 2017; Daskalakis, 2018; Nicol *et al.*, 2019). However, the evidence described so far suggests a rather unspecific localisation and action of the protein within the PSII unit.

Biochemical and computational studies showed that PsbS is capable of sensing pH variations that activate qE (Dominici *et al.*, 2002; Li *et al.*, 2002; Bergantino *et al.*, 2003; Li *et al.*, 2004; Daskalakis and Papadatos, 2017). Site-directed mutagenesis and DCCD binding experiments identified two glutamate residues on the luminal side that can bind H⁺ and, upon whom, the activity of the protein depends entirely (Li *et al.*, 2002, 2004). Early works on maize clearly showed that the protein is found in equilibrium between a dimeric and a monomeric form and that the latter is favoured upon light exposure and lumen acidification (Bergantino *et al.*, 2003). Co-immunoprecipitation experiments have shown that PsbS interacts with

many other membrane components (Teardo *et al.*, 2007). A direct interaction between PsbS and LHCII has been observed when these proteins are reconstituted in liposomes (Wilk *et al.*, 2013). Recently, specific pull-down assays have proven that the capacity of PsbS to interact with other complexes increases when zeaxanthin is present and under NPQ conditions (Correa-Galvis *et al.*, 2016; Sacharz *et al.*, 2017). Moreover, PsbS interacts more specifically with LHCII and antenna components rather than RCs (Sacharz *et al.*, 2017). It appears therefore, that a functional interaction is taking place between PsbS and other LHCs during the onset of NPQ. The exact outcome of these associations has not yet been determined. PsbS has been proposed either to carry a quencher pigment to the antenna complexes or to act as transducer of lumen acidification to a quenching site located inside the antenna system (Ruban, 2016).

Recently, PsbS as a strict requirement for qE has been questioned (Johnson and Ruban, 2010). It was shown that *npq4* plants, lacking PsbS, are able to induce a photoprotective quenching mechanism with all the characteristics of qE of WT plants (535 nm absorption changes, ΔpH dependence). The sole difference was in the kinetics of the process, taking an hour to be completed instead of several minutes (Johnson and Ruban, 2010). Thus, it appeared more likely that PsbS acts as a transducer of lumen acidification, rather than being a quenching site itself. When ΔpH was enhanced in isolated chloroplasts with the artificial proton shuttle diaminodurene (DAD), qE was restored in membranes lacking PsbS.

Fluorescence recovery after photobleaching experiments revealed important details concerning the action of PsbS in the thylakoids. The fluidity of the lipid bilayer was affected by the presence of PsbS (Goral *et al.*, 2012). By simple comparison of the thylakoid membranes in the presence (WT) or absence (*npq4* mutant) of the protein, it was observed that the latter exhibits a smaller fraction of mobile chlorophyll-binding complexes and a higher degree of ordered “semi-crystalline” PSII complexes that were first described by Boekema and coworkers (Kouřil *et al.*, 2013). Experiments on the mutants overexpressing PsbS (L17) revealed greater differences compared to *npq4*. Interestingly, the illumination and activation of the NPQ response induced the opposite phenotype, a reduction of the mobile fraction of membrane-bound complexes (Goral *et al.*, 2012). On the contrary, the absence of PsbS didn’t result in any changes, suggesting that the protein is necessary for

the occurrence of a thylakoid reorganisation associated with qE. The involvement of rearrangements in the thylakoid membranes is also consistent with other works showing that PsbS catalyses the formation of an antenna oligomer that detaches from the PSII unit during qE (Kiss *et al.*, 2008; Betterle *et al.*, 2009) and that aggregation of LHCII occurs when the membranes are in the photoprotective state (Johnson *et al.*, 2011b).

Role of the xanthophyll cycle carotenoids

Evidence for a light-inducible conversion between two Cars was found in the 1950s (Sapozhnikov *et al.*, 1957). It was later that the contribution by Harry Yamamoto established that Vio is reversibly converted to Zea during light exposure of leaves (Yamamoto, 1979). The cycle involves the concerted action of two enzymes, the violaxanthin de-epoxidase, a luminal enzyme activated by low pH and ascorbate (Pfundel and Dilley, 1993; Hager and Holocher, 1994), and a zeaxanthin epoxidase, located in the stroma, which is O₂-dependent and active at neutral pH values (Jahns *et al.*, 2009). The first enzyme catalyses the removal of oxygen atoms from the end ring of the xanthophyll Vio. The Zea epoxidase, instead, is involved in the opposite reaction, the “re-oxygenation” of the Car. These reactions take place in two sequential steps of single oxygenation events, where antheraxanthin, a mono-oxygenated Car, is the intermediate product between Vio and Zea. Despite species-specific differences in the quantity and activity of the xanthophyll cycle enzymes (Horton and Ruban, 1992; Demmig-Adams *et al.*, 2006; Wilson and Ruban, 2019), it is generally true that Zea formation takes a few minutes to occur at a complete extent, while its reconversion to Vio takes tens of minutes or even hours (Siefermann and Yamamoto, 1975).

A great breakthrough in understanding the functional significance of this process was made by Demmig-Adams (Demmig-Adams, 1990), who linked the formation of Zea to qE. Afterwards, Bassi and co-workers (Bassi *et al.*, 1993; Crimi *et al.*, 1998) and later Holzwarth and co-workers (Holzwarth *et al.*, 2009) observed that large amounts of Zea could be reconstituted in minor antenna complexes and that this was linked to Chl fluorescence quenching. Additionally, Gilmore and Govindjee described the enhanced extent of quenching in light exposed thylakoids where the

Zea content is maximised (Gilmore *et al.*, 1995).

This exposed link between Zea and fluorescence quenching readily prompted researchers to attribute a direct role to the Car molecule as a quencher of Chl excited states (Duffy and Ruban, 2015). Among the first proposals, an elegant hypothesis was put forward by Frank and co-workers (Frank *et al.*, 1994; Frank and Cogdell, 1996). The so-called *molecular gear-shift* model is based on the observation that, when Vio undergoes the conversion to Zea, the conjugated chain length N increases to $N=11$ and this causes a significant decrease in the energy level of the S_1 state. The model proposes that, while Vio S_1 energy is higher than the energy of Chl S_1 , the situation is reversed for Zea, making Vio a light harvester and Zea a quencher pigment. Due to the characteristically “dark” Car S_1 state (due to the forbidden $S_0 \rightarrow S_1$ transition and the short excited state lifetime), the assignment of the correct energies has long been a non-trivial task. Chynwat and Frank indirectly inferred these values, using the so-called energy-gap law (Chynwat and Frank, 1995). However, the effective conjugated chain length N is less than the expected values for polyenes with 11 C=C bonds, because the *cis* conformation of these in the end terminal rings effectively extends the π -electron chain to only $N \simeq 10$. This results in a higher than expected value for the Zea S_1 energy. Polívka and co-workers accurately measured the energies of the S_1 states of Vio and Zea, showing that both of them lie below the S_1 of Chl and therefore provided evidence against the gear-shift model (Polívka *et al.*, 1999). In addition, biochemical studies exposed incongruities about the localisation of the xanthophyll-cycle Car in the thylakoid membranes. Contrarily to previous findings (Bassi *et al.*, 1993), these studies showed that a pool of Vio, readily available for conversion into Zea, is found in major LHCII trimers, while Vio bound to minor complexes is buried inside the protein structure and unreachable by the de-epoxidase (Ruban *et al.*, 1999; Jahns *et al.*, 2009). More recently, another photophysical mechanism has been proposed involving Zea as a direct quencher (Holt *et al.*, 2005; Amarie *et al.*, 2007; Ahn *et al.*, 2008; Avenson *et al.*, 2008; Amarie *et al.*, 2009; Dall’Osto *et al.*, 2017; Park *et al.*, 2017). This mechanism involves the formation of a strongly-coupled heterodimer between Chl and Zea, the ultrafast formation of a Zea cation upon excitation of this heterodimer and the non-radiative charge recombination to the ground state. The radical cation signal was readily observed in transient absorption measurements of isolated minor

antenna complexes (Avenson *et al.*, 2008) and thylakoids (Holt *et al.*, 2005).

Alternatively to the role as a quencher, zeaxanthin has been proposed to be an allosteric regulator of the qE switch (Horton *et al.*, 1991; Ruban, 2018). Several findings support this hypothesis: at saturating ΔpH extents, the qE in the presence and absence of Zea reaches similar levels (Rees *et al.*, 1989; Noctor *et al.*, 1993); the effect of Zea in the membranes does not depend upon its excited-state levels, but its rather due to structural details of the Car (Ruban *et al.*, 1998a); Zea amplifies the amplitudes of qE quenching and changes the kinetics of its formation and relaxation (Ruban and Horton, 1999). A hysteretic behaviour of the dependence of qE to ΔpH values have been revealed (Noctor *et al.*, 1993; Ruban and Johnson, 2010). The conversion of Vio to Zea causes a profound shift of the hydrophobicity of the Car, due to the removal of the hydrophylic epoxy groups in the end rings of the Car. The observation that the presence of Zea causes the aggregation of isolated LHCII complexes lead to the proposal that the Car promotes antenna aggregation during qE (Horton *et al.*, 1991). By doing so, it would stabilise the quenched state, producing deeper extents of quenching and delaying its recovery. Alternatively, the creation of a hydrophobic environment could increase the pK of some key luminal amino acids of LHCs, making these promptly responsive at smaller ΔpH values (Mehler *et al.*, 2002; Johnson and Ruban, 2011). In this context, the screening of several mutants with different Car compositions revealed the linear correlation between the hydrophobic character of the Car present and the pK value of NPQ (Ruban and Johnson, 2010).

The conformational change in LHCII

The DCCD experiments by Jahns and Junge revealed the capacity of LHC proteins associated with PSII to sense protons and suggested they might have additional roles to their antenna function, related to their protonation (Jahns and Junge, 1990). The suggestion of a feedback regulatory mechanism to control the excitation energy pressure to PSII (Horton and Ruban, 1992), implied that the ability of LHCs to sense protons was somehow related to this mechanism. Indeed, the key lumen-exposed glutamate and aspartate residues of LHCs were identified and it was shown that their protonation is required for the dissipative switch to occur (Ruban *et al.*, 1992;

Walters *et al.*, 1996; Belgio *et al.*, 2013; Ioannidis *et al.*, 2016). The development of the antenna aggregation model for NPQ control (Horton *et al.*, 1991), was based on observations that the fluorescence yield of LHCII could be modulated, controlling the degree of inter-trimer associations, accompanying spectroscopic changes typical of qE *in vivo*. Moreover, modulation of LHCII function was dependent upon pH and xanthophylls and showed the same responses to activators (Mg^{2+} , dibucaine) and inhibitors (antimycin, cross-linkers) as observed in qE (Horton and Ruban, 1992). Before that time, measurements were performed on fully solubilised LHCII trimers, whereas the LHCs in the thylakoid environment are far from being isolated entities. The thylakoid bilayer is among the most protein-rich biological membranes and in some conditions the molecular crowding is so high that the complexes are almost immobile (Kirchhoff *et al.*, 2008). LHCs have been shown to cluster spontaneously when inserted in a lipid bilayer, leading to a reduction in the chlorophyll excitation lifetime (Moya *et al.*, 2001; Natali *et al.*, 2016). The major spectroscopic change that occurs upon aggregation of LHCII is the appearance of red and FR emitting forms in the emission spectra (Ruban and Horton, 1992). These exhibit a complex temperature-dependent behaviour and are formed by several sub-peaks (Ruban *et al.*, 1995b; Chmeliov *et al.*, 2016). Resonance Raman spectroscopy unveiled the involvement of hydrogen bonds during aggregation of LHCII (Ruban *et al.*, 1995a), in line with the entropy variation between the trimeric and aggregated state, which is $\sim 85 \text{ kJ mol}^{-1}$ (Santabarbara *et al.*, 2009). Additionally, Raman showed conformational changes of Lut and Neo upon the transition to the quenched state (Robert *et al.*, 2004; Ruban *et al.*, 2007), underlying a degree of changes in their relative orientation. Flash photolysis experiments absorbance-detected magnetic resonance confirmed these findings, showing that aggregation induces changes in chlorophyll-xanthophyll electronic interactions (Barzda *et al.*, 1998; Lampoura *et al.*, 2002). Absorption spectroscopy showed alterations of the pigment binding sites, especially related to red-most Chl *a* molecules and the Cars in the L1 site. Circular dichroism described extensive changes occurring in the coupling between pigments and showed the alteration of the terminal emitting Chl *a* and Lut molecules, which are reoriented to be more parallel to the membrane plane (Ruban *et al.*, 1997a; Wentworth *et al.*, 2003).

However, after describing the extensive changes in the structural arrangements

and energetics of the pigments, it was questioned to what extent aggregation of LHCII was necessary for the quenched state. The analysis of LHCII crystals, used to solve the structure of the complex by Liu and co-workers (Liu *et al.*, 2004), provided the first evidence that the dissipative conformation could be found in single complexes rather than originating from interaction with neighbouring complexes. Despite marginal interactions between LHCII complexes in the proteo-liposomes used by Liu and coworkers, the complexes were in a deeply quenched state (Pascal *et al.*, 2005). The Raman and fluorescence changes evidenced from a comparison with detergent-isolated LHCII were identical to those observed in LHCII aggregates and *in vivo* (Ruban *et al.*, 1992, 2007). Following investigations discovered that it was possible to induce fluorescence quenching even in fully solubilised LHCII monomers and trimers. The application of hydrostatic pressure caused a 37% of quenching (van Oort *et al.*, 2007). Calculations pointed towards ΔG values of only -7 kJ/mol, corresponding to variations of the trimer volume of 0.006%. Therefore, only tiny structural perturbations (free-energy changes of the order of an H-bond formation) could give rise to quenching interactions, in line with calculations showing that small structural differences can have significant effects on the Chl-Car resonant couplings. Additional evidence of the inner conformational switch of LHCII complexes came from the immobilisation of single trimers in a polyacrylamide gel matrix (Illoaia *et al.*, 2008, 2011b). The dialysis of detergent molecules from LHCII was shown to induce a dissipative state of the complexes, even in the absence of protein-protein aggregation. The spectral changes observed upon this induction were again resembling the fingerprints of qE *in vivo* and were indicative of a strong perturbation of the L1 site, where the terminal emitting Chl cluster is located (Novoderezhkin *et al.*, 2005; Illoaia *et al.*, 2011b). The application of transient absorption spectroscopy indeed identified a dissipative interaction between Chl and Lut 1 (Ruban *et al.*, 2007). More recently, single molecule spectroscopy techniques were applied to LHCII, revealing a fluorescence “blinking” behaviour of single monomers and trimers (Krüger *et al.*, 2010, 2011b,a; Tutkus *et al.*, 2017). Although the blinking behaviour is generally expected for chromophore binding systems, due to fluctuations of their local environments and variations of their rates of fluorescence and internal conversion (Kondo *et al.*, 2017), the remarkable feature observed in these studies was the sensitivity of this blinking pattern to factors such as pH or Zea that

modulate qE *in vivo*. The dynamic behaviour of LHCII arises from an intrinsic disorder of the protein scaffold that can lead to variations of the distances between the bound pigments. All of the above cited works provided direct experimental evidence that a switch of single LHC proteins could underlie the photoprotective qE state. The core of these studies was to show that the light harvesting and the quenched conformations of LHCII are almost iso-energetic, *i.e.* very small changes can lead to a dramatic decrease in the Chl excited state lifetime. Interestingly, Zea, pH and detergent make this switch more probable, revealing an allosteric modulation that could mirror qE *in vivo*. In this context, the rearrangements of LHC subunits observed in the membranes (Betterle *et al.*, 2009; Johnson *et al.*, 2011b) could be a consequence of the quenched state rather than its cause. It has been proposed that the aggregation of LHCII trimers increases the ability of other subunits to switch to the quenched state, in a cooperative behaviour, by increasing their sensitivity to low pH (Petrou *et al.*, 2014).

The nature of the quenching pigment

In the early 1990s, Peter Horton and colleagues suggested the existence of a Chl-mediated mechanism of Δ pH-dependent dissipation of excess energy (Ruban and Horton, 1992). This was based on the observation that, upon LHCII aggregation, a characteristic fluorescence band at 700 nm (F700) appeared and related to the amplitude of qE quenching. F700 displays some peculiar features, such as a pronounced temperature dependence, originating from low frequency vibrations within the LHCII aggregates. Alfred Holzwarth embraced and expanded this idea, suggesting that energy dissipation occurred in Chl dimers that present a charge transfer character (Holzwarth, 1995; Miloslavina *et al.*, 2008; Müller *et al.*, 2010). Chl-Chl charge transfer states possess enhanced coupling between excited and ground states, resulting in faster rates of internal conversion to S_0 (heat release) as well as red-shift of the fluorescence emission band (low energy, F700) (Ruban, 2012). Recently, Stark fluorescence spectroscopy proved the existence of charge transfer states within the LHCII antenna complex of plants, proposed to be the major site of qE development (Wahadoszamen *et al.*, 2012). An analysis of a pair of Chls embedded in an artificially designed protein environment offered insights into the mechanism of

quenching mediated by the mixing of excitonic and charge transfer states and revealed the influence of the protein scaffold in tuning the non-radiative dissipation (Wahadoszamen *et al.*, 2014). Another study, however, scrutinised the time- and temperature-dependency of the emission spectrum of quenched, aggregated LHCII and found clear evidence against the involvement of Chl charge transfer states in the mechanism of energy dissipation (Chmeliov *et al.*, 2016; Gelzinis *et al.*, 2018). First of all, while the number of LHCII complexes in the quenched state is roughly constant, the number of complexes for which fluorescence is red shifted is decreasing with increasing temperatures. Second, in all comparisons, the decay kinetics of the red emission components were slow and unable to explain the fast quenching of Chl fluorescence. Third, a two-state model describing the spectra (main LHCII emission and F700 as quenching sites) could not explain the data as well as a three-state model did (main LHCII emission, F700 and an additional quenched state), implying the existence of a different mechanism of energy dissipation (Gelzinis *et al.*, 2018). Single molecule spectroscopies have also identified these red-emitting states in LHCs, although they have again been proposed not to play any role in the energy quenching mechanism (Krüger *et al.*, 2014). Charge transfer states, therefore, seem to be simply an unavoidable feature in highly packed Chl-enriched systems. However, it is still not possible to exclude their involvement in qE *in vivo*, since it seems they are a conserved trait of several Chl-binding antenna complexes and appear enhanced upon quenching induction (Krüger *et al.*, 2011b; Pinnola *et al.*, 2016; Wahadoszamen *et al.*, 2016).

Another idea began to emerge in the early 1990s proposing that the photophysical mechanism of excitation energy quenching involves energy transfer from Chl to a Car molecule (Owens *et al.*, 1992; Owens, 1994; Frank *et al.*, 1994). Carotenoids were indeed described as “natural born quenchers”, in virtue of their low-lying first excited state S_1 , characterised by a fast rate of internal conversion to S_0 (Polívka and Sundström, 2009; Duffy and Ruban, 2015). The “molecular gear-shift” mechanism (Frank *et al.*, 1994) was the first complete theorisation of a quenching mechanism involved in NPQ (see “Role of the xanthophyll cycle carotenoids”). However, after the determination of the S_1 energies of Vio and Zea (Polívka *et al.*, 1999), it was clear that the simple conversion of the former to the latter couldn’t account for NPQ. Novel experimental evidence in support of this quenching mechanism came from

transient absorption studies of artificial dyads, which are Chl analogues covalently linked to a Car molecule (Berera *et al.*, 2006). It was directly observed that a Car can act as an acceptor of Chl excitation energy, thereby shortening its excited-state lifetime. The conjugation length was shown to be critical in this mechanism, as the Car S_1 state must be low enough to achieve a downhill energy transfer from Chl S_1 . In a following work, Ruban, Berera and co-workers identified a similar channel of energy dissipation opened in LHCII in the aggregated, quenched state (Ruban *et al.*, 2007). Through target analysis of the time-resolved absorption spectra, they were able to resolve a spectrum of a quencher, highly resembling a Car species, whose identity was assigned to one of the central luteins (Lut 1). Applying Raman spectroscopy to a range of systems, from *in vitro* LHCII aggregates to intact leaves, they demonstrated that the same rearrangements of the pigments bound occurs in all cases, suggesting that the same mechanism of energy dissipation is acting *in vivo* during qE. More recently, a breakthrough was achieved when the incoherent energy transfer from Chl to Car was observed in cyanobacterial HliD (an ancestor of LHCII) (Staleva *et al.*, 2015). HliD dimers contain six Chls *a* and 2 β -carotenes and are found in a constitutively photoprotective state, characterised by a very low fluorescence yield. The advent of a femtosecond stimulated Raman technique to measure time-resolved vibrational spectra of Car allowed the confirmation of the Chl *a* to β -carotene energy transfer mechanism in HliD (Hontani *et al.*, 2018). The difficulty in the interpretation of transient absorption data on complex systems, such as light harvesting complex aggregates, lead to criticisms from Holzwarth' and Croce's groups (Müller *et al.*, 2010; van Oort *et al.*, 2018), who showed that excessive laser powers used to achieve good signal-to-noise ratios could lead to spectral and dynamical artefacts. Testing again the hypothesis of Ruban *et al.* (2007), Muller and coworkers concluded that no Car signal could be detected and proposed instead a Chl-only mechanism of energy dissipation (Müller *et al.*, 2010). Liguori *et al.* (2015) isolated LHCII from a plant able to accumulate exclusively the Car astaxanthin. These complexes were found to be in a quenched state compared to WT plants. Probing the energy transfer pathways, they observed the presence of Car signal after Chl excitation, suggesting this as the mechanism of energy quenching (Liguori *et al.*, 2015). Interestingly, the resolved spectrum of the quencher was blue-shifted compared to the usual Car S_1 spectrum, suggesting the involvement of a different

state. This state was assigned as a potential Car S^* state, which excited-state spectrum has always been observed blue-shifted compared to the S_1 peak (Gradinaru *et al.*, 2001; Staleva *et al.*, 2015). Very recently, the investigation of CP29 lead to similar conclusions, as the spectrum of the quencher extrapolated via target analysis from transient absorption measurements was found to be unusually blue-shifted, although the dynamics correspond to those of a Car first excited state (Mascoli *et al.*, 2019).

Formation of Chl-Car exciton states were also proposed to be a mechanism of NPQ within the LHCII complex (Naqvi *et al.*, 1997; van Amerongen and van Grondelle, 2001). When the molecules are in close van der Waals contact, there could be a mixing of the xanthophyll S_1 and the Chl Q_y (S_1). While this mixing results in hardly any noticeable effect on the Car excited-state dynamics, it has a profound effect on Chl S_1 lifetime, which is shortened to hundreds of ps (van Amerongen and van Grondelle, 2001). The first evidence of this mechanism was provided using intact thylakoid membranes under illumination, where an increase in Car signal appeared immediately after Chl excitation (Ma *et al.*, 2003). Peter Walla and coworkers measured the coupling of Car S_1 state and Chl Q_y *in vivo* on various *Arabidopsis* mutants with two-photon excitation (Bode *et al.*, 2009). The authors found a correlation between the extent of qE induced and the Chl-Car electronic coupling value. The coupling strength was pronounced in mutants overproducing PsbS or Vio de-epoxidase, but significantly reduced in mutants impaired in their qE capacity (*e.g.* *npq4*). Recent results provided fresh evidence in support of this quenching mechanism, both in thylakoid membranes of higher plants and in intact cells of the alga *Nannochloropsis oceanica* (Park *et al.*, 2018, 2019).

An additional mechanism of quenching that could occur is a reductive type of energy transfer, that involves the exchange of electrons instead of purely excitation energy. The proposals of this mechanism in higher plants describe the formation of a Zea radical cation in minor antenna complexes (Holt *et al.*, 2005; Amarie *et al.*, 2007; Ahn *et al.*, 2008; Avenson *et al.*, 2008). This model assumes that strong resonance interaction between pigments can lead to a mixing between excitonic and charge transfer state. Therefore, an excited Chl molecule can receive an electron from the highest occupied molecular orbital (HOMO) localized on Zea to its lowest unoccupied molecular orbital (LUMO). This process is followed by rapid charge

recombination and relaxation to the ground state. The recent characterisation of the “No Minor antennae” (NoM) mutant, revealed the signal of a Zea cation associated with monomeric light harvesting complexes (Dall’Osto *et al.*, 2017; Park *et al.*, 2017, 2018). As for charge transfer states between Chl molecules, it is still uncertain the extent of their role in qE since both are easily occurring in the strongly connected and heterogeneous light-harvesting systems (Duffy and Ruban, 2015). In fact, despite correlating with the extent of energy quenching, the Car cation signal doesn’t offer increased quenching compared to quenching in the absence of Zea (Ahn *et al.*, 2008). It has been proposed that a Lut radical cation compensates for the absence of Zea (Avenson *et al.*, 2008; Li *et al.*, 2009). The Car radical cation mechanism has also been detected in other model organisms and occurs in other members of the LHC family, such as LHCSR1 (Pinnola *et al.*, 2016).

Despite several mechanisms of energy dissipation having been proposed, the scenario could be more complicated than expected and multiple photophysical mechanisms could be acting during the qE formation. This has been proposed in several studies and reflects the heterogeneous process of NPQ, characterised by multiple decay kinetics and spectra (Miloslavina *et al.*, 2008; Holzwarth *et al.*, 2009; Krüger *et al.*, 2011b; Wahadoszamen *et al.*, 2012, 2016; Park *et al.*, 2018; van Amerongen and Chmeliov, 2019).

Current models of qE

An holistic perspective that summarises all the experimental evidence described so far led in the formulation of various models for NPQ and its main component qE. The “LHCII aggregation” model, formulated in 1991 (Horton *et al.*, 1991) was based on observations that the major LHCII antenna complexes can undergo protein protein aggregation, accompanied by an extensive amplitude of Chl fluorescence quenching, readily able to explain the amplitudes of qE *in vivo* (Ruban and Horton, 1992). The model states that conformational changes and thylakoid membrane reorganisation processes occur transiently during qE. These changes are promoted by protonation of antenna components and the conversion of Vio to Zea. In this scenario, Zea is acting not as a direct quencher, but as an allosteric modulator that enhances aggregation of LHCII and therefore promotes the formation of the quencher elsewhere. PsbS was

proposed to act as an intermediary between protons (ΔpH) and LHCII, favouring the switch between the light-harvesting and the photoprotective state (Horton *et al.*, 2005).

Bassi and coworkers (Bassi *et al.*, 1993; Crimi *et al.*, 1998), and later also Fleming (Holt *et al.*, 2005; Ahn *et al.*, 2008; Avenson *et al.*, 2008) proposed instead a different explanation of qE, claiming that the process resides entirely in the minor antenna complexes. In this model, Zea acts as direct energy quencher in what is called “radical cation mechanism”, rather than an allosteric modulator (Holt *et al.*, 2005). Whilst LHCII are the most abundant complexes and entirely perform light-harvesting functions, minor antennae would instead be crucial for the control of the energy fluxes in the PSII supercomplex.

An attempt to reconcile these viewpoints was made by Holzwarth in the so-called “4-state 2-site” model (Holzwarth *et al.*, 2009). This invokes the synergic contribution of two different sites in the establishment of the photoprotective state (Holzwarth *et al.*, 2009). In line with the “LHCII aggregation” model, the “4-state 2-site” states that rearrangements in the thylakoid membranes occur at the onset of qE, but they involve the transient detachment, from PSII supercomplexes, of a fraction of the antenna proteins (specifically LHCII and CP24, see Chapter 5 in Demmig-Adams *et al.* (2014)). ΔpH would promote this rearrangement, which is PsbS-dependent. An additional site would be slowly formed by the accumulation of Zea and would occur specifically in minor antenna complexes. Therefore, while the first site (Q1) is Zea-independent but requires PsbS, the second site (Q2) is PsbS-independent, but strictly requires Zea. Interestingly, the Q1 site proposed by Holzwarth and the LHCII aggregation state proposed by Horton and Ruban are in essence equivalent.

The idea of ΔpH -dependent rearrangements of the thylakoid membrane received extensive support from experimental data (Kiss *et al.*, 2008; Betterle *et al.*, 2009; Johnson *et al.*, 2011b; Gerotto *et al.*, 2015). Recently, however, the occurrence of functional detachment of antenna complexes from the RCs (necessary for the validity of Holzwarth’s two-sites model) was questioned (Johnson *et al.*, 2009; Belgio *et al.*, 2014). Although it is nowadays acknowledged that a quenching site is present in the major LHCII antenna complexes (as proposed by Horton and Ruban and corresponding to the Q1 site in Holzwarth’s model) the debate remains open on

whether an additional Q2 site is involved in qE (Dall'Osto *et al.*, 2017). Similarly, the changes that bring about the quenched state, the photophysical mechanism of quenching and whether Zea has a direct or indirect action during qE remain to be determined.

1.4 Aims of the thesis

The qE scenario includes sequential events aimed to rapidly control light harvesting in function of the environment and the energetic requirements (Figure 1.5).

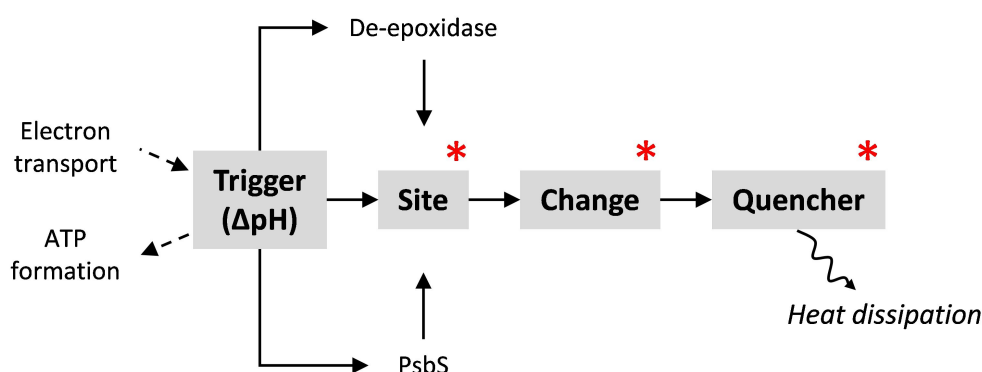


Figure 1.5: **The qE scenario.** Marked in red are the main debated aspects of qE and the focus of this thesis.

ΔpH is the feedback controller that acts as a trigger for the whole process. This signal is then sensed by specific complexes that act as the site of quenching. A change then occurs and brings about the formation of a quencher pigment. While it is well established that pH is the luminal trigger of qE, still largely disputed are the other molecular effectors and mechanisms involved. The objectives of this thesis are to investigate the nature of the qE *site* (Chapter 3), *change* (Chapter 4) and the *quencher* (Chapter 5).

The first part of Chapter 3 describes the characterisation of an *Arabidopsis* mutant lacking minor antenna complexes (*NoM* mutant) in order to determine which is the *site* where qE takes place. The ability of these plants to form qE was measured

and carefully correlated to their capacity to form ΔpH and accumulate zeaxanthin. The role of minor antennae in qE is discussed. In the second part, an *in vivo* model showing a dramatic abundance of major LHCII relative to all other thylakoid membrane complexes is described. qE kinetics and amplitudes and their pH dependence are measured, in relation to the presence or absence of PsbS and zeaxanthin.

Chapter 4 describes the conformational *change* that occur in isolated LHCII upon induction of the quenched state. These are then related to the enrichment of a particular type of xanthophyll-cycle carotenoids (violaxanthin or zeaxanthin) to understand their role in the conformational switch of single complexes.

The first part of Chapter 5 describes an approach to understand how the changes that occur in isolated LHCII are related to the formation of a *quencher* species. The nature of this dissipative interaction is explored. In the second part, these findings are translated into the native state of these complexes in the thylakoid membranes.

Chapter 2

Methodologies and approaches

2.1 Plant material and growth conditions

Young spinach leaves bought from the supermarket were used for the isolation of the LHCII complexes used in the single molecule microscopy measurements (Chapter 4). *Arabidopsis thaliana* was the model organism chosen in all other experiments. Besides the wild-type (WT) Col-0 ecotype, several mutants were used, lacking or over-expressing important components involved in NPQ. Specifically, *npq1*, lacking the gene encoding for the violaxanthin de-epoxidase enzyme and therefore unable to convert Vio into Zea (Niyogi *et al.*, 1998); *npq1lut2*, which in addition lacks the gene encoding for lycopene ϵ -cyclase and is unable to accumulate Lut (Niyogi *et al.*, 2001); *NoM*, knock-out mutant of the *Lhcb4.1*, *Lhcb4.2* and *Lhcb5* genes and thus unable to accumulate minor antenna polypeptides (Dall’Osto *et al.*, 2014a); *NoM* crossed with *npq4*, which in addition lacks the gene encoding for PsbS (Dall’Osto *et al.*, 2017); L17, which contains an additional copy of the gene encoding for PsbS under the control of its endogenous promoter and therefore overexpresses the protein (Li *et al.*, 2002).

Prior to sowing, seeds of *Arabidopsis* were sterilised in 50% ethanol and 0.1% Triton-X 100 and stored for 72 hours at 4°C to obtain an homogeneous germination. Plants were grown on a 6:6:1 ratio of John Innes No. 3 soil, Levington M3 potting compost and perlite (Scotts UK, Ipswich, UK). Due to a variable sensitivity to photodamage during development (Carvalho *et al.*, 2015), the seedlings were grown

under $100 \mu\text{mol m}^{-2} \text{s}^{-1}$ for 1 week before being transferred to $190 \mu\text{mol m}^{-2} \text{s}^{-1}$, with a 10 hours photoperiod at 22 C. Water was added to the trays three times a week. Unless otherwise specified, Chl fluorescence and biochemical measurements were made on plants that were between 40 and 60 days old, before entering the reproductive stage.

To gradually minimise the accumulation of reaction core polypeptides, plants underwent treatment with the chloroplast protein synthesis inhibitor lincomycin. This treatment causes a progressive reduction of the chloroplasts-encoded reaction core complexes, without affecting the accumulation of the nuclear-encoded antennae complexes (Gáspár *et al.*, 2006; Belgio *et al.*, 2012). For WT and L17 plants, the treatment started at the early rosette stage and was delivered three times per week in irrigation water ($0.2\text{-}0.6 \text{ g l}^{-1}$; Sigma Aldrich, Munich, Germany) until Fv/Fm measured on leaves was between 0.1 and 0.25. For *NoM* plants, the treatment (0.4 g l^{-1} , three times a week) started at the adult, full rosette stage and continued for several weeks until Fv/Fm<0.2.

2.2 Isolation of mesophyll cells and sub-cellular membranes

The plant cell wall is a semi-permeable layer surrounding the plasma membrane that confers structural rigidity to cells and anchors them together and to other leaf components. It is composed mainly of cellulose microfibrils coated by hemicellulose and linked one to another by pectins. Protoplasts are plant cells which had their cell wall removed by enzymatic digestion and are very useful preparations to study various aspects of plant physiology and genetics (Yoo *et al.*, 2007; Nishimura and Akazawa, 1975). Protoplasts can be prepared as a source of highly intact and active chloroplasts, capable of fixing CO_2 at elevated rates. Generally, release of chloroplasts can be achieved by mechanical rupture of the fragile membrane of the protoplasts or by osmotic shock. Alternatively, chloroplasts can be isolated mechanically from intact leaves, by homogenisation with a blender or a Polytron. This procedure is much faster, cheaper and yields larger quantities of chlorophyll-enriched material, although the intactness and photosynthetic activity can be even significantly worse

than for the chloroplasts obtained after protoplasts isolation. Osmotic rupture of the chloroplasts releases the chlorophyll-rich thylakoid membranes, useful for biochemical isolation of membrane bound complexes and for studies of photosynthetic processes in the presence of an external electron acceptor such as methyl-viologen.

2.2.1 Isolation of protoplasts

Protoplasts were obtained from the mesophyll layer of dark-adapted leaves from *Arabidopsis* adult plants. To expose the chloroplast-enriched leaf layer to the enzyme solution, the lower epidermis was removed with adhesive tape. Leaves were then floated for 1 hour on a solution containing 0.4 M Mannitol, 20 mM KCl, 20 mM MES, 10 mM CaCl_2 , 0.1% bovine serum albumin (BSA) (pH 5.5) in the presence of 1.5% cellulase Onuzuka R-10 and 0.4% macerozyme R-10 (Serva, Germany). Importantly, mannitol was added as an osmotic agent, salts (especially of divalent cation, such as Ca^{2+}) were added to avoid the clumping of enzymes, BSA to minimise non-specific binding of the proteins and the pH was chosen as the optimal for the cellulase and pectinase activities. Onuzuka R-10 and macerozyme R-10 consist both of enzyme mixtures, and together have high cellulase and pectinase activities, but also degrades hemicelluloses, mannans, xylans, galactomannans, and other polysaccharides of the cell wall. At the end of the incubation period, protoplasts were detected as green clouds in the solution and the exposed leaf tissue layer was fully degraded. This first passage was performed at room temperature, optimal for enzymatic activity, while all subsequent passages were carried out at 4°C to enhance the stability of the biological material. The solution was then filtered in 1 layer of muslin cloth and centrifuged twice (3 minutes, 100 rcf, 4°C). The obtained protoplasts were resuspended in reaction buffer (RC buffer) containing 0.5 M sorbitol, 20 mM HEPES, 20 mM MES, 20 mM Na-citrate, 10 mM EDTA, 10 mM NaHCO_3 , 15 mM MgCl_2 , 0.1% BSA (pH 8). Their intactness was checked with bright-field optical microscope.

2.2.2 Isolation of chloroplasts

When stated, chloroplasts were obtained from osmotic shock of intact protoplasts. To this aim, a small volume of protoplasts resuspended in RC buffer was diluted in a glass cuvette with 1 ml of RC buffer not containing sorbitol. After 30 seconds, an

equal volume of a double-osmotic RC buffer (containing 1 M sorbitol) was added to restore the correct osmotic balance.

In all other experiments, chloroplasts were prepared by mechanical shredding of dark-adapted plant leaves. When possible, healthy adult leaves were used. The middle rib containing vascular tissues was removed and leaves were cut into smaller pieces. Leaf pieces were collected in a pre-cooled Plexiglas container and ground with a Polytron in the presence of ice-cold grinding medium containing 330 mM sorbitol, 5 mM MgCl_2 , 10 mM $\text{Na}_4\text{P}_2\text{O}_7$, 2.5 mM EDTA (pH 6.5). Roughly 130 ml were used every 30 g of leaves. 40 mM D-isoascorbate was added fresh to the buffer right before grinding. The homogenised material was filtered through 4 layers of muslin followed by 2 layers of muslin and cotton wool. The filtrate was centrifuged for 100 s at 4000 rcf. The pellet was resuspended in resuspension medium containing 330 mM sorbitol, 10 mM KCl, 5 mM MgCl_2 , 2.5 mM EDTA, 50 mM HEPES (pH 7.6). The chloroplasts-enriched suspension obtained with this method exhibits a low degree of intactness, since the grinding is a harsh step in the purification procedure. Therefore, the suspension was applied to a 2 cm Percoll cushion (50% Percoll, 50% double osmotic resuspension medium) and centrifuged for 6 min at 4000 rcf. Percoll (Sigma Aldrich) is composed of colloidal silica particles that don't exhibit biological toxicity and can be used to make low-viscosity, low-osmolarity density gradients for the purification of sub-cellular organelles. The floating, less dense fraction was discarded, since it contained mainly broken chloroplasts. The obtained pellet, instead, was resuspended in a small volume of resuspension medium and kept on ice until use. Chloroplasts showed a high degree of intactness, as verified both by observations at the light microscope and measurements of F_v/F_m average values.

2.2.3 Isolation of thylakoids

Thylakoid membranes were obtained by osmotic rupture of intact chloroplasts. Chloroplasts for thylakoid extraction were obtained similarly to how it was described in the previous section, but with some important variations. Magnesium was omitted from all buffers since it promotes stacking of the membranes which in turns affects the solubilisation steps (Ruban and Johnson, 2015). Briefly, the grinding medium used to homogenise leaf material contained 0.33 M sorbitol and 10 mM

$\text{Na}_4\text{P}_2\text{O}_7$, pH 6.5. A washing step with 0.33 M sorbitol and 10 mM MES, pH 6.5 was added after grinding. The pellet was then resuspended in 15 ml of resuspension medium (0.33 M sorbitol, 1 mM EDTA, 50 mM HEPES, pH 7.6), diluted with 25 ml of break medium for 30 seconds (10 mM HEPES, pH 7.6) and then re-equilibrated with 25 ml of osmoticum medium (0.66 M sorbitol, 40 mM MES, pH 6.5). After a last centrifugation step, the thylakoid pellet was resuspended in resuspension medium. Chl concentration was measured as previously described and the thylakoid suspension was diluted to $[\text{Chl}]=2.5$ mg/ml. It was then used immediately for experiments or flash-frozen in liquid nitrogen.

2.2.4 Zeaxanthin enrichment of leaf and thylakoid material

Some variations of the thylakoid isolation protocol were applied to induce the activity of the xanthophyll cycle and the accumulation of Zea. *Arabidopsis* plants were simply illuminated for 2.5 hours with high light ($550 \mu\text{mol m}^{-2} \text{s}^{-1}$). Leaves were sprayed periodically with cold water to dampen the heat originating from the light bulbs. Before measurements, the treated leaves were dark adapted for 5 minutes to relax fast non-photochemical quenching processes and fully re-oxidise the components of the electron transport chain. In experiments involving spinach, detached leaves were placed on a grid with their petiole submerged into cold water, which was fluxed with nitrogen. The oxygen-depleted environment favoured the activity of the violaxanthin de-epoxidase enzyme and minimised that of the zeaxanthin epoxidase. Leaves were then irradiated with high light for 1 hour ($900 \mu\text{mol m}^{-2} \text{s}^{-1}$). For thylakoid extraction, 3 mM D-isoascorbate, a cofactor of the de-epoxidase, was added to the grinding medium prior to leaf homogenisation. An additional step was tailored to the procedure: isolated thylakoids were diluted (final $[\text{chl}]\approx 100 \mu\text{g/ml}$) in resuspension medium also containing 40 mM D-isoascorbate and left at room temperature without stirring for 1 hour. After centrifugation (6 min at 4000 rcf), the thylakoid pellet was resuspended in resuspension medium and used for experiments.

2.3 Pigment analysis

2.3.1 Chlorophyll quantification

Chl quantification was performed spectroscopically, based on the molar extinction coefficients of Chl *a* and *b* provided by Porra *et al.* (1989). For sub-leaf biochemical preparations, a small aliquot of the sample was resuspended in 80% acetone, mixed by inversion and centrifuged at 14000 rpm on a bench-top centrifuge for 2 minutes. The supernatant was collected and its absorption measured at wavelengths 663.6, 646.6 and 750 nm. For measurements of leaves, a circular section with an area of $\sim 3.15 \text{ cm}^2$ was freshly cut from each leaf. This was then frozen with liquid nitrogen and ground with a pestle to a fine powder without allowing it to thaw. It was then resuspended in 1 ml of acetone 80%, mixed vigorously, centrifuged, and its absorption measured. The amount of total chlorophyll ($\mu\text{g/ml}$) was ultimately quantified as the sum of chlorophyll *a* and *b* amounts:

$$\text{Chl } a = 12.25 A^{663.6 \text{ nm}} - 2.55 A^{646.6 \text{ nm}}$$

$$\text{Chl } b = 20.31 A^{646.6 \text{ nm}} - 4.91 A^{663.6 \text{ nm}}$$

where $A^{663.6 \text{ nm}}$ and $A^{646.6 \text{ nm}}$ are the absorption values measured at the corresponding wavelengths.

2.3.2 Carotenoid quantification

The Car mixture was extracted with acetone from leaf or thylakoid samples as described in the previous section. An additional passage of filtration through $0.22 \mu\text{m}$ filters was added after centrifugation, to ensure the complete removal of membrane residues. Separation of the carotenoid molecules was performed via reverse-phase high pressure liquid chromatography (HPLC), using a LiChrospher 100 RP-18 column and Dionex Summit chromatography system, as described before (Farber *et al.*, 1997). The separation was thus achieved by the differences in polarity and interactions with hydrophobic solvents. The solvents used were: 87% acetonitrile, 10% methanol, 3% Tris, pH 8.0 (A) and 80% methanol, 20% hexane (B). The run profile was: 0-9 min A, 9-12.5 A/B gradient, 12.5-18 min B, under a constant 1 ml/min

flow. ~ 50 μ l of sample were injected with a needle in every run. The needle was washed with ethanol between each run and 80% acetone blanks were measured at fixed intervals. Each peak in the resulting chromatogram was analysed with the Chromelion software, by integrating the area below the curve. Pigment concentration was estimated using standards of known concentration.

2.4 Protein purification and analysis

The largest fraction of Chls in the thylakoid membranes is bound to the major LHCII trimers (Peter and Thornber, 1991; Bassi and Dainese, 1992). Among the most used preparative methods to isolate LHCII are gel filtration (separation by size) (Van Roon *et al.*, 2000), sucrose density gradients (separation by density) (Caffarri *et al.*, 2009) and iso-electric focussing (separation by iso-electric point) (Dainese *et al.*, 1990). The last two techniques were used in our studies, in virtue of the low cost of equipment and material needed in relation to the yield and purity of the recovered antennae.

Membrane-bound complexes require a careful solubilisation using detergent before the separation using one of the described methods. This is generally achieved by incubating the thylakoid-enriched suspensions in a buffered solution containing a detergent or a mixture of detergents. The first studies that isolated thylakoid membrane proteins involved solubilisation with harsh ionic surfactants, such as sodium dodecyl sulphate (SDS) (Peter and Thornber, 1991). However, it was later shown that to preserve protein stability and avoid losses of the pigments bound, as well as preserving functionally important inter-complexes interactions, it was necessary to use mild solubilisation steps with gentle non-ionic detergents (Ruban *et al.*, 1999; Boekema *et al.*, 1999b). Among the most used detergents for this purpose is n-dodecyl β -D-maltoside (β -DDM) (Pagliano *et al.*, 2012).

2.4.1 Sucrose density gradient ultracentrifugation

Several methods exist to prepare highly reproducible sucrose density gradients: “freeze-thaw” method, involving the freezing of a buffer containing intermediate concentrations of sucrose (~ 0.5 M) and its slow thawing in the fridge (Caffarri

et al., 2009), a diffusion-based approach involving 2 solutions with different sucrose concentrations laid one on top of the other (Dall'Osto *et al.*, 2006), and a “step gradient” involving the manual creation of layers with different sucrose concentrations (Ruban *et al.*, 1999). In virtue of its rapidity and reproducibility, the latter was chosen in our experiments.

For the experiments described in Chapter 3, two sucrose solutions were prepared, containing 20 mM HEPES, pH 7.8, 0.06% (w/v) β -DDM (Sigma-Aldrich) and either 0.1 M or 1.87 M sucrose. The amount of detergent chosen was well above the critical micellar concentration, to ensure the complete solubilisation of every thylakoid membrane complex (Crepin *et al.*, 2016). Gradients were prepared by the successive addition of fixed volume of solution (1.5 ml) at the bottom of the Ultraclear centrifuge tubes (Beckman Coulter), with increasing concentrations of sucrose, obtained by the gradual addition of a small volume (3 ml) of the more concentrated solution into the less concentrated one. A glass Pasteur pipette was used in the procedure, to which a small piece of cotton was applied to slower the flux of the solution and avoid bubble formation. Ultimately, the gradients formed (7-step, from 0.1 M to 1 M sucrose) were balanced and equal volumes of the solubilised samples were applied on top. The separation was carried out overnight (17 h) by centrifugation at 270000 rcf, at 4°C. Collection of the fractions was performed from the top of each gradient with a 1 ml syringe, carefully washed after every passage.

For the experiments described in Chapter 4, the procedure used was the same, but the buffer used for the sucrose solutions differed, containing 25 mM HEPES, pH 7.8 and 0.01% β -DDM. The concentration of sucrose used remained unaltered. The amount of detergent chosen was just above the critical micellar concentration, meaning that it was high enough to keep the complexes detached from each other and low enough to avoid stripping off pigments and destabilisation of the apoproteins. The LHCII complexes so obtained did not undergo additional purification/wash steps and were used immediately for the measurements or flash-frozen in liquid nitrogen and sent to collaborators.

The same procedure was used for the sucrose gradients described in Chapter 5.

2.4.2 Iso-electric focussing

Flat-bed iso-electric focussing (IEF) is a preparative electrophoretic technique that represents a convenient platform to isolate quickly large amounts of photosynthetic antenna complexes (Dainese *et al.*, 1990; Ruban *et al.*, 1994b). The method exploits the mobility of proteins in an electric field due to their net surface charges and the variability of the latter at different pH values (Scopes, 1987). A mixture of small zwitterionic compounds, called ampholines, are dissolved in the bulk gel buffer and migrate to form a linear pH gradient when an electric field is applied. Therefore, when the sample is applied and a voltage is set, the protein mixture will separate based on the iso-electric point, where the net charge is 0 and the mobility is also null. A gel slurry of volume 100 ml was prepared containing 4.6% Sephadex G-75 Ultrafine (GE Healthcare), 2.5% ampholines (pH 2.5-5; Pharmalyte, GE Healthcare), 1% Glycine and 0.06% β -DDM. The solution was poured into a 25 x 11 cm tray and 37 grams of water were left to evaporate. The tray was then loaded in a pre-cooled (4°C) Pharmacia LKB MultiDrive XL electrophoresis system, carefully putting at the extremes of the gel the electrophoresis strips soaked in either anode (0.5 M H_3PO_4) or cathode (1 M NaOH) solutions. The gel was prefocussed for 1 hour at 8 W, in order for the ampholines to distribute along the block and form a pH gradient. In the meanwhile, unstacked thylakoid membranes (~ 1.7 mg/ml) were solubilised in 1.6% β -DDM for 1 hour on ice. The solubilised sample was then loaded 2 cm from the cathode with a sample applicator (10 x 2 cm). A constant power was applied (8 W) and the focussing was carried on overnight for 17 hours. Separated major LHCII complexes were collected and ampholines were removed using PD-10 desalting column (GE Healthcare). Eventually, these were resuspended a buffer containing 25 mM HEPES and 0.01% β -DDM for all experiments. When needed, LHCII were concentrated in Amicon Ultra-4 centrifugal filter tubes (Sigma-Aldrich), with 30 kDa cut-off for trimers and 3 kDa cut-off for monomers. The Chl content was then quantified and the LHCII were resuspended at the desired concentration (0.5-1 mg/ml of total Chl).

To obtain monomers of major LHCII complexes, a previously described method involving an incubation step with phospholipase A2 (PLA2) was employed (Ruban *et al.*, 1998b; Wentworth *et al.*, 2004). A central phosphatidylglycerol molecule

in LHCII is necessary for trimerisation of the complexes. Its degradation with PLA2, which hydrolyses the bonds forming between glycerol and the fatty acid tails, results in the monomerisation of LHCII. LHCII complexes obtained from IEF were resuspended in a buffer containing 25 mM HEPES, 0.01% β -DDM and 20 mM CaCl_2 (pH 7.6) at a final $[\text{Chl}] = 500 \mu\text{g/ml}$. PLA2 from bee venom (Sigma-Aldrich) was added to the suspension ($10 \mu\text{g/ml}$) and the LHCII were incubated in the dark for 21 hours. Eventually, separation of the obtained monomers from the residual trimers was achieved via sucrose density gradient ultracentrifugation ($[\text{Chl}] = 500 \mu\text{g/ml}$).

2.4.3 Immobilisation of LHCII in polyacrylamide gels

To ensure a homogeneous distribution of LHCII and avoid particle clustering, isolated LHCII were embedded in 1 mm thick poly-acrylamide gels, following a protocol described before, with some modifications (Iliaia *et al.*, 2008). LHCII (final $[\text{Chl}] = 100 \mu\text{g/ml}$) were diluted in a buffer containing 25 mM HEPES, 0.01% β -DDM and mixed with 6% acrylamide/bis-acrylamide mixture (37.5:1). Fresh APS (0.05%) and TEMED (0.03%) were added to the solution. This was then well mixed and rapidly poured between glass plates and left to polymerise at room temperature. The induction of the quenched conformation of LHCII was achieved by removal of detergent bound to LHCII immobilised in gels. To this aim, gels were incubated for 17 hours at room temperature in detergent-free buffer (25 mM HEPES, pH 7.6) under constant slow stirring, allowing the gradual equilibration of the β -DDM bound to LHCII with the bulk solution. To monitor the quenching of Chl *a* fluorescence, the gels were gently pressed between the emitter and detector Perspex rods in a Dual-PAM setup and fluorescence was induced by a weak measuring blue light ($< 12 \mu\text{mol photons m}^{-2} \text{s}^{-1}$).

2.4.4 SDS-polyacrylamide gel electrophoresis

Analytical protein separation was performed through denaturing SDS-polyacrylamide gel electrophoresis (SDS-PAGE). Pre-cast 12% acrylamide/bis-acrylamide linear gels were employed (Mini-PROTEAN TGX Stain-Free Precast Gels, Bio-Rad). Laemmli buffer (Sigma-Aldrich) was mixed with β -mercaptoethanol (9:1).

Isolated protein complexes from sucrose gradients were added to the mixture in a 3:1 ratio. They were then heated in the thermoblock at 37°C for 15 minutes, the optimal conditions to denature membrane proteins (Schaller *et al.*, 2011). After denaturation, equal sample volumes (20 μ L) were loaded onto each gel lane. Weight markers (11-245 kDa) were loaded into the first and last lanes. The gels were inserted into the tank which was then entirely filled with a glycine buffer (25 mM 2-amino-2-(hydroxymethyl)propane-1,3-diol (TRIS), 192 mM glycine, 0.1% SDS, pH \approx 8.3). A constant voltage was then applied (100 V for the first 10 minutes, to allow an even entrance of the samples in the gels, and 180 V thereafter). The total time of the runs, carried out at 4°C was \sim 1.5 hours. Gels were stained using InstantBlue protein stain (Expedeon) and scanned using a ChemiDoc Touch Imaging System (BioRad).

2.5 Fluorescence spectroscopy

2.5.1 Principles of chlorophyll fluorescence spectroscopy and pulse-amplitude modulated (PAM) fluorimetry

Chl *a* fluorescence is a valuable tool to study photosynthetic performance in algae and plants exposed to different stimuli and stresses (Baker, 2008). The principle of fluorescence measurements is summarised in Figure 2.1a. When a Chl molecule is excited (either directly, by a photon of light, or receiving excitation energy by other pigments), it can take different routes to relax to its ground state: in an intact system excitation can result in charge separation and be used in photochemical processes; alternatively, the molecule can relax non-radiatively to the ground state and release energy as heat, or it can be released radiatively, with lower energy, in a process called fluorescence emission. These pathways are in competition with each other. Therefore, knowing the fraction of energy released through fluorescence, one can determine the amount of excitation used in photochemical and non-photochemical processes.

The PAM technique (Figure 2.1b,c) exploits a pulsed weak measuring beam that stimulates chlorophyll fluorescence emission without the closure of reaction centres (Fo). Its detection occurs at the same frequency of the pulses, cutting off

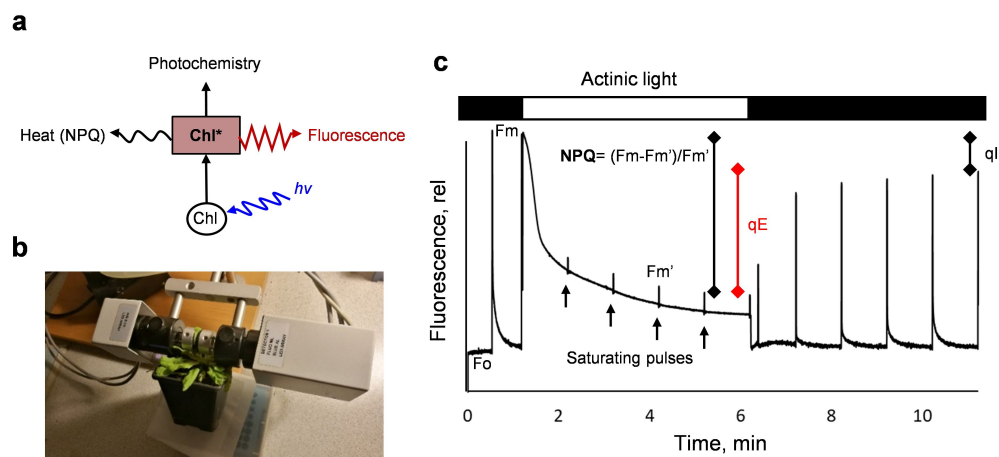


Figure 2.1: Principles of chlorophyll fluorescence spectroscopy and pulse amplitude modulated (PAM) measurements. **a** The fate of excitation energy in a chlorophyll molecule. A blue (or red) photon excites the molecule to an excited state (Chl^*). Depending on its environment, this could lead to energy transfer to another pigment or to one of the 3 following fates: charge separation in the core (photochemistry) release of energy through heat (non-photochemical quenching) or re-emission of a photon (fluorescence). **b** Photograph of a standard PAM setup (Walz) to measure intact leaves. **c** Representative PAM fluorescence trace of a dark-adapted leaf. F_0 is the minimal fluorescence with open reaction centres; F_m is the maximal fluorescence value when all reaction centres are closed, after a saturating pulse. Non-photochemical quenching processes (NPQ) are measured from the difference between F_m and the maximal fluorescence induced during illumination (F_m'). qE is the reversible fraction of NPQ, in contrast to qI which comprises irreversible or slowly reversible processes.

the contribution from ambient light (Schreiber *et al.*, 1986; Murchie and Lawson, 2013). Saturating pulses and external actinic light (AL) sources can thus be applied without interfering with the output fluorescence signal. PAM fluorimetry uses these pulses to close temporarily all reaction centres and gain precise information about their activity (F_m and F_m' , see figure 2.1c for details). In this way, the fraction of excitation dissipated in non-photochemical quenching processes (NPQ) is precisely determined ($\text{NPQ} = (F_m - F_m') / F_m'$). A comparison between alternating periods of illumination and darkness can also yield information about the fraction of NPQ that is quickly reversible (qE) and separate it from photoinhibitory/sustained quenching (qI). qE is measured as $(F_{m_{\text{relaxed}}} - F_m') / F_{m_{\text{relaxed}}}$, where $F_{m_{\text{relaxed}}}$ is the chlorophyll maximal fluorescence values calculated after 5 minutes of relaxation in the dark, following application of AL. In our chlorophyll fluorescence assays, the measuring

heads DUAL-E and DUAL-DB were used (Walz). The latter was used to provide a source of weak blue light (460 nm) for excitation of chlorophyll fluorescence and contains a photodiode detector protected by a long-pass filter (RG9), for the detection of photons emitted at wavelengths >700 nm. Both heads are provided with a chip-on-board LED array coupled to 1 cm x 1 cm. Perspex rods to deliver red AL and saturating pulses (635 nm). Measurements of protoplasts and chloroplasts suspensions, as well as solubilised LHCII, were performed at constant temperature (20 °C).

2.5.2 Imaging PAM

Whole-plant F_o values PSII quantum yield (F_v/F_m) were visualised using a variable chlorophyll fluorescence Imaging-PAM system (Walz). A CCD camera (IMAG-K6) was used to record the images and was coupled to a long-pass filter (RG665) to protect the CCD chip from blue excitation light, while allowing the red fluorescence through. A short-pass filter ($\lambda < 790$ nm) was used to protect the CCD detector against excess near-infrared radiation. Pulse-modulated blue excitation as well as blue saturating pulses were provided by 44 LED lamps. Plants were positioned on a mounting stand, ~ 20 cm below the camera, and enclosed by a red Perspex hood. A controlling unit was connected to a PC running a dedicated software (Imaging Win 2.3).

2.5.3 Electron transport rates

The electron transport rate (ETR) is a simple measurement reflecting the rate of charge separation in PSII reaction centres and is measured as:

$$ETR = Y(II) * PAR * 0.84 * 0.5$$

where $Y(II)$ is the PSII operating efficiency (Baker, 2008), PAR is the photosynthetically active radiation (AL expressed as $\mu\text{mol photons m}^{-2} \text{ s}^{-1}$), 0.84 is a constant value for the fraction of light absorbed by the leaf and 0.5 is an estimate of the fraction of PSII to PSI reaction centres. A preset trigger run for the acquisition of light curves was used to retrieve values of the ETR in intact leaves, with the application

of 11 steps of increasing red light intensities of 1 min duration.

2.5.4 Fast fluorescence induction

OJIP curves

The PSII fluorescence rise kinetics from Fo to Fm display characteristic phases that reflect the accumulation of reduced quinone equivalents (Strasser and Govindjee, 1991; Strasser and Srivastava, 1995; Stirbet and Govindjee, 2011). Fm is reached in about 100 ms from the application of a saturating pulse, coinciding with the accumulation of PQH₂ (fully reduced PQ, called plastoquinol). The logarithmic analysis of this Fo-Fm rise evidences the presence of 2 intermediates (called J and I) between the initial Fo value (O phase) and the PQH₂ product (P phase). The J phase (2 ms) reflect the reduction of both Q_A and Q_B molecules. Previous steps (Pheo and single Q_A reductions) occur in ps and hundreds of ps, respectively, and are out of the limits of instrumental resolution. The I phase (20 ms) reflects the accumulation of double-reduced Q_B (Q_B²⁻).

The OJIP fast fluorescence rise was measured on intact leaves. Prior to measurement, plants were dark adapted for 40 min. Fluorescence was induced using a 1 s saturating pulse of red light (4000 $\mu\text{mol photons m}^{-2} \text{ s}^{-1}$). The fluorescence level (μs acquisition rate) at Fo and Fm were taken as origin (O) and peak (P) phases of the OJIP fluorescence induction transient, respectively. The x-axis is expressed in log₁₀ scale for the correct assignment of the phases.

Fast kinetics with DCMU

DCMU is an herbicide that blocks the electron transfer from Q_A to Q_B. When leaves or chloroplasts are treated with DCMU and illuminated, the fluorescence rises quickly from the O phase to the J phase, where it reaches a plateau (Strasser and Srivastava, 1995). Under low light intensity, this rise can be used to estimate the functional cross-section of PSII, *i.e.* the number of pigment-binding complexes serving the core (Malkin *et al.*, 1981; Belgio *et al.*, 2014).

The fast fluorescence induction kinetics were measured on leaf disks pre-infiltrated with 50 μM DCMU, 150 mM sorbitol and 10 mM Hepes (pH 7.5). Traces

were recorded with a Dual-PAM 100 using a custom-made trigger run providing a 12 mol photons m⁻² s⁻¹ flash. The DCMU was carefully titrated to select the minimum concentration necessary to reach a steady Fm value within 400 μs. To measure the cross-section after NPQ induction, leaf disks were exposed to 5 seconds of low FR light after high light illumination and were then infiltrated with DCMU, the whole process taking roughly 30 s. Estimation of the cross-sections was done integrating the area above the induction curves, after setting the variable fluorescence (Fm-Fo) to 1.

2.5.5 Measurements of ΔpH across the thylakoids and its modulation using chemicals

Among the methods used to measure ΔpH across the thylakoids, the selective pH-dependent uptake of fluorescent amines in the lumen has often offered reproducible results, in good agreement with the thermodynamics of electron transfer (Schuldiner *et al.*, 1972; Kramer *et al.*, 1999). Another common approach has been the measurement of the electrochromic shift of chlorophylls and carotenoids, visible as a red shift of their Soret absorption transitions when exposed to an electric field (Finazzi *et al.*, 2006; Bailleul *et al.*, 2010). In plants, however, this method is spoiled by absorption/scattering changes occurring between 500 nm and 550 nm and due to Zea synthesis and qE formation (Johnson and Ruban, 2014). In our experiments, we thus measured ΔpH monitoring the fluorescence quenching of 9-aminoacridine (9-aa) upon uptake in the lumen (Johnson and Ruban, 2011). The localisation of 9-aa is directly proportional to the proton concentration, as given by the following formula (Schuldiner *et al.*, 1972):

$$\frac{[A]_{in}}{[A]_{out}} = \frac{[H^+]_{in}}{[H^+]_{out}}$$

where $[A]_{in}$ and $[A]_{out}$ are the total amine concentrations inside and outside the lumen, respectively, and $[H^+]_{in}$ and $[H^+]_{out}$ are the total H⁺ concentrations inside and outside the lumen, respectively. To estimate the value of ΔpH, however, one would need to measure accurately the lumen volume, which is still a controversial issue (Kramer *et al.*, 1999) and it is unknown in lincomycin-treated plants where the

chloroplasts ultrastructure is dramatically altered (Belgio *et al.*, 2015). Therefore, in our experiments ΔpH was expressed simply as 9-aa fluorescence quenching relative to the initial value.

5 μM 9-aa was added to the chloroplasts suspensions before each measurement. 9-aa fluorescence quenching was recorded using the Dual-E(mitter)NADPH and Dual-D(etector)NADPH modules for the Dual-PAM 100 fluorimeter, simultaneously to chlorophyll fluorescence. Excitation of 9-aa was provided by 365 nm LEDs in the ENADPH and fluorescence emission was detected between 420 and 580 nm by a photomultiplier built in the DNADPH module. The DNADPH head is highly sensitive to ambient light and therefore was covered with a black cloth during the measurements.

The dependence of qE upon ΔpH was fitted to the Hill equation:

$$qE = \frac{qE_{max} * Q^n}{k_{0.5}^n + Q^n} \quad (2.1)$$

where qE_{max} is the maximum theoretical value of qE , Q is the amplitude of 9-aa quenching, $k_{0.5}$ is the half-maximal concentration constant of 9-aa quenching and n is the Hill parameter.

2,3,5,6-tetramethyl-p-phenylenediamine (diaminodurene, DAD), which stimulates the cyclic electron flow around PSI, was used to enhance ΔpH above the physiological threshold. DAD was added simultaneously to the application of AL. A range of concentrations (20-600 μM) was used to modulate the amplitudes of ΔpH obtained. To block the formation of ΔpH during illumination of isolated protoplasts, nigericin, a H^+ and K^+ ionophore, was added before the measurements. Titrations of nigericin were again performed to determine the minimum concentration needed for the complete dissipation of ΔpH , which was then used in our experiments (50 nM).

2.5.6 Low temperature steady-state fluorescence

Chl fluorescence emission spectra were recorded at 77 K using a Jobin Yvon FluoroMax-3 spectrophotometer equipped with a cryostat filled with liquid nitrogen. A fraction of chloroplasts or LHCII suspensions was injected between two glasses

placed at the end of a metal rod and immediately inserted into the cryostat chamber. In experiments with leaves, a leaf disk ($d=3.15\text{ cm}^2$) was cut from intact leaves and placed between the glasses and used directly for 77 K fluorescence measurements or first subject to illumination under a Dual-PAM fluorimeter. The orientation of the sample was set 45° and scattered light was carefully redirected away from the detector window. Excitation was set at 435 nm (hitting the Soret band of Chl *a*) with a 5 nm spectral bandwidth. The fluorescence emission spectral resolution was instead set at 1 nm. Re-absorption of emitted photons can occur when the chlorophyll concentration of the sample is high and it affects mainly shorter emission wavelengths (Weis, 1984). To avoid the associated spectral distortions, when working with isolated chloroplasts or LHCII the total [Chl] was kept low (10 $\mu\text{g/ml}$ and 3 $\mu\text{g/ml}$, respectively). Spectra were smoothed with a Savitzky-Golay convolution filter and baseline-corrected using the GRAMS/AI software (Thermo-Fisher). Second derivatives were calculated on the smoothed traces to determine accurately the inflection points of the spectra.

2.5.7 Time-resolved fluorescence

Steady-state fluorescence integrates the intensity of all photons emitted in a wide time window at a particular wavelength or set of wavelengths. However, it lacks information concerning the dynamics of the excited states of the chromophores. Time-resolved fluorescence techniques bridge this gap and allow the study of excited-state decay kinetics by taking into account the time gap between excitation of the molecule and detection of the emitted light.

Time-correlated single photon counting (TCSPC)

The term TCSPC refers to the count of every single photon reaching the detector a certain time after excitation (Holzwarth, 1995). In this technique, a weak, pulsed light source excites the sample at high repetition rate (megahertz, MHz). A single-photon resolution photomultiplier detects an emitted photon and simultaneously this signal is digitalised by a time-to-digital converter. This essentially works as a stopwatch, counting the time difference between the excitation pulse photons and the fluorescence emitted photons. These data are then used to create an histogram

that gives information of the average excited state lifetime of the pigment. The time resolution of the technique is then determined by the so-called Instrument Response Function (IRF), which depends on the temporal uncertainties of all the components involved (temporal width of the excitation pulse, photomultiplier response, etc.). In the TCSPC setup used in our experiments (FluoTime 200, PicoQuant), the full-width half-maximum value of the IRF is ~ 30 ps, bringing down the resolution of the system to a few ps. Excitation at 20 MHz repetition rate was provided by a 468 nm laser diode. The power had been previously calibrated to be low enough (~ 30 pJ/pulse) to avoid singlet-singlet annihilation artefacts (Illoaia *et al.*, 2008). Fluorescence was detected at 680 nm with a 2 nm slit width. The IRF was detected at 468 nm after each set of experiments with a Ludox suspension of colloidal silica (Sigma-Aldrich). Experiments on leaves were performed after infiltration of each leaf with a solution containing 150 mM sorbitol, 10 mM HEPES and 50 μ M DCMU (pH 7.5). Measurements of isolated LHCII were performed by resuspending a small aliquot of samples (final [Chl]=3 μ g/ml) in 2 ml of a buffer containing 10 mM HEPES and 0.01% β -DDM. Analysis of fluorescence lifetime histograms was performed with the FluoFit software (PicoQuant). A multi-exponential model was employed with iterative re-convolution of the IRF. The χ^2 parameter and autocorrelation function were used to judge the quality of the fit. Average lifetimes were calculated as:

$$\langle \tau \rangle = \frac{\sum_{i=1}^n A_i \tau_i^2}{\sum_{i=1}^n A_i \tau_i} \quad (2.2)$$

where A_i is the amplitude of i -th lifetime component and τ_i is the respective fluorescence lifetime value, whereas n is the total number of lifetime components. In leaves fixed in the Fm state, τ_i is linked to the quantum efficiency of PSII (Φ_{PSII}) by the equations

$$\Phi_{PSII} = \frac{k_P}{(\tau_i^{-1} + k_P)} \quad (2.3)$$

and

$$\tau_i \approx \frac{1}{(k_F + k_P)} \quad (2.4)$$

where k_F and k_P are the rate constants for fluorescence and photochemistry

of PSII, respectively. For the estimation of Φ_{PSII} , k_P was assumed to be the same in leaves enriched in either Vio or Zea.

Streak camera

Contrarily to TCSPC, streak camera measurements offer simultaneous information about spectral and temporal distribution of the emitted photons. Time-resolved fluorescence spectra at a high temporal resolution can be therefore drawn. After excitation of the sample and fluorescence emission, the emitted photons are dispersed into different colours by a grating system and sent to a photocathode that converts them into electrons in a number directly proportional to the incident intensity (exploiting the photoelectric effect). From here, electrons travel through a chamber where a ramping voltage is applied by a sweep generator, synchronised with the excitation pulse. The electrons are therefore deflected at different times, and at slightly different angles. They are then conducted to a micro-channel plate that multiplies them several thousands of times and are eventually bombarded against a phosphorscreen. An image is produced in which x and y axis are the spectral and dynamical distribution of the fluorescence and the z axis shows the intensity of the signal. In our experiments, a Hamamatsu C5680 streak camera system was used. A femtosecond Yb:KGW oscillator (Pharos, Light Conversion Ltd) with a frequency doubler (HIRO, Light Conversion Ltd) producing 515 nm sub-100 fs pulses at a 76 MHz repetition rate was employed. For ns time scales, the repetition rate was lowered to 20 kHz. The beam intensity was attenuated down to ~ 1 pJ for pulses at the frequency of 76 MHz and to ~ 100 pJ for pulses at the frequency of 20 kHz and was focused on about 80 μm -wide spot on the sample. The temporal resolution was around 10 ps and 100 ps for the 76 MHz and 20 kHz modes, respectively. A liquid helium cold finger cryostat (Janis CCS-100/204) was used for the low temperature measurements.

The measured time-resolved fluorescence spectra $F(\lambda, t)$ of LHCII aggregates and chloroplasts under various temperatures were described in terms of multivariate curve resolution (Chmeliov *et al.*, 2016). This allowed us to describe the data in terms of a minimum number of components with a clear physical meaning, originating from different conformational states of the LHCII trimers. For each dataset,

the factorisation was carried out with the following formula:

$$F(\lambda, t) = \sum_{i=1}^n W_i(t) S_i(\lambda)$$

where W and S are the time dependent weight and spectral shape of the i -th component, respectively. The optimisation procedure resulted into a minimum number of 2 components, sufficient to describe our data, the 680-nm and the red- and FR-emitting forms:

$$F(\lambda, t) = W_{680nm}(t) S_{680nm}(\lambda) + W_{red}(t) S_{red}(\lambda). \quad (2.5)$$

All experimental data were perfectly reproduced by the described model at the initial time delays, but some discrepancies appeared at longer time delays, probably due to population of some additional conformational states of the LHCII or the heterogeneity of the thylakoid membranes. Indeed, beside major LHCII trimers, minor antenna complexes are also present, and possibly some LHCI complexes.

2.5.8 Single molecule fluorescence microscopy

To study the fluorescence dynamics of single LHCII complexes by means of single molecule (SM) fluorescence microscopy. The strategy adopted harbours analogies with a conventional single molecule FRET experiment (Roy *et al.*, 2008). In detail, the molecules under investigation are immobilised to a glass surface and total internal reflection fluorescence (TIRF) is used to selectively excite them (Figure 2.2). TIRF is a technique that was initially designed to study the protein dynamics at the cell boundaries, where conventional fluorescence microscopies inevitably struggle to reduce background noise (Ambrose, 1956). It exploits the evanescent electromagnetic field (E_e) that is generated when a light source reaches a boundary between two media with different refraction indexes at an angle greater than the critical angle, where all light is not transmitted and is instead totally internally reflected. Such generated evanescent field decays exponentially in intensity, which allows for its diffusion up to a hundred nm from the incident spot and thus for a selective excitation of surface-bound chromophores (Axelrod, 2003; Martin-Fernandez *et al.*,

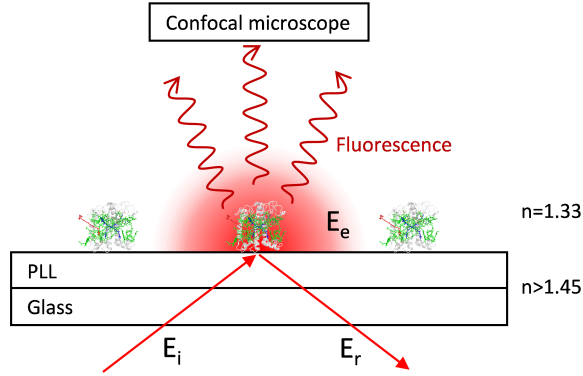


Figure 2.2: **Principles of TIRF exploited in single molecule (SM) fluorescence microscopy.** In the TIRF setup used, protein complexes are linked covalently to poly L-lysine (PLL) layered on top of a glass coverslip. Light from a laser source is directed to the sample compartment with a tilted angle. The difference between the refraction indices determines the existence of an incidence angle at which the beam is totally internally reflected and doesn't penetrate the interface. Under this conditions, only a small portion of the radiation is generated at the boundary where the sample is attached, called evanescent field (E_e). Since its intensity decreases exponentially over tens of nm, single complexes can be selectively excited. The fluorescence from the complexes is then collected through a standard confocal microscope setup. E_i , E_r , E_e = incident, reflected, evanescent electromagnetic radiation, respectively.

2013).

The buffer solutions used in the SM experiments were: buffer 1, containing 10 mM HEPES, 1 mM MgCl_2 , 0.03% β -DDM (pH 7.8); buffer 2 containing 10 mM HEPES, 1 mM MgCl_2 , 0.001% β -DDM (pH 7.8); buffer 3: 10mM HEPES, 1 mM MgCl_2 , 0.001% β -DDM (pH 5). To immobilise LHCII samples, glass coverslips (Menzel-glaser $n^\circ 1.5$) were rinsed 3 times with ultrapure water, once with 1% Alconox detergent solution, sonicated for 10 minutes and finally rinsed again 4 times with ultrapure water. After a final cleaning with isopropanol, coverslips were vacuumed in the plasma machined (PDC-002, Harric plasma) for 20 minutes. One surface of the coverslips was modified by incubating in 0.01% poly L-lysine (PLL) for 10 minutes and then washing with ultrapure water. Coverslips were assembled into the flow cell (sticky-slide VI 0.4, 80608, Ibidi), tubing were inserted in the inlet and outlet port of the cell and the channel was filled with buffer 1. LHCII were diluted in the buffer 10^6 times and injected into the flow cell. After equilibration for 3 minutes, the chamber was flushed with 300 μl of buffer to wash the excess of unbound complexes. When switching between the buffers with different detergent

concentration and/or pH value, 300 μl of the new buffer was flushed in the chamber to exchange with the previous solution. In all conditions of the experiment, a 100 μl volume of buffer containing 10 units/ml of pyranose oxidase (P4234, Sigma-Aldrich), 300 units/ml catalase (C9322, Sigma-Aldrich) and 1% glucose (β -D-glucose, G0047, TCI) was given to deplete the cell of molecular oxygen and prevent the damage from the hydrogen peroxide. O_2 can indeed react easily with the Chl triplets forming in the sample, leading quickly to photobleaching. The setup used for the fluorescence detection relies on a biological inverted Nikon Eclipse Ti-U microscope. The 635 nm laser beam is focused onto the back focal plane of the objective and to achieve TIRF at the glass/water interface, the beam is translated to its periphery by a mirror preceding the objective. The excitation spot is then 80 μm in diameter and the power of the light that excites LHCII is less than 1 W/cm^2 . This is lower than the intensities usually exploited in confocal microscopy and far from the onset of non-linear processes of singlet-singlet and singlet-triplet annihilation (Tutkus *et al.*, 2017). Images were recorded with a 50 ms integration time by a EM-CCD camera. The TIRF setup used is such that a 15 nm distance from the glass surface is excited, yielding a negligible background signal.

2.6 Absorption measurements

The principle of optical absorption spectroscopy is the Lambert-Beer law. The absorption (A) of a sample is the \log_{10} of the ratio between the incident light intensity (I_0) and the one transmitted (I) and is linked to the concentration of the absorbing molecule by the formula:

$$A = \log_{10}\left(\frac{I_0}{I}\right) = \epsilon C d$$

where ϵ is the molar extinction coefficient ($\text{M}^{-1} \text{cm}^{-1}$).

Chls and Cars have usually very high molar extinction coefficients and well defined absorption bands, whose energies correspond to the dipole transitions moments of the pigments. Changes in the surrounding of a pigment (*e.g.* conformational motions of protein clefts) (Illoaia *et al.*, 2008), bending/twisting motions (Llansola-Portoles *et al.*, 2017), dimerisation (Billsten *et al.*, 2005) or cis/trans isomerisations (Schoenlein *et al.*, 1991) can be detectable monitoring perturbations

of its absorption properties, making absorption spectroscopy an invaluable tool in photosynthesis research.

2.6.1 Steady-state absorption

Steady-state absorption spectra were recorded with an Aminco DW-2000 UV/Vis spectrophotometer (Olis Inc.) in dual-beam mode (reference + sample). Slits width was 0.5 mm and the spectral bandwidth 2 nm. The samples were measured within the linear range of absorption ($A=0.2-1$): $[\text{Chl}]_{\text{tot}}=10\text{ }\mu\text{g/ml}$ for LHCII enriched in xanthophyll-cycle carotenoids (Chapter 4), $[\text{Chl}]_{\text{tot}}=100\text{ }\mu\text{g/ml}$ for LHCII in gels (Chapter 5). Sucrose gradient fractions (Chapter 3) were diluted when necessary in buffer containing 25 mM HEPES, 0.01% β -DDM, pH 7.8.

2.6.2 Absorption changes related to NPQ

Kinetics of zeaxanthin formation: 505 nm

The conversion of Vio ($N=9$) to Zea ($N=11$) during the xanthophyll cycle operation is accompanied by characteristic changes in the absorption spectrum, since the carotenoids have different absorption maxima. Following absorption changes at 505 nm, a wavelength falling close to the Zea 0-0 transition maximum, one can monitor the rates of its synthesis *in vivo* (Bilger *et al.*, 1989; Bilger and Björkman, 1990, 1991; Pfundel and Dilley, 1993; Ruban *et al.*, 1993b).

An Aminco DW-2000 UV/Vis spectrophotometer (Olis Inc.) was used to measure the kinetics of Zea accumulation during AL illumination from the initial dark-adapted state. A dual mode setup was used, monitoring simultaneously the changes at the dual-wavelength pair 505 nm and 565 nm. The latter is a wavelength that is close to the isosbestic point of the cytochrome *f* absorption changes. 505 nm-minus-565 nm represents thus an accurate measure of almost exclusively Zea absorption. A fixed-lambda assay collection mode was used, to monitor the kinetics of absorption change over time. Leaf discs were inserted in a custom-made leaf holder with a $\sim 0.8\text{ cm}^2$ round window and placed into a 1 cm^2 cuvette holder positioned at 45° to the incident light beam. The photomultiplier was protected by a Corning 4-96 filter and an OCL1 Cyan T400570 mirror. The red AL from a 250 W tungsten halogen lamp

(1000 $\mu\text{mol photons m}^{-2} \text{ s}^{-1}$) was defined by a Corning 5-58 red filter. Traces are shown after the first 30 s of illumination to avoid the initial contribution of the electrochromic shift, which peaks at around 515 nm and is inevitably partially detected in these experiments. Percentages of initial de-epoxidation rate were calculated from the slopes (m values) of the tangents between 0 and 30 s.

Kinetics of qE: 535 nm

Illumination of thylakoid membranes and creation of a proton gradient are accompanied by scattering changes occurring at ~ 535 nm (Heber, 1969). These changes were shown to correlate well with the amplitudes of NPQ (specifically of its major reversible component qE) (Bilger and Björkman, 1994), reflecting a conformational change occurring in the thylakoid membranes. The true origin of this band is still under debate and one current hypothesis is that it arises from the absorption of zeaxanthin dimers, transiently formed during aggregation under NPQ conditions (Ruban *et al.*, 1993a; Duffy *et al.*, 2010; Iliaia *et al.*, 2011a). The kinetics of the qE-associated conformational changes were monitored on intact leaves using the same setup described in the previous paragraph for 505 nm kinetics. The dual wavelength pair chosen was 540-570 nm, optimised to retrieve the pure dynamics of qE and avoid contributions from electrochromic shift and zeaxanthin absorption. The 535 nm changes are indeed more than 1 order of magnitude smaller than these signals, requiring a careful optimisation of the recording conditions. The temperature of the holder chamber was set to 20 °C throughout the measurements.

2.6.3 Transient absorption spectroscopy

In a pigment-binding photosynthetic complex, the rates of Forster resonance energy transfer can be very high, in the order of femtoseconds (fs, 10^{-12}) or picoseconds (ps, 10^{-9}) (Connelly *et al.*, 1997; Forster, 2012). In order to investigate these events in detail, ultrafast techniques down to a sub-100 fs resolution must be used. The advent of lasers opened scenarios for the application of sub-ps laser pulses for the study of chemical reaction out of equilibrium or, more recently, even sub-fs pulses, which are valuable to study chemical bond formation (Zewail, 2000; Gaumnitz *et al.*, 2017). A useful technique used in the study of photosynthetic complexes exploits

the generation of ultrafast laser pulses to monitor the changes in absorption spectra and kinetics after the initial excitation and is called transient absorption (TA) spectroscopy (van Amerongen and van Grondelle, 1995; Berera *et al.*, 2009). The

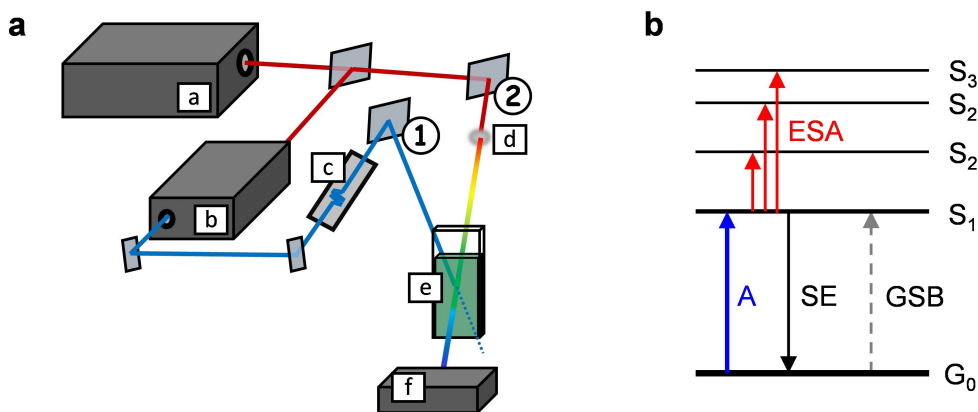


Figure 2.3: **Principles of transient absorption (TA) spectroscopy.** **a** Schematic view of the TA setup used. An amplifier is used to generate primary femtosecond laser pulses (a). A mirror splits each pulse into two different pathways (*pump* ① and *probe* ②). The first path leads to an optical parametric amplifier (b) which is used to generate pulses of different colours, depending on the requirements of the experiment. The beam is then sent to a delay line that sets a time gap between the pump and the probe pulses (c). The second path leads to a sapphire plate, which is used to generate a broad white light continuum (d). Both beams then hit the same spot on the sample (e). The transmitted probe light is collected by a diode array detector (f). **b** Simplified representation of the energy levels of a chromophore and the transitions induced and detected in a pump-probe experiment. The pump beam excites a chromophore to a defined excited state (absorption, A, blue arrow). Stimulated emission (SE, black solid arrow) and ground state bleach (GSB, grey dashed arrow) are detected by the probe beam as negative signals. Excited-state absorption (ESA, red arrows) is detected as a positive signal.

principle of TA is explained briefly in Figure 2.3a. First, a *pump*, monochromatic laser pulse excites a subset of chromophores to their electronically excited states. After a certain amount of time (in the fs-ns range), set mechanically with a delay line, a weak, white *probe* pulse is sent to hit the same spot in the sample. A difference absorption (ΔA) spectrum is then constructed by subtracting spectrum of the probe before and after the pump. ΔA contains information regarding energy migration between pigments, electron and proton transfers as well as intersystem crossing and internal conversion. Each of these processes contribute with distinct signatures to the ΔA spectral evolution (Figure 2.3b):

- *Ground state bleach* (GSB) reflects the depopulation of the ground state of the chromophores, caused by the pump pulse that pushes electron to their excited states. Since it corresponds to the loss of absorption, it appears like a negative peak in the ΔA spectrum. The position of the ground state bleaches mirrors the steady state absorption bands of the chromophores.
- *Stimulated emission* (SE) occurs when the probe stimulates the emission of a photon from a chromophore in its excited state. This emission is usually red-shifted as fluorescence with respect to the GSB. Since SE corresponds to an increase in the light reaching the detector, it is visualised as a negative signal in the ΔA spectrum.
- *Excited-state absorption* (ESA) takes place when a pigment in an excited state is pumped to a higher excited state (usually S_n). Since a fraction of the probe is absorbed and doesn't reach the detector, ESA appears as a positive signal in the ΔA spectrum. Chls have a broad, weak and featureless S_1 ESA signal, while carotenoids S_1 state has a well defined structure and display intense excited state absorption.

In our experiments (described in Chapter 5), transient absorption spectra were measured at room temperature using a femtosecond spectrometer employing Ti:Sapphire amplifier (Spitfire Ace, Spectra-Physics) as the primary source of femtosecond pulses. Excitation pulses (~ 120 fs) were generated at the desired wavelengths (490 nm, 645 nm and 679 nm) in an optical parametric amplifier (Topas-Prime, Light Conversion), while a white-light continuum, generated in a 2 mm sapphire plate, was used as a probe. To avoid unwanted polarisation effects and detect the pure excited-state dynamics, the excitation and probe beams were linearly polarised and set to the magic angle (54.7°). The LHCII gel sample was placed between two quartz glasses separated with a 1 mm Teflon spacer in a round cuvette (1 cm). The cuvette was placed into a holder attached to a Lissajous 2D scanner that moved the sample during the measurement to prevent sample damage. Time-resolved absorption changes were measured from 470 to 720 nm by detecting the dispersed white light of the probe with a CCD detection system (Pascher Instruments). Using neutral-density filters, the excitation intensity in all experiments was kept at about 4×10^{13} photons pulse $^{-1}$ cm $^{-2}$. TA data collected were fitted globally

using CarpetView package (Light Conversion). The software fits the data to a sum of exponentials, and a polynomial to correct chirp artefacts. The latter reflect the wavelength-dependent shifts of time zero (t_0) that arise because of different refraction indices in quartz. To visualise the excited-state dynamics, we assumed that the excited LHCII evolves according to a sequential, irreversible scheme, in which the increasingly slower mono-exponential processes correspond to lifetimes of the individual excited-state species in the sequential scheme. The spectral profile of each species is called evolution-associated difference spectrum (EADS). Although EADSs obtained from the sequential model do not correspond to individual excited states in a complex system such as the LHCII studied here, they help to visualise excited-state processes and carry important information about excited-state dynamics.

Chapter 3

Identification of the qE site

The observations that minor antenna complexes bind large amounts of Vio (the precursor of Zea synthesised during the photoprotective xanthophyll-cycle reactions) and that recombinant complexes reconstituted with Zea exhibit some degree of Chl fluorescence quenching prompted the suggestion that the major site of qE is in the minor antennae (Bassi *et al.*, 1993; Crimi *et al.*, 1998; Bassi and Caffarri, 2000). The creation of antisense or knock-out mutants for specific minor antennae polypeptides challenged this view, since they produced contrasting results on the qE amplitudes and induction kinetics and the fluorescence quenching was never completely abolished (Andersson *et al.*, 2001, 2003; Ruban *et al.*, 2003; Kovács *et al.*, 2006; de Bianchi *et al.*, 2008; van Oort *et al.*, 2010; de Bianchi *et al.*, 2011). Recently, Dall'Osto *et al.* (2014a) reported the creation of a mutant unable to accumulate any minor antenna complexes (No Minor antennae, *NoM*). The mutant has disrupted PSII supercomplexes organisation, is affected in electron transport rates and is prone to photooxidative damage (Dall'Osto *et al.*, 2014a, 2019). It has been reported that the NPQ induction of dark adapted leaves exposed to high actinic light (AL) is impaired, displaying a marked delay in the kinetics of NPQ formation (Dall'Osto *et al.*, 2017). Therefore, it was suggested that two mechanisms take place during fast photoprotection in plants, where major LHCII contribute only to the slowest component of this process and minor antennae are crucial in the first minutes of high light exposure.

In the first part of this chapter, I present a detailed analysis of the fluorescence

quenching induction in *NoM* mutants showing that the impairments originate from disrupted kinetics of pH and zeaxanthin formation, which delay the qE formation, and not from the absence of exclusive quenching sites. In the second part, I present an investigation of qE amplitudes, kinetics and ΔpH dependency in *NoM* mutant treated with lincomycin, to strongly reduce the accumulation of photosystems reaction centres (RCs) in the thylakoid membranes. The results obtained demonstrate that only major LHCII antenna complexes and ΔpH are strict requirements for qE.

3.1 The origin of altered NPQ induction in the *NoM* mutant

3.1.1 Minor antennae mediate the functional connectivity of LHCs in PSII

Figure 3.1a shows the defects of the growth of *NoM* plants exposed to moderate light ($190 \mu\text{mol photons m}^{-2} \text{ s}^{-1}$) under a constant photoperiod in the growth chambers. The tardiness of the growth of these mutants, as attested before, isn't caused by developmental anomalies since the rates of leaf formation are similar to WT plants (Dall'Osto *et al.*, 2017). The lower F_v/F_m values (Figure 3.1c), estimate of the quantum efficiency of PSII, and impairments in electron transport rates (ETR) point towards defects in photosynthetic processes in the absence of minor antenna complexes (Figure 3.2). The reported unusually high level of basal fluorescence (F_o , Figure 3.1b) indicates possible impairments at the level of the PSII organisation, in line with previous results (Dall'Osto *et al.*, 2014a, 2017). The occurrence of a high value of F_o and a concomitant reduction of the F_v/F_m parameter suggest that there are changes in the antennae connectivity in the PSII system, with the possibility that a fraction of the LHCII is functionally disconnected to the RCs and contribute substantially to the F_o level.

To verify this hypothesis, we performed an analysis of the functional antennae cross section of PSII in *NoM* and WT plants (Figure 3.3). The method applied (Malkin *et al.*, 1981; Belgio *et al.*, 2014) provides an estimation of the cross-section of PSII based on the rise kinetics from F_o to F_m in the presence of the herbicide DCMU.

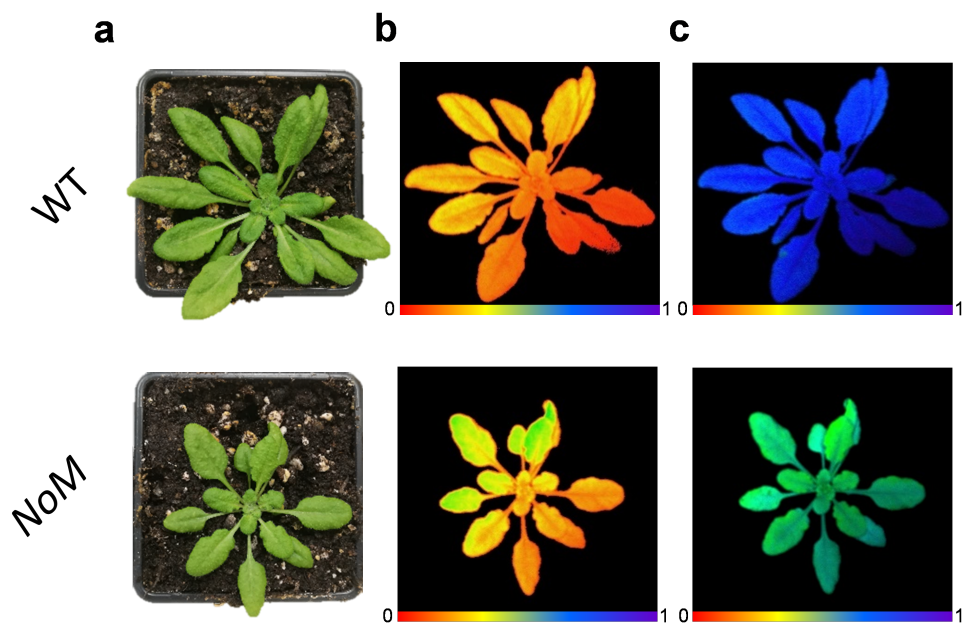


Figure 3.1: ***NoM* plants exhibit disrupted growth rates.** Column **a** shows a comparison of WT and *NoM* plants 5 weeks after sowing. **b**, **c** show a false-colour Chl fluorescence imaging analysis for the two genotypes of Fo and Fv/Fm, respectively. The colour scheme used is displayed at the bottom of each image.

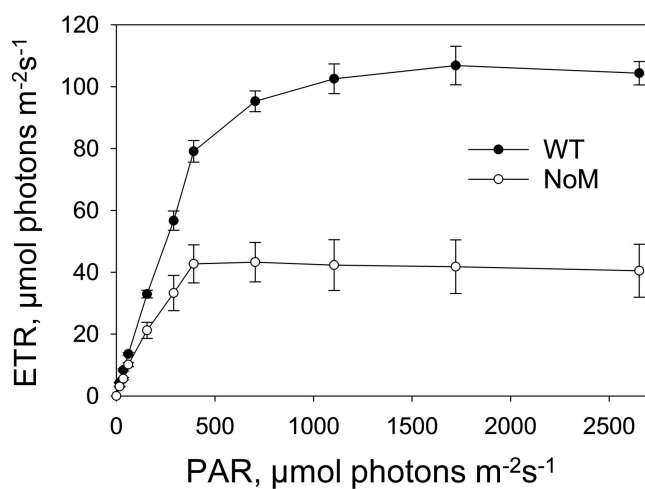


Figure 3.2: **Electron transport rates (ETR) are affected in *NoM* mutants.** Titrations of ETR in function of increasing intensity of photosynthetically active radiation (PAR) for WT and *NoM* plants.

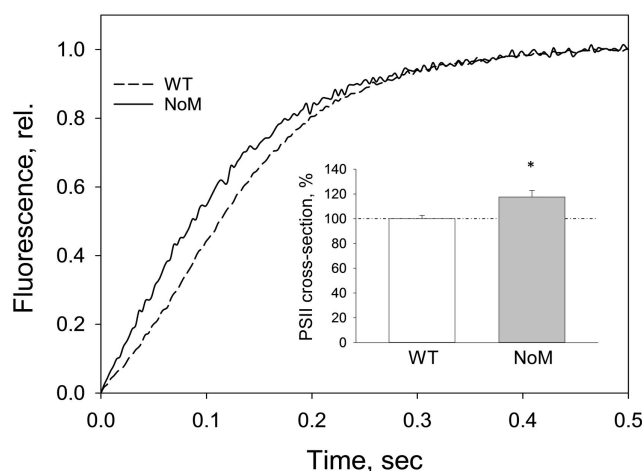


Figure 3.3: **The functional antenna size in mutants lacking minor antennae is increased.** Fast Chl fluorescence kinetics in WT and *NoM* leaves after infiltration with 50 μmol DCMU. The kinetics are normalised at the maximum fluorescence value and offset to 0 at F_0 . The inset shows the calculated PSII-cross section (relative to WT, 100%).

The antenna size is thus estimated calculating the reciprocal value of the area above the induction curve (see “Chapter 2: Methodologies and approaches” for details). The calculated cross-section is increased in *NoM* by a 17% with respect to the WT control (Figure 3.3, inset). This result is apparently contradicting the hypothesis that defects in the functional antennae connectivity are occurring in the absence of minor antennae. However, Dall’Osto *et al.* (2017) reported a protein quantification analysis showing an increase of LHCII in the thylakoids of 60% compared to the control. Our measurements provide an evidence that there is a pool of LHCII ($\sim 43\%$ of the excess accumulated LHCII) that is loosely docked and thus functionally detached from the PSII supercomplexes. These unconnected LHCII complexes could therefore provide additional highly fluorescent sites, contributing to the F_0 increase.

An independent verification of this observation comes from the low temperature fluorescence Chl emission spectra of isolated chloroplasts (Figure 3.4). These steady-state measurements can give informative insights about the presence and organisation of pigment-binding proteins. Performing the measurements at low temperature, pigments site energies are more localised and line narrowing of the

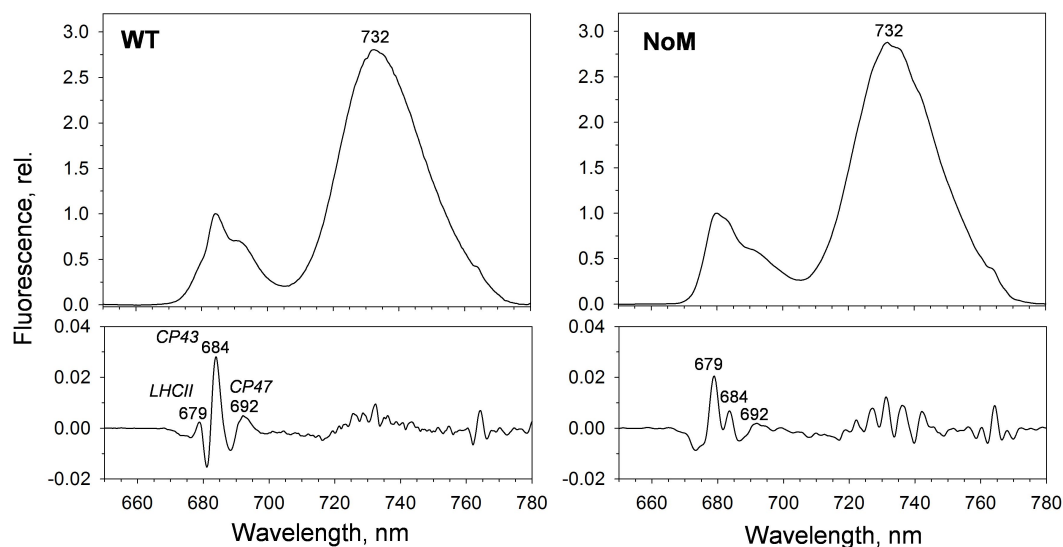


Figure 3.4: **A large pool of weakly coupled LHCII is present in *NoM* thylakoid membranes.** Low temperature (77 K) Chl fluorescence emission of WT and *NoM* chloroplast suspensions. Chloroplasts were diluted to 10 μg total Chl, to avoid reabsorption artefacts. Spectra are averages of at least 3 repeats and are normalised to the maximum fluorescence value below 700 nm. Below each spectrum, the relative second derivatives are displayed.

fluorescence features occurs, bringing about a higher spectral resolution. Moreover, PSI typical far red (FR) emission becomes observable only at low temperature, together with Chl charge transfer states that harbour structural and functional information of the pigment-binding complexes (Krause, 1991). The 670-710 nm region of the spectrum is dominated by the contribution of PSII-related complexes (Figure 3.4). Emission at ~ 679 nm is assigned to peripheral antenna complexes and it is easily distinguishable from the contributions of the core antennae CP43 (~ 684 nm) and CP47 (~ 692 nm) (Krause, 1991; Ruban and Horton, 1992). As revealed in detail with second derivative analysis, the spectrum of *NoM* chloroplasts displays a prominent contribution at 679 nm, while it is present only as an inflection in the WT spectrum. Altogether these findings underline the anomalies in the organisation of the light harvesting structures in *NoM* thylakoid membranes. Nevertheless, they are not sufficient to explain the impairments in growth and electron transport since the calculated functional cross-section of PSII is higher than the WT. A hint towards an explanation of this phenotype comes from fluorescence lifetime measurements

performed with open RCs, that reported a disturbed excitation energy transfer in the absence of minor antennae (Dall'Osto *et al.*, 2014a). The exciton migration time was found to be significantly slower in *NoM*, due to the presence of disconnected or poorly connected antennae in the PSII system. Therefore, although the apparent

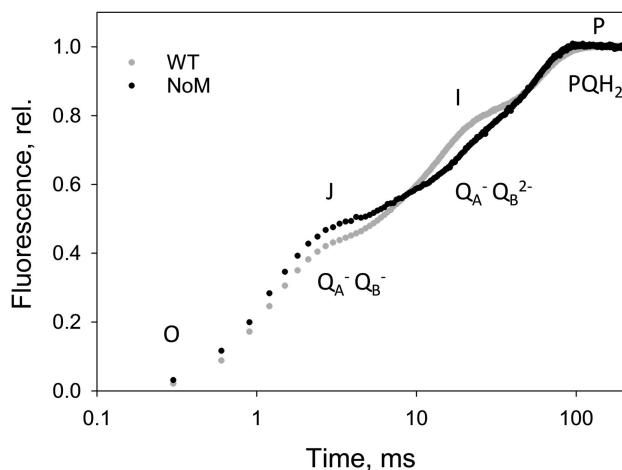


Figure 3.5: **Minor antennae control the dynamics of quinone reduction at the PSII acceptor side.** Millisecond (ms) kinetics of Chl fluorescence rise from F_o to F_m during a saturating light pulse. Traces, averages of 3 independent measurements, were normalised at the F_m plateau, 400 ms after beginning of the pulse, and offset to 0 at the initial F_o level. The x-axis is displayed in logarithmic scale for clarity. OJIP phases are marked (see “Chapter 2: Methodologies and approaches” for details).

increase in PSII cross-section, the presence of minor antennae seems to be crucial for an efficient connectivity of the proteins within PSII, which could alone explain the defects in electron transport in *NoM* (van Oort *et al.*, 2010; Dall'Osto *et al.*, 2014a). It was attested that the extensively affected macroorganisation of PSII in the absence of CP24 could be the reason of limited diffusion of plastoquinone (PQ) to the Q_B site (de Bianchi *et al.*, 2008).

To check whether this occurs in the absence of all minor antenna complexes, we analysed on leaves the kinetics of the rise of the variable fluorescence of PSII triggered by a saturating pulse of light, without the addition of electron transport inhibitors (Figure 3.5). The so-called OJIP curves are kinetics in the $\mu s/ms$ range that reflect the first transfer processes of electrons from Q_A to the PQ pool. The I

phase, occurring between 10 and 80 ms from the beginning of the pulse, is notably lacking in *NoM*, compared to WT plants (Figure 3.5). The finding is similar to previous results where DCCD-incubated thylakoids were shown to be affected in the proton translocation pattern of PSII (Jahns *et al.*, 1988; Jahns and Junge, 1989, 1990). In these experiments, a proton short-circuit was proposed to occur, which impairs the proton gradient generation via the uptake of the H^+ released in the lumen and their unusual release on the stromal side. The main substrates for DCCD binding were afterwards identified as CP26 and CP29 (Walters *et al.*, 1994, 1996). Thus, it is possible that minor antennae mediate a pathway for the correct proton translocation after water oxidation. Their absence results in a proton short-circuit that in turn could limit the photosynthetic ΔpH gradient.

To verify this possibility, ΔpH amplitudes and kinetics were measured through the quenching of 9-aminoacridine (9-aa, Figure 3.6) (Schuldiner *et al.*, 1972). The

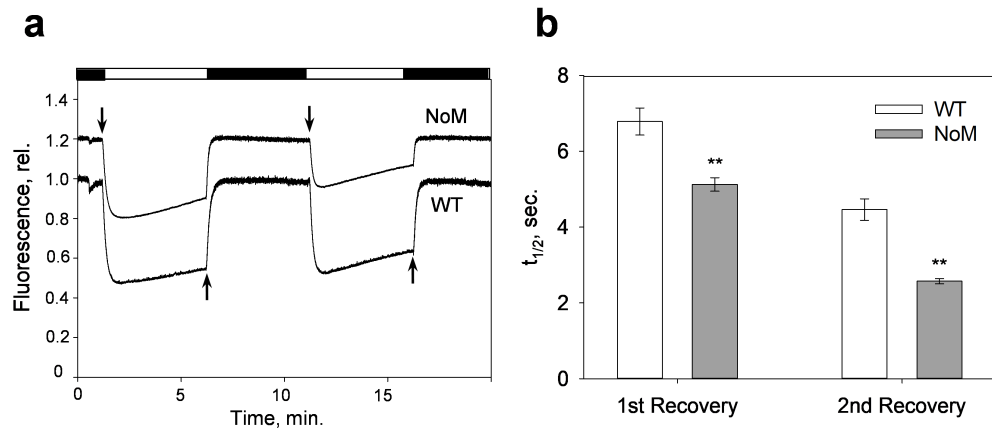


Figure 3.6: **ΔpH generation and maintenance are compromised in the *NoM* mutant.** **a** Fluorescence quenching of 9-aminoacridine (9-aa) measured in isolated WT and *NoM* chloroplasts during 2 cycles of illumination ($1382 \mu\text{mol photons m}^{-2} \text{s}^{-1}$) + darkness, marked with white and black bars on top of the graph (5 minutes each). **b** Half-times ($t_{1/2}$) of the recovery rates of 9-aa fluorescence during the light-to-dark switch. Data presented are mean \pm SE of 5 repeats. Asterisks represent $P \leq 0.01$ (Student's t-test).

lower amplitude of ΔpH in *NoM* (38% of 9-aa quenching compared to 44% in WT) is consistent with the findings of altered proton translocation to the lumen and with previously reported data for single deletion mutants of Lhcb5 (CP26) and Lhcb6 (CP24) (de Bianchi *et al.*, 2008). It is also noticeable a more pronounced recov-

ery rate of the 9-aa fluorescence quenching during illumination (linear regression fit $m=0.030 \pm 0.001$) relative to WT chloroplasts ($m=0.013 \pm 0.001$; $P \leq 0.01$). Additionally, the kinetics of recovery in the light-to-dark transition are significantly different (Figure 3.6b), being faster in *NoM* ($t_{1/2}=5.1$ compared $t_{1/2}=6.8$ in WT during the first transition; t-test, $**P \leq 0.01$). This indicates a marked proton leakage of *NoM* chloroplasts, which struggle to maintain a stable pH gradient across the thylakoid membranes. Altogether, these results unravel the pivotal role of monomeric LHCs to assure an efficient photon energy utilisation in the PSII system. Their absence causes impairments both in exciton migration in the supercomplex and correct proton release in the lumen with formation of ΔpH .

3.1.2 The fast NPQ development in *NoM* is independent of the presence of reaction centres and zeaxanthin

The knock-out mutant of all minor antennae offers unprecedented possibilities to unveil the role of these complexes in photoprotection, particularly their role in fast dissipative processes that plants exploit to adapt to high light intensities (NPQ). The kinetics of the dark-to-light transition in *NoM* plants display an atypical delay in the Chl fluorescence quenching (Figure 3.7a,b,c). In particular, it is possible to distinguish 3 phases in the fluorescence kinetics during the first illumination cycle (Figure 3.7): a fast quenching component, at the onset of AL that reaches its maximal value in ~ 30 s (II); a transient recovery of fluorescence (III); a second, slower, quenching component (IV). This is in agreement with the previous report from Dall'Osto *et al.* (2017), although the transient fluorescence relaxation component is more pronounced in our study, likely due to difference in the AL intensities used. The Chl fluorescence quenching induction are reflected in the kinetics of NPQ induction, which display the same “wavy” pattern upon the dark-to-light transition (Figure 3.7d,e,f). The NPQ amplitude during the fast quenching induction (phase I in Figure 3.7b) is significantly larger in *NoM* (Figure 3.8; 1.07 ± 0.07 compared to 0.83 ± 0.06 in WT, t-test, $*P \leq 0.05$). This phase was suggested to originate from a very fast fluorescence quenching mediated by closed RCs of PSII (Finazzi *et al.*, 2004; Dall'Osto *et al.*, 2017). This hypothesis is weakened by the observation that plants treated with the antibiotic lincomycin exhibit virtually unaltered NPQ

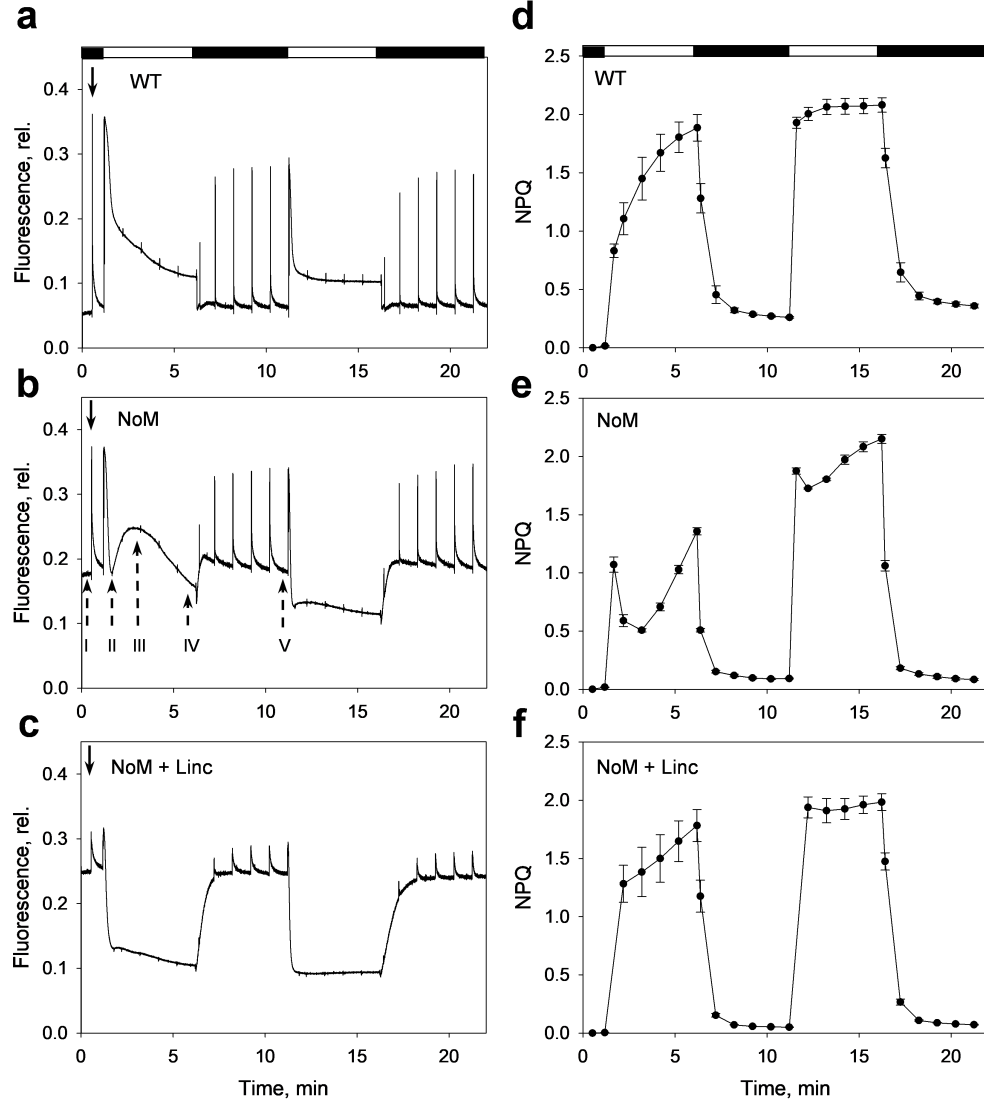


Figure 3.7: **The altered Chl fluorescence quenching induction in the *NoM* mutant.** **a, b, c** Chl fluorescence induction during 2 cycles of 5 minutes light ($1382 \mu\text{mol photons m}^{-2} \text{s}^{-1}$) + 5 minutes dark, marked with white and black bars on top of the first graph. **d, e, f** NPQ values calculated from fluorescence traces during saturating pulses. *NoM* + Linc, *NoM* mutants treated with lincomycin.

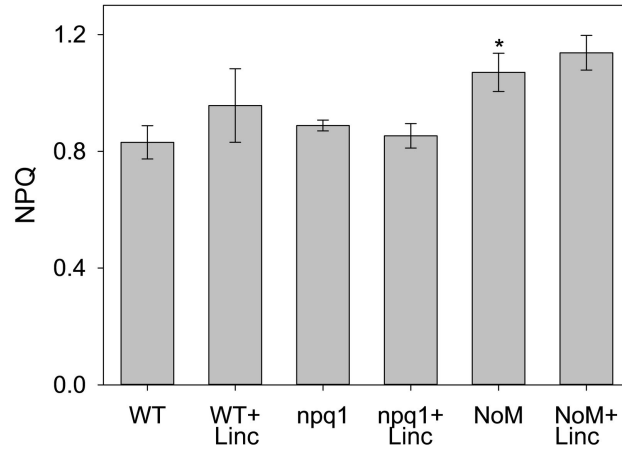


Figure 3.8: **The fast quenching phase is independent of RCs, minor antennae and Zea.** NPQ values calculated from fluorescence induction of WT, *npq1* and *NoM* leaves, 30 seconds after the beginning of the illumination period. +Linc, plants treated with lincomycin. Data presented are mean \pm SD of at least 3 repeats. Asterisk represents $P \leq 0.05$ (Student's t-test).

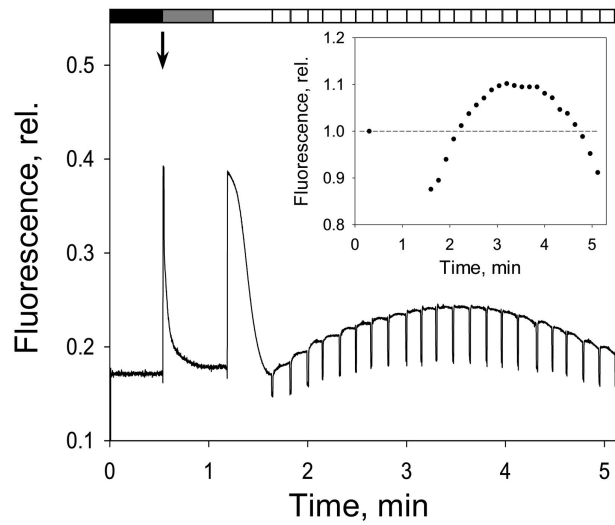


Figure 3.9: **Fo fluorescence dynamics indicate antenna rearrangements during quenching induction.** Fo determination during light induction of *NoM* leaves. Fo values were recorded every 10 s by transiently switching off AL ($1382 \mu\text{mol photons m}^{-2} \text{s}^{-1}$) and quickly providing far red (FR) light. The inset shows the evolution of the Fo values over time upon illumination, normalised to the initial Fo value. Black, grey and white bars represent periods of darkness, FR and AL, respectively.

amplitude 30 seconds after AL illumination, or even slightly higher, with respect to the untreated controls (Figure 3.8). The treatment inhibits the synthesis of chloroplasts encoded proteins, causing a strong decrease (~ 5 -fold) in the amounts of RC proteins in the thylakoid membranes (Belgio *et al.*, 2012). The kinetics of NPQ induction in lincomycin-treated plants are different from the untreated (Figure 3.7c). It could be speculated that the altered thylakoid membrane architecture, in which LHCII is overexpressed and found in a pre-aggregated state (Belgio *et al.*, 2012), makes the NPQ state more accessible for these plants and easier to sustain. To understand if Zea plays any role in the fast quenching phase, we tested the ability of the mutant *npq1*, which lacks the Vio de-epoxidase and can't accumulate Zea during illumination, to form NPQ. The mutant displays NPQ values after 30 seconds that are similar to WT plants (0.89 ± 0.02), ruling out a role for Zea during this fast phase (Figure 3.8). Moreover, its treatment with lincomycin does not impair this rapid quenching induction, excluding once again the role of RCs in this phase. The *NoM npq4* mutant, knock-out of the PsbS protein, was reported by Dall'Osto *et al.* (2017) to be defective in this induction phase, pointing towards a role of PsbS in the rapid quenching formation even in the absence of minor antennae. Therefore, the fast quenching induction is not mediated by minor antennae, RCs and Zea. The data overall indicate that this quenching component is mediated by the joint activity of LHCII and PsbS.

The low level of Fo fluorescence, that occurs in the presence of open RCs, arises from the antenna component of PSII (Krause, 1991). Therefore, the kinetics of Fo during illumination are a distinct marker of antenna reorganisation/quenching. To independently verify whether RCs are involved in Chl fluorescence quenching, Fo values were determined during the induction of the first illumination cycle by transiently switching off the AL at constant intervals and applying 3 seconds of FR light (Figure 3.9). FR light is specifically absorbed by red-shifted Chl *a* molecules associated with PSI and drives a faster re-oxidation of the PSII quinone pool. Thus, its application causes a quick re-opening of the RCs while maintaining the structural rearrangements of the antenna proteins and the antenna-associated non-photochemical processes occurring. 30 seconds after the beginning of illumination, the quenching of the Fo value below its initial level in the dark is significant of a quenching component originating in LHCII within this time scale, providing again evidence against

a RC-mediated mechanism (inset in Figure 3.9).

3.1.3 The origin of the transient fluorescence recovery during illumination in *NoM*

The temporary relaxation of NPQ in *NoM* mutants has previously been attributed to the lack of specific quenching sites normally present in minor antenna complexes (Dall'Osto *et al.*, 2017). In detail, two mechanisms of energy dissipation were identified, one occurring between 1 and 4 minutes of illumination, residing in minor antennae and another one, with slower kinetics, activated later in the major LHCII. However, the observation that the NPQ relaxation in *NoM* occurs concomitantly to a transient increase of the F_o values (compare Figures 3.7e and 3.9), suggest that the lack of a quenching phase is due to changes occurring in the antenna complexes still present in the mutant, *i.e.* LHCII. Notably, during the second illumination cycle, when Zea has accumulated, the wave of Chl fluorescence recovery is strongly attenuated and NPQ amplitudes of WT and *NoM* are very similar (Figure 3.7a,b). The peculiar course of the F_o fluorescence during light suggests that a rearrangement occurs within the LHCII domain, bringing about a transient relaxation of the quenched conformation.

To investigate this hypothesis low temperature Chl fluorescence emission spectra were measured for WT and *NoM* leaves after 2 minutes of illumination (Figure 3.10). An enhanced emission shoulder at 679 nm was present in illuminated *NoM* compared to the dark-adapted control plants. (inset in Figure 3.10b). On the contrary, no appreciable changes occurred in WT samples (Figure 3.10a). As previously discussed (see Figure 3.4), this denotes the emission contribution of unquenched LHCII complexes and is possibly reflecting an uncoupling of LHCII trimers from the bulk PSII antenna (Ruban *et al.*, 1992, 1997a).

It is likely that minor LHCs are essential to warrant not only the correct PSII superstructure but also functional changes occurring during light exposure (Belgio *et al.*, 2014). To test this hypothesis, fluorescence induction of leaves infiltrated with DCMU was recorded during 2 and 5 minutes of illumination and compared to dark adapted leaves or 5 minutes after recovery from the illumination time (Figure 3.11). Up to 5 seconds of FR light were applied after AL to re-oxidise the quinone

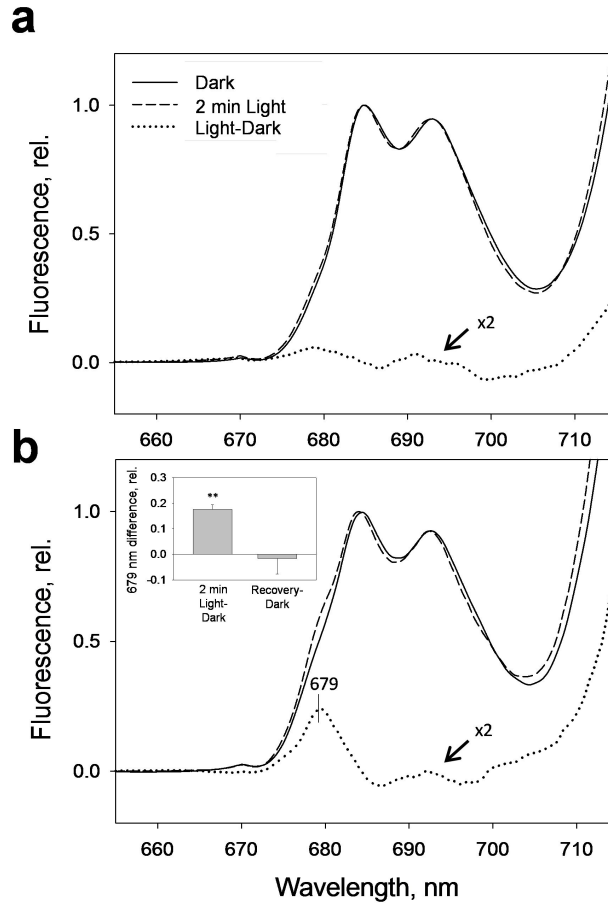


Figure 3.10: **Transient highly fluorescent state of LHCII during light induction in *NoM*.** 77K fluorescence emission spectra of **a** WT and **b** *NoM* leaves. All spectra were normalised at the ~685 nm emission maximum. Measurements were taken on dark-adapted leaves (solid line) or after 2 minutes of illumination ($1382 \mu\text{mol photons m}^{-2} \text{s}^{-1}$, dashed line). A dark minus light difference spectrum is shown (dotted line). Each spectrum is the average of at least 3 repeats. The inset shows the fluorescence difference at 679 nm between light and dark, and recovery and dark. Asterisks represent $P < 0.01$ (Student's t-test). Data presented are average of 3 repeats \pm SE.

pool. Note that this method doesn't assess the fraction of LHCII in the quenched state, because the qE process relaxes almost completely during the time of infiltration, but it is suitable to monitor the (relatively) slower relaxing features of antenna reorganisation. Remarkably, the induction kinetics didn't display any change, remaining essentially unaltered during all the physiological phases tested. Therefore, the fraction of LHCII functionally bound to PSII core does not vary upon light induction, contrarily to what was previously reported in WT (Belgio *et al.*, 2014).

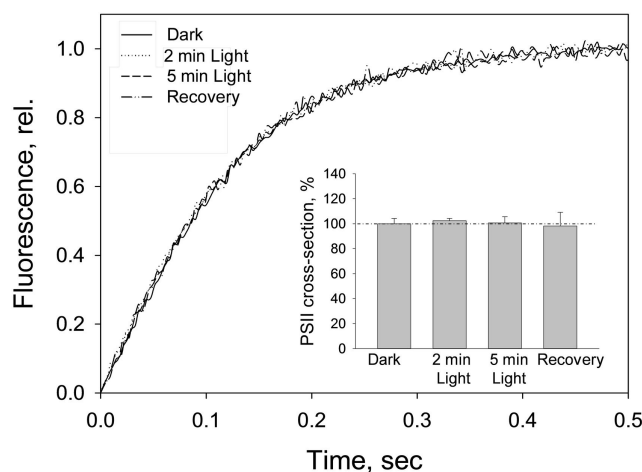


Figure 3.11: **No changes in functional antenna cross section occur during Chl fluorescence induction in *NoM*.** Normalised fast fluorescence induction kinetics in *NoM* leaves after infiltration with 50 μ M DCMU during the different phases of quenching induction: dark-adapted state, transient fluorescence recovery (2 min of illumination), maximum qE (5 min of illumination), and recovery (5 min of illumination followed by 5 min of darkness, see figure 3.7b as a reference). Leaves taken during illumination were briefly exposed to 3 seconds of FR light after switching off AL and before infiltration. The inset shows the calculated values of antenna cross-section as percentages relative to WT.

While on one side there is no increase in the cross-section during illumination, a trait indicating the economic nature of NPQ in WT plants (Belgio *et al.*, 2014), on the other side there isn't even a decrease, excluding the possibility of functional detachment of LHCII from the supercomplexes. Therefore, the observed increase in LHCII emission (Figure 3.10) should originate from a relaxation of quenching processes, not accompanied by functional changes in the organisation of LHCII. We speculate that the observed impairments in OJIP kinetics and Δ pH formation, considering especially the pronounced proton leakage across the thylakoid membranes, cause the anomalous recovery of fluorescence quenching, (phase III in the induction in Figure 3.7b). An initial burst of protons in the lumen, driven by PSII and cytochrome b_6f , could result in a dramatic activation of the quenching mechanism in LHCII (phase II in Figure 3.7b). Following the activation of ATPase, partial dissipation of the H^+ gradient, already reduced in amplitude compared to WT, would cause the observed phenotype of NPQ relaxation.

In plants, Zea plays a crucial role during NPQ (Demmig-Adams, 1990). Its

presence positively influences the kinetics and amplitude of NPQ formation (Ruban and Horton, 1999). However, Zea is normally not constitutively present in plants and needs to be synthesised during the so-called xanthophyll cycle, activated during illumination (Sapozhnikov *et al.*, 1957; Yamamoto, 1979). The activity of the Vio de-epoxidase enzyme, that converts Vio to Zea, exhibit a strong dependency to luminal pH (Pfundel and Dilley, 1993). Thus, the anomalous induction and maintenance of ΔpH in *NoM*, could determine a delayed induction of Zea synthesis, which in turn could contribute to the observed partial recovery of NPQ. To investigate this hypothesis, Zea synthesis was probed in *NoM* leaves. To this aim, the kinetics of Zea formation in the first minutes of illumination were probed spectroscopically, measuring the changes in absorption occurring at 505 nm, a wavelength lying on the shoulder of 0-0 absorption transition of the xanthophyll (Ruban *et al.*, 2001). Absorption changes can be very informative, since they correlate well with the amount of Zea formed and therefore mirror the kinetics of its accumulation in the thylakoid membranes (Pfundel and Dilley, 1993; Ruban *et al.*, 1993b). The results obtained are shown in Figure 3.12. During the initial seconds of the first illumination cy-

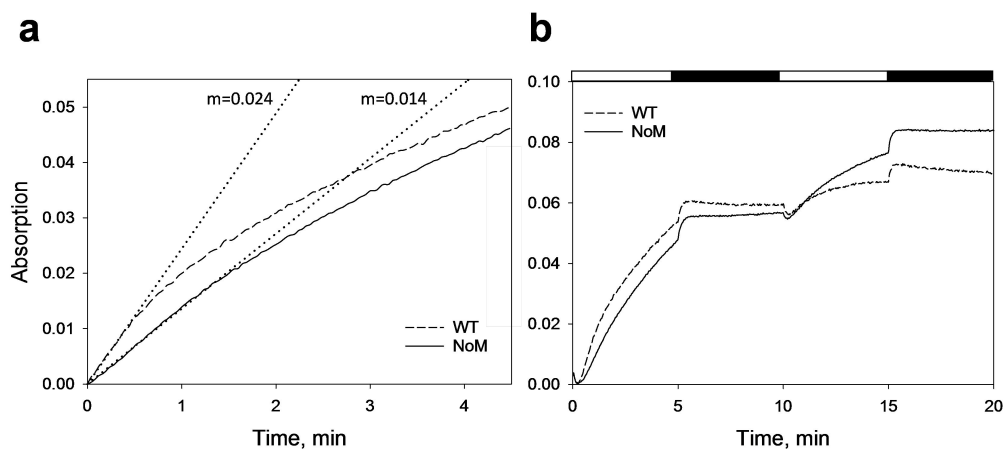


Figure 3.12: **Zea formation is delayed during *NoM* induction.** **a** Kinetics of 505 nm absorption changes during 5 min of illumination of WT and *NoM* leaves (AL=1000 $\mu\text{mol photons m}^{-2} \text{s}^{-1}$). Straight dotted lines represent the tangents of the kinetic curves between 0 and 30 s of illumination. m values represent the slopes of the tangents (OD/min). **b** Complete time courses of the absorption changes related to Zea formation, showing a two cycle induction of 5 min light + 5 min dark. All traces are the average of 5 repeats.

cle there is a 58% faster rate of Zea formation in WT compared to *NoM* (Figure

3.12a; $m=0.024$, WT; $m=0.014$, *NoM*; fitted with linear regression of the absorption values in the first 30 seconds of light). Therefore, even though the Vio pool available for de-epoxidation is higher (60% increase in the LHCII content in *NoM*, Dall'Osto *et al.* (2017)), the xanthophyll cycle activity is impaired, likely because of the documented defects in ΔpH formation. In the second illumination phase, Zea synthesis in WT becomes slower and soon reaches a plateau, while in *NoM* it continues to increase, an effect that could reflect the higher availability of Vio for the de-epoxidation (Figure 3.12b).

3.1.4 Discussion

In the present and in a previous study (Dall'Osto *et al.*, 2017), NPQ amplitudes and kinetics were measured of the triple knock-out mutant unable to accumulate all minor antennae of PSII. The kinetics of quenching induction were found to be altered compared to WT (Figure 3.7) (Dall'Osto *et al.*, 2017). However, the reported NPQ amplitude at the end of 5 minutes of illumination were 90% of the total NPQ seen in WT. The fluorescence quenching induction in *NoM* can be explained considering three characteristic phases: a fast quenching component, a transient fluorescence recovery and a second quenching component with slower kinetics (marked as phases II, III and IV in Figure 3.14, respectively). In the present study, we identified the origin of these physiological stages and propose a model for the quenching induction in the absence of minor antennae (Figure 3.14).

The fast quenching components (phase II) peaks 30 seconds after the beginning of illumination. Dall'Osto *et al.* (2017) assigned this component to a RC-mediated quenching, reported to take place quickly during the transition of leaves from dark to light (Finazzi *et al.*, 2004). In this work, lincomycin-treated *NoM* plants, exhibiting largely decreased amounts of photosystem RCs, were probed for their capacity to form NPQ. They were shown to possess amplitudes of NPQ in the first 30 seconds of light that are comparable to those in the untreated counterparts, and even slightly higher, disproving the hypothesis of a RC-mediated quenching component. The quenching of Fo during illumination below its initial level in the dark suggest that the fast quenching resides in the LHCII present in *NoM* thylakoids. The analysis of this NPQ induction phase in the mutants *npq1* and *npq4* suggests that this is

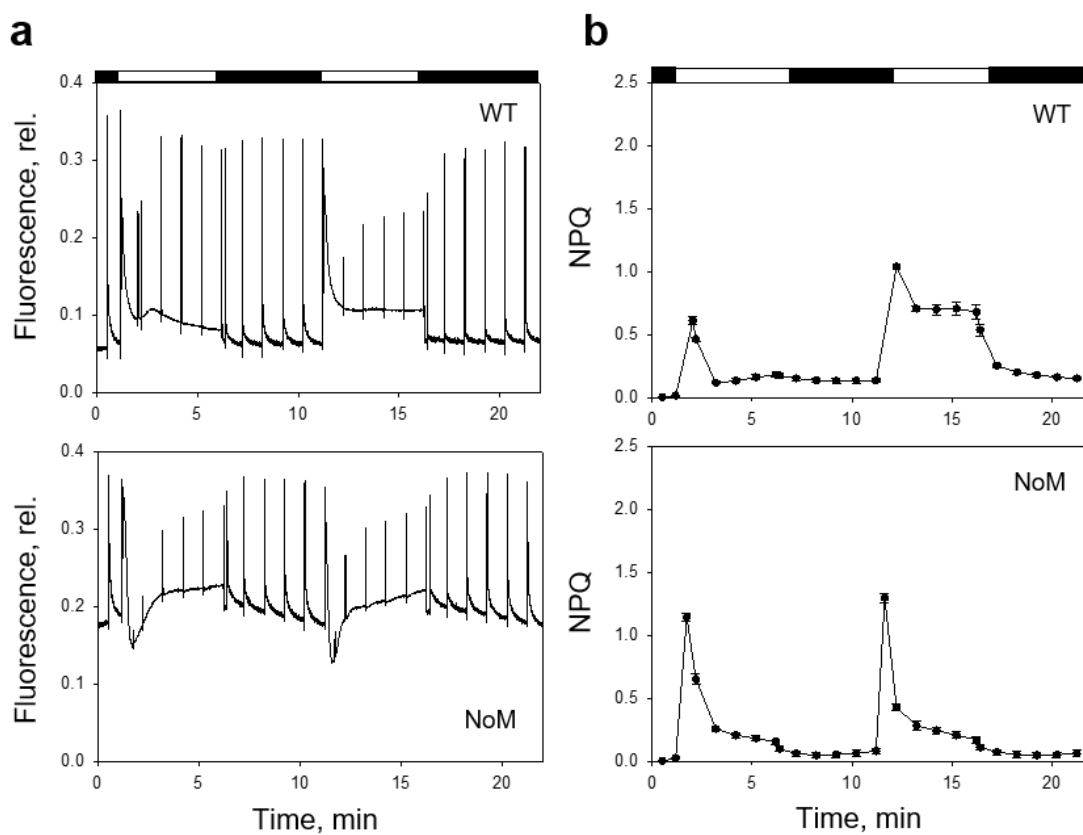


Figure 3.13: **The altered Chl fluorescence induction in plants exposed to limiting light intensities.** **a** Chl fluorescence induction in WT and *NoM* leaves during 2 cycles of 5 minutes low-light ($216 \mu\text{mol photons m}^{-2} \text{s}^{-1}$) + 5 minutes dark, marked with white and black bars on top of the graph. **b** NPQ values calculated from fluorescence traces with the application of saturating pulses.

dependent upon PsbS presence and independent upon Zea.

The following transient fluorescence recovery in the induction kinetics (phase III), was assigned to the lack of an intermediate quenching mechanism residing in the missing minor antenna complexes. However, our data suggest that this mechanism arises from a transient relaxation of the quenching state of trimeric LHCII. The transient increase in F_0 fluorescence during illumination indicates that there is a higher fluorescence emission occurring in the antenna components of PSII present in *NoM*. The increased fluorescence emission at 679 nm and the analysis of the functional PSII cross-section suggest that there might occur a detachment of LHCII from its quenched state in the already uncoupled LHCII bulk antenna, which con-

Fast quenching	Transient recovery	Second quenching
<ul style="list-style-type: none"> • Quenching of <i>Fo</i> • ΔpH-dependent • <i>PsbS</i>-dependent • RCs-independent • Zea-independent 	<ul style="list-style-type: none"> • Increased <i>Fo</i> • Impaired Zea synthesis • Proton short-circuit • LHCII uncouples from bulk antenna 	<ul style="list-style-type: none"> • Quenching of <i>Fo</i> • ΔpH-dependent • <i>PsbS</i>-dependent • RCs-independent • Zea-enhanced

Figure 3.14: **Features of NPQ induction phases in *Arabidopsis* plants lacking minor antenna complexes.** “Fast quenching”, “transient recovery” and “second quenching” indicate the phases observed in the Chl fluorescence induction traces in *NoM* (marked II, III and IV in Figure 3.7b).

sequently possesses a longer fluorescence lifetime and this in turn results in a higher steady-state fluorescence yield. Importantly, the fraction of complexes functionally connected to RCs remains unaltered suggesting that, the occurring rearrangements concern only the fraction of poorly connected LHCII. Since plants lacking specific minor antenna polypeptides were shown to be affected in ΔpH formation and Zea (de Bianchi *et al.*, 2008), we hypothesised that these effects could also be present in the complete antenna-deficient mutant *NoM* and result in the observed impairments in the fluorescence induction. Dall’Osto *et al.* (2017) reported an analysis of the pigment composition of *NoM* plants at fixed intervals during illumination by means of HPLC. No significant difference was reported in the concentration of Zea at each time probed. Reported values were similar after 20 minutes of illumination in the mutant and the WT. In our study, we employed a more sensitive approach to measure of Zea formation, by recording the kinetics of the xanthophyll formation probing absorption changes in intact leaves. This analysis allowed us to spot differences in the very first minutes of illuminations, where the differences in the fluorescence induction occur, with *NoM* exhibiting a considerably slower induction of Zea synthesis (Figure 3.12). Similarly, in their study, no statistically significant difference was observed in the kinetics of ΔpH formation during illumination, although smaller average values in *NoM* were reported at the AL intensities probed in the fluorescence induction (Dall’Osto *et al.*, 2017). However, in our study, differences were observed both in the amplitudes and in the dynamics of ΔpH formation and retention of the gradient, with *NoM* showing lower pH and pronounced proton

leakage visible as a relaxation of the 9-aa quenching during light exposure and a fast dissipation of the gradient during recovery in the dark. These discrepancies could be due to the use of methyl-viologen in their experiment, which acts as an exogenous electron acceptor that saturates the electron transport rate. Therefore, its addition could bias the 9-aa detection method, by artificially amplifying the ΔpH and levelling the existing differences between WT and *NoM*.

Thus, our results indicate that the combination of the defects in ΔpH and Zea formation can explain the differences in the observed quenching induction without taking into account the existence of an intermediate quenching component localised in minor antennae. A further support to this interpretation comes from the analysis of WT plants subject to low AL illumination (Figure 3.13). Under such conditions, the limited proton gradient imitates the *NoM* phenotype, where quenching induction is impaired and Zea synthesis is slowly activated. In particular, it is interesting to notice the occurrence of similar phases in the fluorescence induction during the first illumination period to those reported in *NoM*: fast quenching, transient fluorescence recovery and second slower quenching (compare Figures 3.13 and 3.7). The second illumination period, once Zea is formed, harbours comparable amplitudes and kinetics of NPQ in WT and *NoM* (Figure 3.7d,e and 3.14). What is causing in *NoM* the altered dynamics of ΔpH formation resulting in anomalies during the first fluorescence induction? The altered redox reactions at the PSII acceptor side (Figure 3.5) suggest that a proton short circuit, which impedes the vectorial H^+ flux from the stroma to the lumen, could be the explanation for such impairments. The basic functional unit of PSII supercomplexes is C2S2M2, where the monomeric light-harvesting complexes are found as linkers of the RCs and the major trimeric antenna components (Boekema *et al.*, 2006; Dekker and Boekema, 2005). The robustness of the light-harvesting system of PSII is evidenced by the ability of plants to compensate for the lack of specific antenna polypeptides by increasing the synthesis of other LHCs proteins (Ruban *et al.*, 2003; Damkjær *et al.*, 2009; Dall'Osto *et al.*, 2017). The modularity and resulting plasticity of PSII give rise to uncertainties in assigning a quenching mechanism to specific LHCs. Mutants lacking components of the minor antenna system were found to possess fewer PSII supercomplexes and disrupted in their macroorganisation, defective functional connection within supercomplexes, decreased ETR, lower values of ΔpH and Zea accumulation,

increased membrane rigidity (Kovács *et al.*, 2006; de Bianchi *et al.*, 2008; van Oort *et al.*, 2010; de Bianchi *et al.*, 2011; Dall’Osto *et al.*, 2014a). Interestingly, state transitions are also impaired in the absence of minor antennae (Kovács *et al.*, 2006; Dall’Osto *et al.*, 2019). Together with our data showing that there are no changes in the analysed PSII cross-section (Figure 3.11), this could indicate an important role for minor antennae in the dynamic changes of the photosynthetic membranes occurring during adaptations to different light environments. The absence of CP24 brings about the most pronounced phenotype: exaggeration of the crystallinity of PSII the membranes and a considerable decrease in the mobile fraction of LHCs in the membranes (Goral *et al.*, 2012). The described Lhcb6 knock-out mutant exhibit the most notable changes in NPQ formation (de Bianchi *et al.*, 2008). The changes in membrane rigidity are remarkably similar to the same differences evidenced in *npq4* and L17 mutants, lacking or overexpressing PsbS, respectively (Goral *et al.*, 2012). Therefore, the deficiencies in fast photoprotection in the absence of minor antennae, could originate from a combination of functional (Δ pH and Zea) as well as structural (mobility of LHCs) impairments. Their presence is therefore crucial *in vivo* for the integrity of the PSII supercomplexes and for the efficiency and plasticity of light harvesting processes.

Its disputed whether minor antenna complexes are themselves sites of quenching during NPQ induction. *In vitro* studies of minor antenna complexes highlighted the inclination of CP26 and CP29 to bind DCCD, suggesting the presence of proton-sensing residues (Walters *et al.*, 1994, 1996), to bind large amounts xanthophyll cycle Cars (Bassi and Caffarri, 2000) and the ability to induce large amplitudes of Chl fluorescence quenching (Ruban *et al.*, 1996). A proposed quenching mechanism occurs in minor antenna complexes (especially in CP29) and involves a charge transfer state to a Zea molecule after Vio deepoxidation (Holt *et al.*, 2005; Ahn *et al.*, 2008; Avenson *et al.*, 2008). The following charge recombination results in the non-radiative dissipation of the excitation energy. This mechanism was proposed by Dall’Osto *et al.* (2017), to occur in WT and be absent in *NoM*. However, the L2 Car pocket in CP29 complex is embedded in the polypeptide scaffold and the Vio it incorporates is not readily available for deepoxidation since it is inaccessible for enzymatic conversion and tightly hydrogen-bound to the protein (Pan *et al.*, 2011; Duffy and Ruban, 2012). Moreover, the presence of Zea in *NoM* brings

about amplitudes of NPQ comparable to WT plants, disproving the hypothesis of an additional Zea-dependent mechanism occurring and being differentially present in the two genotypes. In addition, the knock-out and antisense mutants for minor LHCs so far mentioned, revealed up to a 50% reduction in qE, whilst deletion of two polypeptides of the major LHCII determine a 35% reduction, with CP26 assembling in trimeric form to compensate for the lack of trimeric LHCII (Ruban *et al.*, 2003, 2006; Andersson *et al.*, 2003).

NPQ is an additive process if multiple independent NPQ sites are active. When photochemistry is inhibited by saturating light pulses, the non-photochemical quenching parameter NPQ can be described as $k_D/(k_f+k_d)$, that relates the rate constant for a non-radiative dissipative process (k_D) to the sum of all other rates at the conditions of closed RCs, namely k_f , rate constant for fluorescence, and k_d , rate constant for the other dissipative processes. If multiple independent mechanism of fluorescence quenching take place, then their rate constants would sum up in an additive way. In particular, in *NoM*, two mechanisms of energy dissipation were proposed (Dall'Osto *et al.*, 2017). Within this model, NPQ can be described as $(k_{D1} + k_{D2})/(k_f+k_d)$, where k_{D1} is the rate constant for quenching taking place in minor antennae and k_{D2} the one for trimeric LHCII. Given that, once Zea is accumulated, the NPQ value is the same in WT and *NoM* (~ 2) and assuming that in the absence of minor antennae $k_{D1}=0$, this implies that k_{D1} is also null in WT plants, thereby proving that minor antennae play no exclusive role in excitation energy quenching.

3.2 Fast photoprotection (qE) in plants lacking minor antennae and RCs

The data so far collected on *NoM* mutants suggest that the LHCII proteins are the NPQ site in higher plants and that minor LHCs and RC proteins of the photosystems don't harbour excitation energy quenching sites. The now simplified scheme of NPQ strict requirements contains only ΔpH , LHCII. However, factors such as PsbS and the xanthophyll cycle activation are also needed for the correct dynamics of this photoprotective process and various models suggest that they might be important sites of NPQ (Holt *et al.*, 2005; Niyogi *et al.*, 2005; Bennett *et al.*, 2019). We

decided therefore to undertake a more complete analysis of NPQ by adopting a substantially reductionist approach and analysing the dynamics of the process in plants lacking minor antennae and RCs and possessing varying amounts of PsbS and Zea. We focused especially on the quickly forming and reverting phase of NPQ, called qE, energy-dependent quenching, the main NPQ component that protects plants from sudden light intensity changes. We determined the kinetics, amplitude and pH requirements of qE and their allosteric modulation, in order to understand the interplay between the factors that are absolutely essential for qE and those that are instead only components of its regulation.

3.2.1 Making the thylakoid membranes enriched only in major LHCII

Arabidopsis NoM plants used in this study were treated for up to 3 weeks with lincomycin during the full rosette developmental stage. In line with previously reported observations of treated WT plants (Belgio *et al.*, 2015), prolonged antibiotic treatment resulted in an extremely affected morphology of the chloroplasts, with enhancement of senescence-related traits (not shown): increased number of plastoglobules in the stroma; almost absent accumulation of starch; affected integrity of the stroma lamellae; loss of specific orientation of thylakoid grana. Among others, also the formation of characteristic “megagrana” made up by several tens of stacked thylakoid membranes was observed. Fractionation of the thylakoid membranes with detergent and separation of the complexes via sucrose density gradient ultracentrifugation evidenced a poor distribution of the Chl content alongside the tube compared to the untreated control, with a dark green band corresponding to antenna proteins harbouring 81% of the total Chl content (Figure 3.15a). Just 6% of the total Chl was found in lower density bands associated with RCs of PSII and PSI, while up to a 36% was present in the control. The identity of each fraction in the tube was determined with SDS-PAGE and absorption spectra (Figures 3.15 and 3.16). As expected, the *NoM* mutant utilised in the study presented only a band corresponding to trimeric antenna complexes, while monomeric complexes were undetectable. An intermediate band between LHCII and PSII core proteins and a higher density band towards the end of the tube, previously assigned in WT to the presence of CP24-CP29-LHCII

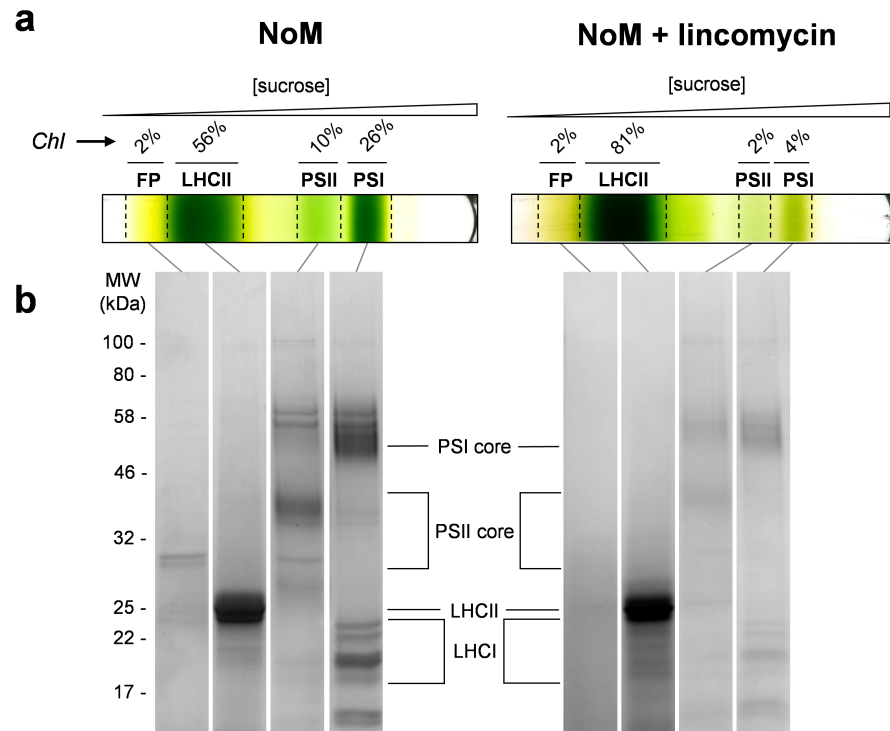


Figure 3.15: **Lincomycin-treated *NoM* plants have thylakoids greatly enriched in LHCII.** **a** Representative sucrose density gradients of solubilised thylakoid membranes isolated from *NoM* and lincomycin-treated *NoM* plants. Analysed fractions are labelled and their relative Chl content is shown (the same amount of Chl was loaded in each gradient). **b** SDS-PAGE of the main sucrose gradient fractions. The gel lanes displayed were cropped from the same pictures of the gels for clarity. Equal sample volumes were loaded in each lane. FP, free pigment.

associates and PSII megacomplexes, respectively, (Caffarri *et al.*, 2009), were undetectable in both conditions, in line with previous studies (Dall'Osto *et al.*, 2014a, 2017). The proteomic profile highlighted a drastically changed composition of the thylakoid membranes (Figure 3.15b), severely impaired in the accumulation of RC-related polypeptides. Instead, the nuclear encoded LHCII components were unaffected (Jansson, 1994). Minor antennae polypeptides (Lhcb4, Lhcb5, Lhcb6) were not present in the gel lanes, confirming previous data about the characterisation of the *NoM* mutant (Dall'Osto *et al.*, 2014a, 2017). The presence of Lhca polypeptides, that are part of LHCI proteins, was partially altered as already observed in treated WT plants (Belgio *et al.*, 2012), possibly because of the lack of docking sites in PSI of the final complexes. Indeed, some core PSI proteins are crucial for the

stability of the supercomplexes and their loss results in disrupted accumulation of Lhca polypeptides (Varotto *et al.*, 2002; Caffarri *et al.*, 2014). Thus, the analysis of protein accumulation evidenced a minimal composition of the thylakoid membranes after lincomycin treatment, similar to a polypeptide analysis after pull-down specific purification, where only one type of complexes (LHCII) is largely represented. The absorption spectra of the main sucrose density gradient bands clearly mark the presence of the LHCII as the main contributor to the overall absorption profile (Figure 3.16).

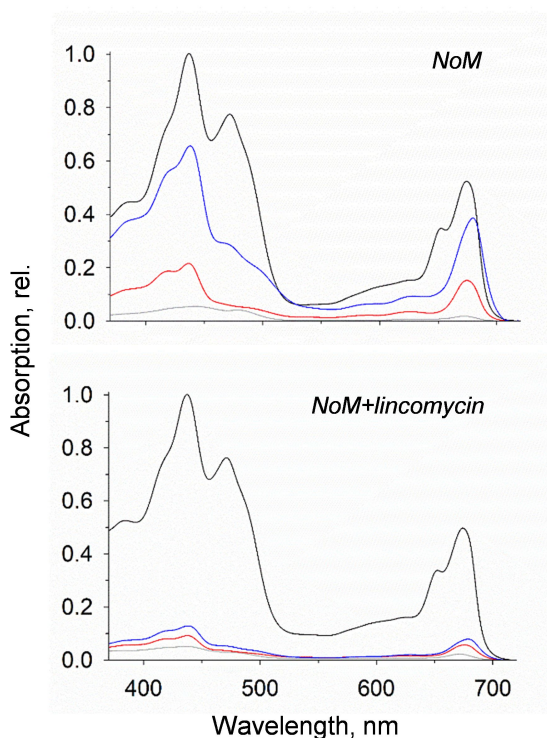


Figure 3.16: **Absorption profiles attest a selective enrichment of LHCII in *NoM* + lincomycin plants.** Spectra of the four sucrose gradient fraction retrieved from solubilised *NoM* and lincomycin-treated *NoM*, as shown in Figure 3.15a (black, LHCII; blue, PSI; red, PSII; grey, FP). Each spectrum was normalised at the maximum Soret absorption of the fraction enriched in LHCII trimers.

A last independent evidence of the strong reduction of the content of RCs comes from the analysis of the pigments purified from leaves (Table 3.1). In particular, the lower values of Chl a/b ratio for treated plants support the findings of a large abundance of LHCII ($a/b=1.33$) relative to RCs (that carry only Chl a) as

	Chl a/b	%N/Car	%V/Car	%A/Car	%L/Car	%Z/Car	% β -car/Car	DEP (%)
WT	3.45 \pm 0.09	12.47 \pm 0.42	10.09 \pm 2.46	-	64.78 \pm 1.24	-	22.48 \pm 0.9	-
NoM	3.02 \pm 0.34	14.3 \pm 0.96	8.27 \pm 0.26	-	67.73 \pm 1.35	-	18.47 \pm 0.93	-
NoM+lincomycin (v)	2.08 \pm 0.07	16.04 \pm 0.29	11.15 \pm 0.39	0.629 \pm 0.57	54.95 \pm 1.69	-	7.4 \pm 1.42	2.56 \pm 2.3
NoM+lincomycin (z)	2.05 \pm 0.07	15.88 \pm 0.32	3.83 \pm 0.94	3.63 \pm 0.66	59.96 \pm 0.83	2.57 \pm 0.447	6.35 \pm 0.78	43.73 \pm 6.96

Table 3.1: **Pigment composition of *Arabidopsis* WT, NoM and NoM + lincomycin plants.** Chl and Car content in leaves of WT, NoM and lincomycin-treated NoM plants, the latter either enriched in Vio (v) or Zea (z). Chl a/b, chlorophyll a/b ratio; %N(V,A,L,Z,-car)/Car, relative % percentage of Neo (Vio, antheraxanthin, Lut, Zea, -carotene) relative to total Car content; DEP (%), de-epoxidation parameter calculated as $([Z]+0.5*[A])*100/([Z]+[A]+[V])$. Data are the average of 4 independent experiments \pm SD.

well as the lower value for β -carotene, which is found only in core complexes. From the ratios of Chl content of the sucrose gradient band corresponding to PSII and PSI cores (Figure 3.15a), we estimated in lincomycin-treated samples a protein content reduction by $\sim 80\%$ and $\sim 85\%$, respectively.

3.2.2 qE is formed in the absence of minor antennae and reaction centres

We therefore tested the ability of these plants with drastically changed thylakoid composition to form and relax NPQ and especially its energy-dependent component qE. To evaluate the maximum extent of qE and compare it between genotypes in the course of an induction cycle (5 minutes light, 5 minutes dark), WT, untreated NoM and treated NoM plants were high light treated previous to the NPQ induction to induce maximum Vio de-epoxidation. To independently assess the dynamics of qE formation in leaves, two methods were employed: one consisted in the traditional detection of Chl fluorescence quenching associated with the determination of the NPQ parameter from the traces; the other relied on the detection of absorption changes related to qE. The advantage of looking at the absorption changes at 535 nm relies on the fact that the parameter, despite being an indirect measurement of the NPQ phenotype, correlates linearly with it and offers the possibility to study in detail the kinetics of its formation and relaxation (Ruban *et al.*, 1993b; Johnson *et al.*, 2009). Figure 3.17 shows the results obtained. In all cases, similar NPQ induction were observed (column a). The NPQ values are the same within experimental error, although the averages are slightly higher for NoM and NoM

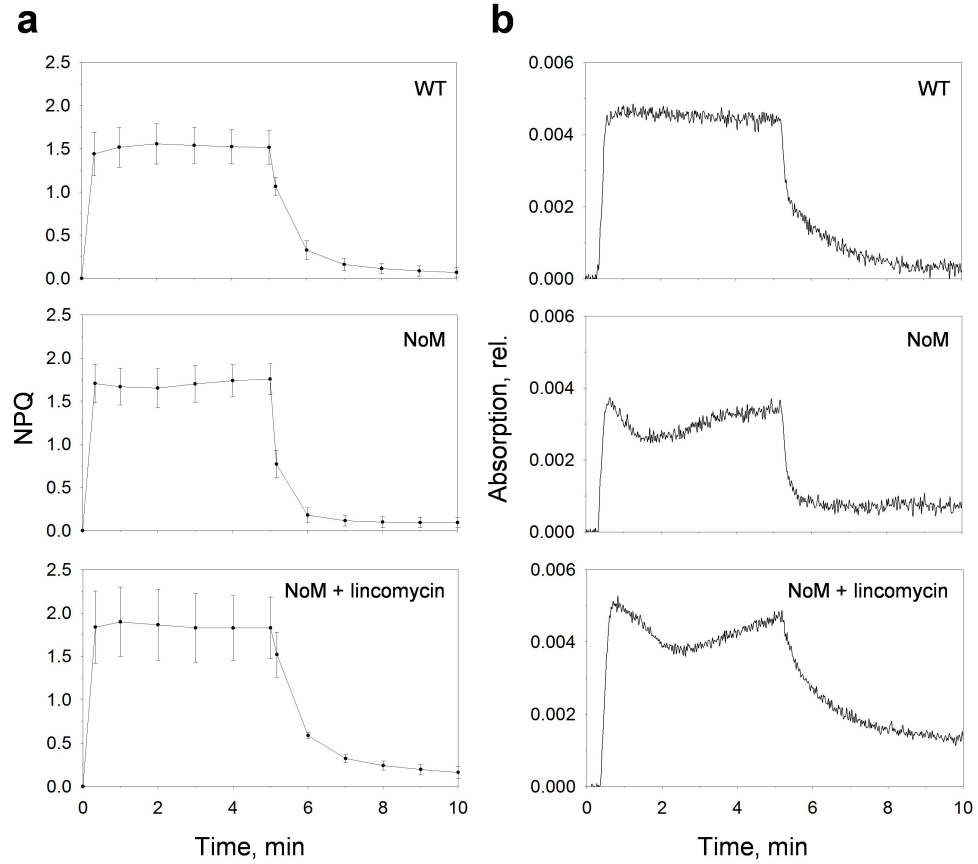


Figure 3.17: **qE** is formed in plants lacking minor antennae and RCs. **a** NPQ values measured in WT, NoM and lincomycin-treated NoM leaves enriched in Zea during 5 min light ($1100 \mu\text{mol photons m}^{-2} \text{s}^{-1}$) + 5 min dark induction. **b** Absorption changes at 535 nm measured during the induction. Traces represent the mean of 3-5 replicates.

+ lincomycin ($P=0.19$, One-way ANOVA on NPQ values after 5 minutes of illumination), as suggested in our previous study (Townsend *et al.*, 2018b). The 535 nm changes exhibit some variability with respect to the NPQ trend, particularly during illumination and the strong correlation between NPQ and 535 nm values in WT is seemingly lost in *NoM* mutants (column b). This result, which was already detectable in a previous report on single antisense and knock-out mutants (Johnson *et al.*, 2009), is explained considering the origin of 535 absorption changes, which was ascribed to Zea dimers transiently formed during LHCII clustering (Duffy *et al.*, 2010). Absorption changes related to qE in *NoM* could thus mirror the altered

LHCII organisation and dynamics during light induction in the mutant, which also partially occur when Zea is accumulated (Dall’Osto *et al.*, 2014a; Townsend *et al.*, 2018b). Therefore, 535 nm absorption changes lose partially linearity with the NPQ parameter in these mutants. In all three conditions tested, NPQ was formed at virtually identical amplitudes and was quickly reversible (qE). Remarkably, not only plants lacking minor antenna complexes displayed unaltered capacity to form qE, but also exhibited a tendency for it to be faster, an effect particularly pronounced in the kinetics of its recovery (Figure 3.18). This trait, which is probably due to

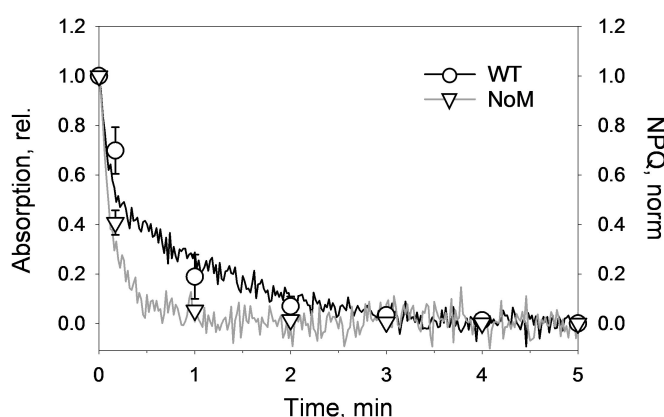


Figure 3.18: **The qE recovery kinetics are accelerated in the plants lacking minor antenna complexes.** Comparison of the NPQ values and the 535 nm absorption changes during the recovery in the dark of the traces showing in Figure 3.17. To compare the kinetics, normalisation was done at the maximum value right after the end of illumination and traces were offset to 0 at the end of the 5 min of dark.

the altered thylakoid membrane architecture and PSII macro-organisation in *NoM* plants (Dall’Osto *et al.*, 2014a), highlights the capacity of LHCII alone to undergo a transient switch between on and off states, corresponding to light-harvesting and dissipative functions, respectively, as hinted in single molecule fluorescence studies (Krüger *et al.*, 2010, 2013). A faster switch makes qE a less wasteful process since the interplay between photochemistry and photoprotection is improved to avoid the unnecessary dissipation of collected photon energy. It has been recently proven that bioengineering the qE switch to make it faster results in improved biomass accumulation of plants in field (Kromdijk *et al.*, 2016). The lincomycin treatment abolishes this phenotype, as the kinetics of qE relaxation are visibly slower with respect to the

untreated counterpart, again possibly because of varied arrangement and dynamics of the thylakoid membrane complexes (Belgio *et al.*, 2012).

By definition, qE, the energy-dependent fraction of NPQ, is triggered by the formation of ΔpH across the thylakoid membrane (Briantais *et al.*, 1979). We therefore examined the dependence of the observed quenching in lincomycin-treated *NoM* plants upon ΔpH , by investigating the effects of the uncoupler nigericin on qE. A gentle protoplast preparation was employed, that yielded a very high degree of chloroplasts intactness (Figure 3.19). In this way, the essay was performed in a near

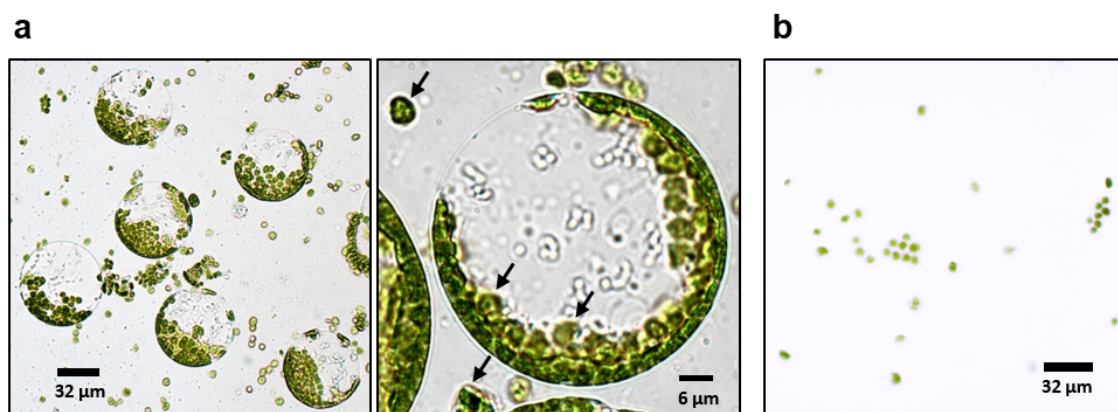


Figure 3.19: **Microscopy assessment of the intactness of cellular and subcellular preparations from *Arabidopsis*.** Brightfield optical microscopy images of protoplasts isolated from *Arabidopsis NoM* plants (a) and diluted chloroplasts obtained after osmotic rupture of the protoplasts (b). Arrows in a indicate intact chloroplasts.

native thylakoid membrane state, whilst guaranteeing a homogeneous infiltration with the chemicals used, unattainable on leaves. When nigericin was added to a protoplast suspension from lincomycin-treated *NoM* plants, the reversible quenching component was completely lost (Figure 3.20a). The effect of nigericin is to completely dissipate the ΔpH gradient created during the light-harvesting reactions. Therefore, the quenching observed in the *Arabidopsis* model studied is still triggered by ΔpH and retains the characteristics of the qE observed in WT plants. It was shown that a condition sufficient for qE is the acidification of the lumen (Rees *et al.*, 1992; Johnson and Ruban, 2011). Lowering the pH from 8 to 5.5 of the reaction medium where chloroplasts were suspended caused a marked inhibition of the relaxation of quenching (Figure 3.20b). The addition of the base KOH,

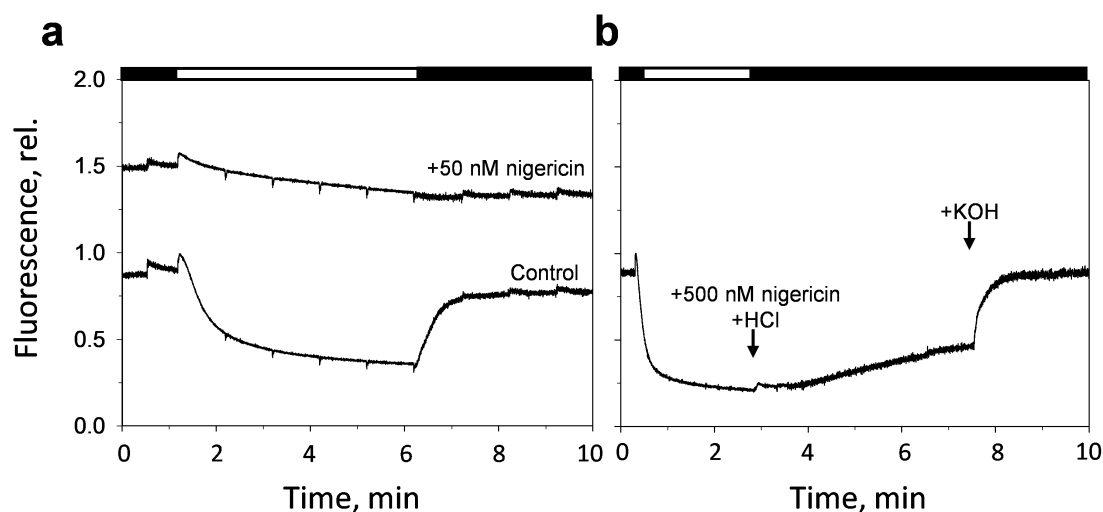


Figure 3.20: **The pH dependence of quenching in lincomycin-treated *NoM* mutants.** Chl fluorescence induction traces of protoplasts (a) and chloroplasts (b) obtained from lincomycin-treated *NoM* plants. **a** Effect of nigericin addition on the formation of qE. Traces are the means of 3 independent measurements, normalised at the maximum of fluorescence after the onset of AL and offset for clarity. A saturating pulse was applied every minute to retrieve the NPQ values. **b** Control of qE by bulk pH variations. After illumination, pH was lowered to 5 by simultaneous addition of HCl and nigericin. In the dark, pH was restored to 8 by the addition of KOH. Black and white bars represent periods of darkness and AL illumination ($900 \text{ mol m}^{-2} \text{ s}^{-1}$), respectively. A saturating concentration of nigericin was added to ensure complete equilibration of lumen and bulk pH (Rees *et al.*, 1992).

to restore the initial pH value of the medium, caused the quick relaxation of the quenching, showing that quenching in the absence of minor antennae and RCs can be modulated by pH. It is likely that the residual amounts of PSII and PSI retained in the membranes of lincomycin-treated plants (see Figure 3.15), together with the cytochrome *b₆f*, are sufficient to provide the ΔpH needed for the onset of qE in the thylakoids of these plants (Belgio *et al.*, 2012).

3.2.3 Zea and PsbS exert an allosteric control of qE

So far, we reported the NPQ amplitudes of plants in which Zea accumulation was induced by pre-exposure to high light. To understand what is the role of the xanthophyll cycle during qE induction, we measured the fluorescence induction traces of leaves subject to a prolonged dark-adaptation, to induce a maximum pool of Vio,

and compared them with leaves pre-treated with light (Figure 3.21). The pigment

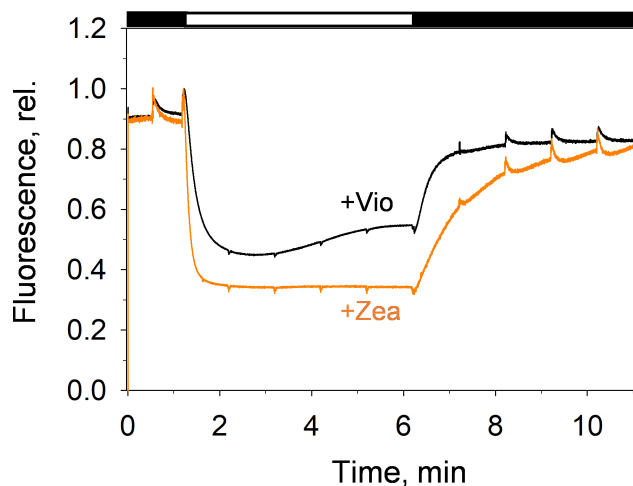


Figure 3.21: **Zea controls the kinetics and maximum amplitude of qE.** Fluorescence quenching induction traces of leaves from lincomycin-treated NoM plants, either dark-adapted (+Vio, black line) or light-treated (+Zea, orange line). Each trace is the average of at least 4 independent measurements. A saturating pulse was applied every minute to retrieve the NPQ value.

composition of the plants used in the experiment is shown in Table 3.1. We found that fluorescence quenching also occurs in the presence of Vio, however, greater quenching was achieved upon Zea accumulation ($\text{NPQ}=1.22\pm0.36$ for Vio-enriched, $\text{NPQ}=1.94\pm0.35$ for Zea-enriched, $P\leq0.01$, two-tailed t test; Figure 3.21). The induction kinetics differ between the two conditions, reaching faster a stationary phase of maximal quenching in Zea-enriched plants. In Vio-enriched plants, instead, the induction is slower and the quenching isn't sustained, beginning to relax after the first 2 minutes of light exposure. This relaxation may be conspicuous in NoM plants due to the slower induction of Zea synthesis (Figure 3.12 and Townsend *et al.* (2018b)), which could be even more pronounced in the absence of the PSII RCs contribution to the overall ΔpH formation required for the activation of the Vio de-epoxidase.

Besides quenching induction, we also investigated the steady-state quenching effect that was associated with the slowly-relaxing qZ component of NPQ. Such component relates to the presence of Zea, which is slowly re-epoxidised to Vio in the dark (Siefermann and Yamamoto, 1975; Gilmore *et al.*, 1994). qE and qZ were shown to take place in shared site of the membrane and the latter provides a memory func-

tion for plants during consecutive qE induction (Noctor *et al.*, 1991; Johnson *et al.*, 2009; Ruban and Johnson, 2010). An investigation of the Chl fluorescence lifetimes during the Fm state, where the fraction of remaining photosystems is closed and no additional NPQ processes are active, provided an evidence that the mere presence of Zea in the membrane causes a degree of energy quenching in dark-adapted leaves (Figure 3.22a) (Johnson *et al.*, 2010). The average lifetime in Zea-enriched leaves is lowered to 1.73 ± 0.18 ns from 2.17 ± 0.03 ns in Vio-enriched leaves, in line with the effect caused by Zea overexpression in plants with the normal thylakoid membrane organisation (Ware *et al.*, 2016). The detailed analysis of the exponential components used in the reconvolution fitting procedure yielded unaltered lifetime values of the components used, in both conditions (Figure 3.22b). However, changes in the

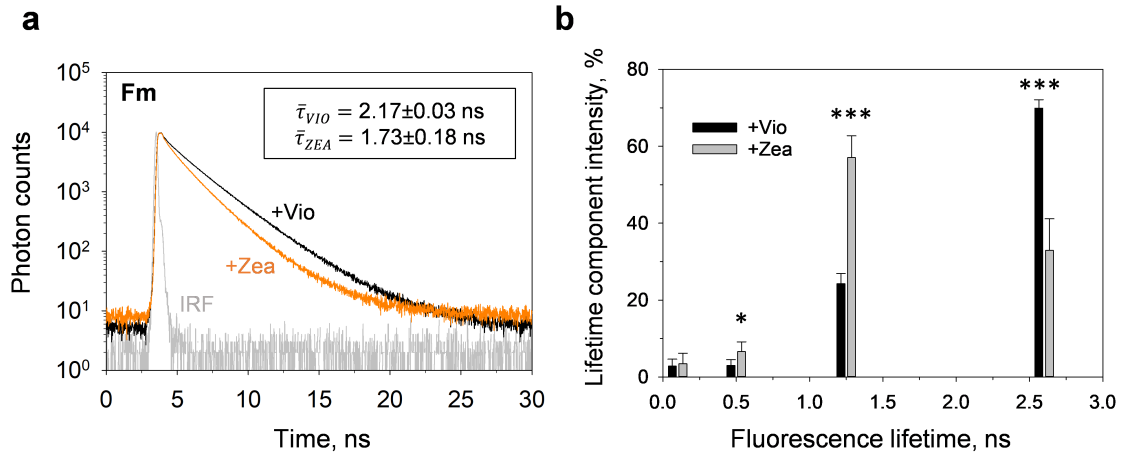


Figure 3.22: **Zea retention in the thylakoids causes partial quenching in the dark.** **a** Chl *a* fluorescence lifetime measurements of Vio- (black) and Zea-enriched (orange) leaves of lincomycin-treated *NoM* plants. Prior to measurements, leaves were infiltrated with 50 μ M DCMU, to fix the Fm state. Traces are averages of at least 4 independent measurements. The instrument response function (IRF) trace is shown in grey. **b** Intensity-weighted components (%) obtained from Chl fluorescence lifetime traces. The components were calculated after exponential reconvolution of lifetime traces with the IRF. The fitting procedure yielded good results using 4 exponential components of lifetimes 0.1, 0.5, 1.25 and 2.6 ns. The fastest component originates from PSI contribution (Chukhutsina *et al.*, 2019), while the other components were attributed to LHCs in different quenching conformations (Belgio *et al.*, 2012). Error bars represent SD and asterisks mark statistical significance (two-tailed t test: * $P < 0.05$, *** $P < 0.001$).

intensities of the components was noticeable, with the Zea-enriched sample exhibiting a reduction of the intensity of the longer lifetime components and an increase of the 1 ns component.

We then investigated whether PsbS, which was recently shown to preferentially interact with major LHCII complexes during NPQ (Sacharz *et al.*, 2017), retains its function in the LHCII-enriched thylakoids under examination. *NoM npq4* mutants lacking PsbS and lincomycin-treated *NoM npq4* exhibit both a greatly impaired capacity to form qE (Figure 3.23b,c). It was previously observed that the modulation of ΔpH can restore the WT quenching phenotype in plants lacking PsbS (Johnson and Ruban, 2011). Interestingly, the addition of diaminodurene (DAD), a proton shuttle that acts as a mediator of cyclic electron flow around PSI, is able to restore qE also in plants lacking minor antennae and RCs, as well as PsbS (Figure 3.23). The simultaneous measurements of ΔpH by monitoring the fluorescence quenching of 9-aminoacridine (9-aa) was used to determine the extent of the pH gradient formed during the light induction and enhanced by the addition of DAD (Schuldiner *et al.*, 1972). The additional infiltration with DCMU, of chloroplasts from lincomycin-treated *NoM npq4*, which blocks the residual PSII activity and linear electron flow, did not impede the restoration of qE by DADs (Figure 3.23), thus being an ultimate proof that control of qE can derive exclusively from the concerted action of LHCII and ΔpH . By modulating the extent of ΔpH using different light intensities as well as the addition of increasing amounts of DAD, it was possible to determine the correlation between lumen pH (measured as 9-aa quenching) and the reversible qE quenching (Figure 3.24). The data fitting revealed a sigmoidal behaviour of the relationship between ΔpH and qE, as previously observed (Johnson and Ruban, 2011). This dependency suggests that the absence of PsbS shifts the pK of qE to higher values (the 9-aminoacridine quenching value at half qE maximum, $k_{0.5}=0.24\pm0.03$ for *NoM* and $k_{0.5}=0.39\pm0.06$ for *NoM npq4*) and changes the cooperativity of the process (Hill parameter $n=2.58\pm0.69$ for *NoM* and $n=6.17\pm0.62$ for *NoM npq4*; Figure 3.24).

3.2.4 LHCII aggregation: tuning the activity of LHCII to regulate light harvesting

It was shown by freeze-fracture electron microscopy in conjunction to confocal analysis of fluorescence recovery after photobleaching that qE is accompanied by a reversible clustering of LHC proteins in the thylakoids (Johnson *et al.*, 2011b). The

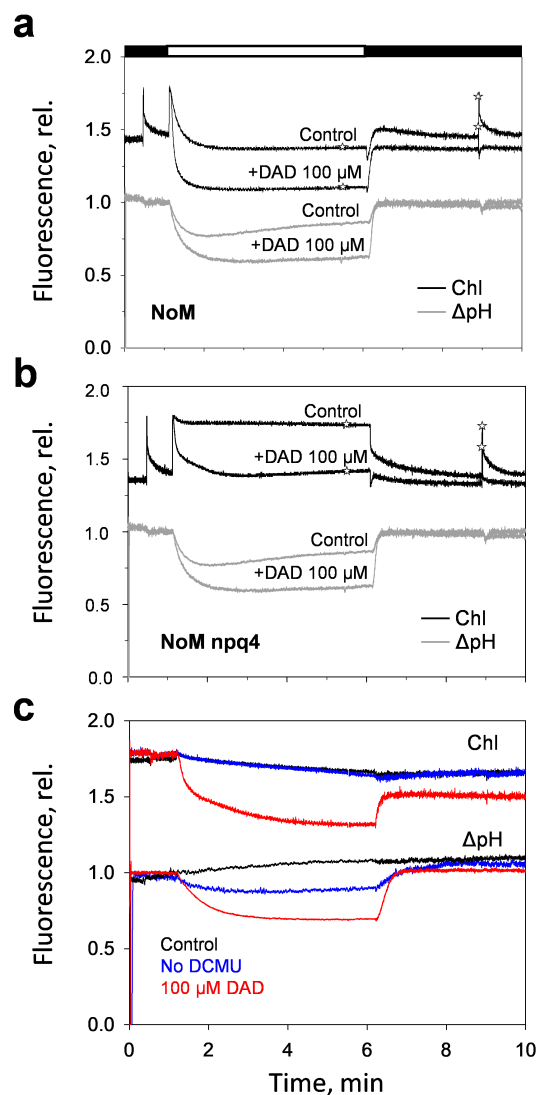


Figure 3.23: **Enhancing ΔpH causes a restoration of qE in the absence of PsbS.** **a,b** Representative traces of Chl fluorescence (black lines) and ΔpH (grey lines) induction in *NoM* and *NoM npq4* chloroplasts, respectively. When specified, 100 μM diaminodurene (DAD) was added to the suspension at the beginning of the illumination period. Open stars indicate the Fm and Fm' values assessed by saturating pulses. **c** Induction of Chl fluorescence and ΔpH formation on chloroplasts of lincomycin-treated *NoM npq4* plants. 50 M DCMU was added prior experiments to close the remaining fraction of PSII RCs (black and red lines). 100 μM DAD was added at the beginning of the illumination phase (red lines). In blue, a control without addition of DCMU and DAD is shown. In all experiments, ΔpH was measured by the fluorescence quenching induction of 9-aminoacridine (9-aa) added before each measurement (5 μM).

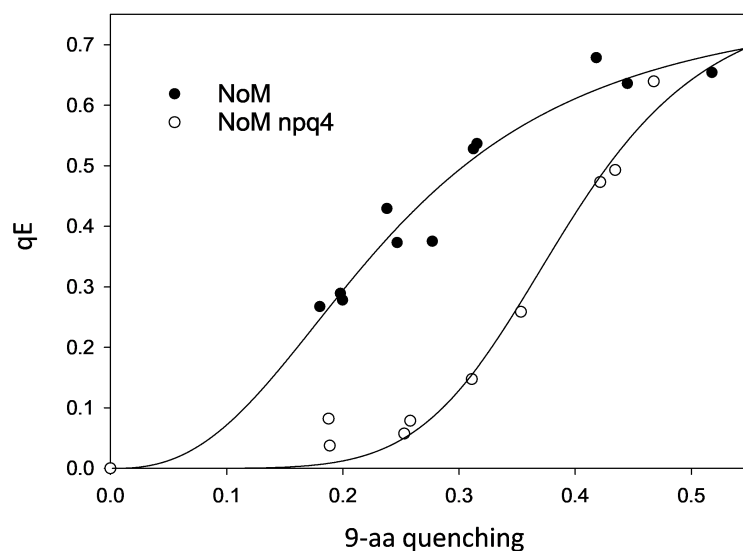


Figure 3.24: **PsbS presence alters the pH sensitivity of LHCII for the activation of qE.** Relationship between reversible Chl fluorescence quenching (qE , $(F_{m_{relaxed}} - F_{m'})/F_{m_{relaxed}}$) and 9-aa fluorescence quenching. Data range was obtained either by changing AL intensity or DAD concentration. Data were fitted to a Hill equation (equation 2.1 in “Chapter 2: Methodologies and approaches”; $R^2=0.96$ and 0.98 for *NoM* and *NoM npq4* chloroplast, respectively).

data of 535 nm absorption changes (Figure 3.17) suggest that this correlation of qE with aggregation of LHCII could be preserved in plants lacking minor antennae and RC proteins since these absorption parameter has been linked to clustering of LHCII particles (Ruban and Horton, 1992; Duffy *et al.*, 2010). To address this aspect, we monitored the 77K fluorescence spectra evolution across a range of NPQ values obtained by high light exposure of lincomycin-treated *NoM* chloroplasts (Figure 3.25). The obtained spectra revealed a simplified structure compared to that of WT and *NoM* chloroplasts, because of the absence of PSII core emission (compare to Figure 3.4). The main detectable bands peaked at 682, 695-699 and 728 nm, where the first two belong to trimeric and clustered LHCII, respectively, and the latter could arise from red shifted forms of LHCI (Ruban and Horton, 1992; Croce *et al.*, 1998). The trimeric LHCII emission is somewhat red-shifted from the emission peak of detergent-solubilised LHCII (situated at 679 nm), a factor observed when LHCII is in a partially quenched state (Illoaia *et al.*, 2008; Tutkus *et al.*, 2019). This occurs in thylakoid membrane where the average Chl fluorescence lifetime is 2 ns instead

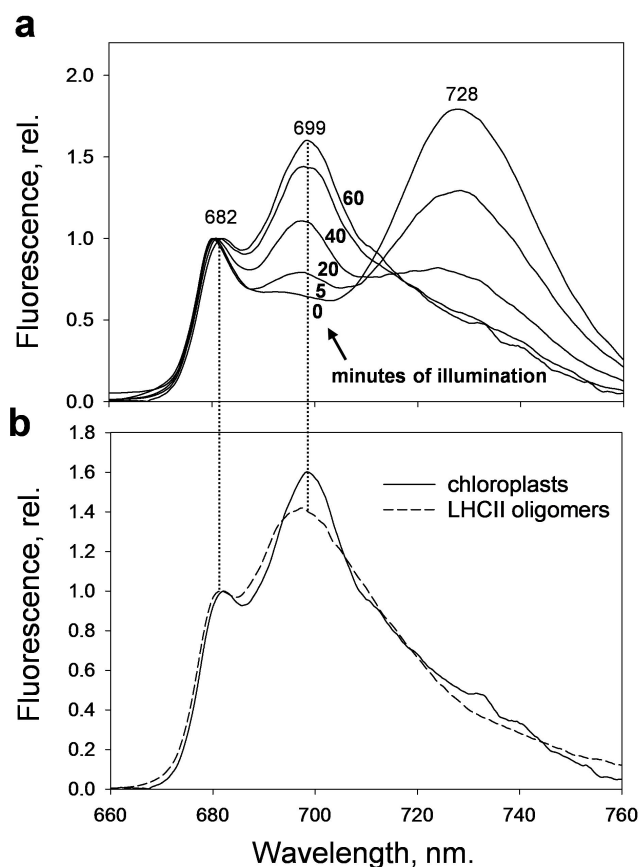


Figure 3.25: **Photoprotective quenching in LHCII-enriched thylakoid membranes exhibits the fluorescence markers of antenna aggregation.** Low temperature Chl fluorescence emission spectra of chloroplasts isolated from lincomycin-treated *NoM* plants after exposure to high light ($2000 \mu\text{mol m}^{-2} \text{s}^{-1}$). **a** Comparison between samples dark-adapted and samples taken after 5, 20, 40 and 60 minutes of AL illumination. **b** Comparison of the fluorescence emission spectra of lincomycin-treated *NoM* chloroplasts (exposed to 60 minutes of high light) with that of isolated LHCII oligomers with a similar fluorescence quenching value. Traces are normalised at ~ 680 nm.

of 4 ns observed in detergent-isolated LHCII (Belgio *et al.*, 2012). The red emission peaking at wavelengths close to 700 nm is not arising from CP47 core antenna protein, since the contribution of the latter is strongly diminished after lincomycin treatment together with the other RC polypeptides. The most likely explanation is therefore that it is the so-called F700 emission, arising from antenna proteins in the aggregated state (Chmeliov *et al.*, 2016). The FR broad emission is shifted 4 nm compared to the untreated control plants (728 nm vs 732 nm; compare to Figure 3.4).

The origin of this shift is more difficult to determine, as it could be due to (i) a loss of PSI superstructure concomitant to decreased amounts of PSI core proteins with an increased emission of LHCI or (ii) a relatively high contribution of FR spectral forms of LHCII (Krüger *et al.*, 2010; Wahadoszamen *et al.*, 2012). During induction of NPQ, the F700 band progressively increases, indicating the gradual increase of the extent of LHCII aggregation (Figure 3.25a). The FR emission, however, exhibits the opposite trend, being quenched upon NPQ increase. Again it isn't straightforward to attribute this effect correctly, as it could originate from the quenching of PSI-related complexes, as previously attested (Giovagnetti *et al.*, 2015; Ware *et al.*, 2015b), or from unfavourable thermodynamics of the LHCII FR states after the onset of quenching (Chmeliov *et al.* (2019) and see Chapter 5). The fluorescence spectrum of chloroplasts obtained after 1 hour of illumination resembles that of *in vitro* clustered LHCII with a comparable reduction of the fluorescence yield, further supporting the correlation between NPQ and LHCII aggregation (Figure 3.25b).

3.2.5 Discussion

Our results demonstrate the ability of LHCII alone in the thylakoid membranes to mediate the qE process, suggesting that the sole site of this photoprotective response is the major trimeric antenna complex of PSII. We demonstrated that Zea and PsbS are only allosteric factors in the control of light harvesting, as their presence is not necessary for qE. This essentially narrows down its requirements to the LHCII (*site*) and ΔpH (*trigger*). Despite being crucial for the integrity of PSII supercomplexes, the correct pH gradient formation and the electron transport efficiency, my data show that minor antenna complexes are not involved as specific sites in qE, as they affect neither the amplitude, nor the kinetics of the process (Townsend *et al.*, 2018b). The partial relaxation of qE during illumination of Vio-enriched plants was observed in previous studies (Dall'Osto *et al.*, 2017; Townsend *et al.*, 2018b) (Figure 3.17) and supports early findings suggesting the occurrence of two distinct kinetic components for qE, with the fast one assigned to lutein-mediated quenching of Chl excitation and the slower one assigned to the presence of Zea (Gilmore and Yamamoto, 1992; Pogson *et al.*, 1998). The sites where Zea-dependent and Zea-independent quenching mechanisms take place were later shown to be the same, within the antenna system

(Johnson *et al.*, 2009, 2011b). In this work, we restricted further the site of action of xanthophyll cycle Cars, which appears to be exclusively LHCII, in agreement data showing that these complexes harbours the fraction of Vio readily available for depoxidation in the membrane (Ruban *et al.*, 1999; Duffy and Ruban, 2012). Indeed, the Zea effect on the kinetics and extent of qE is identical to what was previously observed in WT genotypes (Ruban and Horton, 1999). The average fluorescence lifetime value τ for Zea-enriched leaves was reduced from 2.17 ± 0.03 ns to 1.73 ± 0.18 ns with respect to Vio-enriched leaves (Figure 3.21b). If we assume a value of 0.8 for quantum efficiency of PSII (Φ_{PSII}) in dark adapted WT plants, the determined reduction in τ results in a value of Φ_{PSII} of 0.76, which is in line with previously reported values of Zea-enriched leaves (equations 2.3 and 2.4 in “Chapter 2: Methodologies and approaches”) (Ruban and Horton, 1999). It is also interesting that the presence of this Car alters specifically the Chl fluorescence lifetime components measured for intact leaves, by increasing the intensity of a middle lifetime component at the expenses of the long one, whose intensity is proportionally decreased (Figure 3.22). A similar effect was previously reported by (Gilmore *et al.*, 1995; Frank and Cogdell, 1996), with the proposal that this redistribution of lifetimes occurs because of Zea binding to inner LHCs. In our studied model, however, inner (minor) antennae are not present and a possible explanation for this effect is that Zea alters the fluorescence dynamics of LHCII by increasing the probability of accessing intermediately quenched states (Schlau-Cohen *et al.*, 2015; Tutkus *et al.*, 2017). Recently, this effect on the lifetime component distribution has also been reported for LHCII purified from the mutants *npq2lut2* largely enriched in Zea (Tutkus *et al.*, 2017), reinforcing the idea that the interaction between LHCII and Zea somehow eases the access to quenched conformations by the complexes. The PsbS subunit (and its homologous LHCSR and LHCX in green algae and diatoms, respectively) are crucially involved in the NPQ response (Giovagnetti and Ruban, 2018). The PsbS knock-out in plants exhibits a dramatic phenotype, with the complete suppression of qE (Li *et al.*, 2000). Recently, computational and biochemical methods showed that PsbS senses pH variations in the range of the proposed activation of the qE mechanism (Daskalakis and Papadatos, 2017; Sacharz *et al.*, 2017; Liguori *et al.*, 2019). Our work shows that the PsbS action is also exerted in the absence of minor antennae and RCs, in line with findings showing that its main interaction partners are LHCII

complexes (Teardo *et al.*, 2007; Wilk *et al.*, 2013; Correa-Galvis *et al.*, 2016; Sacharz *et al.*, 2017). Our data suggests that, contrarily to earlier proposals (Niyogi *et al.*, 2005; Bennett *et al.*, 2019), PsbS does not constitute a specific site for qE, but rather is controlling the pH dependence of the quenching sites in LHCII to tune accordingly the qE response. Low temperature fluorescence spectroscopy and the occurrence of absorption changes related to qE (Figures 3.17 and 3.10) are fingerprints of antenna aggregation and constitute evidence of the “LHCII aggregation” model as a mechanism of NPQ (Horton *et al.*, 1991). However, we acknowledge that the F700 fluorescence band was observed only when chloroplasts were shone with high light and the quenching obtained was irreversible. Although earlier proposals that the red-shifted fluorescence emissions associated with irreversible quenching originate from RCs, this is not applicable to lincomycin-treated plants, since they lack core proteins (Nematov *et al.*, 2017). However, F700 was also observed in LHCII crystals, where protein-protein interactions are not prominent, suggesting that the parameter is not strictly correlated with LHCII aggregation (Pascal *et al.*, 2005). In the future, electron microscopy methods should be used to unequivocally address the occurrence of aggregation-mediated quenching in LHCII-only thylakoid membranes. Overall, we demonstrated that LHCII in the thylakoid membranes possess an intrinsic flexibility that allows them to switch between light harvesting and photoprotective conformations in function of changing environmental and metabolic conditions, as already attested in isolated complexes (Krüger *et al.*, 2013). Plants must regulate their photosynthetic processes in a tight window of physiological ΔpH to guarantee that photochemical reactions of energy storage take place and simultaneously avoid photoinhibition (Horton *et al.*, 1996). Consequently, qE is a highly cooperative process and allows plants to respond efficiently to small ΔpH changes to regulate photosynthesis. Our results point towards an allosteric action of PsbS and Zea, to control the relationship between qE and ΔpH and the cooperativity of quenching *in vivo*. Aggregation of LHCII is possibly the strategy adopted by plants to finely and reversibly tune their light harvesting efficiency, allowing for a robust and “economic” photoprotection to occur (Horton *et al.*, 2000; Belgio *et al.*, 2014).

Chapter 4

Investigation of the conformational change of LHCII associated with qE

4.1 Isolation of LHCII enriched in xanthophyll cycle carotenoids

The structural details of the major LHCII monomer are displayed in Figure 4.1a. Among the four Car binding sites present, the site that incorporates the xanthophyll cycle Cars (violaxanthin, Vio and zeaxanthin, Zea), called the V1 site, is situated at the periphery of the complex. In the native trimeric form of LHCII, this site is easily reached by the luminal de-epoxidase that converts Vio to Zea during high light exposure (Figure 4.1b) (Liu *et al.*, 2004). A combination of low pH and the presence of the cofactor ascorbate are required to modulate the activity of the enzyme (Jahns *et al.*, 2009). On the opposite side, upon exposure to low light or darkness, the activity of the de-epoxidase ceases whilst that of the stromal epoxidase increases. Molecular oxygen was catalogued among the cofactors required for the activity of this latter enzyme, that catalyses the reconversion of Zea to its original form, Vio (Siefermann and Yamamoto, 1975). To study the effects of the accumulation of Zea in LHCII, we aimed to isolate LHCII with a large fraction of xanthophyll cycle Cars bound in the V1 site. The procedure of thylakoid extraction from spinach leaves

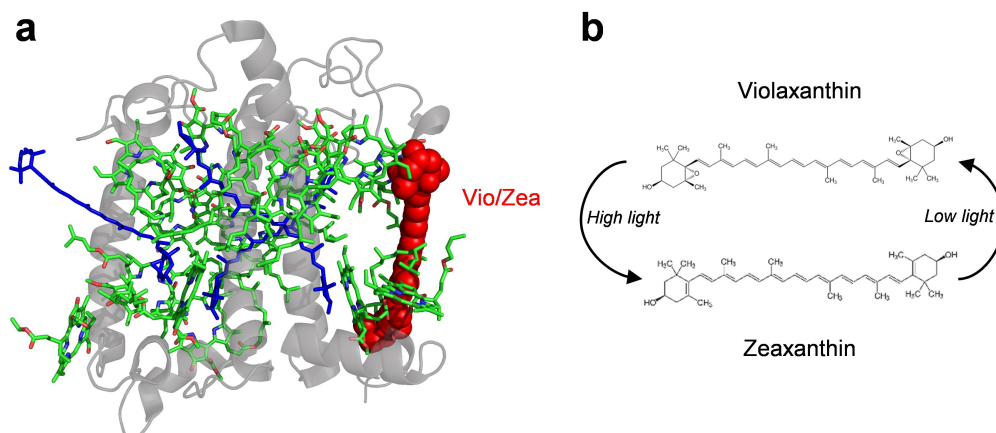


Figure 4.1: **LHCII has a peripheral Car binding site involved in the xanthophyll cycle operation.** **a** Structure of the LHCII monomer represented with PyMol software. The protein scaffold is shown as grey cartoon. Chls and Cars are shown as green and blues sticks, respectively. In red, represented as filled spheres, the xanthophyll cycle Car (Vio or Zea) is displayed. **b** Simplified scheme of the xanthophyll cycle operations, whereby Vio is de-epoxidised to Zea and Zea is epoxidised back to Vio. The intermediate reaction that leads to antheraxanthin formation is omitted for clarity, as well as the cofactors required for the enzymatic reactions.

was modified to achieve a great extent of deepoxidation and at the same time inhibit epoxidation to occur. Spinach leaves were first subject to a light treatment for 1 hour with high light ($900 \mu\text{mol m}^{-2} \text{s}^{-1}$) in an atmosphere saturated with nitrogen ($\text{N}_2 \geq 98\%$, $\text{O}_2 \leq 2\%$). In these conditions the deepoxidase works at maximal rates and Zea accumulates. Both enzymes exhibit a strong dependence upon temperature and epoxidation is slowed down significantly at 5°C (Reinhold *et al.*, 2008). Therefore, all the following steps of thylakoid extraction were rigorously performed on ice, to maintain high the amount of Zea synthesised. The so-prepared thylakoids were then incubated for 1 hour in a low pH medium (pH 5.5) in the presence of exogenously added ascorbate, to progress further the de-epoxidation reaction. After obtaining Zea-enriched thylakoids, a solubilisation with the mild non-ionic detergent β -DDM was employed to retrieve the fraction of LHCII trimers in the most intact state possible. Through careful biochemical solubilisation assays, it was shown that the xanthophyll cycle Cars are loosely bound to the protein scaffold and therefore are easily lost upon purification (Ruban *et al.*, 1999). Thus, in our approach, we first titrated the ratio of detergent to Chl required for a full solubilisation of the LHCII complexes by separating with sucrose density gradient ultracentrifugation or

size exclusion chromatography thylakoid membranes solubilised with different concentrations of β -DDM (data not shown). The appearance of the trimeric LHCII band, at a concentration of sucrose of ~ 0.3 M in the density gradients, was detected for β -DDM/Chl ratios of ~ 10 for Vio-enriched thylakoid membranes and ~ 7 for Zea enriched. These slight differences could reflect a differential tendency to solubilise due to reorganisation during high-light treatment of the thylakoid membranes, that exhibit a high flexibility in response to the light environment (Ruban and Johnson, 2015).

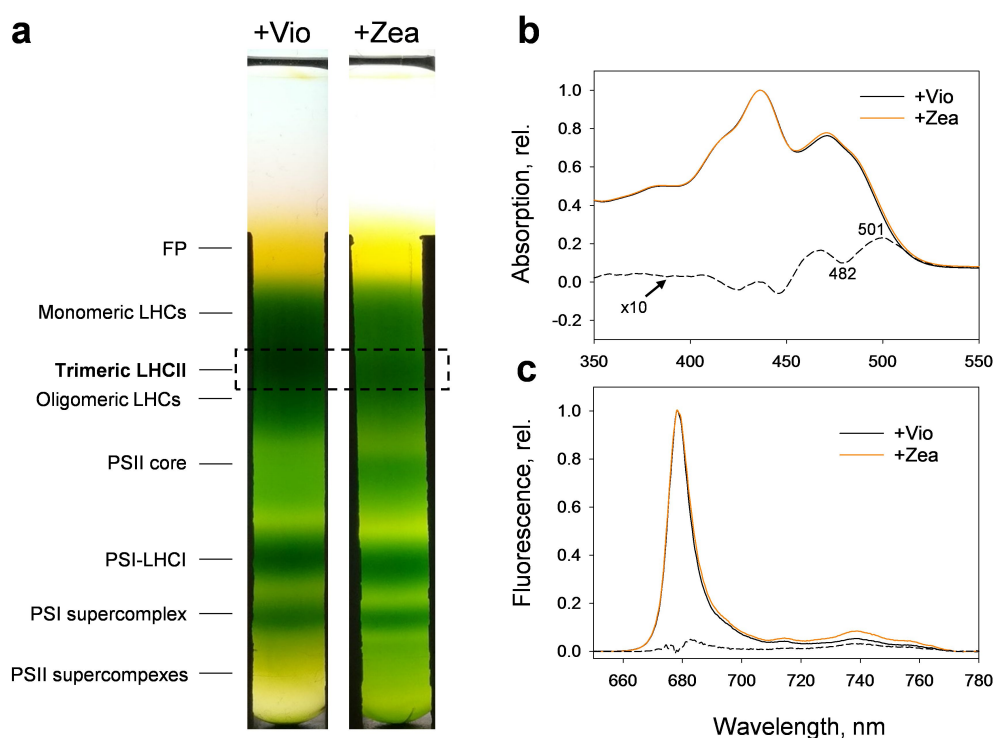


Figure 4.2: **Isolation of LHCII enriched in Vio or Zea.** **a** Representative sucrose density gradients after centrifugation of fractionated thylakoids. Solubilisation of the membranes was achieved by incubating them for 1 hour on ice in the presence of 25 mM β -DDM (β -DDM/Chl=13). The fraction of trimeric LHCII collected and used in the experiments is shown delimited by a dashed box. **b** Absorption spectra of Vio-LHCII (black) and Zea-LHCII (orange), normalised at the maximum of the Soret band. **c** 77K fluorescence emission spectra of LHCII, normalised to their maximum. To avoid reabsorption artefacts, LHCII were diluted to 3 μ g/ml of total Chl. The difference spectra (Zea-Vio) are plotted as dashed lines.

Figure 4.2 a shows the representative sucrose gradient obtained after solubilisation at a β -DDM/Chl ratio of 13. These conditions were chosen for the experiment

CHAPTER 4. INVESTIGATION OF THE CONFORMATIONAL CHANGE OF LHCII ASSOCIATED WITH QE

Sample	Chl a/b	DES	%Vio/Car	%Zea/Car
LHCII + Vio	1.48 ± 0.01	-	17.25 ± 0.82	-
LHCII + Zea	1.42 ± 0.01	76.19 ± 1.52	3.84 ± 0.36	12.27 ± 0.29

Table 4.1: **Pigment composition of Vio- and Zea- enriched LHCII.** LHCII samples were taken directly after purification via sucrose density gradients and pigments were extracted in 80% acetone/20% water for HPLC measurements. Chl a/b, Chl *a* to Chl *b* ratio; DES, de-epoxidation state. Amounts are expressed as percentage relative to the total Car pool.

since the LHCII thus retrieved showed a high retention of xanthophyll cycle Cars and were characterised by a Chl *a/b* ratio close to 1.33, typical of the major LHCII complex (Table 4.1) (Liu *et al.*, 2004). This value was slightly higher in our preparations, indicating a smaller contamination with minor antenna complexes. Based on the Chl ratios reported of 2.6, 1.9 and 1.2 for CP29, CP26 and CP24, respectively (Ruban, 2012; Peter and Thornber, 1991), and assuming a homogenous distribution of the complexes within the LHCII band, the calculated contamination of the collected LHCII fraction with minor complexes is around 10% or less which is negligible in our analysis. The total amount of xanthophyll cycle Cars in the two preparations is comparable (17.25% for Vio-enriched LHCII and 3.84+12.27=16.11% for Zea-enriched LHCII) and these values correspond to a xanthophyll binding ≥ 0.64 mol per monomer. The de-epoxidation index (DES) is high for the light treated samples (76.19±1.52%) but does not reach 100% as the values attested during *in vitro* de-epoxidation of LHCII (Jahns *et al.*, 2009), indicating that a minor fraction of Zea was either not formed or was reconverted back to Vio and reflecting possibly the small amounts of Vio bound to minor complexes. This eventually results in a binding of roughly 0.5 molecules of Zea per LHCII monomer compared to the value of 0.7 of Vio. The efficiency of de-epoxidation was also evaluated by comparing the differences in the LHCII absorption spectra between the dark-adapted and the light-treated conditions (Figure 4.2 b). The absence of the oxygen atom in the head groups of the Car Zea effectively increases the conjugation length (N) of the carbon double-bond chain compared to Vio, shifting the absorption transition to the second excited state (S_2) by several nm to the red. The difference absorption spectrum showed a characteristic wavy pattern that mirror the 3-finger vibronic band of the absorbing Cars (corresponding to 0-0, 0-1 and 0-2 vibronic transitions). The positions of the red-most maximum and minimum, 501 nm and 482 nm, correspond

to the increase in Zea absorption and the decrease in Vio absorption, respectively, thereby confirming the selective enrichment of Zea in the light-treated samples. It has been reported that the binding of Zea does not alter the spectroscopic characteristics of LHCII (Caffarri *et al.*, 2001). Nevertheless, precise low-temperature measurements of reverse transmittance have indicated that there could be a small contribution of Zea during excitation energy transfer. Moreover, it has been recently suggested that the accumulation of Zea in the thylakoids could lead to the formation of strong excitonic interaction between Chl *a* and this Car, correlating to the non-photochemical quenching of excess energy (Bode *et al.*, 2009; Park *et al.*, 2018). The low temperature fluorescence emission spectrum of Vio and Zea enriched LHCII differs subtly, suggesting some changes in the site energies of the emitting Chls in the complex (Figure 4.2). A small red shift occurs in the presence of Zea, as highlighted in the difference spectrum. This feature is maintained in the room temperature fluorescence spectrum where the Zea-enriched sample is composed of two sub-peaks, 3 nm far apart, and the red sub-peak is not present in Vio-enriched samples (Tutkus *et al.*, 2019). Curiously, such broadening of the LHCII fluorescence main peak, bears similarities with a mutant where the terminal emitted locus is disrupted by site mutations in the protein scaffold (Ramanan *et al.*, 2015; Malý and Van Grondelle, 2018). A reduction of the coupling strengths between pigments can indeed result in an increased delocalisation of the excitation over multiple emitting Chl molecules. Our results suggest that some pigment interactions are changing when Zea binds to LHCII, possibly leading to small changes in the coupling that result in observable differences of the fluorescence spectra. To some extent, also the vibronic satellite band differs between Vio- and Zea- enriched samples, being more pronounced in the former.

4.2 The dissipative conformational change in LHCII

To investigate the photoprotective switch that the protein undergoes during the onset of NPQ, aggregation of the isolated LHCII complexes was achieved by dilution in a low detergent and low pH buffer to achieve a final concentration of detergent lying

significantly below the critical micellar concentration and a pH of 5.5 (Figure 4.3). These conditions mimic the state of the thylakoid membrane during high light ex-

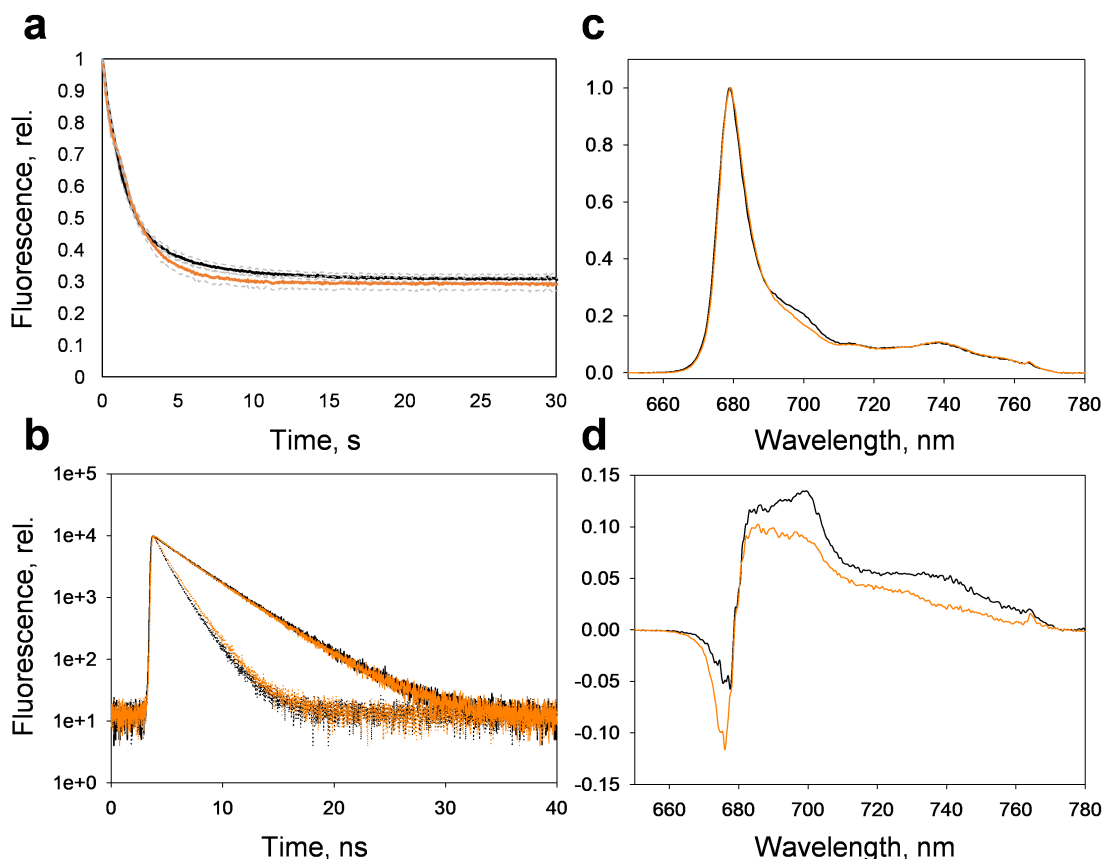


Figure 4.3: **Induction of the photoprotective conformation in LHCII.** **a** Chl fluorescence quenching induction traces of Vio- (black) and Zea- (orange) enriched LHCII, measured with steady-state PAM fluorimetry. At time 0, LHCII were resuspended in a low-pH/low-detergent buffer for a final $[\beta\text{-DDM}] = 6 \mu\text{mol}$. **b** Chl fluorescence lifetime decays measured for samples in **a** before (solid lines) and after (dotted lines) quenching induction. **c** Steady-state 77 K fluorescence emission spectra measured for samples in **a** after quenching induction. **d** 77 K fluorescence difference spectra (quenched-minus-unquenched) of samples in **a**.

posure, where the lumen pH is significantly lowered by the proton pumping activity of the photosynthetic complexes and the antenna proteins form aggregates (Horton *et al.*, 1991; Betterle *et al.*, 2009; Johnson *et al.*, 2011b; Ruban, 2018). The change of buffer was immediately accompanied by a sustained decrease in the fluorescence yield (Figure 4.3 a), that reaches a plateau at $\sim 30\%$ of residual fluorescence signal. It has been previously reported that the differential presence of the xanthophyll

CHAPTER 4. INVESTIGATION OF THE CONFORMATIONAL CHANGE OF LHCII ASSOCIATED WITH QE

Sample	A ₁ (%)	μ_1 (ns)	A ₂ (%)	μ_2 (ns)	$\langle\mu\rangle$ (ns)
Vio-LHCII, pH 7.8, 0.03% DDM	93	3.78 0.01	7	1.54 0.1	3.62
Zea-LHCII, pH 7.8, 0.03% DDM	90	3.74 0.02	10	1.67 0.08	3.53
Vio-LHCII, pH 5.5, low DDM	63	1.73 0.01	37	0.85 0.02	1.4
Zea-LHCII, pH 5.5, low DDM	55	1.93 0.02	45	1.08 0.02	1.55

Table 4.2: **Bi-exponential description of the fluorescence decay kinetics in Vio- and Zea-enriched LHCII trimers before and after quenching induction** Exponential components used to fit the fluorescence lifetimes data (Figure 4.3b) with their relative amplitudes (%). The amplitude weighted average lifetime is shown ($\langle\mu\rangle$).

cycle Cars interferes with the amplitudes and the rates of the dissipative switch in LHCII (Ruban *et al.*, 1994a; Ruban and Horton, 1999). The effect however, was very evident only when exogenously applied Cars were added in the solution with LHCII. Our results displayed in Figure 4.3a show the effect of endogenously accumulated Zea or Vio and their binding to LHCII. The induction traces highlight that the extent of energy dissipation is virtually identical in both the conditions ($69.16 \pm 1.37\%$ and $70.89 \pm 1.97\%$ for Vio- and Zea- enriched samples, respectively). This suggests that there is no major quenching channel opened by the mere binding of Zea to the complex. By looking at the kinetics of the dissipative switch in more detail, it is noticeable, that their behaviour is multi-exponential, and can be described by at least two components. The initial, very fast drop in the fluorescence yield is attributable to an effect mediated by protonation, which becomes more favourable when the detergent concentration in the medium is low (Petrou *et al.*, 2014). The second, slower phase is likely due to aggregation of the complexes, triggered by interactions between the hydrophobic regions of the proteins freed by detergent molecules. These multi-meric interactions, in turn, are thought to stabilise the quenched conformation, by decreasing the activation energy between the light-harvesting and photoprotective state (Wentworth *et al.*, 2003; Santabarbara *et al.*, 2009). Therefore, the ongoing LHCII aggregation pushes further the quenched conformation. A somewhat faster decline of the fluorescence intensity in samples containing Zea is observable (Figure 4.3a). While the first, fast phase of the induction is identical for both samples, the differences seem to affect the slower exponential decay component. This suggests that Zea favours the aggregation of light harvesting complexes, in line with previous

results showing that Zea and Vio modulate the oligomerisation of LHCs by an agonistic and antagonist effect, respectively (Ruban *et al.*, 1994a, 1997b; Ruban and Johnson, 2010). The difference in the kinetics is reproducible, but is small and not statistically proven due to great variability between samples. This is likely due to the fact that we are working with physiological amounts of xanthophylls and not with Cars added in excess to the reaction medium. Furthermore, a hysteretic behaviour of the qE dependence on ΔpH was observed in the membranes, where the accumulated Zea shifts the pH requirements to less acidic environments. Due to the design of our experiments, since we aimed to investigate the switch of LHCII between the two extreme functional states, it was not possible to grasp in detail the xanthophyll effect during states of intermediate pH or detergent values.

Chl fluorescence lifetime decays show a very similar trend in Vio- and Zea-enriched LHCII, both before and after quenching induction (Figure 4.3b). A more detailed look to the components used to fit the lifetime data reveal the markedly similar bi-exponential behaviour, and the amplitudes and lifetimes of the components used almost unaltered, resulting in very close values of mean lifetime kinetics ($\langle\mu\rangle$).

On a similar note also the fluorescence spectra, measured at a steady-state fluorescence value after the quenching induction, show a nearly identical profile, suggesting that the nature of the quenching switch is common, regardless of the xanthophyll-cycle profile (Figure 4.3c). The difference spectra (quenched-minus-unquenched) for Vio- and Zea-enriched LHCII show a common pattern of changes occurring upon quenching, involving the red-shift of the main fluorescence band and the small increase in fluorescence at 700 nm. All peaks are conserved, independently of Car composition.

4.3 Fluorescence blinking of single LHCII trimers

To further investigate the LHCII conformational switch we studied the Chl fluorescence behaviour of single LHCII complexes through single-molecule (SM) fluorescence microscopy. This way, we were able to retrieve the fluorescence profile of isolated LHCII in controlled conditions while avoiding protein-protein interactions to take place. SM fluorescence microscopy is useful to resolve spectral and dynam-

ical features that can be hidden in ensemble measurements (Kondo *et al.*, 2017) and to resolve protein motions ($1\text{-}10\text{ s}^{-1}$) that are impossible to retrieve from bulk measurements (Krüger *et al.*, 2011a). As a result, this approach allowed us to clarify whether the observed differences in ensembles (Figure 4.3) are due to intrinsic conformational dynamics of single proteins or to structural rearrangements occurring during LHCII aggregation. The method applied, based on Total Internal Reflection Fluorescence (TIRF) was recently applied by Valkunas and co-workers to shed light on the effect of a different Car composition on the conformational dynamics of LHCII (Tutkus *et al.*, 2017). Single trimers were exposed to 635 nm red light, preferentially absorbed by Chl *b*, and their fluorescence intensity was monitored for several seconds with 50 ms integration time. The acquired fluorescence signal coming from the single LHCII complexes exhibited a well-known blinking behaviour, where the fluorescence intensity switches quickly and reversibly between several stable emitting states and dark, non-emitting states, as a result of the conformational changes occurring in the protein scaffold (Krüger *et al.*, 2011b; Iliaia *et al.*, 2011b; Tutkus *et al.*, 2017; Schlau-Cohen *et al.*, 2015). By averaging >200 distinct complexes, the time dependent distribution of the various intensities was obtained (Figure 4.4), for samples enriched in Vio or Zea, under light harvesting- (high pH, high detergent, panels a and b) or NPQ-mimicking conditions (low pH, low detergent, panels c and d). The colour of the plots represents the number of complexes in that particular fluorescence state and therefore its probability to occur at a certain time after excitation. At earlier time delays, more complexes are present in a highly fluorescent state, which is partly due to the absence of photobleaching and to the fact that only emitting states were originally detected under the microscope at the beginning of the experiments. At later times, the zero-intensity population decreases, due to reversible switching of the protein to non-fluorescent states and to the irreversible photobleaching processes. After 30 seconds, photobleaching affected almost all complexes. Notably, under an NPQ-mimicking environment (low pH, low detergent), the probability of emitting states decreased steeply over a few seconds from the beginning of the measurements (Krüger *et al.*, 2012). This feature is particularly evident in Figure 4.4e and f, that show the integration of the first points from 0 to 10 seconds. Within this time window, most trimers are still in an active, non-bleached form, which guarantees the study of the true dynamics due to protein conforma-

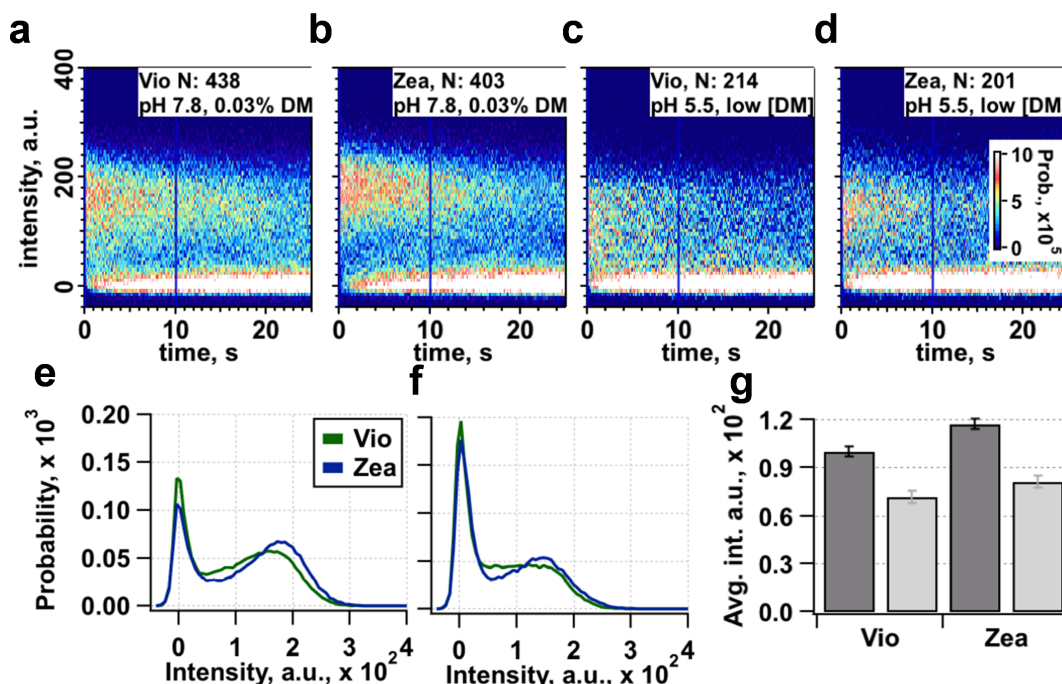


Figure 4.4: **Zea doesn't induce changes in the fluorescence intensity profiles of single LHCII trimers.** **a-d** Single molecule (SM) fluorescence emission plots. The emission intensity (y-axis, a.u.) is correlated to the time of its detection (x-axis, s). Each plot is the average of N measurements, specified in its top-right corner. **a,b** High detergent and high pH conditions; **c,d** Low detergent and low pH conditions. Vio- enriched samples are displayed in panels **a** and **c**, while Zea-enriched in panels **b** and **d**. The colour scale represents probability density. **e,f** Graphs showing the integration of the first 10 seconds of the recordings as marked with vertical lines in panels **a,b** and **c,d**, respectively.

g Average intensity of population of SM traces from 0 to 10 s. Black, high detergent, high pH conditions, grey, low detergent low pH.

tional fluctuations and their modulations by external cues. No major differences in the profiles are present comparing Vio and Zea enriched samples, showing that no specific quenching site seems to be active in the presence of Zea. Figure 4.4g shows the average intensity values under all conditions probed. A $\sim 30\%$ reduction of the fluorescence level was measured upon induction of the photoprotective state. This value is far from the nearly 70% quenching observed in bulk measurements (Figure 4.3) and may reflect the importance of protein-protein interactions to achieve the sustained quenched conformations observed in the crowded thylakoid membranes. A partial explanation for this result could also come from the omission of deeply

quenched complexes from the analysis, which were too dim to be detected under the microscope. It was estimated, however, that their consideration in the calculations would stretch the quenching extent to $\sim 50\%$, a value still far from the 70% of ensemble measurements (Tutkus *et al.*, 2019). Unexpectedly, LHCII trimers enriched in Zea showed a higher value of fluorescence intensity under the light harvesting conditions. Upon induction of quenching, the differences compared to Vio-LHCII become less pronounced, reflecting a higher extent of quenching in the presence of Zea. This is somewhat in line with the effect reported for the xanthophyll on WT chloroplasts (Johnson and Ruban, 2009) and it can underline differences in the extent of the inherent switch of LHCII with different Car compositions (Johnson *et al.*, 2010). A similar finding was also observed in ensemble measurements (shown only normalised in figure 4.3), where a $\sim 15\%$ larger fluorescence value was registered in the presence of Zea ($P < 0.05$).

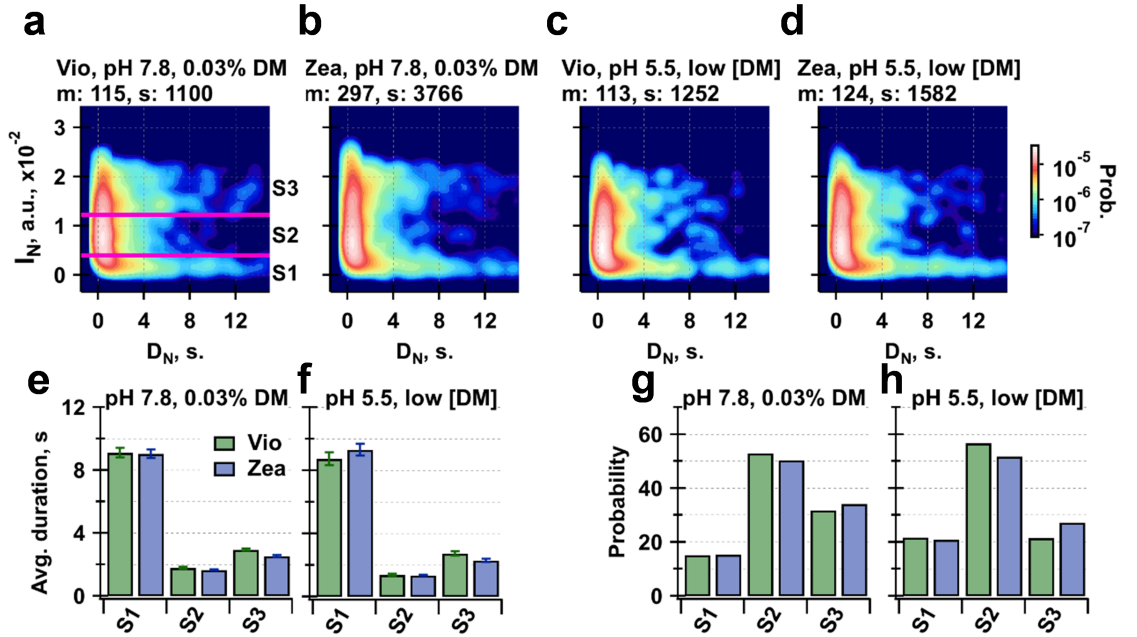


Figure 4.5: **The duration of LHCII conformational states is not significantly altered by xanthophyll cycle Cars.** a-d Intensity of the N-state (I_N) vs its duration (D_N). a,b High detergent high pH conditions, c,d Low detergent low pH. Number of included molecules (m) and detected intensity states (s) are indicated at the top of each graph. Plots are normalised to their total area. Logarithmic colour scale represents probability density. e,f Mean duration and g,h probability of S1,S2 and S3 fluorescent states marked in plot a.

An Intensity Point Change (IPC) detection algorithm was used to analyse in greater detail the fluorescence intensity variations (Krüger *et al.*, 2011b; Tutkus *et al.*, 2017, 2019). The time-resolved traces are scanned point-by-point with an 8-point window. Averages of the first and last 4 points are calculated and compared to retrieve a value of a step amplitude (the difference between the averages) within that selection window. This is then compared to a threshold value, found empirically by testing different numerical values, to determine if a conformational change, leading to a switch between different fluorescing states, is occurring. This way, it is possible to correlate the intensity of a certain emitting state to its duration. Figure 4.5a-d shows the graphs of the states duration under different buffer conditions and Car compositions. In the majority of the cases, the duration of a state does not exceed 2-3 seconds and after this time the LHCII switches conformation and accesses another state. Some trimers however, were found in the same fluorescent state for up to 15 seconds. With this analysis it was possible to distinguish between the populations of at least three different intensity states, namely S1, a dim or dark state (<20 a.u.), S2, an intermediate intensity state (>20 a.u. and <130 a.u.), and S3, a highly fluorescent state (>130 a.u.) (Figure 4.5a). The average duration of these states is almost identical for Vio- and Zea- enriched LHCII (Figure 4.5e,f). The mean duration of the S1 state is ~ 3 times higher than the one of the fluorescing states S2 and S3. Among them, the intermediate S2 state is the shorter one and on average it doesn't exceed 2 seconds of duration. Although inducing only small alterations of the duration/intensity distributions, the reduction of detergent concentration and pH level lead mainly to the shortening of S2 and increased probability for the S1 state at the expense of S3. It is worth to note that the analysis we performed was coarse due to resolution limitations and did not take into account for example the possibility of peculiar highly fluorescing states accessed only during "light-harvesting" conditions, which were more evident in a previous work (Tutkus *et al.*, 2017). Plots of the probability of LHCII to be found in a certain state show that S3 and S1 populations are affected by the different buffer conditions (Figure 4.5g,h). When pH and detergent are lowered, S1 increases probability by a 5-6% and S3 access is decrease by up to a 10%. Although the S2 state duration is short, on average, it is the most populated state and probably several LHCII configurations bring about similar intermediately fluorescing states. Again, no significant differ-

ences are evident between Vio- and Zea- enriched samples. It is only noticeable a tendency for S3 to be more represented in the presence of Zea and for S2 to be proportionately less populated.

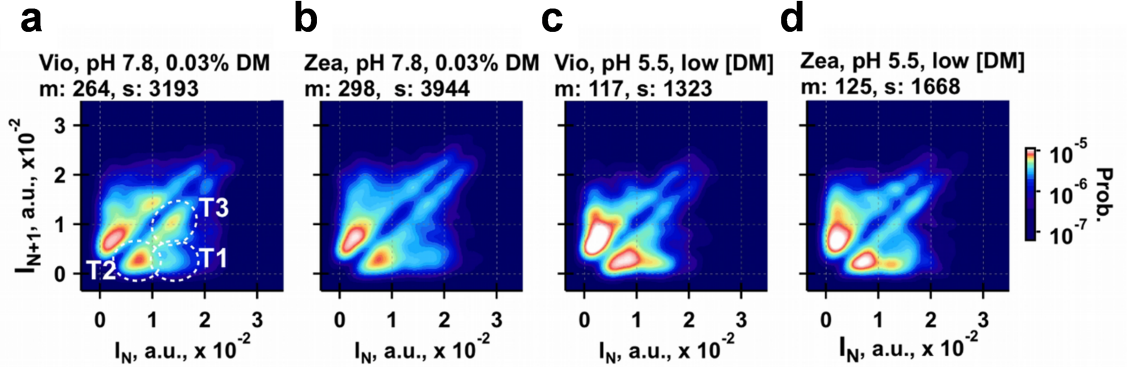


Figure 4.6: **Zea marginally affects the switch of LHCII complexes between different conformational states under NPQ conditions.** Transition density plots correlating the average intensity of a certain state N (I_N) to the average intensity of the following state $N+1$ (I_{N+1}). **a,b** High detergent high pH; **c,d** low detergent low pH conditions. Number of included molecules (m) and states (s) are indicated above each graph. Plots are normalised to probability density function. Logarithmic colour scale represents probability density.

Additional to changes associated with the intensity-to-duration correlations, we checked whether the pathways of transition between different states are affected. For this purpose, transition density maps were prepared, in which the intensity of a particular state is correlated with the fluorescence intensity of the next one directly accessed. The results are presented in Figure 4.6. The plots represent a dispersed distribution of the data, but some dominating transitions are detectable, which are marked in Figure 4.6a. T1 identify the transition from the strongly emitting state S3 to the dark/dim S1 state; T2 represent the transition from the intermediate S2 to S1; T3 marks the transition from S3 to S2. The maps are highly symmetrical, meaning that the forward and backward transition between a set of conformations is equally probable. This is somewhat different from what was previously reported on LHCII from mutants unable to accumulate luteins (Tutkus *et al.*, 2017). It means that the free energies of the states engaged in these transitions are very similar. Although being almost iso-energetic, however, the accessibility of these states varies based on the external buffer and Car composition. The differences between Vio and Zea enrichment is once again subtle, but it is noticeable that, in the presence of Zea,

T3 is strongly diminished, while transitions between lower fluorescence intensities and dark states is favoured (T2). Switching to buffer conditions mimicking the NPQ state, LHCII exhibit a shift in the probability of these transitions and T3 becomes infrequent whilst the T2 transition becomes strongly predominant.

4.4 Conclusions

In this study, we compared the conformational dynamics of LHCII with a different composition of the externally bound, xanthophyll cycle Cars. The light treatment and the careful solubilisation conditions used in the study allowed us to achieve a good de-epoxidation state and a good retention of Vio and Zea to the isolated LHCII (Figure 4.2 and Table 4.1). With the aid of fluorescence spectroscopy, we probed both the ensemble and the SM dynamics, showing that a selective enrichment in either of the two xanthophylls does not induce major changes in the switch of LHCII to the quenched state. However, marginal differences were observed in steady-state spectra of the unquenched state (Figure 4.3b) as well as in the transition between conformational states (Figure 4.6a,b) suggesting that the Vio-Zea enzymatic conversion induces some changes in the pigment energies due to the alteration of some pigment-pigment interactions. These changes can hardly be correlated to the NPQ induction from our results, because we observed that there aren't differences in the final quenching amplitudes reached (Figure 4.3a), nor in the distribution of fluorescence intensities of single trimers (Figure 4.4). Under typical low-light conditions (*i.e.* high pH level, high detergent concentration) the presence of Zea results in stronger fluorescence compared to the Vio-samples, that might even reduce the unnecessary loss of excitation energy. Additionally, the transition plots are virtually identical between the two Car subsets upon induction of the photoprotective state showing that Zea does not alter the probability of the conformational states accessible by the LHCII trimers (Figure 4.6c,d). Interestingly a difference was noticed in the fluorescence quenching induction of LHCII, whose kinetics exhibit a steeper decrease in the presence of Zea (Figure 4.3a). The results underline the ability of the latter sample to switch faster to a dissipative state and, since only the slower component of quenching is affected and the fast, pH-dependent component is unaltered, it suggests that this may be due to Zea favouring aggregation of the complexes (Ruban

et al., 1997b; Ruban and Johnson, 2010; Horton *et al.*, 2000). Antenna aggregation was shown to occur *in vivo* (Johnson *et al.*, 2011b) and is thought to stabilise the quenched state, providing a fine control of the light harvesting function of LHCII in the membrane (Ruban, 2018). Our results match nicely the recent findings of Croce and coworkers (Xu *et al.*, 2015) showing that Zea binding doesn't induce any quenching effect on isolated LHCII proteins or supercomplexes, but it only exerts its effects on intact thylakoid membranes. The integration of this knowledge with our findings suggests that endogenously accumulated Zea is not involved *per se* in the formation of the quenched state in LHCII, but is likely related to a structural effect of the Car on the dynamics of inter-complexes interactions (Phillip *et al.*, 1996; Ruban *et al.*, 1997b, 1998a). Prominent among the alternative views concerning the role of Zea are the proposals that Zea binding to LHCs induces the formation of a channel for energy dissipation through a mechanism involving direct excitation energy transfer or charge transfer states (Avenson *et al.*, 2008; Dall'Osto *et al.*, 2005; Ruban and Johnson, 2010; Bode *et al.*, 2009; Holt *et al.*, 2005; Park *et al.*, 2017, 2018). These proposals, therefore, suggest a photophysical effect of Zea during NPQ induction, with a direct effect on the energy transfer and trapping dynamics. Initial proof of these theories was obtained through the analysis of reconstituted recombinant LHCs or antenna complexes isolated from Arabidopsis strains over-expressing the xanthophyll (*i.e.* *npq2* mutants) (Crimi *et al.*, 1998; Bassi and Caffarri, 2000; Bassi *et al.*, 1993; Dall'Osto *et al.*, 2005; Fuciman *et al.*, 2012). In these cases, the internal L1 and L2 sites of the complexes were shown to incorporate efficiently Zea leading to a quenching effect. However, it has been debated the relevance of this mechanism in a more native environment, as the efficiency of Vio de-epoxidation was reported to be very low for the inner binding sites, being inaccessible to the de-epoxidase enzyme (Jahns *et al.*, 2001; Ruban *et al.*, 1999; Wehner *et al.*, 2006; Jahns *et al.*, 2009). More recent works (Park *et al.*, 2017, 2018) make use of pump-probe techniques to study native thylakoid membranes, but these are subject to artefacts due to non-linear optical effects such as singlet-singlet annihilation, which alters kinetics as well as time-resolved spectra of the probed samples (van Oort *et al.*, 2018), making ambiguous the assignment of Car signals to a specific xanthophyll. Also, the correlation between the signal attributed to Zea and the de-excitation of Chl excited states have not been strongly assessed. Understanding the physiologically relevant

role of Zea binding to LHCII after the de-epoxidation reactions is a difficult task, since no structural details are available about the binding site of this xanthophyll. Our work bears intrinsic limitations, one being that we recorded the dynamics of single LHCII under two particular conditions that represent the extremes of the light-harvesting and the dissipative state. It is possible that Zea exerts an effect under intermediate pH values and detergent concentrations and this will need to be tested in the future. It has indeed been shown that its accumulation shifts the pH dependence of quenching to higher values, thus suggesting that its physiological significance lies on the facilitation of the switch to a dissipative state (Johnson and Ruban, 2011; Ruban and Johnson, 2010). Moreover, the ensemble kinetics of the quenching induction showed some differences in the kinetics, while the initial and final fluorescence values were not affected. The SM experiments probe “snapshots” of LHCII in a steady state, not during the induction, therefore potentially losing the details of the transition between the unquenched and the quenched state. In the future therefore, new strategies should be envisaged to study the changes in the fluorescence dynamics of single trimers during the induction of the dissipative switch. Zea and PsbS are both crucial modulators of NPQ in plants. It is debated whether PsbS binds Zea to create a quenching site (Aspinall-O’Dea *et al.*, 2002; Dominici *et al.*, 2002). More recently, it was proven that the two factors are working independently and on apparently different time scales (Crouchman *et al.*, 2006; Sylak-Glassman *et al.*, 2014). Whilst both of them promote LHCII aggregation and accelerate the switch to the quenched state (this study and Johnson *et al.* (2011b)), their effect on the relaxation kinetics is markedly different. While PsbS is acting as a fast switch that allows for quick kinetics of formation and relaxation of the quencher, the de-epoxidation of Vio has a rather opposite effect, being activated relatively slowly and persisting in the dark, delaying the recovery of Chl fluorescence. The relevance of this difference is to be found in the adaptation of plants to sunflecks when PsbS-mediated prompt response of the regulation of the photosynthetic machinery is essential together with the establishment of a Zea-induced memory of illumination history (Ruban and Johnson, 2010), whereby the photosynthetic membrane is more prone to the dissipation of excess, potentially harmful excitation energy.

Chapter 5

Identification of the qE quencher

Chapter 3 provided experimental evidence that the site of excitation energy quenching during the onset of qE is the major LHCII trimer of PSII. In Chapter 4, the modulation of the qE process by the xanthophyll cycle Cars was determined and it was observed that the accumulation of zeaxanthin (Zea) is not a pre-requisite for quenching and the identity of the quenching pigment is different. In this last result Chapter of the results, I present the data collected with time-resolved absorption and fluorescence techniques that shed light on the quenching mechanism in LHCII. The nature of the quencher has been the conundrum of NPQ research since the 90s. At the beginning of that decade, the connection between the xanthophyll cycle and NPQ had emerged (Demmig-Adams, 1990). It was soon after that Owens and Frank groups (Owens *et al.*, 1992; Frank *et al.*, 1994) proposed a role for Cars (specifically Zea) as direct energy quenchers. Naqvi embraced these ideas and suggested that a variable coupling strength between Chls and Cars, enhancing dissipative interactions, could underlie the non-photochemical quenching processes in photosynthetic organisms (Naqvi *et al.*, 1997; van Amerongen and van Grondelle, 2001). Horton and coworkers suggested an alternative mechanism, based on the observation that long-wavelength Chls emerge after induction of NPQ. Their hypothesis was that Chl-Chl interactions could be enhanced during NPQ, as observed in quenched aggregates of isolated LHCII (Ruban *et al.*, 1991), giving rise to quenching Chl dimers (Horton and Ruban, 1992). More recently, the application of ultrafast transient absorption (TA) techniques, found the contribution of a Car excited state in the

de-excitation of Chls, prompting to the proposal that Cars in LHCII may serve as “natural born quenchers” of excess energy and act like a safety valve during photoprotection (Ruban *et al.*, 2007; Duffy and Ruban, 2015; Mascoli *et al.*, 2019). Although potentially being an extremely insightful technique, TA spectroscopy relies on the use of high laser powers, focused on small spots on the sample, and is subject to a series of undesirable drawbacks. Among these, singlet-singlet annihilation arises when the excitation density is high and two different excited states in the same pigment matrix meet on the same molecule, causing the net disappearance of one excitation (van Grondelle, 1985). Annihilation was shown to produce artefacts that can be deceiving and spoil the interpretation of the results, especially when analysing large multimeric systems, since it shortens the total excitation lifetime and affects the spectral shapes at early lifetimes (van Grondelle, 1985; Müller *et al.*, 2010; van Oort *et al.*, 2018). Based on this, Holzwarth and colleagues suggested to revisit the involvement of Cars during the process of NPQ, proposing instead that Chl interactions are the sole contributors to energy quenching *in vivo* (Müller *et al.*, 2010).

In the first part of the Chapter, I describe the approach that we adopted to investigate the nature of the quencher in isolated LHCII (*in vitro*), with high resolution and in the absence of annihilation artefacts. I will present the TA data obtained on *in vitro* isolated LHCII stabilised in the energy dissipative form, where the annihilation problem is bypassed by immobilising the complexes in polyacrylamide gels, impeding the formation of large aggregates. The second part seeks to describe the NPQ molecular mechanism in the native thylakoid membrane. I will present the time- and temperature-resolved fluorescence analysis (TRF) of intact chloroplasts isolated from lincomycin-treated plants, that are lacking photosystems RC proteins and therefore represent a simplified model to study the NPQ dynamics involving LHCII in their “natural” environment. Red spectral forms, that often correlate with NPQ formation *in vivo*, originate from Chl charge-transfer states, that are in this work disentangled from the quenching mechanism. The fluorescence data suggest that the nature of the quenching mechanism is an additional dark state which likely involves the participation of a Car molecule, supporting the findings on isolated LHCII complexes. A comparison with *in vitro* isolated LHCII aggregates evidences the similarity between the two fluorescence profiles, suggesting that re-

versible antenna aggregation is nature's pick to control light-harvesting efficiency in plant thylakoid membranes.

5.1 *In vitro*

5.1.1 Induction of efficient energy dissipation in isolated LHCII in the absence of protein aggregation

The preparation of LHCII immobilised in gels is described schematically in Figure 5.1. Major trimeric LHCII complexes were isolated from *Arabidopsis thaliana* plants via iso-electric focussing (IEF) following the solubilisation with β -DDM (1). After washing the LHCII fraction with fresh buffer to remove co-migrating ampholines (2), this fraction was embedded in the matrix of polyacrylamide gels, in order to immobilise single complexes and prevent their interactions (3). The gels were either kept in the fluorescent, unquenched state or underwent a procedure to induce and stabilise the dissipative, quenched state, as described by Iliaia and coworkers (Iliaia *et al.*, 2008). To this purpose, they were incubated overnight in a detergent-free solution and the fluorescence quenching was periodically monitored (4). Since LHCII were stuck in the gel matrix, no aggregation of complexes occurred, which would instead happen for complexes solubilised in buffer, in liquid phase. The possibility to quench single LHCII particles in the absence of clustering suggests that the latter is not required for the pigment quenching interactions and that the switch is internal to the single complexes. This was elegantly proved with the single molecule spectroscopy of LHCII that described the presence and interplay of “on”, highly fluorescent states alternating to “off”, dark forms of the complexes (Krüger *et al.*, 2010; Iliaia *et al.*, 2011b; Krüger *et al.*, 2013; Tutkus *et al.*, 2017, 2019). These works showed how factors such as pH, detergent and Car composition, affect the equilibrium of LHCII between the unquenched and the quenched conformations. The detergent bound to LHCII stabilises the protein on a similar way to how MGDG and other lipids provide support to it in the thylakoid membrane (Seiwert *et al.*, 2017; Thallmair *et al.*, 2019). A low detergent concentration provokes the collapse of the LHCII protein scaffold and brings about the formation of new quenching interactions between pigments. LHCII in gels could be quenched, following this principle, up to 5.5-fold

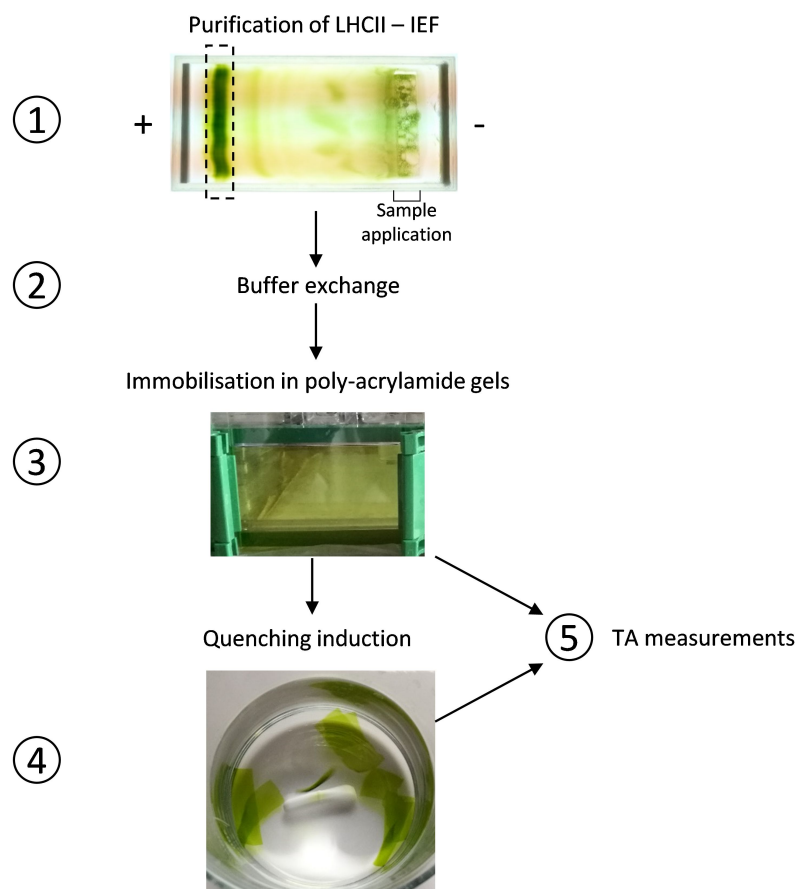


Figure 5.1: **Trapping of LHCII trimers into polyacrylamide gels.** Schematic representation of the procedure for isolation of LHCII trimers from *Arabidopsis thaliana* WT leaves, embedding into polyacrylamide gels and induction of the quenched conformation. IEF, iso-electric focussing; TA, transient absorption spectroscopy. See text for further details.

compared to the initial fluorescence intensity value (Figure 5.1; compare also Figure 5.11a). The so-prepared LHCII gels were then used in steady state spectroscopy and in TA measurements.

As briefly discussed above, singlet-singlet annihilation is a phenomenon in non-linear spectroscopy associated with the use of high laser powers on complexes that bind a high density of pigments (van Grondelle, 1985). If two excited states are present at the same time in a single complex, the probability of them to meet on the same molecule is very high, due to the fast energy equilibration in the system. Upon meeting, one excitation is boosted to a higher excited state level and rapidly decays

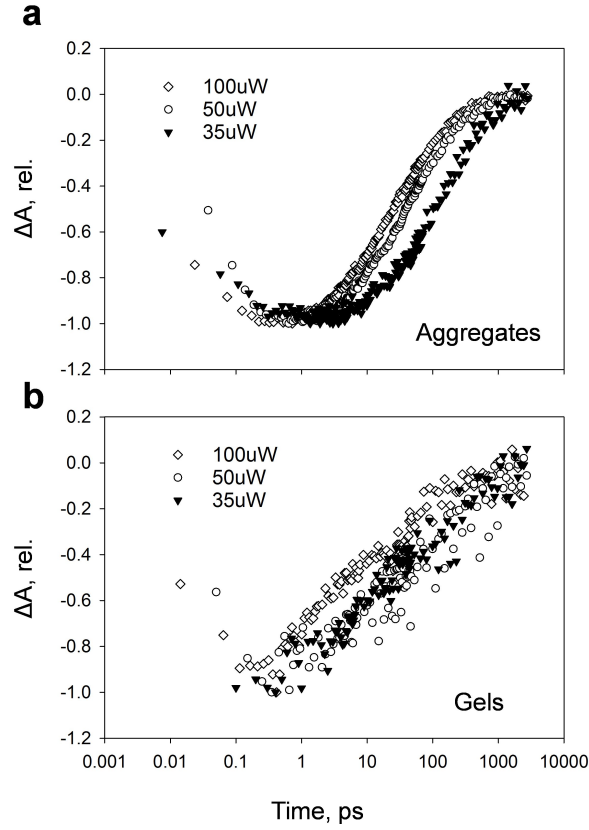


Figure 5.2: **LHCII in gels exhibit a negligible degree of singlet-singlet annihilation during TA measurements.** Power dependence study of aggregated LHCII (a) and LHCII in gels (b). Traces represent the decay kinetics of Chl Q_y ground state bleach (GSB) measured at 678 after direct Chl excitation at 674 nm using different laser powers. x-axis is shown in log scale and the kinetics are normalise to the minimum value of ΔA (difference absorption, see “Chapter 2: Methodologies and approaches” for details).

back to the lowest excited state, while the other one is lost, leading to a net loss in excitation energy of the ensemble. Therefore, as a result, the decay kinetics of the excited state are faster than the expected true dynamics of the system. Not only there is a discrepancy in the excitation dynamics, but it was also shown that the presence of singlet-singlet annihilation involves artefactual spectral changes in the timescale of picoseconds (ps) and that these resemble a coupled Chl-Car heterodimer, which could mistakenly be assigned to a quenching interaction (Müller *et al.*, 2010; van Oort *et al.*, 2018). Therefore, it is crucial when setting up experiments involving laser pulses to carefully determine the contribution of singlet-singlet annihilation and

to work when possible in “annihilation-free” conditions. Previously, it was shown that the removal of detergent bound to LHCII in gel is not leading to aggregation of the complexes and therefore embedding in gels minimises the impact of annihilation on the dynamics of LHCII pigments (Illoaia *et al.*, 2008; Rutkauskas *et al.*, 2012). Figure 5.2 shows the power study of LHCII used in our transient absorption experiments. As expected (Barzda *et al.*, 2001; Illoaia *et al.*, 2008), there is a marked dependence of the signal of the Chl excited state in LHCII aggregates on the laser power used. Already at the intermediate intensity value used in this study (50 μ W), the excited states decay visibly quicker than with the lower power tested (35 μ W, Figure 5.2a). On the other hand, this is not observed clearly in the quenched LHCII in gels, whose decay kinetics are comparable between the two conditions (Figure 5.2b). At the highest laser power tested (100 μ W) Chl excited states of LHCII in gels starts also to decay faster, since the excitation density increases significantly even in non-interacting LHCII trimers. Therefore, the gel system, by preventing aggregation of the complexes, offers an almost “annihilation-free” platform to study the true excited-state dynamics of quenched LHCII.

5.1.2 A new spectroscopic marker appears upon incorporation of LHCII in gels

Since the formation of the quenching interactions in LHCII decreases the excited-state lifetime of Chl *a*, traditionally, a TA experiment could help identifying the nature of this mechanism by investigating the events that follow the direct Chl *a* excitation. This was the experimental design that led to the finding that an energy transfer between Chl *a* and Lut 1 is responsible for energy quenching in LHCII aggregates (Ruban *et al.*, 2007). Figure 5.3a shows the comparison of the spectra of LHCII in gels and aggregates, obtained 10 ps after Chl *a* excitation.

Unexpectedly, profound differences are visible when comparing LHCII in buffers and in gels. Upon immobilisation in gels, a new excited state absorption (ESA) signal appears, peaking around 515 nm and displaying negative inflections reminiscent of Car ground state bleach (GSB). Induction of the quenched conformation enhances the amplitude of this new spectroscopic marker. However, no evident changes are associated with aggregation of LHCII in buffer. The spectrum of LHCII

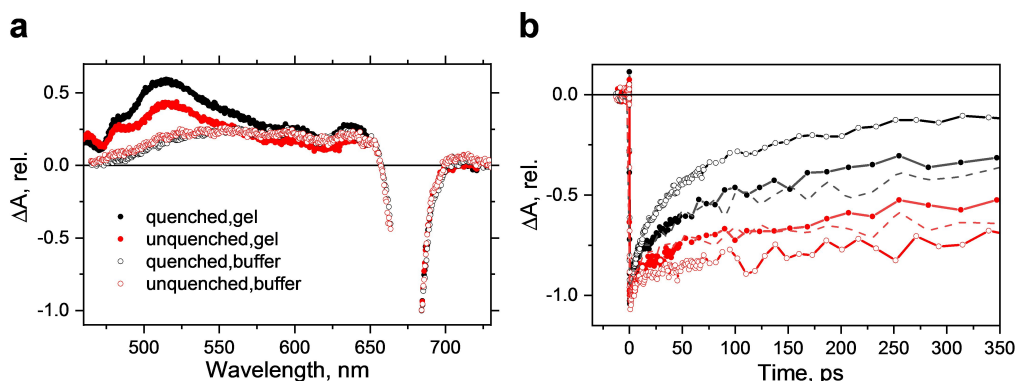


Figure 5.3: **A new spectroscopic marker appears upon incorporation of LHCII in gels.** **a** Spectra of quenched LHCII in gels or buffer (unquenched trimers and quenched aggregates) 10 ps after Chl *a* excitation at 674 nm. Spectra are normalised to the maximum value of Chl *a* Q_y GSB. **b** Normalised kinetics monitoring the Chl *a* Q_y signal decay, measured at 684 nm after excitation at 674 nm.

resuspended in solution is rather broad and featureless, which is characteristic of the S_1 - S_n transition of Chl molecules (Croce *et al.*, 2001). The kinetics of Chl *a* GSB display also some variations between LHCII in the two compared environments (Figure 5.3b). The extent of quenching is larger for LHCII in buffer, showing that LHCII aggregation apparently leads to deeper quenching than for complexes in gels, although similar Chl *a* fluorescence quenching amplitudes were measured for both from steady-state fluorescence (data not shown). An explanation for this discrepancy can be surely found in the higher extent of annihilation occurring in aggregates, which shortens the lifetime of Chl molecules (see Figure 5.2). Moreover, immobilisation on a gel offers a more controlled system for quenching induction, while the process of aggregation is more difficult to monitor and could progress even after the removal of adsorbent polystyrene beads from the buffer (see “Chapter 2: Methodologies and approaches” for details). On the other hand, the procedure of incorporation in polyacrylamide gels itself induces a certain degree of excitation energy quenching in LHCII, as the kinetics of Chl *a* are slightly faster than those of LHCII trimers in buffer, confirming previous data (Rutkauskas *et al.*, 2012).

5.1.3 The new marker is associated with a Car dark excited state and correlates to the quenching of Chl excitation

The new ESA signal recorded upon Chl excitation in LHCII in gels, appears to be blue shifted compared to all reported values of Car S_1 - S_n transitions (Fuciman *et al.*, 2012). A comparison with direct excitation of Car molecules highlights a blue-shift

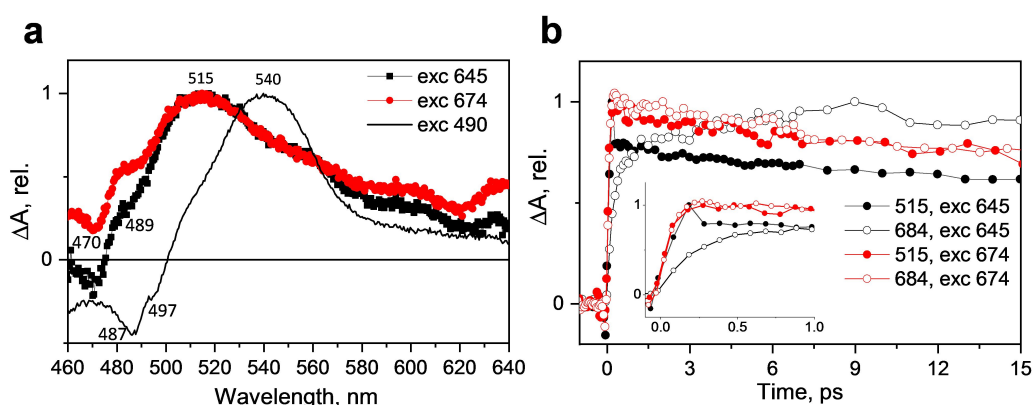


Figure 5.4: **The newly found Car signal differs from Car S_1 state.** **a** Spectra of LHCII in gels 10 ps after excitation at 674 nm, 650 nm and 490 nm, normalised at the maximum positive ΔA signal. **b** Kinetics in the first picoseconds of the new Car signal, measured at 515 nm (filled dots), and Chl *a* signal, measured at 684 nm (open dots), upon excitation of Chl *a* (674 nm, red) or Chl *b* (645 nm, black). The inset shows a close-up of the first picosecond after excitation.

of the newly found signal by 25 nm, from 540 nm of the measured Car S_1 absorption to 515 nm, after Chl excitation (Figure 5.4a). Negative inflections, attributable to Cars GSB are found at 487 nm and 497 nm upon direct Car excitation, and represent the signals from Neo and Lut molecules, respectively. Indeed, the 490 laser is not selective, since it falls exactly on the 0-0 absorption transition of both Cars, which are thus both excited. However, the negative signals after Chl excitation do not superimpose precisely with the Car GSB wavelengths, being found at 470 nm and 490 nm. Comparing the kinetics of Chl and the 515 nm absorption signal, it appears impossible to resolve a rising time for the latter, as its increase is almost instantaneous and follows the kinetics of Chl molecules (Figure 5.4a). Surprisingly, both the excitation of Chl *a* and that of Chl *b* offer the picture, since the 515 nm signal appears always immediately (within experimental resolution). To our knowledge, this is the first observation of a Car-like signal populated instantaneously

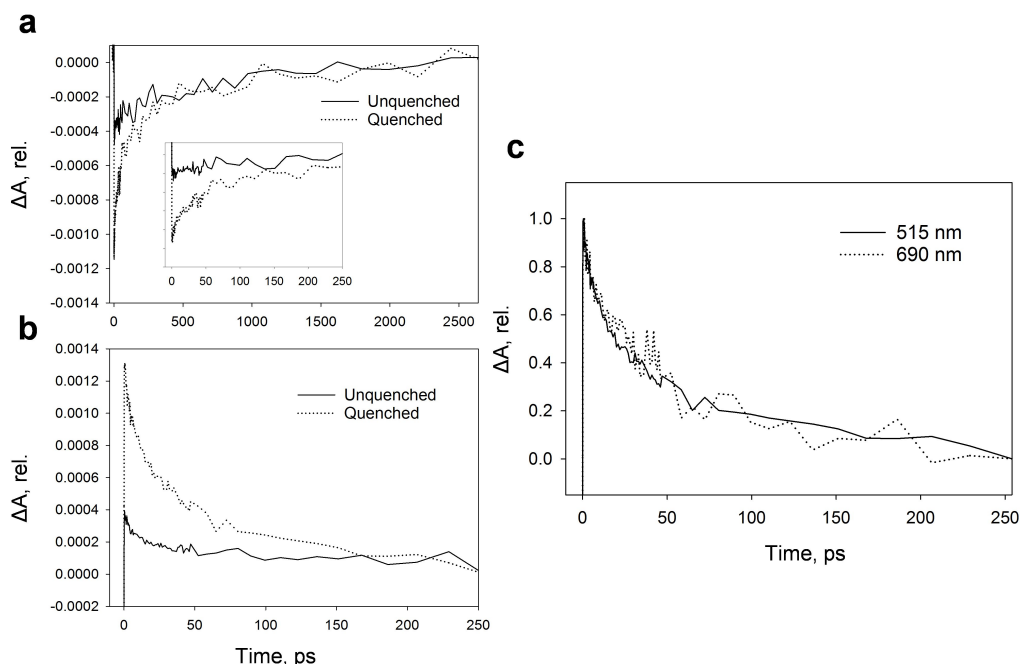


Figure 5.5: **The new Car excited state correlates with the de-excitation of Chls.** **a, b** Dynamics of Chl *a* Q_y and Car new excited state, respectively, after Chl *a* excitation (674 nm). All kinetics are not normalised, for a truthful comparison of the signal intensities between unquenched and quenched LHCII in gels. **a** Full length kinetics measured at 684 nm. The inset shows the details in the first 200 ps. **b** Kinetics measured at 515 nm. **c** Superimposition of the dynamics of Chl *a* and the new Car excited states signals. Kinetics were offset after 250 ps and normalised to the maximum absolute absorption signal.

after excitation of both Chl *a* and *b* molecules.

Figure 5.5 shows the dynamical description of Chls and the newly found Car signal. The raw kinetics of Chl Q_y and the new Car band shown in panels a and b, respectively, highlight their similar kinetics and depict their similar behaviour when switching between the unquenched and the quenched conformation of LHCII. Stabilising the quenched conformation, indeed, brings about a faster decay for both for Chl and Car signal. The correlation between them becomes obvious when the kinetics are normalised to 1 to their maximum absolute absorption value and offset to 0 after 250 ps, when in quenched samples both signals have decayed and the remaining background absorption is a leftover of the broad Chl S₁-S_n ESA (Figure 5.5c). It is clear that there is a good correlation between the two kinetics, suggesting that the 515 nm state is involved in the de-excitation of Chl molecules.

The identity of this state remains dubious, due to the different position relative to the S_1 - S_n band. It retains the characteristic of an S^* state, which has been invoked in other reports as the dark state involved in energy dissipation (Liguori *et al.*, 2017; Mascoli *et al.*, 2019). The bleaching negative inflections reasonably match the 0-0 and 0-1 transition maxima of Lut in the L1 site (Ruban *et al.*, 2000). Moreover the position of this signal matches nicely the blue shoulder of the S_1 - S_n Car ESA, which have been previously assigned to S^* (Polívka and Sundström, 2009). The presented data are therefore in agreement with the hypothesis that Chl transfer energy to a Lut, similarly to what has been reported for isolated LHCII (Ruban *et al.*, 2007) as well as for other systems (Pinnola *et al.*, 2016; Staleva *et al.*, 2015; Hontani *et al.*, 2018; Park *et al.*, 2018). Despite this, the kinetics of appearance and decay of the 515 nm signal contradict the existence of a mechanism of incoherent energy transfer and suggest that dissipative excitonic interactions between Chl and Car molecules are present, that lead to the ultrafast population of a Car dark state and subsequent energy release as heat (Bode *et al.*, 2009). Indeed, beside observing an instantaneous population of the 515 nm absorbing state, the kinetics of decay are longer than expected for a pure Car dark excited state, which generally decays in tens of ps (Frank *et al.*, 1997). The observed 515 band is instead long-lived and decays in hundreds of ps, following the decay of Chl signal.

To investigate in more detail the kinetics and spectra of the quencher differences between the quenched and unquenched samples were calculated (Figure 5.6). The derived kinetics of the putative “quencher”, shown in panel a, are in the order of tens of ps, in line with the decay time of Car S_1 state to the ground state (Frank *et al.*, 1997). However, they are longer than what is expected from a Lut S_1 state (~ 15 ps) and match more closely those of Neo (~ 35 ps) (Niedzwiedzki *et al.*, 2006). Neo in LHCII forms contacts with both Chl *a* and *b* (Croce *et al.*, 1999b; Liu *et al.*, 2004), which would explain, if we assume Neo can be the quencher responsible for the 515 nm ESA, why we observe its signal after the excitation also of Chl *b*. It was calculated that potentially every Car could act as a quencher of excitation energy, provided that its coupling with Chl molecules is strong enough to allow energy transfer from the latter (Fox *et al.*, 2017). However, this explanation of our data is a mere hypothesis and should be carefully tested. Indeed, assigning the identity of a specific Car by deriving the difference in the kinetics between quenched and

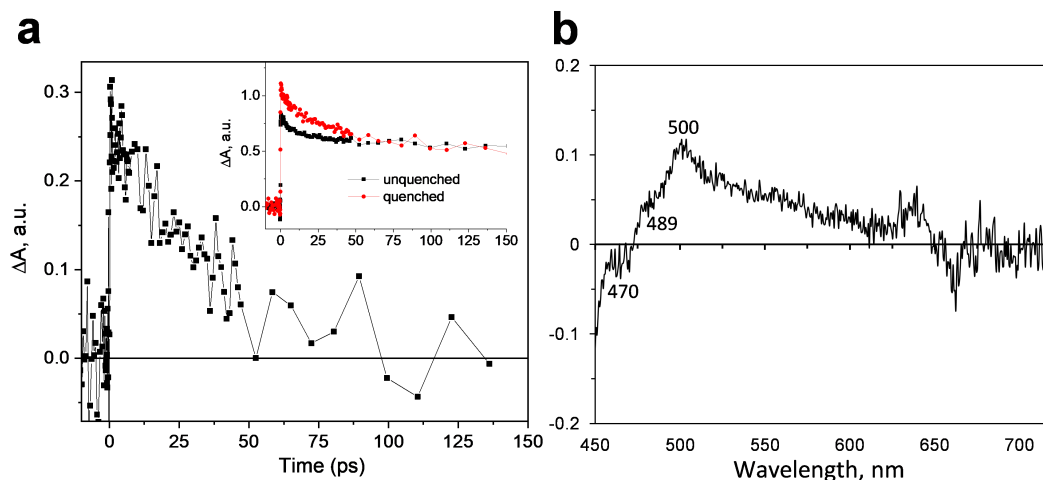


Figure 5.6: **Derived kinetics of the “quencher” signal indicate the possible contribution of neoxanthin.** **a** Difference between the kinetics of quenched and unquenched LHCII in gel measured at 515 nm after Chl *a* excitation. The inset shows the raw traces, normalised to the signal after 150 ps. **b** Difference between the spectra of quenched and unquenched LHCII in gel measured at 515 nm after Chl *a* excitation.

unquenched, which is often used in TA studies (Ma *et al.*, 2003; Park *et al.*, 2018), bears intrinsic weaknesses since it is very sensitive to the components of annihilation present in the measurements and since the LHCII protein scaffold exerts a strong effect on the dynamics of the pigments bound (Polívka *et al.*, 2002). The difference spectrum, shown in Figure 5.6b, is difficult to explain too, since it appears strongly blue-shifted from a Car S_1 - S_n ESA. Strikingly, it is very similar in shape to what was recently reported in CP29 complexes, where it was retrieved via the application of global and target analysis to the experimental data (Mascoli *et al.*, 2019). Despite this, the dynamics of this band do not match those reported in that work, being populated quickly and decaying on hundreds of ps, compared to the ~ 6.3 ps decay kinetics reported for CP29 (Mascoli *et al.*, 2019).

As discussed before, excitation of Cars in LHCII lead to the ultrafast appearance of the Car S_1 - S_n excited state absorption (Figure 5.4a). The 515 nm state instead does not stand out in the spectrum in the first tens of ps. However, it appears to be present 100 ps after Car excitation (Figure 5.7, black line). When normalising to the amplitude maximum of this signal, the spectrum closely resembles the one obtained after Chl excitation (Figure 5.7, red line) and retains also the

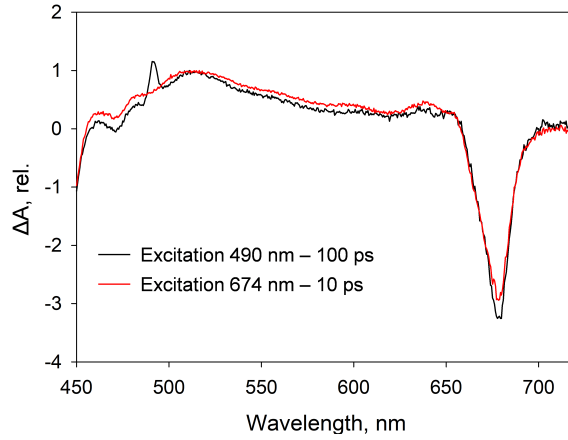


Figure 5.7: **Direct Chl excitation is not needed to populate the new Car state.** Normalised spectra of quenched LHCII in gels obtained 100 ps after direct Car excitation (490 nm, black) or 10 ps after Chl *a* excitation (674 nm, red).

same position of Car GSB. It appears therefore that this state is populated independently of the excitation energy route (either immediately after Chl excitation or after Chl receives energy from the Car S_1 and S_2 states).

The Car S_2 state is a bright excited state which transition from the ground state is strongly dipole-allowed and thus participates in light harvesting processes (Polívka and Sundström, 2004; Polívka and Frank, 2010). Conventionally, in TA experiments, excitation of Car to their S_2 state is used to gain insights into the dynamics of the lowest excited states of Car and Chl molecules, which in turn help understanding how strongly these are coupled to allow energy transfer between them to occur (Croce *et al.*, 2001). Figure 5.8 shows spectral and dynamical properties of the lowest excited states of Chl *a*, *b* and Car. The spectrum of Car S_1 , shown in panel a, exhibit differences between the unquenched and quenched LHCII conformations, being slightly red-shifted in the latter. This could arise from a twisted conformation of an end ring of a xanthophyll molecule in LHCII induced upon quenching, which effectively increases the conjugation length of its double carbon backbone, hence changing the energetic level of the S_1 state (Llansola-Portoles *et al.*, 2017). Such changes have been previously associated with energy quenching, either by a direct effect on the Car S_1 energy level, or by changes in the excitonic coupling strengths with neighbouring Chl molecules (Pascal *et al.*, 2005; Liguori *et al.*, 2015, 2017; Fox

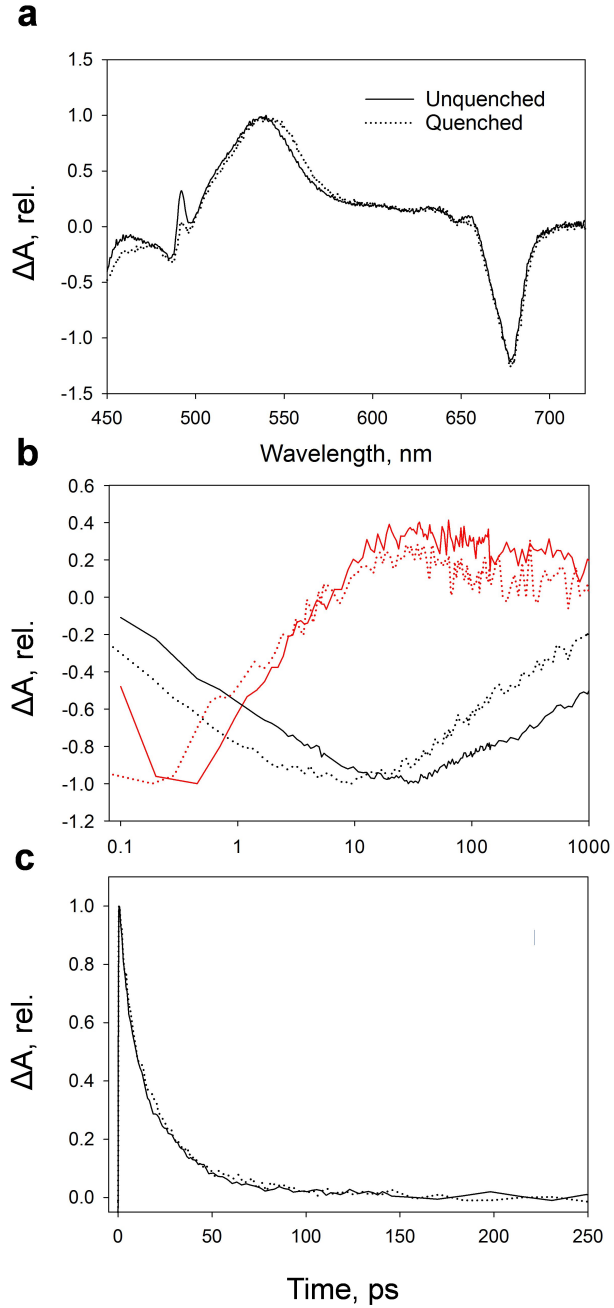


Figure 5.8: **Structural changes of LHCII cause alterations of the spectroscopic properties of the bound pigments.** **a** Normalised spectra of unquenched (solid line) and quenched (dotted line) LHCII in gels, 10 ps after Car excitation at 490 nm. **b** Normalised kinetics of Chl *a* (black) and Chl *b* (red) signal, measured at 650 and 675 nm, respectively, after Car excitation. **c** Normalised kinetics of Car S_1 signal decay, measured at 540 nm, after Car excitation.

et al., 2015; Llansola-Portoles *et al.*, 2017). Induction of quenching induces also some changes in the kinetics of the Chl *b* and Chl *a* S_1 states, which appear to be populated faster in the quenched LHCII (Figure 5.8b). This could underline a stronger Car-Chl coupling, which enables a quicker energy transfer from the former. This conclusion is somewhat weakened by the observation that the decay kinetics of the Car S_1 state are identical for both unquenched and quenched LHCII conformations, while they should be faster in the latter if energy is transferred faster to Chl (Figure 5.8c). However, we note that this analysis of the kinetics concerns the integrated signal from all Car in LHCII and thus the individual contributions are indiscernible.

5.1.4 Induction of the quenched conformation is independent of Car composition

So far, the new 515 nm band has been described and has been associated with a Car dark excited state and shown to be related to energy quenching in the LHCII complex. To help us understand better how the LHCII structure can give rise to the so described quenching interaction, we investigated in more details the induction of the dissipative switch in monomeric LHCII immobilised in gels, isolated from WT *Arabidopsis* plants or from a mutant lacking Lut.

The internal Car binding pockets in an LHCII monomer, called L1 and L2 (Liu *et al.*, 2004), constitute the core of the complex and incorporate Lut molecules in WT plants (Figure 5.9). Both are conserved, at different extents, across different members of the LHC superfamily (Premvardhan *et al.*, 2010; Pan *et al.*, 2011; Bo-

Sample	<i>a/b</i>	%Neo/Car	%Vio/Car	%Ant/Car	%Lut/Car	%Zea/Car
WT	1.39±0.06	26.85±2.67	3.37±0.71	-	69.77±3.09	-
npq1lut2	1.46±0.14	27.43±1.42	63.6±1.93	-	-	-

Table 5.1: **Pigment composition of the LHCII samples used in the study.** Pigment composition of isolated LHCII. LHCII samples were taken after purification through IEF and pigments were extracted in 80% acetone/20% water for HPLC measurements. *a/b*, Chl *a* to Chl *b* ratio; Ant, antheraxanthin. Amounts are expressed as percentage relative to the total Car pool. Note that the sum of the Car percentages of *npq1lut2* is slightly less than 100%, due to minor contamination with degradation products in the preparative steps that were not taken into account in the analysis.

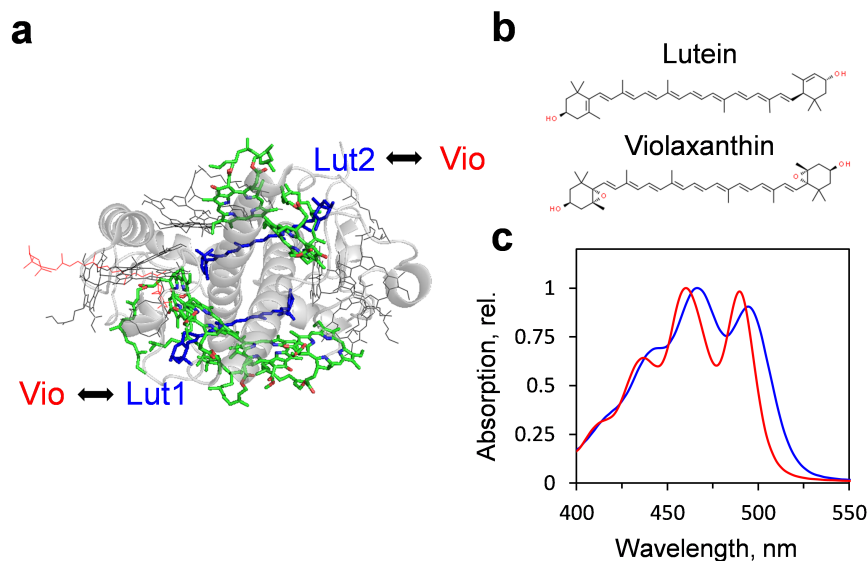


Figure 5.9: **Genetic alteration of Car biosynthesis pathways changes the xanthophyll composition of LHCII complexes.** **a** Stromal view of the LHCII monomer (Liu *et al.* (2004), represented with PyMol software) showing in blue the Lut molecules binding to sites L1 and L2 and the neighbouring Chl molecules in green (Chl 610, 611, 612 for Lut 1 and Chl 602, 603, 604 for Lut 2). The remaining Chl are displayed as black lines and the Neo molecule as a red line. The *lut2* mutation affects the lycopene ϵ -cyclase, resulting in the lack of Lut (Pogson *et al.*, 1998). In the *npq1lut2* mutant violaxanthin (Vio) replaces Lut in the L1 and L2 sites (Dall’Osto *et al.*, 2006). **b** Chemical structures of Lut and Vio. **c** Absorption spectra of Lut and Vio isolated via reverse-phase HPLC (Farber *et al.*, 1997).

nente *et al.*, 2008; Staleva *et al.*, 2015), where they have been shown to participate in photoprotective processes. In reconstitution experiments, Lut was found to be critical for the correct refolding of the complexes and the stability of the trimeric state (Dall’Osto *et al.*, 2006). However, reconstitution with different xanthophylls, structurally similar, occupying these sites was found to be achievable (Dall’Osto *et al.*, 2006, 2012; Fuciman *et al.*, 2012). These works reveal a somewhat flexible LHCII protein scaffold, therefore it was not surprising that we were able to isolate biochemically intact LHCII complexes from *Arabidopsis* mutants (*npq1lut2*) unable to accumulate Lut, where Vio compensates stoichiometrically for its absence (Table 5.1). It was previously found that such isolated complexes are always found in monomeric state, due to the absence of Lut 2 that is critical for trimerisation, and Vio is bound to the L1 and L2 sites, normally occupied by Lut (Dall’Osto *et al.*, 2006) (Figure 5.9a). To be consistent with the interpretation of our results, we com-

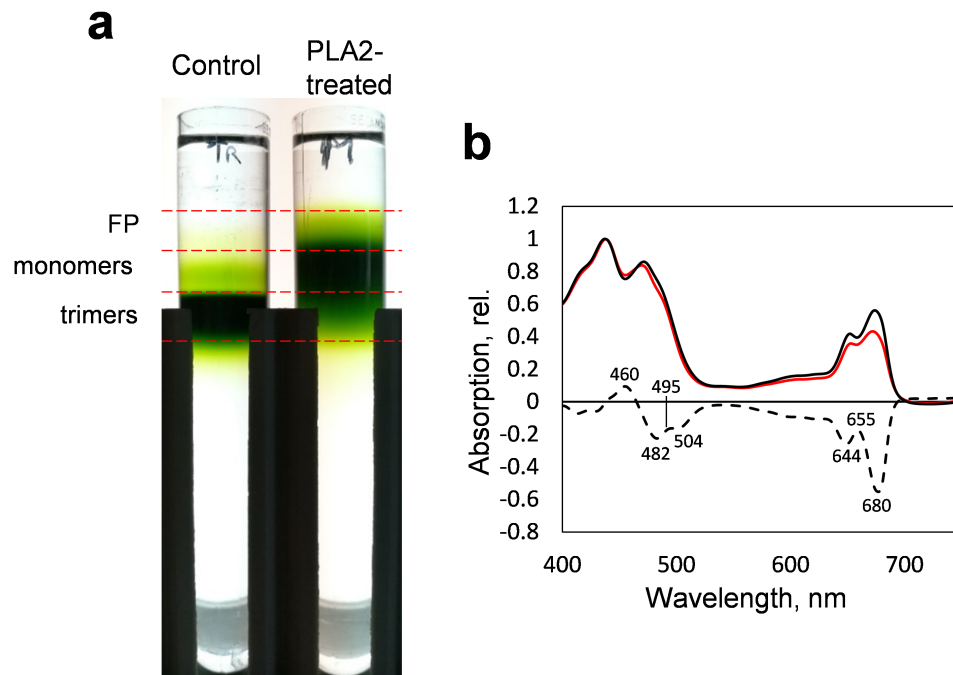


Figure 5.10: **Enzymatic removal of phosphatidylglycerol causes monomerisation of LHCII.** **a** Sucrose density gradients showing the composition of the LHCII fraction isolated from IEF, before (left) or after (right) the treatment with phospholipase A2 (PLA2). The fractions of trimeric LHCII, monomeric LHCII and free pigment (FP) are labelled. **b** Normalised absorption spectra of the LHCII trimers (black) and monomers (red) collected respectively from the control and the PLA2-treated gradients in **a**. The difference spectrum (monomers-minus-trimers) is shown as a dashed line.

pared the LHCII monomers obtained from the mutant with both trimers of LHCII in their native state and with monomers of LHCII, obtained from a monomerisation procedure performed after isolation of the trimeric complexes (Figure 5.10). The procedure involves the enzymatic removal of the phosphatidylglycerol molecule that “glues” together the three monomers of LHCII in the trimer (Wentworth *et al.*, 2004). The monomers so obtained, after separation on a sucrose density gradient, display changes in the absorption that reflect the structural relaxation of the Lut in the L2 site, that is distorted in the LHCII trimer and hence display a red-shifted 0-0 transition maximum (Ruban *et al.*, 2000) (Figure 5.10). These changes are visible as a decrease in absorption >500 nm and a relative small increase of the ~ 495 nm maximum belonging to a structurally relaxed Lut (Figure 5.10b). As describe before (Wentworth *et al.*, 2004), other changes occur, mainly associated with Chl *a*

molecules and its Q_y absorption transition.

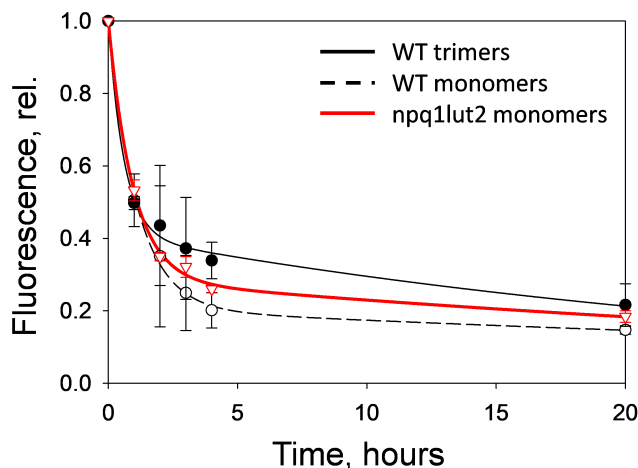


Figure 5.11: **Lutein replacement does not hinder the dissipative switch in LHCII.** Comparison of quenching induction traces of LHCII in gels isolated from WT and *npq1lut2* *Arabidopsis* plants. Gels were incubated in buffer without detergent overnight and fluorescence quenching was monitored with a Dual-PAM fluorometer at 0, 1, 2, 3, 4 and 20 hours.

Vio is a xanthophyll with 9 conjugated carbon double bonds in its polyenic chain (Figure 5.9b). On the contrary, Lut lacks the epoxy groups at the end rings (as Zea, its isomer) and presents 10 conjugated C=C bonds. These features have a quite marked impact on the energetics of the molecule as a shorter conjugation length results in blue shifted absorption transitions for Vio (Figure 5.9c). It was shown that the absence of Lut and the accumulation of Vio in the *npq1lut2* plants have a dramatic effect on the fluorescence dynamics of the thylakoid membranes, impairing the formation of NPQ (Niyogi *et al.*, 2001) and triplet quenching photo-protective mechanisms (Dall’Osto *et al.*, 2006). Several reports concluded that Vio is an antagonist of energy quenching induction and its presence affects negatively the kinetics and amplitudes of the energy dissipation (Ruban *et al.*, 1994a; Ocampo-Alvarez *et al.*, 2013; Kana *et al.*, 2016). However, it has been shown that Lut is not essential for NPQ and that the dynamics of qE quenching could be restored also in mutant plants, simply enhancing the ΔpH across the thylakoid membrane (Johnson *et al.*, 2012). Monomeric LHCII from WT and *npq1lut2* plants were embedded in polyacrylamide gels as described before (Figure 5.1). Quenching induction was achieved again via incubation overnight in a medium without added detergent and

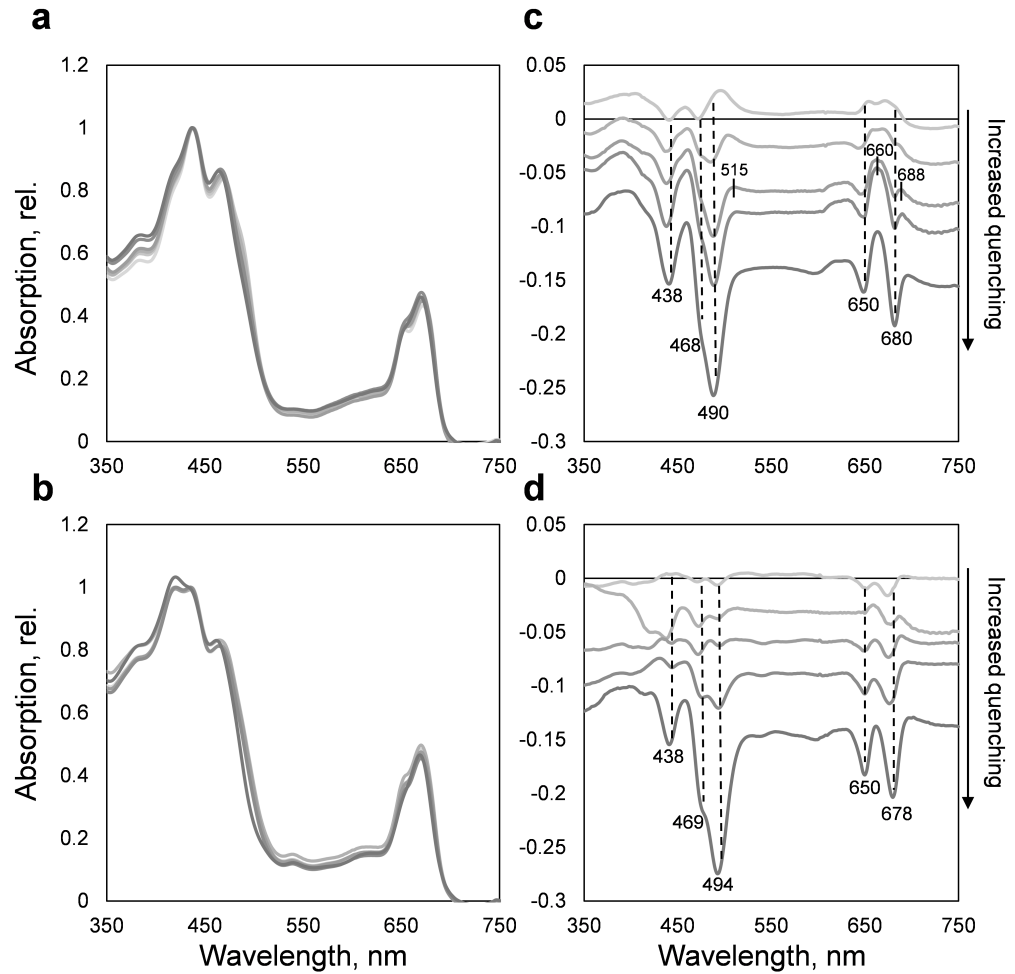


Figure 5.12: **Absorption spectroscopy reveals dramatic changes in the Lut 1 site upon quenching induction.** **a,b** Normalised absorption spectra and **c,d** quenched-minus-unquenched difference absorption spectra of LHCII monomers (obtained after treatment with phospholipase A2) in gels isolated from WT (**a,c**) and *npq1lut2* (**b,d**) plants. A progressively increasing degree of fluorescence quenching is displayed in a colour scale, from light grey (less quenched) to dark grey (more quenched). Difference spectra are offset for clarity.

the fluorescence quenching was monitored at fixed time points. Strikingly, not only were *npq1lut2* LHCII able to switch to a dissipative conformation, but they followed the same induction kinetics of WT trimers and monomers and reached similar amplitudes (Figure 5.11). Therefore, our data provide new evidence that the molecular switch governing the transition of LHCII from a light-harvesting to a quenched state is independent of Car composition, complementing previous studies on isolated com-

plexes (Johnson *et al.*, 2010; Tutkus *et al.*, 2017).

In order to understand what changes occur in the pigment binding sites in LHCII upon quenching induction, absorption spectra were recorded of samples at different extents of the energy quenching (Figure 5.12). The protein environment can shape profoundly the absorption and fluorescence properties of LHC proteins, since specific amino acids pose structural constraints for each pigment binding site and affect also pigment site energies (Scholes *et al.*, 2007; Müh *et al.*, 2010). It was shown that the heterogeneous dielectric environment in LHCII can lead to a two-fold increase in energy transfer rates between chromophores (Curutchet *et al.*, 2011). Cars are particularly sensitive to structural perturbations and variations in the polarizability of the environment (Robert *et al.*, 2004; Mendes-Pinto *et al.*, 2013). Only small variations are visible in the normalised spectra (Figure 5.12a,b), but the differences become more evident when analysing difference absorption spectra (Figure 5.12c,d). At intermediate extents of quenching (middle grey line in panel c), the difference spectrum of WT LHCII is in very good agreement with the first reports on LHCII aggregates, at room temperature (Ruban and Horton, 1992) and at 77K (Ruban *et al.*, 1997a). Besides negative bleaching in the Soret bands of Chls, three prominent positive peaks arise around 515 nm, 660 nm and 688 nm, similarly to the aggregates. Therefore, their presence seems to depend upon the intrinsic conformational state of the complexes, rather than their oligomeric form. Pushing further the quenched state (dark grey line), a drastic decrease in absorptivity occurs around 490 nm. This is associated with changes occurring in the Lut 1 domain, where the terminal emitting Chls are bound (Illoaia *et al.*, 2008, 2011b). Interestingly, these changes have also been shown to correlate quantitatively with qE *in vivo*, thereby showing that this site is subject to wide structural fluctuations during photoprotection (Johnson *et al.*, 2009). Theoretical works support these findings too, showing that environmental factors such as pH, Zea and aggregation foster these changes (Liguori *et al.*, 2015; Belgio *et al.*, 2013; Balevičius *et al.*, 2017; Fox *et al.*, 2017). Generally, it appears that the conformational change affects, to different extents, the majority of the pigments bound to LHCII and impacts both Chl *a* and Chl *b*, testified by the presence of negative inflections/peaks at 438 and 680 nm (Chl *a*) and 468 and 650 nm (Chl *b*). *npq1lut2* LHCII complexes exhibit a similar pattern of absorption changes and once again show a sharp decrease in absorption at 494

nm, closely matching the site energy of the L1 locus (Figure 5.12b,d).

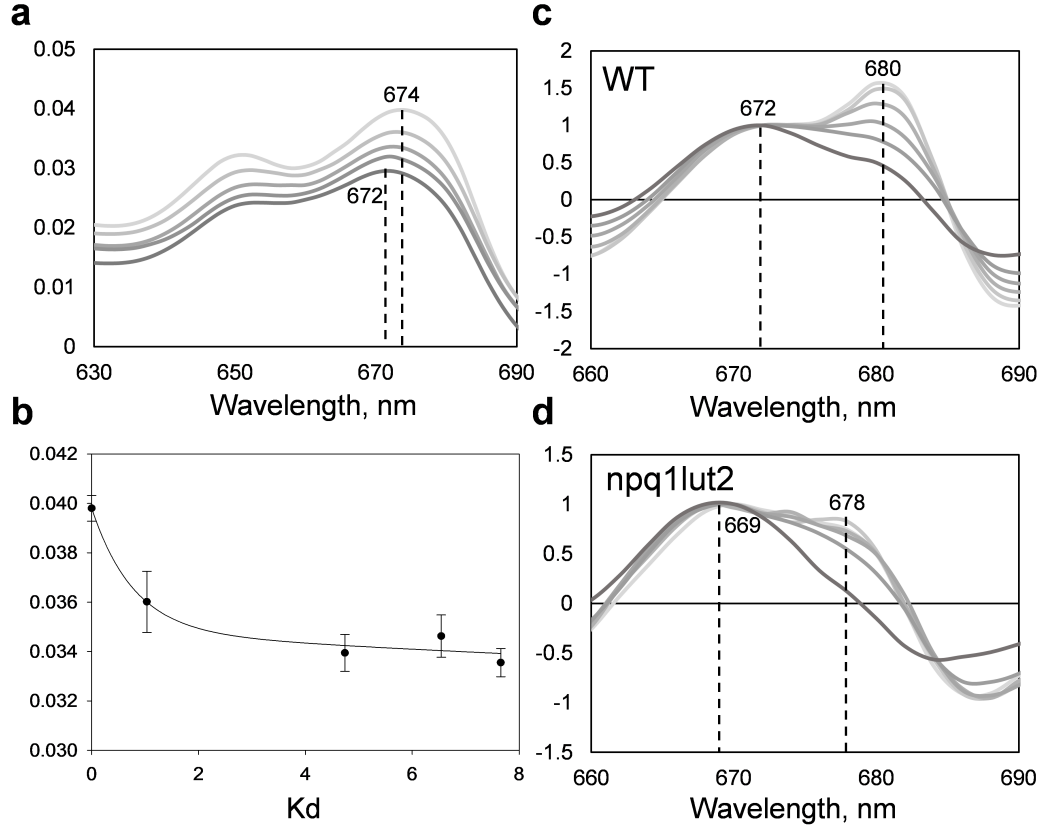


Figure 5.13: Low-energy forms of Chls are mostly affected by the LHCII conformational change. **a.** Zoom-in of the Chl Qy absorption band in LHCII monomers, showing a characteristic blue-shift correlating to the quenching induction. **b** Raw intensity values of the Chl *a* Qy band, evidencing the net decrease in absorptivity upon quenching (measured as $K_d = (F_m - F_q)/F_q$, where F_m is the initial fluorescence value of the gels and F_q is the value after quenching). Points are the averages of 3 independent measurements \pm SD, fitted with a double-exponential decay function. **c,d** Second derivatives of the Chl *a* Qy absorption band from WT and *npq1lut2* samples, respectively. Second derivatives were normalised at 672 nm (WT) or 669 nm (*npq1lut2*). A progressively increasing degree of fluorescence quenching is displayed in a colour scale, from light grey (less quenched) to dark grey (more quenched).

Figure 5.13 shows a more detailed analysis of the Chl *a* Qy absorption transition. It is noticeable an overall blue shift of the band, going from 674 nm to 672 nm, which is accompanied by a net decrease in absorptivity (panels a and b). At room temperature, absorption bands are broad and largely overlapping, but a deeper analysis, obtaining second derivatives of the spectra, provides a clearer picture (panels c and d). It becomes therefore obvious a decrease in the red-most region of the spec-

trum (peaking at 680 nm), upon quenching induction, relative to the blue part (672 nm). The presence of different sub-peaks in the Qy band reflects the presence of Chl *a* molecules with different site energies in LHCII, where the red-most is attributed to the terminal emitting pigments (Novoderezhkin *et al.*, 2005). Hence, the largest amplitude of absorption changes affects the terminal Chls (Chl *a* 610, 611 and 612) in line with previous observations (Johnson and Ruban, 2009). Still, *npq1lut2* LHCII exhibit a similar set of changes, suggesting again that the Car composition is not the major determinant of the quenching switch, which is rather stringently controlled by a switch of the protein backbone.

Fluorescence data provide good support to the absorption data so far described and show again the commonalities between WT and *npq1lut2* in the conformational change of LHCII (Figure 5.14). Upon quenching, the LHCII is subject to homogeneous broadening of the main emission peak at around 680 nm and to its red-shift, by a few nm. Broadening of a fluorescence emission band is due to specific interactions of the electronic transitions with the protein and pigment vibrational motions (referred to as “phonons”) (Fassioli *et al.*, 2014; Krüger and van Grondelle, 2017). A red shift is therefore associated with changes in the environment surrounding the pigments and it is the result of a change in the site energy of the terminal emitting Chl. A perturbation in the local environment of the terminal emitter excitonic cluster produces appreciable changes of its energetics and therefore of the fluorescence profile (Ramanan *et al.*, 2015). Interestingly, the evolution of the fluorescence profile is different for LHCII monomers immobilised in gels and for LHCII aggregates (inset in Figure 5.14a). The intensity of the F700 fluorescence band previously described (see Figure 3.10 in “Chapter 3: Identification of the qE site”) increases only upon aggregation and is not appreciable in immobilised complexes. This finding strengthen the hypothesis that F700 is strongly linked to the aggregation process but is loosely associated with the energy quenching (Chmeliov *et al.*, 2016). Thus, quenching of LHCII in gels brings about variations of the site energy of the terminal emitting cluster of Chls, as already evidenced by absorption measurements. These changes could modify the interactions between them and the Car in L1 site, in close van der Waals contact, possibly opening a dissipative channel through the S₁/S* route of the Car.

Eventually, after having zoomed into the molecular details of the quenching

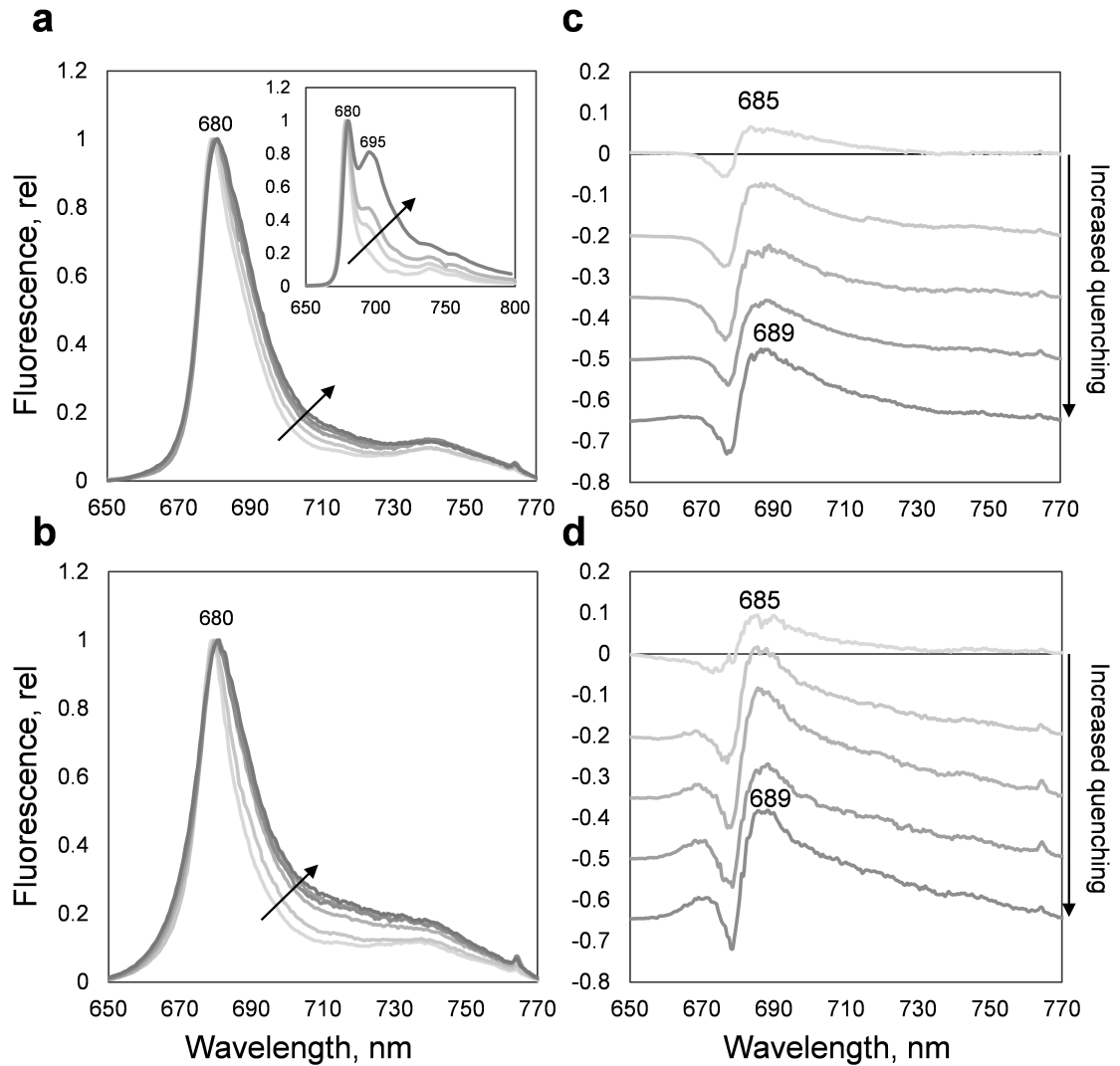


Figure 5.14: **Fluorescence spectroscopy reveals changes in the terminal emitting Chls that are independent of Car composition.** (a,b) Normalised 77K fluorescence emission spectra and (c,d) the relative quenched-minus-unquenched difference spectra of LHCII monomers in gels isolated from WT (a,c) and *npq1lut2* (b,d) plants. A progressively increasing degree of fluorescence quenching is displayed in a colour scale, from light grey (less quenched) to dark grey (more quenched). Difference spectra are offset for clarity. The inset in panel a shows the fluorescence spectra of LHCII aggregates during quenching induction.

conformational change in LHCII and having found that the Car composition doesn't affect the dynamic switch, we applied TA to understand if the quenching mechanism is conserved also in *npq1lut2* LHCII. To this aim, we excited the Chl in LHCII

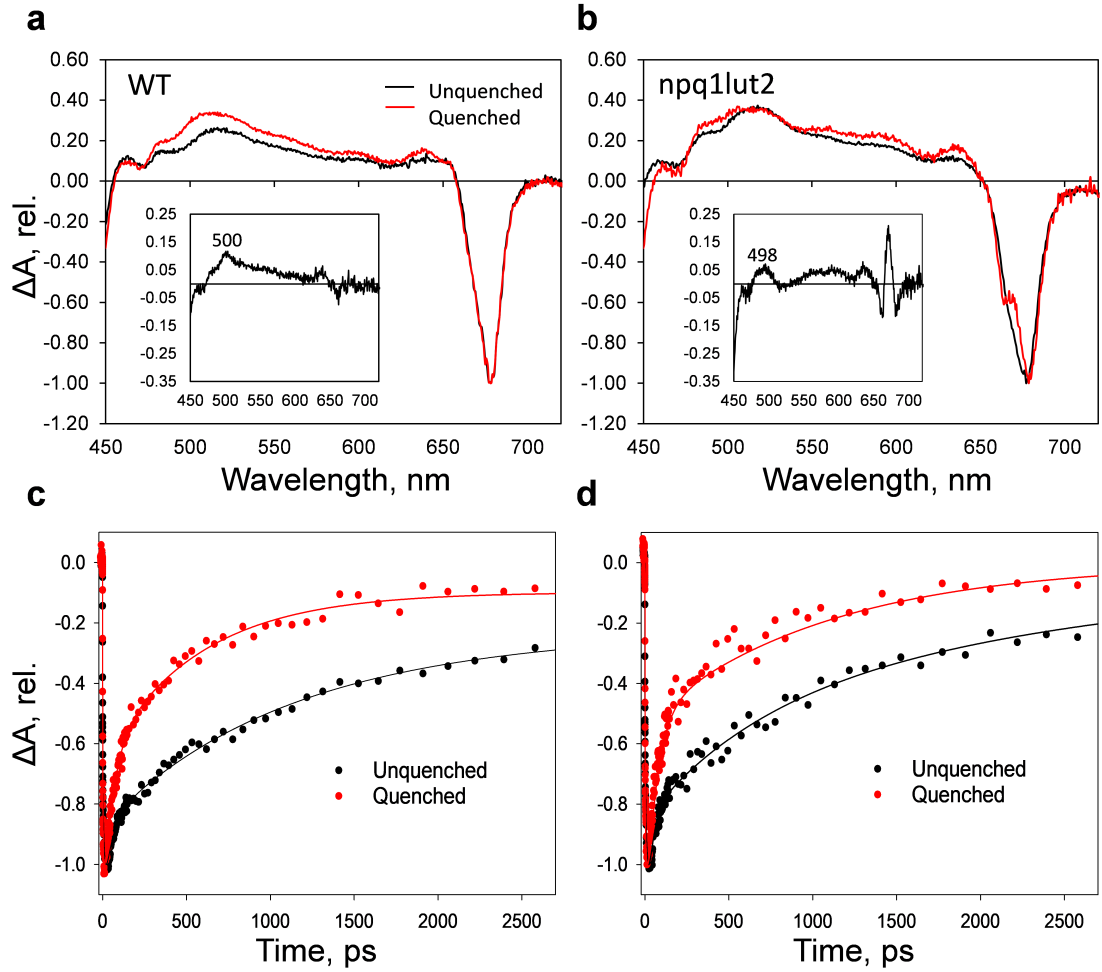


Figure 5.15: **Spectra of the quencher from WT and *npq1lut2* LHCII share marked similarities.** Spectra of unquenched (black) and quenched (red) LHCII in gels for WT (a) and *npq1lut2* (b) samples, 10 ps after Chl *a* excitation at 674 nm. Spectra are normalised to the maximum value of Chl *a* Q_y GSB. b,c Normalised kinetics monitoring the Chl *a* Q_y signal decay, measured at 684 nm after excitation at 674 nm, for WT and *npq1lut2* samples, respectively.

isolated from this mutant and monitored the changes occurring in the the Car ESA region, as previously shown for the WT (Figure 5.15). It is immediately evident the resemblance of the spectra obtained after Chl excitation, that exhibit conserved position of the GSB and the excited state absorption (panels a and b). As already shown previously in quenching induction traces (Figure 5.11), the extent of quenching is similar for LHCII from both genotypes and this is supported by the likeness of the Chl *a* signal decay kinetics (panels c and d). A closer inspection of the spec-

tra shows that there is a common change shared in WT and *npq1lut2* LHCII. The difference spectra indeed show that the maximum of the change in the Car signal (below 550 nm) occurs around 500 nm, slightly blue-shifted by 2 nm in the mutant (498 nm). This is again in line with the spectrum of the quencher in CP29, recently resolved by Croce and co-workers (Mascoli *et al.*, 2019). The strong resemblance of the two spectra reflects the structural homology between the complexes investigated (major LHCII and CP29) and suggests that a common mechanism could be shared across other members of the LHC family.

5.1.5 The internal Car pockets in LHCII shape the functional properties of the xanthophylls bound

Having identified the possible quenching mechanism in LHCII, describing the involvement of Lut 1 enclosed by the terminal emitting Chl cluster, the remaining open question is why the substitution of Lut with Vio in the L1 site doesn't affect quenching. Vio has indeed a higher excited state energy compared to Lut and is therefore reasonably expected to antagonise the quenching pathway (see Figure 5.9 and related discussion).

Figure 5.16 shows that indeed differences are present in LHCII from WT and *npq1lut2*. Steady-state absorption spectra (panel a) show a negative bleach in the difference spectrum that arises from an absorption loss of the Lut bound in the L1 site, which is substituted by Vio that has a blue shifted 0-0 transition. A variation of the Chl binding sites is also reported, as the 682 nm bleach evidences a blue-shift of the Qy band. The positive peaks at 540 nm and 418 nm correspond to the absorption transitions of pheophytin (Pheo). Pheo is formed when Chl *a* molecules lose their Mg atom positioned at the centre of the chlorin ring and it is frequently found as a by product of harsh biochemical preparations. It is possible that the lack of Lut in the mutant, that stabilise the LHCII complexes, makes Chl *a* more susceptible to damage from preparative steps and this results into a significant amount of Pheo in our *npq1lut2* LHCII samples. However, no contribution of this product was visible in transient absorption spectra and excitation fluorescence spectra were identical for WT and the mutant (data not shown), suggesting that Pheo is not energetically connected to other pigments in the complexes and therefore does not contribute to

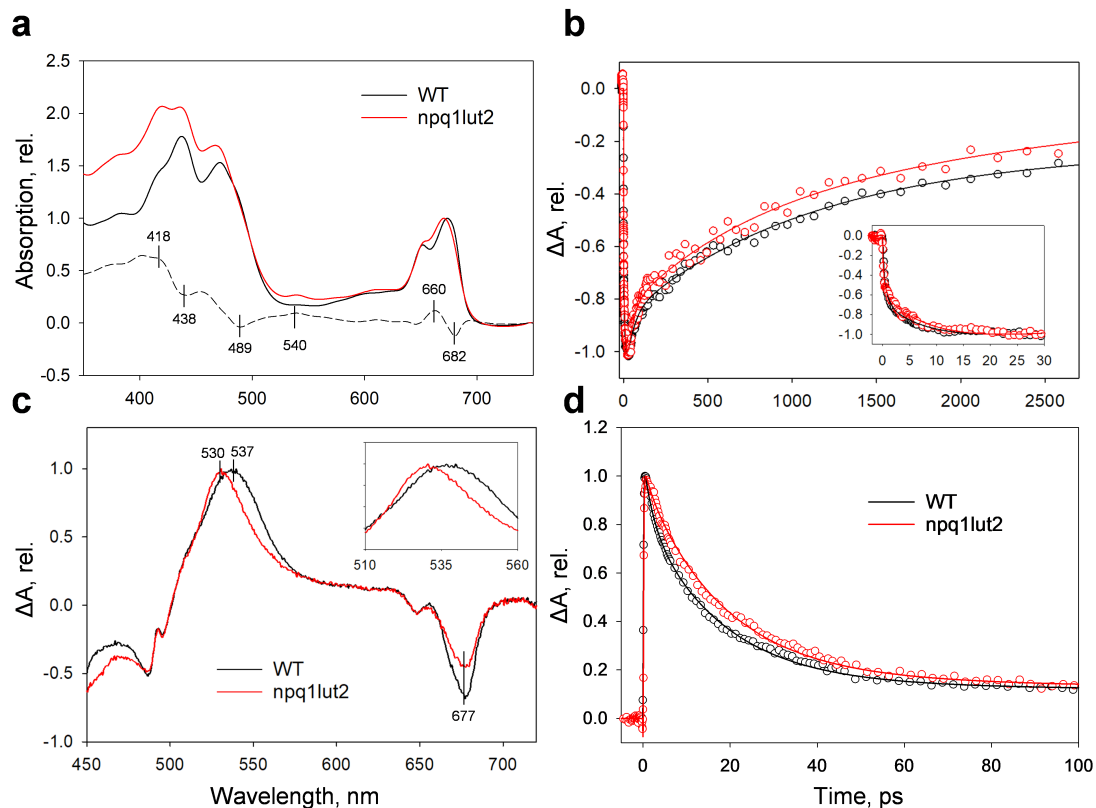


Figure 5.16: **Vio can replace Lut in the internal Car binding pockets in LHCII.** **a** Absorption spectra of WT and *npq1lut2* LHCII complexes, normalised at the peak of Chl *a* Q_y absorption. **b** Kinetics monitoring the Chl *a* ΔA signal in WT (black) and *npq1lut2* (red) LHCII. Inset shows the kinetics in the first 30 ps **c** Transient absorption spectra measured 10 ps after Car excitation at 490 nm and normalised to the maximum value of Car S_1 absorption. **d** Decay kinetics in the first 100 ps of the Car S_1 state, measured the wavelength of its maximum intensity (537 and 530 nm for WT and *npq1lut2*, respectively).

the observed dynamics of the LHCII pigments. The region in the absorption spectra in the gel below 500 nm is higher in the mutant compared to WT, due to differences in the scattering of the gel samples. The Chl *a* dynamics are only marginally affected by different Car composition (Figure 5.16b). The rise of Chl *a* Q_y signal after Car excitation, which is almost exclusively due to Chl *b* to Chl *a* energy transfer (Croce *et al.*, 2001), is nearly identical in both LHCII complexes (see inset in panel b). This is in line with earlier report on ultrafast dynamics of various LHCII mutants (Fuciman *et al.*, 2012) showing that replacement of Lut by Vio in LHCII complex leaves the energy transfer properties of the LHCII complex nearly unaltered. The

decay of the Chl *a* is multi-exponential in both complexes, characterised by the time constants of 0.5, 1.1, and 3 ns (Saccon *et al.*, 2019), suggesting some conformational heterogeneity of the LHCII bound in gel (Mascoli *et al.*, 2019). Car S_1 - S_n ESA and relative kinetics, in Figure 5.16c and d, respectively, evidence differences that are related to the Lut-Vio exchange. From one side, the ESA transition is spectrally narrower and blue-shifted in *npq1lut2*, in line with the presence of Vio. The decay kinetics of this peak, measured at its maximum (537 nm for WT and 530 nm for *npq1lut2*) are longer for the mutant, again reflecting the shorter conjugation length of Vio (Figure 5.16d) (Niedzwiedzki *et al.*, 2006).

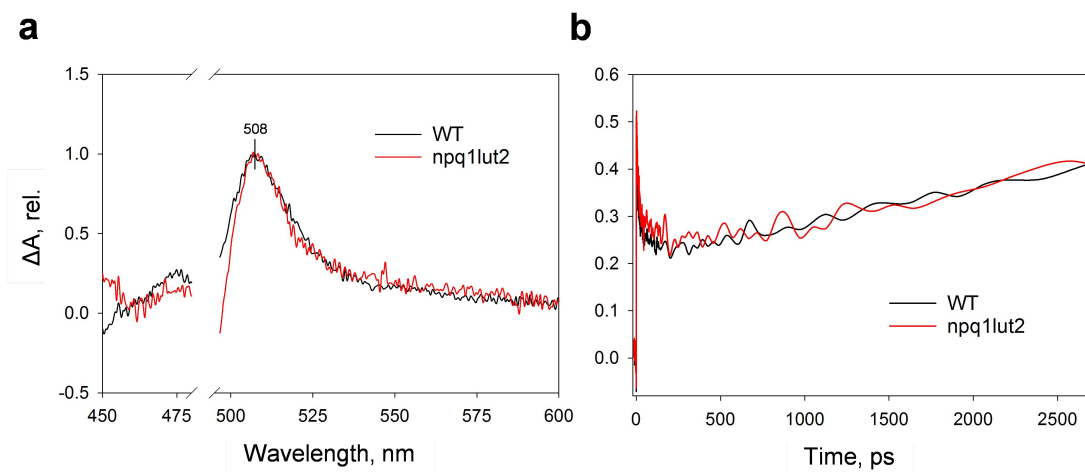


Figure 5.17: **Lut and Vio triplets in LHCII are spectroscopically identical.** **a** Spectra of WT and *npq1lut2* LHCII in gels 2.7 ns after excitation at 490 nm, normalised at the maximum triplet absorption. **b** ΔA kinetics measured at 508 nm, monitoring the time course of Car triplet formation. The kinetics were normalised to the maximum GSB of the Chl *a* Q_y transition.

After a complete energy equilibration in the complexes, the long term absorption dynamics present a dominant contribution of Car triplet states (Figure 5.17) (Mozzo *et al.*, 2008). Strikingly, despite the changes in the dynamics of singlet excited states, the Car triplets in LHCII from both samples are virtually identical (Figure 5.17). Earlier reports showed instead that, for Car in solution, the spectra of the triplets for Lut and Vio differs as the Car S_1 - S_n ESA, being blue-shifted for Vio (Jhutti *et al.*, 1998). The conservation of this photoprotective mechanism (triplet-triplet energy transfer) and its independence of Car composition, suggest that the L1 site is structurally very robust and shapes the functional properties of

the Cars it accommodates (Saccon *et al.*, 2019).

5.1.6 Discussion

The major LHCII complex is the most abundant pigment-binding membrane protein in the thylakoids and is responsible for the fast quenching of excess energy (qE, see “Chapter 3: Identification of the qE site”). Our data show that the dissipative switch lies within the LHCII complex itself and is not to be sought in particular under-represented proteins (such as PsbS or minor antennae). LHCII has a *flexible* and *robust* design, that on one side allow the protein to switch reversibly between light-harvesting and photoprotective conformations and on the other side presents conserved pigment binding pockets where the protein scaffold exerts a strong effect on the function of the chromophores it accommodates. This is the reason why Car composition is important but not crucial for the function of the LHCII complexes (Johnson *et al.*, 2010; Tutkus *et al.*, 2017). *Arabidopsis* plants lacking Lut and Zea (*npq1lut2*) accumulate LHCII where Vio is bound to the L1 and L2 pockets and their fitness is only marginally affected (Dall’Osto *et al.*, 2006; Niyogi *et al.*, 2001). Our data, in particular, show an optimal conservation of the L1 site, which normally incorporates a Lut (Lut 1). The close contacts between Lut 1 and the terminal emitter Chls (~ 6 Å), makes the former a good candidate for the quencher pigment (Figure 5.18). Car are indeed “natural born quenchers”, since their optically dark first excited state has a very short lifetime compared to Chls and could act as a relief valve for excitation energy pressure. The spectrum of the quencher that we obtained in our analysis, although clearly showing features of a Car molecule, differs from the S_1 - S_n spectrum, pointing out the involvement of a different state. Importantly, the characteristic blue-shift of its ESA compared to the S_1 - S_n transition suggest that its identity could be an S^* state, frequently invoked as a contributor during energy dissipation (Figure 5.18) (Liguori *et al.*, 2017; Mascoli *et al.*, 2019). The identity of this state is still disputed and it is unsure whether it represents a define state (Gradinaru *et al.*, 2001) or a “hot” ground state (Andersson and Gillbro, 1995). Indeed, the photochemistry of Cars is very complex compared to Chls, due to their flexible backbone giving rise to a multitude of molecular vibrations that contribute to Raman and absorption signals (Robert *et al.*, 2004). By contrast, the chlorin rings of

Chls are rather rigid and don't exhibit many degrees of freedom. When considering local heating effects on the Car molecule, the presence of additional dark states beside S_1 becomes unlikely as these can be explained simply as contribution from non-equilibrium vibronic population of the ("hot") ground state (Balevičius *et al.*, 2019). It remains unexplained the observation of an "instantaneous" population of this state in LHCII after both Chl *a* and *b* excitation. One possibility is the involvement of strong excitonic interactions between both Chl and the Car molecule, as suggested by Walla and colleagues (Bode *et al.*, 2009). It is also possible that Neo, sitting in a Chl *b*-enriched pocket, could contribute as well to the quenching process.

To conclude, therefore, our data suggest that the conformational change of LHCII brings some Chl and Car molecules (possibly Lut 1) in closer association and thus allow efficient energy transfer to the latter, followed by energy release as heat (Figure 5.18). It is still not trivial to assign a particular mechanism to this energy transfer, since it is not clear the involvement of excitonic interactions or incoherent energy transfer and since it is not clear the Car state involved, whether it is S_1 or a "hot" ground (or S^*) state. The quest for the quencher in the thylakoid membranes of higher plants is still ongoing (Ma *et al.*, 2003; Holt *et al.*, 2005; Ruban *et al.*, 2007; Bode *et al.*, 2009; Dall'Osto *et al.*, 2017; Park *et al.*, 2018; Mascoli *et al.*, 2019) and has been leading relentlessly to new mechanistic proposals (Dall'Osto *et al.*, 2017; Bennett *et al.*, 2019). Since the techniques adopted in these investigations suffer inevitably from artefacts and variability when applied to heterogeneous pigment-enriched systems (van Oort *et al.*, 2018), the interpretation of the results is often biased by personal inclinations towards a particular view of energy quenching mechanism. Thus, while the conundrum of the nature of the quenching mechanism in LHCII remains unsolved, our data indicate that the LHCII function is tuned dramatically by changes in the surrounding local environment and these can be the driving force in its photoprotective switch during NPQ. Our data also show that there could be more than one dissipative pathway involved in photoprotection, reflecting the heterogeneity in the structure of the pigments bound to LHCII and their relative orientations and coupling.

LHCII is an intrinsically dissipative system and, as such, maintaining a light-harvesting state is less trivial than achieving the quenched state (Duffy and Ruban,

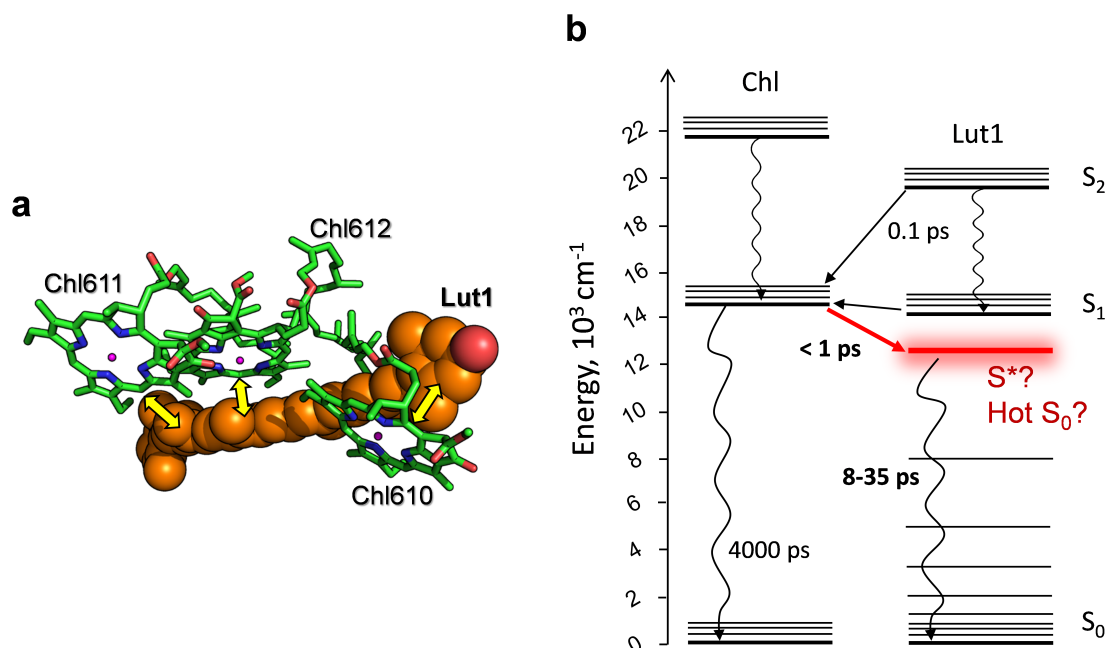


Figure 5.18: **Model of the dissipative switch in LHCII.** **a** Structure of the Chl *a* 610, 611, 612 and Lut 1 excitonic cluster represented with PyMol software. Chls are shown as green sticks, while Lut is displayed in orange, space-filling mode. Yellow arrows indicate the possible increase of the coupling strength of Chl and Lut (Yan *et al.*, 2007; Ruban *et al.*, 2007; Bode *et al.*, 2009; Duffy *et al.*, 2014), resulting from structural changes in that site during NPQ induction (Johnson and Ruban, 2009; Iliaia *et al.*, 2011b). **b** Schematic Jablonski diagram showing the excitation energy transitions and transfers of Chls and Lut 1 in LHCII. Wavy arrows represent internal conversion relaxation pathways within molecules. Straight arrows represent energy transfer pathways between molecules. The red arrow marks the possible energy quenching route, whereby Chls feed an unknown Car state that is likely an S^* state or a vibrationally "hot" ground state. Rate constants of the main pathways are shown in ps and are shown in bold for the pathways related to the quencher state. The energy levels shown are approximate values in line with the experiments performed and the literature (Polívka *et al.*, 1999).

2015; Chmeliov *et al.*, 2015). Membrane phospholipids are crucial for the structural stabilisation of antenna proteins and their functionality of in the native thylakoids (Schaller *et al.*, 2011; Seiwert *et al.*, 2017). The local environment of membrane proteins has also a strong impact on their mobility and control their tendency to interact with other proteins (Killian, 1998; Quemeneur *et al.*, 2014). Recently, it has been hypothesised that a reorganisation of the lipids bound to LHCII is associated with a hydrophobic mismatch around the complexes and this in turn locks the dissipative state of the antennae in the thylakoid membrane (Daskalakis *et al.*, 2019; Ruban, 2019). It thus seems that LHCII evolved a flexible structure, enabling it to

transiently switch off during qE and this process is essentially governed *in vivo* by the interplay between membrane and protein dynamics. More effort in the future should be put forwards to understand what are the factors that *in vivo* are controlling the optimal light-harvesting function of LHCII and largely prevent quenching interaction to occur with such high pigment densities.

5.2 *In vivo*

Investigating the excitation energy transfer and trapping pathways of a dynamic and heterogeneous system such as the thylakoid membrane is a difficult task. Whilst, as discussed in the previous section, ultrafast pump-probe techniques involving high laser powers are not suitable for this purpose, the application of time-resolved fluorescence (TRF) spectroscopy can overcome these limitations. This technique indeed uses low laser powers, that lessen drastically the probability to generate singlet-singlet annihilation artefacts, even in the presence of large interconnected antennae systems. The properties of aggregated LHCs have been therefore investigated several times in such way (Mullineaux *et al.*, 1993; Holzwarth, 1995; Moya *et al.*, 2001; Miloslavina *et al.*, 2008). More recently, Valkunas and colleagues presented the first detailed description of the spectral and dynamical properties of LHCII aggregates and their temperature dependence (Chmeliov *et al.*, 2016). However, straightforward spectroscopic studies aimed to identify the nature of the quenching mechanism in the thylakoid membranes are hindered the multiplicity of pigment-binding complexes, each of them binding an array of different chromophores and contributing to the overall spectral and dynamical response of the system.

In this work I present the solution we adopted to overcome this problem. We investigated the fluorescence behaviour of intact chloroplasts isolated from *Arabidopsis* plants treated with the antibiotic lincomycin. In this way, as presented in “Chapter 3: Identification of the qE site”, we could examine thylakoid membranes in which the contribution of PSII and PSI core proteins is largely suppressed, therefore constituting a simplified system to study NPQ dynamics.

5.2.1 NPQ induction in the absence of reaction centre proteins

Arabidopsis plants in the full rosette stage were watered twice a week with lincomycin to achieve $F_v/F_m \leq 0.25$. Under this conditions, plants retain only about 20% of the core complexes (Belgio *et al.*, 2012) (see also “Chapter 3: Identification of the qE site”). To investigate the role of the protein PsbS during NPQ, we compared the WT genotype to the mutant L17, which present an additional copy of the gene encoding PsbS and accumulate several times more protein than the WT (Li *et al.*, 2002). The ability to form NPQ is affected by the amounts of PsbS present, and L17 plants can form NPQ of amplitudes more than 4 times higher than the WT. The NPQ induction traces show also that the fraction of NPQ affected is specifically qE, the quickly forming component (Li *et al.*, 2000, 2002). It was shown that the PsbS-mediated effect on qE is maintained even after the lincomycin-treatment, a strong evidence that the complex does not have a characteristic binding site within the photosystem and that interactions with antenna complexes define its activity in the thylakoids (Ware *et al.*, 2015b; Sacharz *et al.*, 2017).

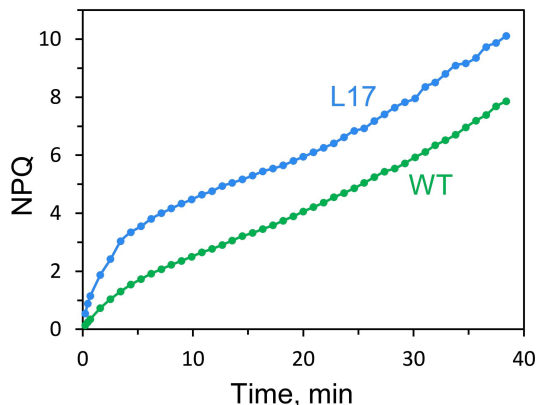


Figure 5.19: **PsbS enhances NPQ in isolated chloroplasts from lincomycin-treated *Arabidopsis* plants.** NPQ induction traces of chloroplasts from lincomycin-treated WT and L17 plants upon prolonged high light exposure ($2000 \mu\text{mol photons m}^{-2} \text{s}^{-1}$). NPQ is calculated as $(F_m - F_m')/F_m'$.

Figure 5.19 shows the NPQ induction traces measured for the isolated chloroplasts of both plants considered in this study. Chloroplasts were treated with high light ($2000 \mu\text{E}$) to ensure the induction of a sustained NPQ state, irreversible dur-

ing the time span of the TRF measurements. Since the antibiotic treatment results almost in the lack of PSII, which is highly susceptible to excess excitation energy damage (Powles, 1984), the sustained quenching is not originating from photoinhibition but rather relates to a sustained component of quenching in the antennae (Björkman and Demmig, 1987; Ruban and Horton, 1995). A clear PsbS-dependent effect can be spotted from early times, as L17 chloroplasts reach a higher amplitude of NPQ compared to WT (~ 3.5 versus ~ 1.8 within the first 4 minutes). As the illumination proceeds, the NPQ amplitudes keep rising, to values largely above the physiological threshold registered in intact leaves. However, it should be noted that NPQ was calculated following the Stern-Vollmer fluorescence quenching equation, with the expression $(F_m - F_m')/F_m'$, in which small variations in the extent of quenching result in notable NPQ changes (Bilger and Björkman, 1990). Eventually, the maximum NPQ reached was ~ 7.8 for WT and ~ 10.5 for L17 chloroplasts.

5.2.2 Stabilisation of a strongly quenched state in chloroplasts leads to a redistribution of the fluorescence spectral components

In the early 1990s, it was shown that upon LHCII aggregation, there is the appearance of several red-shifted emitting forms, that exhibit a strong temperature dependency (Mullineaux *et al.*, 1993; Ruban *et al.*, 1995b). These results were corroborated by the TRF analysis carried out recently by Valkunas' group (Chmeliov *et al.*, 2016). The TFR spectrum measured at 130 K for the WT dark-adapted chloroplasts, presented as a two-dimensional map, is shown in Figure 5.20a. Already at a first glance, the TRF plot of isolated chloroplasts resembles the spectrum of the LHCII aggregates presented in the previous study (Chmeliov *et al.*, 2016), showing the presence of red (~ 700 nm) emitting forms, flanked by an intense peak at 683 nm and a broader FR (~ 720 nm) band. However, the FR emission is present only as a faint shoulder in *in vitro* aggregates, while it is a main contributor to the spectrum of the chloroplasts analysed (compare to figure 5.20c, red lines, and see also steady-state spectra in Figure 3.4 in “Chapter 3: Identification of the qE site”). On a closer inspection, it can be seen that the behaviour of the red and FR bands is strongly temperature-dependent (Figure 5.20b). The ~ 700 nm band emerges at

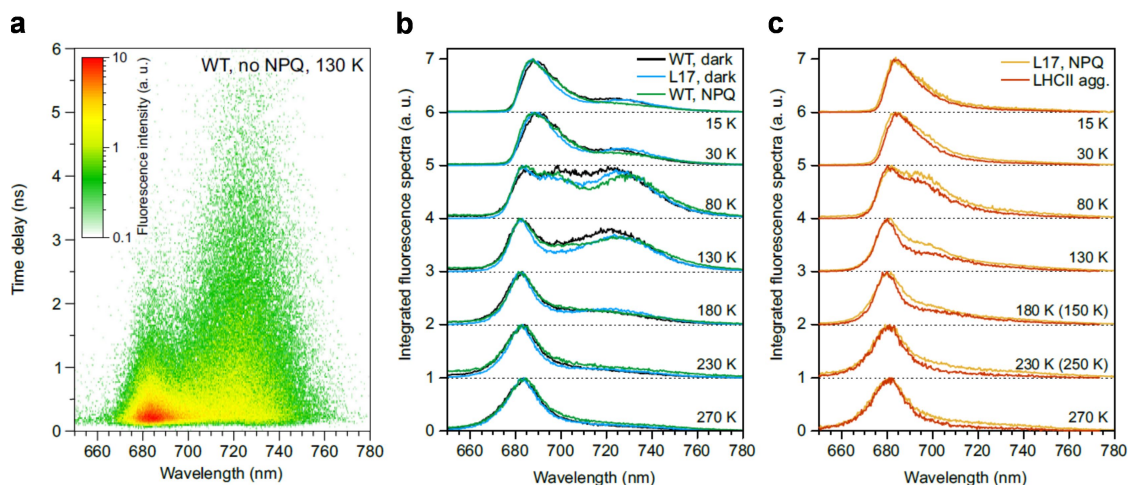


Figure 5.20: **The time- and temperature-resolved fluorescence spectra of chloroplasts from lincomycin-treated plants.** **a** 2-dimensional map showing the TRF data measured at 130 K of dark-adapted chloroplasts (no NPQ) isolated from lincomycin-treated WT. **b** Fluorescence spectra of the WT and L17 chloroplasts at different temperatures (black and blue lines, respectively), obtained by integrating the corresponding TRF maps over the 0-12 ns time window. Fluorescence spectra of the WT chloroplasts under NPQ conditions are also shown (green lines), whose spectra were obtained by integrating the corresponding fluorescence maps over 0-2 ns time window. **c** Fluorescence spectra of the L17 chloroplasts under NPQ conditions (orange lines), obtained at different temperatures by integrating the corresponding TRF maps over 0-1.5 ns (for $T \leq 80\text{K}$) or 0-0.8 ns (for $T \geq 130\text{K}$) time windows. The fluorescence spectra from LHCII aggregates at the corresponding temperatures are also shown (red lines, 150 and 250 K data is shown instead of the lacking 180 and 230 K spectra; spectra obtained by integrating TRF maps over the same time window as for the L17 chloroplasts).

$T < 130\text{ K}$ and gradually blue-shifts, a behaviour already assigned to mixed excitonic and charge-transfer states in Chl clusters (Chmeliov *et al.*, 2016). Dark-adapted WT and L17 exhibit a very similar fluorescence behaviour. The PsbS overexpression, therefore, does not affect the “Fm” state (fluorescence intensity in the absence of quenching), unlike Zea (see Figure 3.22b in “Chapter 3: Identification of the qE site”), providing support to previous studies (Li *et al.*, 2002; Ware *et al.*, 2015b). Upon quenching induction, almost no difference is visible in the spectra of the WT, across a range of temperatures (Figure 5.20b). In particular, it is interesting to note that the 700 nm red band remains unchanged, suggesting that these forms are unrelated to quenching (Chmeliov *et al.*, 2016; Gelzinis *et al.*, 2018), unlike previous claims (Miloslavina *et al.*, 2008). Unlike in WT, dramatic changes occur in fluores-

cence profile of L17 upon induction of the quenched state, in which the FR emitting forms are almost absent (Figure 5.20c). Superimposing the traces at different temperatures with those obtained for isolated LHCII aggregates reveal the exceptional similarities between the two systems. The absence of the FR band also disproves the hypothesis that this is related to the quenching mechanism (Wahadoszamen *et al.*, 2012).

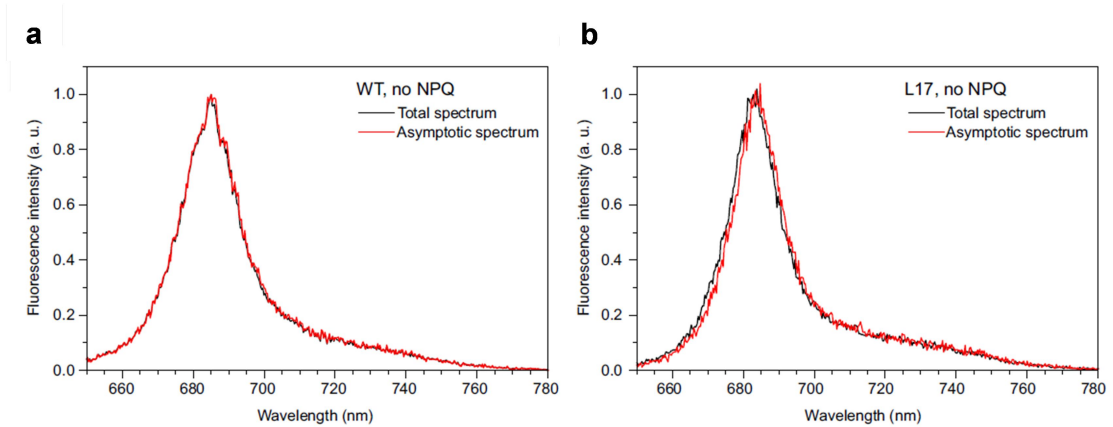


Figure 5.21: **Lincomycin treatment strongly diminishes the fluorescence emission contribution from RC complexes of PSI.** Comparison of the total integrated and asymptotic (integrated over 1-8 ns time window) room-temperature fluorescence spectra of the dark-adapted chloroplasts from lincomycin-treated WT (a) and L17 (b).

As discussed above, the additional FR fluorescence band around 720 nm in the chloroplasts is only marginally present in the aggregates and could originate from PSI-related complexes. This band, however, almost completely disappears at higher temperature, unlike in the fluorescence spectra of the thylakoids containing both PSII and PSI (Farooq *et al.*, 2018). Since the amounts of PSI and partially LHCI are greatly diminished after the lincomycin treatment but the intensity of the FR emission band is not appreciably undermined (see also Figure 3.4 in “Chapter 3: Identification of the qE site”), attributing a physical origin to it is not trivial. PSI acts as a very efficient trap of excitation energy and therefore its fluorescence emission has a characteristic sub-100 ps lifetime at room temperature, faster than any other component in the thylakoid membrane (Chukhutsina *et al.*, 2019). Thus, to understand how the residual amounts of PSI RCs can contribute to the intensity of this band, we measured the asymptotic spectra of the samples (integrated

in the window 1-8 ns) and compared it with the steady state spectrum. Given the characteristic short lifetime of PSI fluorescence, the asymptotic spectrum is by definition lacking any possible signal from PSI. On the contrary, the steady-state spectrum should include the contribution of PSI since it integrates the fluorescence signal from time zero. In our analysis, the two spectra are identical, suggesting that the thylakoid membranes from both WT and L17 lincomycin-treated samples are almost PSI-deficient. Therefore, the origin of the FR emission band is likely in the LHCII complexes themselves, which by means of single-molecule and Stark spectroscopy were found to occasionally switch to the FR emitting form (Krüger *et al.*, 2010; Wahadoszamen *et al.*, 2012). Moreover, a similar band was observed, although much weaker, at longer time delays in LHCII aggregates (Chmeliov *et al.*, 2016). It is worth noting that the LHCI polypeptides are nuclear encoded and therefore in principle should not be affected by the lincomycin treatment (Jansson, 1994). However results on treated WT and *NoM* plants (see for example Figure 3.15 in “Chapter 3: Identification of the qE site”) hints towards a decrease in the amounts of LHCI in the membrane (Gáspár *et al.*, 2006; Belgio *et al.*, 2012), which is possibly related to the lack of docking sites in PSI core polypeptides (Varotto *et al.*, 2002). Given the variety of Lhca polypeptides, their differences in lifetimes and spectral shapes and the variability of polypeptide composition in lincomycin-treated plants, assessing their contribution in the TFR spectra is virtually impossible. Therefore we can’t exclude *a priori* a partial contribution due to free LHCI in the thylakoids to the FR emission fluorescence.

A detailed analysis of the fluorescence kinetics of the peaks at ~ 680 nm and ~ 720 nm is presented in Figure 5.22. Especially at the lowest temperatures probed, the decay at 720 nm is considerably slower than that at 680 nm and this behaviour is independent of NPQ. Not only the spectra presented in Figure 5.20, but also the kinetics in the FR region exhibit a marked temperature dependency. These observations support further the conclusion that red and FR emitting states are not correlated to quenching. The decay of dark-adapted WT and L17 chloroplasts is very similar, or even slightly slower in the overexpressor strain, suggesting again that PsbS acts in the pH-dependent induction of NPQ and does not cause any “pre-quenching” effect, unlike when Zea is accumulated in the membranes. On the contrary, when the chloroplasts are exposed to high light during NPQ induction,

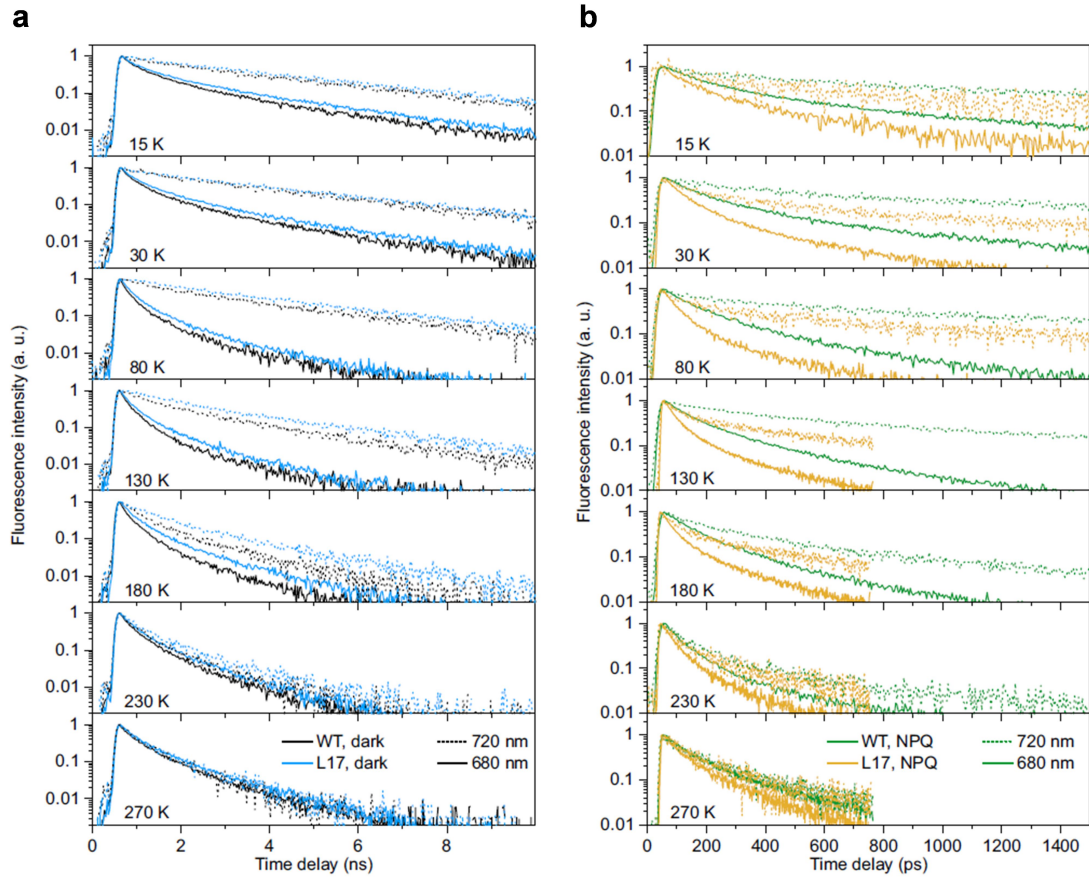


Figure 5.22: **Red and FR emitting forms decays significantly slower than the 680 nm emitting state.** **a** Fluorescence decay kinetics in the dark-adapted WT (black) and L17 (blue) chloroplasts at 680 nm (solid lines) and 720 nm (dots). **b** Fluorescence decay kinetics, obtained from the WT (green) and L17 (yellow) chloroplasts under NPQ condition.

ΔpH is generated across the thylakoids, PsbS is protonated and becomes active after monomerisation and forms quenching interactions with LHCII (Bergantino *et al.*, 2003; Sacharz *et al.*, 2017). Therefore, as already visible from NPQ induction traces (Figure 5.19), the fluorescence decay of L17 under NPQ conditions becomes significantly more pronounced relative to the WT (Figure 5.22b) since the membranes reach a deeper quenching state. Compared to aggregated LHCII (Chmeliov *et al.*, 2016), fluorescence kinetics in chloroplasts decay slower than the aggregates in the absence of NPQ processes, while they decay faster in quenched samples.

5.2.3 Red and FR emitting states are not involved in energy quenching

To gain more insights into the fluorescence state and their contribution to energy quenching, we performed a multivariate curve resolution analysis, that allows describing the fluorescence data in terms of a minimum number of fluorescing components with a clear physical meaning (equation 2.5 in “Chapter 2: Methodologies and approaches”) (Chmeliov *et al.*, 2016). The results are presented in Figure 5.23. While the data, at a first glance, suggest the presence of 3 distinct state (683 nm, 700 nm and 720 nm), the red (700 nm) and FR (720 nm) states were in fact well described treating them as a single component. Hence, the data were eventually described using two fluorescing states, “680 nm” and “red” components (Figure 5.23). With this analysis, we were able to fully separate the spectral and dynamical properties of these two LHCII states in the chloroplasts. Overall, once again it is clear the similarity of the obtained spectra and kinetics with those presented for LHCII aggregates (Chmeliov *et al.*, 2016). As described for raw traces in the above section, we were able to confirm the different behaviour of the two states and to verify both that the blue shift and temperature dependency are exclusive features of the “red” states and that these are long lived compared to the “680 nm” state. The analysis confirmed also that the “red” forms are not linked to quenching, since WT and L17 exhibit a different fluorescence profile under NPQ conditions. Therefore, all the results point towards the presence of an additional “dark” state that is responsible for energy quenching. The red emitting forms are loosely related to quenching and seem rather markers for the aggregation of LHCII (Akhtar *et al.*, 2019). Curiously, however, these forms are not enhanced in chloroplasts under NPQ conditions, and this could be due to the presence of additional factors such as lipids and PsbS that exert control over the structure of LHCII and vary the accessibility to the red and FR states. Even tiny structural differences were indeed found to result in pronounced perturbations of the fluorescence dynamics in LHCs (Krüger *et al.*, 2011a).

CHAPTER 5. IDENTIFICATION OF THE QE QUENCHER

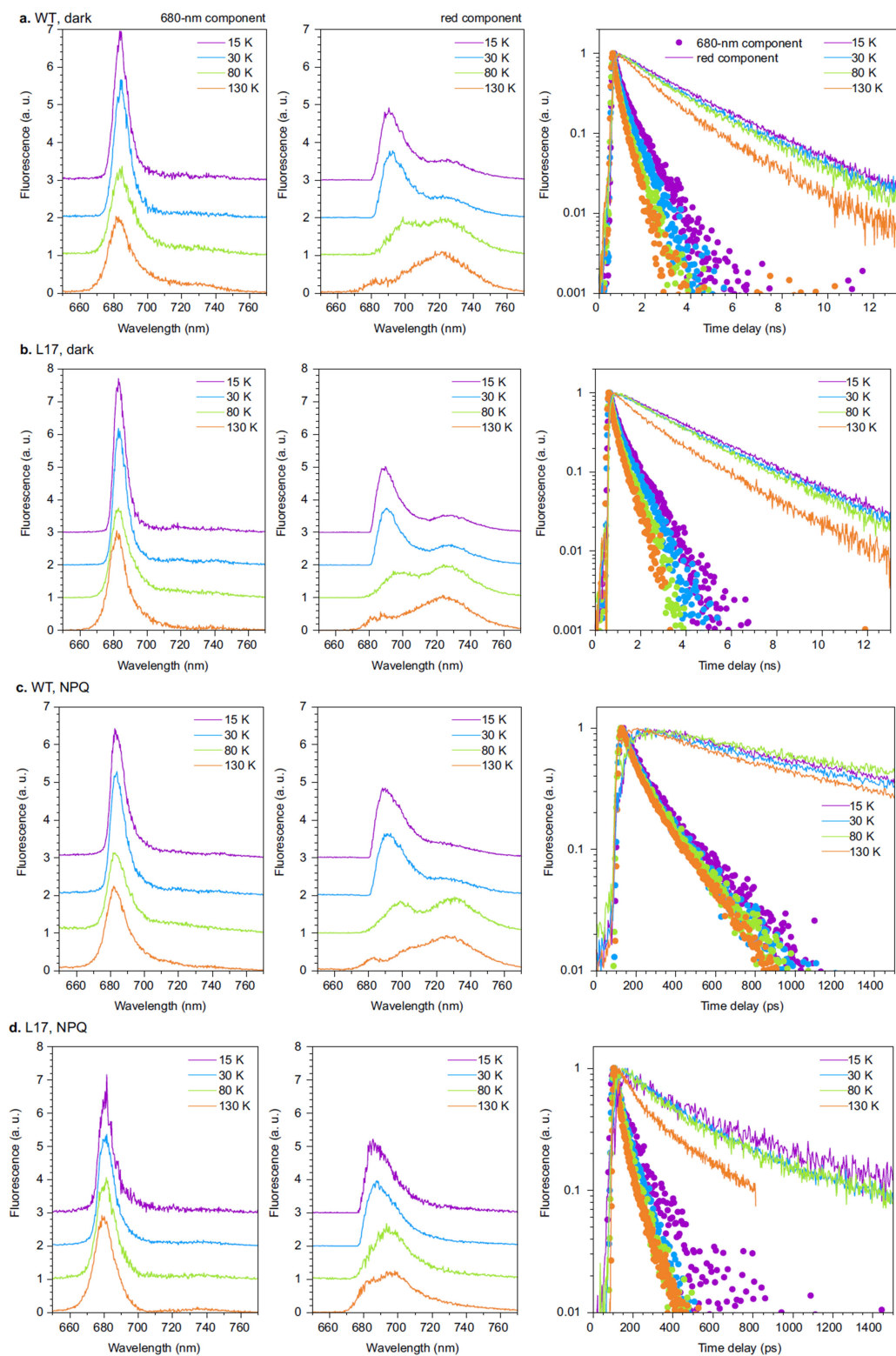


Figure 5.23: \curvearrowright **TFR data can be analytically described by a two-(emitting)-state model.** Results of the 2-state multivariate curve resolution analysis of the fluorescence from WT and L17 chloroplasts (equation 2.5 in “Chapter 2: Methodologies and approaches”). Left and middle, temperature-dependent fluorescence spectra of the dominating “680 nm” and the “red” emitting states, respectively. All fluorescence spectra are normalised to the area below them and offset for clarity. Right, normalised temperature-dependent fluorescence decay kinetics of the “680 nm” (dots) and the “red” (solid lines) emitting states.

5.2.4 The deeply quenched state of chloroplasts bears marked similarities with *in vitro* LHCII aggregates

The results of the spectral decomposition of L17 under NPQ conditions and their comparison with LHCII aggregates is shown in Figure 5.24. The spectral components (“680 nm” and “red”) of both conditions compared reveal a strikingly similar profile. The corresponding kinetics, shown in the multivariate curve analysis (Figure

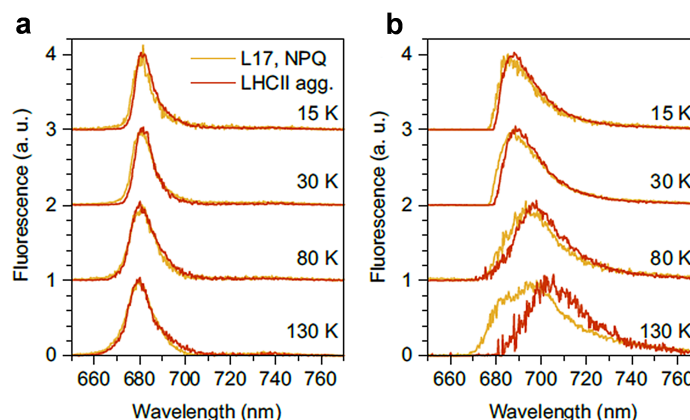


Figure 5.24: **The spectral decomposition of L17 chloroplasts under NPQ conditions and LHCII aggregates exhibit similar profiles.** **a** Extracted fluorescence spectra of the “680 nm” component obtained for the L17 chloroplasts under NPQ conditions (orange) and that obtained for LHCII aggregates from spinach (red). **b** Corresponding extracted fluorescence spectra of the “red” emitting component.

5.23) are notably faster than those in LHCII aggregates. However, the property that the “680 nm” component decays faster than the “red” one is still preserved. These results again imply that in the light-adapted thylakoids more antenna complexes compared to *in vitro* LHCII aggregates switch into the quenching conformational state since the switch become statistically more probable due to the presence of protonated, “active” PsbS. Therefore, the TRF spectra are very similar between

the *in vivo* chloroplasts and *in vitro* LHCII aggregates, even though the decay rates are somewhat different. This suggests that both these systems can be understood in terms of a the same model. In the previous work on LHCII aggregates (Chmeliov *et al.*, 2016), it was shown that the system can be described by a three-state model, with each state representing a specific conformational state of a LHCII monomer: one is the dominating state, responsible for emission at ~ 680 nm, and the other two are a red-emitting state, responsible for emission at ~ 700 nm and a non-emitting state, responsible for energy trapping and dissipation. Given the described similarity of the LHCII aggregates and the L17 chloroplasts under NPQ conditions, the same description can be applied to the fluorescence properties of both systems (Figure 5.25). The differences in decay rates can be attributed to a larger number of antenna complexes being in a quenching state, while spectral differences might be related to the presence of the minor antenna complexes, free remaining LHCI complexes and perturbations of their structure due to the lipid environment/PsbS presence, factors that are absent in the LHCII aggregates.

5.2.5 Discussion

In conclusion, our study on the lincomycin-treated chloroplasts that severely lack PSI and PSII RCs allowed us to detect the TRF signature of the light harvesting antenna complexes in native thylakoid membrane, in a simplified system where the fluorescence contribution from core complexes is suppressed. This work is a follow-up of the previous study of TRF on *in vitro* LHCII aggregates by Valkunas and co-workers (Chmeliov *et al.*, 2016). Here, we provided clear evidence of the similarity between spectral responses from both intact chloroplasts and artificially prepared LHCII aggregates, probed across a wide range of temperatures. These similarities further support the “LHCII aggregation” model of NPQ (Horton *et al.*, 1991, 2005; Ruban, 2018), which was supported by experimental data showing a higher degree of protein interactions correlated to the NPQ induction (Johnson *et al.*, 2011b). We demonstrated that the TFR data obtained from the thylakoid membranes can be easily understood in terms of the same model previously used to describe the behaviour of LHCII aggregates (Chmeliov *et al.*, 2016). Therefore, the previous conclusions derived from *in vitro* aggregates regarding the mechanism of energy

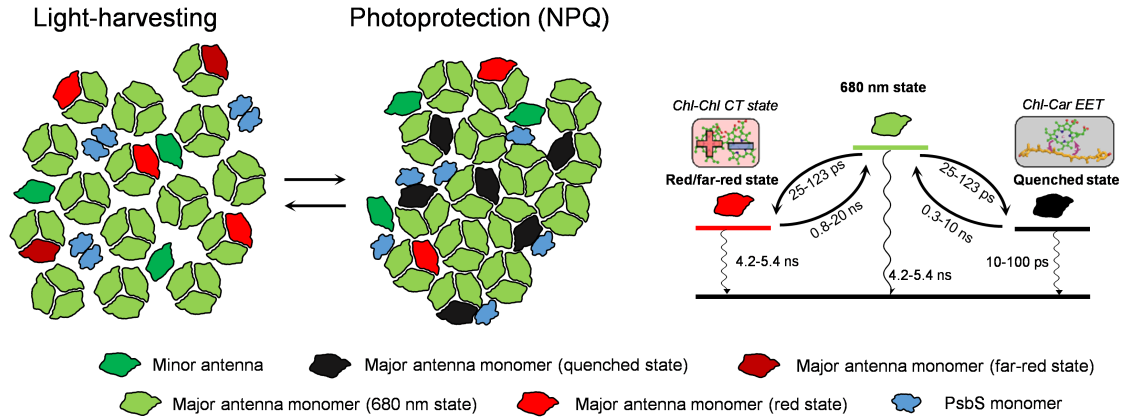


Figure 5.25: **NPQ shifts the conformational equilibrium of LHCII in the thylakoid membrane.** Schematic representation of the changes in the LHCII conformation associated with the onset of NPQ in the thylakoids from lincomycin-treated plants. Minor antennae are not involved in the in the dissipation of excess energy during NPQ, therefore don't switch to the dissipative conformation, unlike major LHCII complexes (Townsend *et al.*, 2018b). LHCII complexes undergo clustering during intense illumination (Betterle *et al.*, 2009; Johnson *et al.*, 2011b). Concomitantly, PsbS monomerises (Bergantino *et al.*, 2003) and interacts with LHCII, providing plasticity in the control of the quenching switch. (Wilk *et al.*, 2013; Correa-Galvis *et al.*, 2016; Sacharz *et al.*, 2017; Gerotto *et al.*, 2015). LHCII is in equilibrium between different conformational states ("680 nm", "red", "far-red", "quenched") and this equilibrium is shifted by variations in the thylakoid environment associated with NPQ (Krüger *et al.*, 2010, 2013). On the right, the 3-state model that describes the experimental data is presented (adapted from Chmeliov *et al.* (2016)) It comprises 2 emitting states ("680 nm" and "red/far-red") and a dark state, corresponding to the quencher. Energy transfer rates and decay kinetics to the ground state are shown in ps and ns. "Red/far-red" forms originate from Chl-Chl charge transfer (CT) interactions, while the "quencher" state involves likely a Chl-Car excitation energy transfer (EET). Both states show a very slow back-transfer to the "680 nm" state, constituting therefore efficient energy traps, but the "red/far-red" decays slowly to the ground state, while the "quencher" displays very fast kinetics of internal conversion.

quenching can be translated to *in vivo* chloroplasts, that constitute a considerable step towards a more "native" picture of the NPQ scenario. Particularly interesting is the behaviour of the red emitting states, which were variably found in isolated LHCII (Ruban and Horton, 1992; Pascal *et al.*, 2005; Illoaia *et al.*, 2008) and were associated *in vivo* to the quenching conformation (Miloslavina *et al.*, 2008). From our analysis, it emerges that neither red- nor FR-emitting states, occurring at temperatures below 130 K, are related to NPQ and should be attributed to the formation of the Chl-Chl charge-transfer states (Chmeliov *et al.*, 2016). These states are inevitably present in such a congested system, where pigment-pigment associations are very tight, but our results show that they do not positively correlate with energy quenching. By

contrast, the conformational state responsible for NPQ has a different nature and most likely involves excitation energy transfer from Chls to Cars (Ruban *et al.*, 2007). This is in line with the results presented in the first part of the Chapter (“*In vitro*”), where it was shown the probable involvement of Lut 1 in quenching excitation energy of the terminal emitter Chls. Additional insights into the action of the PsbS protein were obtained in this study, showing that it provides an allosteric control of the quenching switch of LHCII, without affecting the “light-harvesting” (Fm) state, in line with the results described in “Chapter 3: Identification of the qE site”. This allosteric control exerted over LHCII aggregation and quenching adds flexibility to NPQ and determines further the “economic” nature of the quenching mechanism (Belgio *et al.*, 2014), allowing the LHCII to perform an efficient function both as an energy harvester, under optimal light conditions, and as energy sink, under excessive excitation pressure.

Chapter 6

Conclusions

6.1 Plasticity in the regulation of light harvesting: the duality of LHCII purpose

The photosynthetic membrane is a dynamic micro-cosmos, unceasingly moving, renewing its components and adapting to external cues. The protein density in the thylakoids is among the highest in all known biological membranes, a property that can impact/control the mobility of complexes in the lipid bilayer and their interactions (Kirchhoff, 2014). Such high macromolecular crowding is efficiently exploited by nature to capture a large fraction of the dilute sunlight energy by a vast array of antenna complexes. LHCs are optimised to bind a considerable number of pigments while at the same time avoiding concentration quenching effects (Horton *et al.*, 1996). A remarkable property of this natural system is to control quickly and reversibly its efficiency during light capture.

In this work, I presented an investigation of the *site*, *change* and *quencher* of qE in plants (Figure 6.1a; see also “Aims of the Thesis” in “Chapter 1: Introduction”). While many factors have been linked to the dissipation of excess energy (major LHCII, minor LHCs, PsbS, Zea, RCs) this work showed that the sole crucial requirements of qE are LHCII trimers and ΔpH (“Chapter 3: Identification of the qE site”). Minor antenna complexes are not responsible for energy quenching, although they are critical for the optimal assembly of supercomplexes, excitation energy transfer to the core, electron transfer, ΔpH formation and dynamic reorganisation of the

membrane complexes during adaptive responses (*e.g.* state transitions). The major LHCII complex is capable of undergoing an intrinsic conformational *change* to tune its light-harvesting function and induce energy quenching. Components such as PsbS and Zea are found to be allosteric regulators, contributing to the plasticity of the LHCII quenching response, shaped on environmental cues and metabolic needs. More specifically, while exerting some minor effects on the energetics of single LHCII complexes, Zea doesn't substantially change their fluorescence emission properties and doesn't cause additional quenching effects ("Chapter 4: Investigation of the conformational change of LHCII associated with qE"). Therefore, the prominent effect of Zea accumulation during NPQ on the amplitudes and kinetics of the process is unlikely to arise from an *in situ* change on single LHCII. Instead, it probably relates to changes in the hydrophobicity of the membrane, that causes an increased tendency of LHCII to aggregate and leads to the stabilisation of the quenching state. Despite having shown the indirect effect of Zea during NPQ, the nature of the *quencher* remains a question mark. While many dissipative mechanisms have been identified, none of them has been so far unequivocally correlated to energy quenching during qE. The results presented in "Chapter 5: Identification of the qE quencher" clearly show that the environment of LHCII is a crucial factor and determines its functionality. A dynamic lipid bilayer around LHCII complexes could thus be the cornerstone controlling the conformational changes associated with qE. In virtue of their short excited state lifetime, Cars are good candidates for energy dissipation, making them "natural-born quenchers". Transient absorption measurements performed on isolated LHCII immobilised in gels suggests that a relief valve for excitation pressure involving Chl-to-Car energy transfer could be enhanced during the induction of the dissipative state. The changes that occur in the terminal emitter locus prompt towards an involvement of the Car in the L1 site, namely a lutein (Lut 1) in LHCII.

6.2 Physiological significance of qE control

Several models of qE have been proposed over the years (Horton *et al.*, 1991; Krieger and Weis, 1993; Holt *et al.*, 2005; Holzwarth *et al.*, 2009; Ruban, 2016; Dall'Osto *et al.*, 2017; Bennett *et al.*, 2019; Nicol *et al.*, 2019). Most of them invoke the action

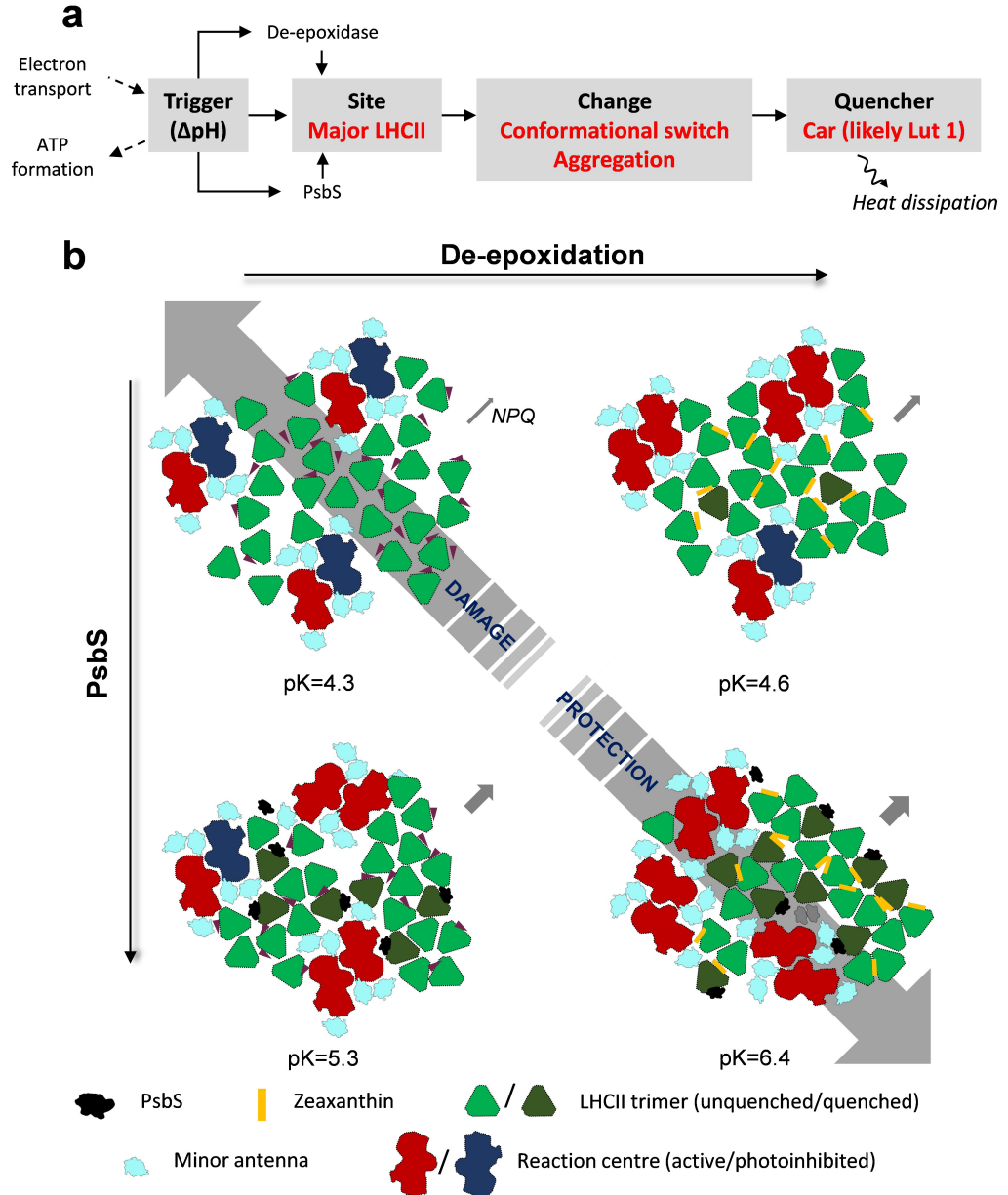


Figure 6.1: **Outcome of the thesis.** **a** The qE scenario, as described in section “Aims of the thesis” in “Chapter 1: Introduction”. In red, the novel findings described in the thesis concerning *site*, *change* and *quencher* identity. **b** The physiological significance of qE regulation. pK values for each scenario described were taken from (Johnson and Ruban, 2011).

of specific pigment-binding complexes and specific pigments in the quenching of excess energy, such as minor antennae and Zea (Holt *et al.*, 2005; Ahn *et al.*, 2008).

Further, they suggest the existence of multiple processes and sites, accounting for the multitude of kinetic components of qE (Holzwarth *et al.*, 2009; Dall'Osto *et al.*, 2017; Park *et al.*, 2018). Our results, however, suggest that the major LHCII complexes have an inherent capacity to regulate their function and protect themselves via conformational changes. Altogether, this is in line with the “LHCII aggregation” model proposed by Horton and co-workers (Horton *et al.*, 1991).

The most important difference between the “LHCII aggregation” model and all other qE hypothesis is the concept of *control* over qE, which is contemplated only in the former. ΔpH in the thylakoids is the intermediary product between the harvesting of sunlight energy and its storage in a stable chemical form. High amplitudes of ΔpH , however, can be limiting, causing the inhibition of electron transport (Schönknecht *et al.*, 1995; Hurry *et al.*, 1996; Krieger-Liszka *et al.*, 2000), or even detrimental, being linked to photoinhibitory processes (Spetea *et al.*, 1997). It is likely, therefore, that ΔpH is regulated within narrow limits (Schönknecht *et al.*, 1995; Kramer *et al.*, 1999). For this reason, qE is a highly controlled process, characterised by an allosteric and cooperative regulation given by Zea and the protein PsbS (Figure 6.1b). This has profound physiological implications. LHCII trimers alone have a limited ability to sense protons (Petrou *et al.*, 2014) and are, in fact, irresponsive to physiological ΔpH variations. PsbS and Zea act synergically as allosteric modulators of the proton-sensitivity of LHCII, tuning its activation to less acidic luminal pH values (Figure 6.1b). This model is therefore able to readily explain the roles of Zea and PsbS, which seem to act independently on the same process (*i.e.* LHCII aggregation/conformational change). Thus, both factors add flexibility to the qE mechanism and make it tunable in relation to environmental conditions and metabolic needs. Offering a dynamic adaptation of qE to the light environment, the allosteric control defined by PsbS and Zea is necessary to preserve its economic nature (Belgio *et al.*, 2014; van Amerongen and Chmeliov, 2019). The function of LHCII is therefore optimally modulated to ensure the correct balance between protection and photosynthetic productivity. The cooperativity between LHCII units offers an additional control of the qE switch, allowing its complete induction within small pH changes. Superimposed to this allosteric regulation of light harvesting, natural genetic variation of PsbS and Zea-related genes grant different plant species a high adaptability to diverse natural environments (Demmig-Adams *et al.*, 2006;

Wilson and Ruban, 2019; Rungrat *et al.*, 2019).

6.3 Improving solar energy utilisation in a dynamic environment

The industrial revolution of the 18th and 19th centuries kicked off a prosperous era for humanity, which resulted in the tremendous increase of the growth rate of the world population. As progress led to improved technologies, infrastructures, food safety and healthcare, humankind is facing new, unprecedented challenges. With this trend, the global population is expected to exceed 10 billion individuals by the end of the current century (source: <https://www.worldometers.info>).

Firstly, to deal with the incumbent issue of feeding an exponentially-increasing number of people, it is calculated that the current crop yields need to double within the next 40-50 years (Zhu *et al.*, 2010).

The second issue concerns energy consumption. Fossil fuels are still the predominant sources that drive industries, transports, heating systems *etc.* Since fossil fuels contribute severely to CO₂ emissions and their reserves are gradually depleting, their use needs to shift in favour of renewable and cleaner resources.

Additionally, we are experiencing a climate emergency. Extreme weather events, such as heat waves, are becoming more frequent (Tebaldi *et al.*, 2006). Fossil fuel burning and deforestation have led to a conspicuous amount of CO₂ released in the atmosphere during the Anthropocene era (Sabine, 2004). This release has contributed to the substantial and continuous rise of the average temperature of the planet, that is disturbing the current equilibrium of the biosphere, with effects such as biome loss or latitude shifts (Long and Ort, 2010), loss of permafrost (Chadburn *et al.*, 2017), increased ocean acidification (Caldeira and Wickett, 2003) *etc.* In September 2019, at the United Nations Climate Action Summit, a report was redacted to update the current status of the environment and set new goals to cut carbon emissions thus putting a stop to global warming (source: https://public.wmo.int/en/resources/united_in_science). It emerged that we are quickly approaching a tipping point that, if crossed, would irreversibly lead to a “hothouse” Earth (Steffen *et al.*, 2018). In order to meet the goals set by the

2016 Paris Agreement and contain global warming within a 2 °C increase, countries must triple their policies on reducing carbon emissions.

Luckily, we live in a historical moment of great awareness of these issues. Under countless aspects, plants represent a vital resource to fight back and solve them. Crops are factories not just for the production of food, but also for biofuels and can potentially mitigate the effect of climate change by helping to sequester atmospheric CO₂ (Kantola *et al.*, 2017). But since the arable land is limited and its expansion has considerable environmental drawbacks, it is necessary to improve the biomass yields of current crop cultures. Conventional breeding has been crucial to select convenient agronomic traits and to fuel the “Green Revolution” in the 20th century. However, the advances made during this period mainly affected the so-called “harvest index”, which measures the amount of biomass that is partitioned into grain, but this is now close to its theoretical limit (Blankenship *et al.*, 2011; Ort *et al.*, 2015). By contrast, the efficiency of photosynthesis is still far from its theoretical limit, but these traits have proven to be hard to select through standard breeding procedures (Zhu *et al.*, 2010). Advances in genetic engineering and biotechnologies will likely be crucial for a scientific breakthrough that relieves humanity from the burdens of food, energy and climate crises.

It is often overlooked that plants are living in a dynamic world, where improving the efficiency of light energy utilisation could be a more rewarding approach than simply increasing the quantity of energy captured. Indeed, a remarkable property of living systems is their ability to regulate, adapt and repair themselves, in a relentless struggle with other organisms and environmental factors. As an outcome of competitive evolution, energy losses can be considerably large during sunlight energy harvesting in plants (Ruban, 2012; Krüger and van Grondelle, 2017). Some of these losses are inevitable and often extensive. They reflect the processes of internal conversion from higher pigment excited states and the directionality of the excitation energy transfer, where only energies around red wavelengths are utilised to store chemical potential. Others are avoidable and reflect simply the evolutionary constraints that prioritised survival traits over primary production yields. Among these, NPQ is often an inefficient valve for the regulation of excitation energy pressure on PSII (Ruban, 2017). The induction of NPQ upon high-light exposure can be fast but is never instantaneous in nature, implying that a fraction of absorbed

photons is persisting in the photosystem before it can be safely dissipated (“Insufficient protection”, Figure 6.2a). The rate of NPQ relaxation is even slower than the rate of induction, leading to wasteful dissipation of absorbed photons (“Wasteful protection”, Figure 6.2a). It was predicted that a “lossy” NPQ induction could have severe repercussions on the yield of CO_2 assimilation under field conditions (dynamic light environments) (Zhu *et al.*, 2004). An important advance has been recently presented by Long and co-authors (Kromdijk *et al.*, 2016), confirming these predictions and proving that engineering the NPQ switch to make it faster and more efficient can increase the biomass yield of plants in the field by up to 20% (Figure 6.2b).

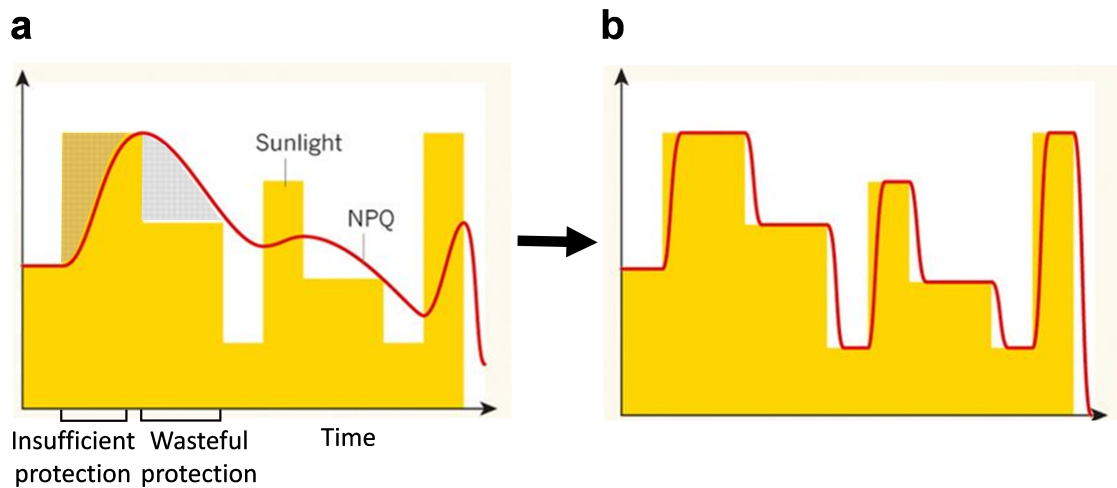


Figure 6.2: **Re-engineering the NPQ switch.** **a** NPQ allows plants to track the changes in light intensity and regulate the energy fluxes during light harvesting. However, the slow kinetics of the xanthophyll cycle operations are a major bottleneck to the rates of induction and relaxation of the process. **b** Kromdijk and co-workers (Kromdijk *et al.*, 2016) have shown that re-engineering NPQ, accelerating the switch between light-harvesting and quenched state, can improve the yield of plants in field by up to 20%. Adapted from Ruban (2017), Nature.

Photoinhibition (qI) is another common source of energy loss and occurs even in plants exposed to moderate amounts of light (Murchie *et al.*, 1999). While a fraction of this sustained decline of PSII efficiency is ascribed to slowly reverting NPQ processes (Ruban and Horton, 1995), the rest is due to damage of core proteins, whose repair has a metabolic cost (Raven, 1989). If under some conditions qI may be even beneficial for plants, protecting other photosynthetic complexes such as PSI

(Tikkanen and Aro, 2014), in most cases it is a limiting factor for photosynthesis (Murchie and Ruban, 2019). NPQ is strongly interlinked to photoinhibition and it has been shown in several experiments that enhancing the NPQ capacity reduces the extent of photoinhibition (Li *et al.*, 2002; Hubbart *et al.*, 2018). Early works on *Arabidopsis* NPQ mutants demonstrated that NPQ impacts the fitness of plants in the field (Külheim *et al.*, 2002; Krah and Logan, 2010). A recent study on rice showed that, by lessening the detrimental photoinhibitory effects, the improvement of NPQ results in increased biomass production (Hubbart *et al.*, 2018). Despite the clear link between NPQ and photoinhibition, remaining debated is true impact of NPQ as a photoprotective mechanism and the avoidance of photooxidative damage (Santabarbara *et al.*, 2001; Ruban, 2016). Recently, efforts have been made to understand the photoprotective effectiveness of NPQ. A new non-invasive method based on PAM fluorimetry has been described, which enabled the separation of the contribution of NPQ and other metabolic processes such as D1 repair in plant light tolerance (Ruban and Murchie, 2012; Townsend *et al.*, 2018a). Its accuracy has been tested on several *Arabidopsis* NPQ mutants and other related Brassicaceae, showing in all cases that NPQ plays a crucial role in photoprotection (Ware *et al.*, 2015a, 2016; Wilson and Ruban, 2019). Particularly pronounced is the increase of maximum light tolerance in plants overexpressing PsbS, where qE is enhanced (Ruban and Belgio, 2014).

Constant inspiration to understand photoprotection and its impact on fitness and productivity comes from natural organisms that are capable of sophisticated mechanisms to cope with sporadic or persistent high light exposure. For example, the recently characterised green alga *Chlorella ohadii* is extremely resistant to photodamage and its PSII core complexes are barely affected by strong irradiance (Treves *et al.*, 2016). On a similar note, the diatom *Pheodactylum tricornutum* is capable of inducing a huge extent of NPQ, which is possibly a reason contributing to their ecological success (Giovagnetti and Ruban, 2017; Cardona *et al.*, 2018).

It appears that NPQ affects several cellular processes, interacting for example with defence pathways involving ROS signalling (Murchie and Ruban, 2019). Importantly, a recent study demonstrated that the PsbS protein is involved in the control of stomatal aperture and affects the water use efficiency of plants (Głowacka *et al.*, 2018). Overall, these works suggest that NPQ exerts a pleiotropic effect on

plant growth traits, demonstrating the economic importance of this physiological process and justifying the efforts invested toward its improvement.

6.4 The future of qE research.

Our knowledge of qE has greatly improved over 50 years of research. At the time of writing of this thesis, there is a large body of evidence that the trigger of qE is thylakoid ΔpH , the site of quenching is the major LHCII antenna and that conformational changes and rearrangements in the membranes occur to achieve the photoprotective state. Despite this, some mechanistic gaps remain to be filled. One such area is the detail of how the protein PsbS acts. PsbS is likely not involved directly in the quenching of excess energy since the need for PsbS could be bypassed by varying ΔpH amplitudes in intact chloroplasts (see “Chapter 3: Identification of the qE site”). Its presence interferes with the fluidity of the thylakoid membrane, increasing the size of the mobile fraction of membrane bound complexes, while “freezing” them in the qE state (reducing greatly their mobility) (Goral *et al.*, 2012). This suggests that PsbS could be acting as a membrane re-modeller, possibly interacting specifically with thylakoid lipids, to control the activity and the interactions of antenna complexes. Moreover, PsbS has been shown to interact with antenna complexes and these interactions are enhanced during qE and associated with energy quenching (Correa-Galvis *et al.*, 2016; Sacharz *et al.*, 2017). Are these interactions specific or merely due to the high hydrophobicity of PsbS? Are they promoting the conformational change of LHCII? If this is true, is it due to an increase in the pK of proton-sensing residues on the luminal side of LHCII, making the protein more sensitive to pH? Molecular details of these interactions are missing.

Whilst it is accepted that a reorganisation of the thylakoid membrane occurs at the onset of qE, the mechanism that drives these transient changes is still not well understood. As early as 1970, it was observed that a ΔpH -dependent thinning of the thylakoid occurs (Murakami and Packer, 1970). This was later shown to be correlated to qE (Johnson *et al.*, 2011a). Up to a 25% thinning of the thylakoids has been observed, which is sufficient to cause hydrophobic mismatch between membrane proteins and the lipid bilayer (Killian, 1998). In turn, this hydrophobic mismatch causes a thermodynamic instability of the membrane complexes, that are forced

into a conformational change and to find relief in protein-protein interactions. This has been recently suggested as a possible scenario for the conformational switch of LHCII and its enhanced aggregation observed during qE, although it remains to be verified (Ruban, 2019).

Yet another question mark concerns the identity of the qE quencher. The work presented on this thesis showed the probable direct involvement of Lut 1 as a quencher and the indirect effect of Zea as an allosteric modulator. However, we are still lacking irrefutable proof that this is indeed the mechanism of quenching in the intact thylakoids. The thylakoid membrane is a congested system, with an incredibly high concentration of pigments and variety of chemical structures, interactions, deformations *etc.* This makes the study of the quencher *in vivo* a seemingly impossible challenge. The study of the quenched state *in vivo* at high atomic resolution would require a fundamentally new approach, possibly coming from recent advances in cryo-electron microscopy (Engel *et al.*, 2015; van Bezouwen *et al.*, 2017; Nagao *et al.*, 2019) or from time-resolved vibrational techniques, that are able to chase with high specificity subtle molecular motions (Fang *et al.*, 2009; Hontani *et al.*, 2018).

The results presented in this thesis represent a small contribution to the knowledge of the dynamics of light harvesting in the photosynthetic membrane and its regulation, providing a potential basis for future biotechnological improvement. It is shown here that the beauty of the light harvesting regulation lies in the simplicity of its components and not in overly-complicated networks of photoprotection: the LHCII function is controlled in a negative feedback loop by enhanced ΔpH across the thylakoid and these two factors are the sole essential components of the qE processes in plants. Cooperativity and allostery, given by accessory factors such as PsbS and zeaxanthin are key traits in this control and it is where bioengineering approaches should look for improvement. It is clear that membrane dynamics largely govern the plasticity of the light harvesting machinery and its adaptability to the external cues. In light of the temperature rise caused by climate change, understanding the regulation of these processes would provide invaluable tools to fight back the crash of natural constants and represent solutions to improve the yield of photosynthesis under ever-changing conditions.

Bibliography

- Ahn, T. K., Avenson, T. J., Ballottari, M., Cheng, Y. C., Niyogi, K. K., Bassi, R., and Fleming, G. R. (2008). Architecture of a charge-transfer state regulating light harvesting in a plant antenna protein. *Science* **320**(5877): 794–797.
- Akhtar, P., Görföl, F., Garab, G., and Lambrev, P. H. (2019). Dependence of chlorophyll fluorescence quenching on the lipid-to-protein ratio in reconstituted light-harvesting complex II membranes containing lipid labels. *Chemical Physics* **522**: 242–248.
- Allen, J. F., Bennett, J., Steinback, K. E., and Arntzen, C. J. (1981). Chloroplast protein phosphorylation couples plastoquinone redox state to distribution of excitation energy between photosystems. *Nature* **291**(5810): 25–29.
- Amarie, S., Standfuss, J., Barros, T., Kühlbrandt, W., Dreuw, A., and Wachtveitl, J. (2007). Carotenoid radical cations as a probe for the molecular mechanism of nonphotochemical quenching in oxygenic photosynthesis. *Journal of Physical Chemistry B* **111**(13): 3481–3487.
- Amarie, S., Wilk, L., Barros, T., Kühlbrandt, W., Dreuw, A., and Wachtveitl, J. (2009). Properties of zeaxanthin and its radical cation bound to the minor light-harvesting complexes CP24, CP26 and CP29. *Biochimica et Biophysica Acta - Bioenergetics* **1787**(6): 747–752.
- Ambrose, E. J. (1956). A Surface Contact Microscope for the study of Cell Movements. *Nature* **178**(4543): 1194–1194.

- Anderson, J. M. and Boardman, N.** (1966). Fractionation of the photochemical systems of photosynthesis I. Chlorophyll contents and photochemical activities of particles isolated from spinach chloroplasts. *Biochimica et Biophysica Acta (BBA) - Biophysics including Photosynthesis* **112**(3): 403–421.
- Andersson, J., Walters, R. G., Horton, P., and Jansson, S.** (2001). Antisense inhibition of the photosynthetic antenna proteins CP29 and CP26: implications for the mechanism of protective energy dissipation. *The Plant cell* **13**(5): 1193–1204.
- Andersson, J., Wentworth, M., Walters, R. G., Howard, C. A., Ruban, A. V., Horton, P., and Jansson, S.** (2003). Absence of the Lhcb1 and Lhcb2 proteins of the light-harvesting complex of photosystem II - Effects on photosynthesis, grana stacking and fitness. *Plant Journal* **35**(3): 350–361.
- Andersson, P. O. and Gillbro, T.** (1995). Photophysics and dynamics of the lowest excited singlet state in long substituted polyenes with implications to the very long-chain limit. *The Journal of Chemical Physics* **103**(7): 2509–2519.
- Aspinall-O'Dea, M., Wentworth, M., Pascal, A., Robert, B., Ruban, A., and Horton, P.** (2002). In vitro reconstitution of the activated zeaxanthin state associated with energy dissipation in plants. *Proceedings of the National Academy of Sciences of the United States of America* **99**(25): 16331–16335.
- Athanasίου, K., Dyson, B. C., Webster, R. E., and Johnson, G. N.** (2010). Dynamic acclimation of photosynthesis increases plant fitness in changing environments. *Plant Physiology* **152**(1): 366–373.
- Avenson, T. J., Tae, K. A., Zigmantas, D., Niyogi, K. K., Li, Z., Ballottari, M., Bassi, R., and Fleming, G. R.** (2008). Zeaxanthin radical cation formation in minor light-harvesting complexes of higher plant antenna. *Journal of Biological Chemistry* **283**(6): 3550–3558.
- Axelrod, D.** (2003). Total internal reflection microscopy in cell biology. *Methods in Enzymology* **361**(2): 1–33.

- Bailey, S., Walters, R. G., Jansson, S., and Horton, P.** (2001). Acclimation of *Arabidopsis thaliana* to the light environment: The existence of separate low light and high light responses. *Planta* **213**(5): 794–801.
- Bailleul, B., Cardol, P., Breyton, C., and Finazzi, G.** (2010). Electrochromism: a useful probe to study algal photosynthesis. *Photosynthesis research* **106**(1-2): 179–189.
- Baker, N. R.** (2008). Chlorophyll Fluorescence: A Probe of Photosynthesis In Vivo. *Annual Review of Plant Biology* **59**(1): 89–113.
- Balevičius, V., Fox, K. F., Bricker, W. P., Jurinovich, S., Prandi, I. G., Mennucci, B., and Duffy, C. D. P.** (2017). Fine control of chlorophyll-carotenoid interactions defines the functionality of light-harvesting proteins in plants. *Scientific Reports* **7**(1): 13956.
- Balevičius, V., Wei, T., Di Tommaso, D., Abramavicius, D., Hauer, J., Polívka, T., and Duffy, C. D.** (2019). The full dynamics of energy relaxation in large organic molecules: From photo-excitation to solvent heating. *Chemical Science* **10**(18): 4792–4804.
- Ballottari, M., Dall'Osto, L., Morosinotto, T., and Bassi, R.** (2007). Contrasting behavior of higher plant photosystem I and II antenna systems during acclimation. *Journal of Biological Chemistry* **282**(12): 8947–8958.
- Barzda, V., Peterman, E. J., Van Grondelle, R., and Van Amerongen, H.** (1998). The influence of aggregation on triplet formation in light-harvesting chlorophyll a/b pigment-protein complex II of green plants. *Biochemistry* **37**(2): 546–551.
- Barzda, V., Gulbinas, V., Kananavicius, R., Cervinskis, V., van Amerongen, H., van Grondelle, R., and Valkunas, L.** (2001). Singlet-Singlet Annihilation Kinetics in Aggregates and Trimers of LHCII. *Biophysical Journal* **80**(5): 2409–2421.

- Bassi, R. and Dainese, P.** (1992). A supramolecular light-harvesting complex from chloroplast photosystem-II membranes. *European journal of biochemistry* **204**(1): 317–26.
- Bassi, R., Pineau, B., Dainese, P., and Marquardt, J.** (1993). Carotenoid-binding proteins of photosystem II. *European journal of biochemistry* **212**(2): 297–303.
- Bassi, R. and Caffarri, S.** (2000). Lhc proteins and the regulation of photosynthetic light harvesting function by xanthophylls. *Photosynthesis Research* **64**(2-3): 243–256.
- Beddard, G. S. and Porter, G.** (1976). Concentration quenching in chlorophyll. *Nature* **260**(5549): 366–367.
- Belgio, E., Johnson, M. P., Jurić, S., and Ruban, A. V.** (2012). Higher plant photosystem II light-harvesting antenna, not the reaction center, determines the excited-state lifetime - Both the maximum and the nonphotochemically quenched. *Biophysical Journal* **102**(12): 2761–2771.
- Belgio, E., Duffy, C. D. P., and Ruban, A. V.** (2013). Switching light harvesting complex II into photoprotective state involves the lumen-facing apoprotein loop. *Physical Chemistry Chemical Physics* **15**(29): 12253.
- Belgio, E., Kapitonova, E., Chmeliov, J., Duffy, C. D. P., Ungerer, P., Valkunas, L., and Ruban, A. V.** (2014). Economic photoprotection in photosystem II that retains a complete light-harvesting system with slow energy traps. *Nature Communications* **5**(1): 4433.
- Belgio, E., Ungerer, P., and Ruban, A. V.** (2015). Light-harvesting superstructures of green plant chloroplasts lacking photosystems. *Plant, Cell and Environment* **38**(10): 2035–2047.
- Bellafiore, S., Barneche, F., Peltier, G., and Rochaix, J.-D.** (2005). State transitions and light adaptation require chloroplast thylakoid protein kinase STN7. *Nature* **433**(7028): 892–895.

- Ben-Shem, A., Frolov, F., and Nelson, N.** (2003). Crystal structure of plant photosystem I. *Nature* **426**(6967): 630–635.
- Bennett, D. I. G., Amarnath, K., Park, S., Steen, C. J., Morris, J. M., and Fleming, G. R.** (2019). Models and mechanisms of the rapidly reversible regulation of photosynthetic light harvesting. *Open Biology* **9**(4): 190043.
- Bennett, J.** (1977). Phosphorylation of chloroplast membrane polypeptides. *Nature* **269**(5626): 344–346.
- Bennett, J.** (1979). Chloroplast Phosphoproteins. Phosphorylation of Polypeptides of the Light-Harvesting Chlorophyll Protein Complex. *European Journal of Biochemistry* **99**(1): 133–137.
- Bennett, J.** (1980). Chloroplast Phosphoproteins. Evidence for a Thylakoid-Bound Phosphoprotein Phosphatase. *European Journal of Biochemistry* **104**(1): 85–89.
- Bennett, J., Shaw, E. K., and Michel, H.** (1988). Cytochrome b6f complex is required for phosphorylation of light-harvesting chlorophyll a/b complex II in chloroplast photosynthetic membranes. *European Journal of Biochemistry* **171**(1-2): 95–100.
- Berera, R., Herrero, C., van Stokkum, I. H. M., Vengris, M., Kodis, G., Palacios, R. E., van Amerongen, H., van Grondelle, R., Gust, D., Moore, T. A., Moore, A. L., and Kennis, J. T. M.** (2006). A simple artificial light-harvesting dyad as a model for excess energy dissipation in oxygenic photosynthesis. *Proceedings of the National Academy of Sciences* **103**(14): 5343–5348.
- Berera, R., van Grondelle, R., and Kennis, J. T. M.** (2009). Ultrafast transient absorption spectroscopy: Principles and application to photosynthetic systems. *Photosynthesis Research* **101**(2-3): 105–118.
- Bergantino, E., Segalla, A., Brunetta, A., Teardo, E., Rigoni, F., Giacometti, G. M., and Szabò, I.** (2003). Light- and pH-dependent structural changes in the PsbS subunit of photosystem II. *Proceedings of the*

- National Academy of Sciences of the United States of America* **100**(25): 15265–15270.
- Betterle, N., Ballottari, M., Zorzan, S., de Bianchi, S., Cazzaniga, S., Dall'Osto, L., Morosinotto, T., and Bassi, R.** (2009). Light-induced dissociation of an antenna hetero-oligomer is needed for non-photochemical quenching induction. *Journal of Biological Chemistry* **284**(22): 15255–15266.
- Bilger, W., Björkman, O., and Thayer, S. S.** (1989). Light-Induced Spectral Absorbance Changes in Relation to Photosynthesis and the Epoxidation State of Xanthophyll Cycle Components in Cotton Leaves. *Plant Physiology* **91**(2): 542–551.
- Bilger, W. and Björkman, O.** (1990). Role of the xanthophyll cycle in photoprotection elucidated by measurements of light-induced absorbance changes, fluorescence and photosynthesis in leaves of *Hedera canariensis*. *Photosynthesis Research* **25**(3): 173–185.
- Bilger, W. and Björkman, O.** (1991). Temperature dependence of violaxanthin de-epoxidation and non-photochemical fluorescence quenching in intact leaves of *Gossypium hirsutum* L. and *Malva parviflora* L. *Planta* **184**(2): 226–234.
- Bilger, W. and Björkman, O.** (1994). Relationships among violaxanthin deepoxidation, thylakoid membrane conformation, and nonphotochemical chlorophyll fluorescence quenching in leaves of cotton (*Gossypium hirsutum* L.). *Planta* **193**(2): 238–246.
- Billsten, H. H., Sundström, V., and Polívka, T.** (2005). Self-Assembled Aggregates of the Carotenoid Zeaxanthin: Time-Resolved Study of Excited States. *The Journal of Physical Chemistry A* **109**(8): 1521–1529.
- Björkman, O., Boardman, N., Anderson, J., Thorne, S., Goodchild, D., and Pyliotis, N.** (1972). Effects of light intensity during growth of *Atriplex patula* on the capacity of photosynthetic reactions, chloroplast components and structures. *Carnegie Inst. Wash. Yrbk.* **71**: 115–135.

- Björkman, O. and Demmig, B.** (1987). Photon yield of O₂ evolution and chlorophyll fluorescence characteristics at 77 K among vascular plants of diverse origins. *Planta* **170**(4): 489–504.
- Björn, L. O., Papageorgiou, G. C., Blankenship, R. E., and Govindjee** (2009). A viewpoint: Why chlorophyll a? *Photosynthesis Research* **99**(2): 85–98.
- Blankenship, R. E.**, *Molecular Mechanisms of Photosynthesis* (Blackwell Science Ltd, Oxford, UK, 2002).
- Blankenship, R. E., Tiede, D. M., Barber, J., Brudvig, G. W., Fleming, G., Ghirardi, M., Gunner, M. R., Junge, W., Kramer, D. M., Melis, A., Moore, T. a., Moser, C. C., Nocera, D. G., Nozik, A. J., Ort, D. R., Parson, W. W., Prince, R. C., and Sayre, R. T.** (2011). Comparing Photosynthetic and Photovoltaic Efficiencies and Recognizing the Potential for Improvement. *Science* **332**(6031): 805–809.
- Boardman, N. K.** (1977). Comparative Photosynthesis of Sun and Shade Plants. *Annual Review of Plant Physiology* **28**(1): 355–377.
- Bode, S., Quentmeier, C. C., Liao, P.-N., Hafi, N., Barros, T., Wilk, L., Bittner, F., and Walla, P. J.** (2009). On the regulation of photosynthesis by excitonic interactions between carotenoids and chlorophylls. *Proceedings of the National Academy of Sciences* **106**(30): 12311–12316.
- Boekema, E. J., Dekker, J. P., van Heel, M. G., Rögner, M., Saenger, W., Witt, I., and Witt, H. T.** (1987). Evidence for a trimeric organization of the photosystem I complex from the thermophilic cyanobacterium *Synechococcus* sp. *FEBS Letters* **217**(2): 283–286.
- Boekema, E. J., Van Roon, H., Calkoen, F., Bassi, R., and Dekker, J. P.** (1999a). Multiple types of association of photosystem II and its light-harvesting antenna in partially solubilized photosystem II membranes. *Biochemistry* **38**(8): 2233–2239.
- Boekema, E. J., Van Roon, H., Van Breemen, J. F., and Dekker, J. P.** (1999b). Supramolecular organization of photosystem II and its light-harvesting

- antenna in partially solubilized photosystem II membranes. *European Journal of Biochemistry* **266**(2): 444–452.
- Boekema, E. J., Hankamer, B., Bald, D., Kruip, J., Nield, J., Boonstra, A. F., Barber, J., and Rogner, M.** (2006). Supramolecular structure of the photosystem II complex from green plants and cyanobacteria. *Proceedings of the National Academy of Sciences* **92**(1): 175–179.
- Bonaventura, C. and Myers, J.** (1969). Fluorescence and oxygen evolution from *Chlorella pyrenoidosa*. *Biochimica et Biophysica Acta (BBA) - Bioenergetics* **189**(3): 366–383.
- Bonente, G., Howes, B. D., Caffarri, S., Smulevich, G., and Bassi, R.** (2008). Interactions between the photosystem II subunit PsbS and xanthophylls studied in vivo and in vitro. *Journal of Biological Chemistry* **283**(13): 8434–8445.
- Briantais, J.-M., Vernotte, C., Picaud, M., and Krause, G.** (1979). A quantitative study of the slow decline of chlorophyll a fluorescence in isolated chloroplasts. *Biochimica et Biophysica Acta (BBA) - Bioenergetics* **548**(1): 128–138.
- Büchel, C.** (2015). Evolution and function of light harvesting proteins. *Journal of Plant Physiology* **172**: 62–75.
- Burton-Smith, R. N., Watanabe, A., Tokutsu, R., Song, C., Murata, K., and Minagawa, X. J.** (2019). Structural determination of the large photosystem II-light-harvesting complex II supercomplex of *Chlamydomonas reinhardtii* using nonionic amphipol. *Journal of Biological Chemistry* **294**(41): 15003–15013.
- Caffarri, S., Croce, R., Breton, J., and Bassi, R.** (2001). The Major Antenna Complex of Photosystem II Has a Xanthophyll Binding Site Not Involved in Light Harvesting. *Journal of Biological Chemistry* **276**(38): 35924–35933.

- Caffarri, S., Kouřil, R., Kereïche, S., Boekema, E. J., and Croce, R.** (2009). Functional architecture of higher plant photosystem II supercomplexes. *The EMBO Journal* **28**(19): 3052–3063.
- Caffarri, S., Tibiletti, T., Jennings, R., and Santabarbara, S.** (2014). A Comparison Between Plant Photosystem I and Photosystem II Architecture and Functioning. *Current Protein & Peptide Science* **15**(4): 296–331.
- Caldeira, K. and Wickett, M. E.** (2003). Anthropogenic carbon and ocean pH. *Nature* **425**(6956): 365.
- Cardona, T., Shao, S., and Nixon, P.** (2018). Enhancing photosynthesis in plants: the light reactions. *Essays In Biochemistry* **62**(1): 85–94.
- Carvalho, F. E. L., Ware, M. A., and Ruban, A. V.** (2015). Quantifying the dynamics of light tolerance in Arabidopsis plants during ontogenesis. *Plant, Cell and Environment* **38**(12): 2603–2617.
- Chadburn, S. E., Burke, E. J., Cox, P. M., Friedlingstein, P., Hugelius, G., and Westermann, S.** (2017). An observation-based constraint on permafrost loss as a function of global warming. *Nature Climate Change* **7**(5): 340–344.
- Chmeliov, J., Bricker, W. P., Lo, C., Jouin, E., Valkunas, L., Ruban, A. V., and Duffy, C. D.** (2015). An 'all pigment' model of excitation quenching in LHCII. *Physical Chemistry Chemical Physics* **17**(24): 15857–15867.
- Chmeliov, J., Gelzinis, A., Songaila, E., Augulis, R., Duffy, C. D., Ruban, A. V., and Valkunas, L.** (2016). The nature of self-regulation in photosynthetic light-harvesting antenna. *Nature Plants* **2**(5): 16045.
- Chmeliov, J., Gelzinis, A., Franckevičius, M., Tutkus, M., Saccon, F., Ruban, A. V., and Valkunas, L.** (2019). Aggregation-Related Nonphotochemical Quenching in the Photosynthetic Membrane. *The Journal of Physical Chemistry Letters* **10**(23): 7340–7346.

- Chukhutsina, V. U., Holzwarth, A. R., and Croce, R.** (2019). Time-resolved fluorescence measurements on leaves: principles and recent developments. *Photosynthesis Research* **140**(3): 355–369.
- Chynwat, V. and Frank, H. A.** (1995). The application of the energy gap law to the S1 energies and dynamics of carotenoids. *Chemical Physics* **194**(2-3): 237–244.
- Cogdell, R. J., Gall, A., and Köhler, J.** (2006). The architecture and function of the light-harvesting apparatus of purple bacteria: From single molecules to in vivo membranes. *Quarterly Reviews of Biophysics* **39**(3): 227–324.
- Connelly, J., Müller, M., Hucke, M., Gatzen, G., Mullineaux, C., Ruban, A., Horton, P., and Holzwarth, A.** (1997). Ultrafast spectroscopy of trimeric light-harvesting complex II from higher plants. *Journal of Physical Chemistry B* **101**(10): 1902–1909.
- Correa-Galvis, V., Poschmann, G., Melzer, M., Stühler, K., and Jahns, P.** (2016). PsbS interactions involved in the activation of energy dissipation in Arabidopsis. *Nature Plants* **2**(2): 1–8.
- Crepin, A., Santabarbara, S., and Caffarri, S.** (2016). Biochemical and spectroscopic characterization of highly stable photosystem II supercomplexes from arabidopsis. *Journal of Biological Chemistry* **291**(36): 19157–19171.
- Crimi, M., Dona, D., Bösiinger, C. S., Giuffra, E., Bassi, R., and Holzwarth, A. R.**, Zeaxanthin-induced fluorescence quenching in the minor antenna CP29. In *Photosynthesis: Mechanisms and Effects*, 333–336 (Springer Netherlands, Dordrecht, 1998).
- Croce, R., Zucchelli, G., Garlaschi, F. M., and Jennings, R. C.** (1998). A thermal broadening study of the antenna chlorophylls in PSI- 200, LHCI, and PSI core. *Biochemistry* **37**(50): 17355–17360.
- Croce, R., Weiss, S., and Bassi, R.** (1999a). Carotenoid-binding sites of the major light-harvesting complex II of higher plants. *Journal of Biological Chemistry* **274**(42): 29613–29623.

- Croce, R., Remelli, R., Varotto, C., Breton, J., and Bassi, R.** (1999b). The neoxanthin binding site of the major light harvesting complex (LHCII) from higher plants. *FEBS Letters* **456**(1): 1–6.
- Croce, R., Müller, M. G., Bassi, R., and Holzwarth, A. R.** (2001). Carotenoid-to-chlorophyll energy transfer in recombinant major light-harvesting complex (LHCII) of higher plants. I. Femtosecond transient absorption measurements. *Biophysical Journal* **80**(2): 901–915.
- Croce, R. and Van Amerongen, H.** (2011). Light-harvesting and structural organization of Photosystem II: From individual complexes to thylakoid membrane. *Journal of Photochemistry and Photobiology B: Biology* **104**(1-2): 142–153.
- Crouchman, S., Ruban, A., and Horton, P.** (2006). PsbS enhances nonphotochemical fluorescence quenching in the absence of zeaxanthin. *FEBS Letters* **580**(8): 2053–2058.
- Curutchet, C., Kongsted, J., Muñoz-Losa, A., Hossein-Nejad, H., Scholes, G. D., and Mennucci, B.** (2011). Photosynthetic light-harvesting is tuned by the heterogeneous polarizable environment of the protein. *Journal of the American Chemical Society* **133**(9): 3078–3084.
- Dainese, P., Hoyer-Hansen, G., and Bassi, R.** (1990). The resolution of chlorophyll a/b binding proteins by a preparative method based on flat bed isoelectric focusing. *Photochemistry and Photobiology* **51**(6): 693–703.
- Dall’Osto, L., Caffarri, S., and Bassi, R.** (2005). A Mechanism of Nonphotochemical Energy Dissipation, Independent from PsbS, Revealed by a Conformational Change in the Antenna Protein CP26. *The Plant Cell* **17**(4): 1217–1232.
- Dall’Osto, L., Lico, C., Alric, J., Giuliano, G., Havaux, M., and Bassi, R.** (2006). Lutein is needed for efficient chlorophyll triplet quenching in the major LHCII antenna complex of higher plants and effective photoprotection in vivo under strong light. *BMC Plant Biology* **6**: 1–20.

- Dall'Osto, L., Holt, N. E., Kaligotla, S., Fuciman, M., Cazzaniga, S., Carbonera, D., Frank, H. A., Alric, J., and Bassi, R.** (2012). Zeaxanthin protects plant photosynthesis by modulating chlorophyll triplet yield in specific light-harvesting antenna subunits. *Journal of Biological Chemistry* **287**(50): 41820–41834.
- Dall'Osto, L., Caner, ., Cazzaniga, S., and Van Amerongen, H.** (2014a). Disturbed excitation energy transfer in *Arabidopsis thaliana* mutants lacking minor antenna complexes of photosystem II. *Biochimica et Biophysica Acta - Bioenergetics* **1837**(12): 1981–1988.
- Dall'Osto, L., Bassi, R., and Ruban, A.**, Photoprotective Mechanisms: Carotenoids. In *Plastid Biology*, vol. 14, 393–435 (Springer New York, New York, NY, 2014b).
- Dall'Osto, L., Cazzaniga, S., Bressan, M., Paleeèk, D., Židek, K., Niyogi, K. K., Fleming, G. R., Zigmantas, D., and Bassi, R.** (2017). Two mechanisms for dissipation of excess light in monomeric and trimeric light-harvesting complexes. *Nature Plants* **3**(5): 17033.
- Dall'Osto, L., Cazzaniga, S., Zappone, D., and Bassi, R.** (2019). Monomeric light harvesting complexes enhance excitation energy transfer from LHCII to PSII and control their lateral spacing in thylakoids. *Biochimica et Biophysica Acta (BBA) - Bioenergetics* in press.
- Damkjær, J. T., Kereïche, S., Johnson, M. P., Kovacs, L., Kiss, A. Z., Boekema, E. J., Ruban, A. V., Horton, P., and Jansson, S.** (2009). The Photosystem II Light-Harvesting Protein Lhcb3 Affects the Macrostructure of Photosystem II and the Rate of State Transitions in *Arabidopsis*. *The Plant Cell Online* **21**(10): 3245–3256.
- Daskalakis, V. and Papadatos, S.** (2017). The Photosystem II Subunit S under Stress. *Biophysical Journal* **113**(11): 2364–2372.
- Daskalakis, V.** (2018). Protein-Protein Interactions within Photosystem II under Photoprotection: The Synergy between CP29 Minor Antenna, Subunit S (PsbS)

- and Zeaxanthin at all-atom resolution. *Physical Chemistry Chemical Physics* **20**: 11843–11855.
- Daskalakis, V., Papadatos, S., and Kleinekathöfer, U.** (2019). Fine tuning of the photosystem II major antenna mobility within the thylakoid membrane of higher plants. *Biochimica et Biophysica Acta (BBA) - Biomembranes* **1861**(12): 183059.
- de Bianchi, S., Dall'Osto, L., Tognon, G., Morosinotto, T., and Bassi, R.** (2008). Minor Antenna Proteins CP24 and CP26 Affect the Interactions between Photosystem II Subunits and the Electron Transport Rate in Grana Membranes of Arabidopsis. *The Plant Cell* **20**(4): 1012–1028.
- de Bianchi, S., Betterle, N., Kouril, R., Cazzaniga, S., Boekema, E., Bassi, R., and Dall'Osto, L.** (2011). Arabidopsis Mutants Deleted in the Light-Harvesting Protein Lhcb4 Have a Disrupted Photosystem II Macrostructure and Are Defective in Photoprotection. *The Plant Cell* **23**(7): 2659–2679.
- Dekker, J. P. and Boekema, E. J.** (2005). Supramolecular organization of thylakoid membrane proteins in green plants. *Biochimica et Biophysica Acta (BBA) - Bioenergetics* **1706**(1-2): 12–39.
- Demmig-Adams, B.** (1990). Carotenoids and photoprotection in plants: A role for the xanthophyll zeaxanthin. *Biochimica et Biophysica Acta (BBA) - Bioenergetics* **1020**(1): 1–24.
- Demmig-Adams, B. and Adams, W. W.** (2000). Harvesting sunlight safely. *Nature* **403**(6768): 371–373.
- Demmig-Adams, B., Ebbert, V., Mellman, D. L., Mueh, K. E., Schaffer, L., Funk, C., Zarter, C. R., Adamska, I., Jansson, S., and Adams, W. W.** (2006). Modulation of PsbS and flexible vs sustained energy dissipation by light environment in different species. *Physiologia Plantarum* **127**(4): 670–680.

- Demmig-Adams, B., Garab, G., Adams, W. W., and Govindjee,** *Non-Photochemical Quenching and Energy Dissipation in Plants, Algae and Cyanobacteria*, vol. 40 of *Advances in Photosynthesis and Respiration* (Springer Netherlands, Dordrecht, 2014).
- Depege, N.** (2003). Role of Chloroplast Protein Kinase Stt7 in LHCII Phosphorylation and State Transition in *Chlamydomonas*. *Science* **299**(5612): 1572–1575.
- Dexter, D. L.** (1953). A theory of sensitized luminescence in solids. *The Journal of Chemical Physics* **21**(5): 836–850.
- Di Valentin, M., Biasibetti, F., Ceola, S., and Carbonera, D.** (2009). Identification of the sites of chlorophyll triplet quenching in relation to the structure of LHC-II from higher plants. Evidence from EPR spectroscopy. *Journal of Physical Chemistry B* **113**(39): 13071–13078.
- Di Valentin, M. and Carbonera, D.** (2017). The fine tuning of carotenoid-chlorophyll interactions in light-harvesting complexes: An important requisite to guarantee efficient photoprotection via triplet-triplet energy transfer in the complex balance of the energy transfer processes. *Journal of Physics B: Atomic, Molecular and Optical Physics* **50**(16).
- Dominici, P., Caffarri, S., Armenante, F., Ceoldo, S., Crimi, M., and Bassi, R.** (2002). Biochemical properties of the PsbS subunit of photosystem II either purified from chloroplast or recombinant. *Journal of Biological Chemistry* **277**(25): 22750–22758.
- Duffy, C. D. and Ruban, A. V.** (2012). A theoretical investigation of xanthophyll-protein hydrogen bonding in the photosystem II antenna. *Journal of Physical Chemistry B* **116**(14): 4310–4318.
- Duffy, C. D., Pandit, A., and Ruban, A. V.** (2014). Modeling the NMR signatures associated with the functional conformational switch in the major light-harvesting antenna of photosystem II in higher plants. *Physical Chemistry Chemical Physics* **16**(12): 5571–5580.

- Duffy, C. D. P., Johnson, M. P., MacErnis, M., Valkunas, L., Barford, W., and Ruban, A. V. (2010). A theoretical investigation of the photophysical consequences of major plant light-harvesting complex aggregation within the photosynthetic membrane. *Journal of Physical Chemistry B* **114**(46): 15244–15253.
- Duffy, C. D. P. and Ruban, A. V. (2015). Dissipative pathways in the photosystem-II antenna in plants. *Journal of Photochemistry and Photobiology B: Biology* **152**: 215–226.
- Duysens, L. N. M. (1989). The discovery of the two photosynthetic systems: a personal account. *Photosynthesis Research* **21**(2): 61–79.
- Engel, B. D., Schaffer, M., Cuellar, L. K., Villa, E., Plitzko, J. M., and Baumeister, W. (2015). Native architecture of the chlamydomonas chloroplast revealed by in situ cryo-electron tomography. *eLife* **2015**(4): 1–29.
- Fan, M., Li, M., Liu, Z., Cao, P., Pan, X., Zhang, H., Zhao, X., Zhang, J., and Chang, W. (2015). Crystal structures of the PsbS protein essential for photoprotection in plants. *Nature Structural & Molecular Biology* **22**(9): 729–735.
- Fang, C., Frontiera, R. R., Tran, R., and Mathies, R. A. (2009). Mapping GFP structure evolution during proton transfer with femtosecond Raman spectroscopy. *Nature* **462**(7270): 200–204.
- Farber, A., Young, A. J., Ruban, A. V., Horton, P., and Jahns, P. (1997). Dynamics of Xanthophyll-Cycle Activity in Different Antenna Subcomplexes in the Photosynthetic Membranes of Higher Plants (The Relationship between Zeaxanthin Conversion and Nonphotochemical Fluorescence Quenching). *Plant Physiology* **115**(4): 1609–1618.
- Farooq, S., Chmeliov, J., Wientjes, E., Koehorst, R., Bader, A., Valkunas, L., Trinkunas, G., and Van Amerongen, H. (2018). Dynamic feedback of the photosystem II reaction centre on photoprotection in plants. *Nature Plants* **4**(4): 225–231.

- Fassioli, F., Dinshaw, R., Arpin, P. C., and Scholes, G. D.** (2014). Photosynthetic light harvesting: excitons and coherence. *Journal of The Royal Society Interface* **11**(92): 20130901.
- Finazzi, G., Johnson, G. N., Dall'Osto, L., Joliot, P., Wollman, F.-A., and Bassi, R.** (2004). A zeaxanthin-independent nonphotochemical quenching mechanism localized in the photosystem II core complex. *Proceedings of the National Academy of Sciences* **101**(33): 12375–12380.
- Finazzi, G., Johnson, G. N., Dall'Osto, L., Zito, F., Bonente, G., Bassi, R., and Wollman, F. A.** (2006). Nonphotochemical quenching of chlorophyll fluorescence in *Chlamydomonas reinhardtii*. *Biochemistry* **45**(5): 1490–1498.
- Fox, K. F., Bricker, W. P., Lo, C., and Duffy, C. D.** (2015). Distortions of the Xanthophylls Caused by Interactions with Neighboring Pigments and the LHCII Protein Are Crucial for Studying Energy Transfer Pathways within the Complex. *Journal of Physical Chemistry B* **119**(51): 15550–15560.
- Fox, K. F., Balevičius, V., Chmeliov, J., Valkunas, L., Ruban, A. V., and Duffy, C. D. P.** (2017). The carotenoid pathway: what is important for excitation quenching in plant antenna complexes? *Physical Chemistry Chemical Physics* **19**(34): 22957–22968.
- Forster, T.** (2012). Energy migration and fluorescence. *Journal of Biomedical Optics* **17**(1): 011002.
- Frank, H. A., Cua, A., Chynwat, V., Young, A., Gosztola, D., and Wasielewski, M. R.** (1994). Photophysics of the carotenoids associated with the xanthophyll cycle in photosynthesis. *Photosynthesis Research* **41**(3): 389–395.
- Frank, H. A. and Cogdell, R. J.** (1996). Carotenoids in Photosynthesis. *Photochemistry and Photobiology* **63**(3): 257–264.
- Frank, H. A., Chynwat, V., Desamero, R. Z., Farhoosh, R., Erickson, J., and Bautista, J.** (1997). On the photophysics and photochemical properties of

- carotenoids and their role as light-harvesting pigments in photosynthesis. *Pure and Applied Chemistry* **69**(10): 2117–2124.
- Fuciman, M., Enriquez, M. M., Polívka, T., Dallosto, L., Bassi, R., and Frank, H. A.** (2012). Role of xanthophylls in light harvesting in green plants: A Spectroscopic investigation of mutant LHCII and Lhcb pigment-protein complexes. *Journal of Physical Chemistry B* **116**(12): 3834–3849.
- Funk, C., Schroeder, W. P., Napiwotzki, A., Tjus, S. E., Renger, G., and Andersson, B.** (1995). The PSII-S Protein of Higher Plants: A New Type of Pigment-Binding Protein. *Biochemistry* **34**(35): 11133–11141.
- Gall, A., Berera, R., Alexandre, M. T. A., Pascal, A. A., Bordes, L., Mendes-Pinto, M. M., Andrianambinintsoa, S., Stoitchkova, K. V., Marin, A., Valkunas, L., Horton, P., Kennis, J. T. M., Van Grondelle, R., Ruban, A., and Robert, B.** (2011). Molecular adaptation of photoprotection: Triplet states in light-harvesting proteins. *Biophysical Journal* **101**(4): 934–942.
- Gáspár, L., Sárvári, E., Morales, F., and Szigeti, Z.** (2006). Presence of PSI free LHCI and monomeric LHCII and subsequent effects on fluorescence characteristics in lincomycin treated maize. *Planta* **223**(5): 1047–1057.
- Gaumnitz, T., Jain, A., Pertot, Y., Huppert, M., Jordan, I., Ardana-Lamas, F., and Wörner, H. J.** (2017). Streaking of 43-attosecond soft-X-ray pulses generated by a passively CEP-stable mid-infrared driver. *Optics Express* **25**(22): 27506.
- Gelzinis, A., Chmeliov, J., Ruban, A. V., and Valkunas, L.** (2018). Can red-emitting state be responsible for fluorescence quenching in LHCII aggregates? *Photosynthesis Research* **135**(1-3): 275–284.
- Genty, B., Goulas, Y., Dimon, B., Peltier, G., Briantais, J., and Moya, I.**, Modulation of efficiency of primary conversion in leaves, mechanisms involved at PS2. In **Murata, N.** (editor), *Research in photosynthesis, Vol. IV: Proceedings of IXth International Congress on Photosynthesis*, vol. August 30-, 603–610 (Nagoya, Japan, 1992).

- Gerotto, C., Franchin, C., Arrigoni, G., and Morosinotto, T.** (2015). In Vivo Identification of Photosystem II Light Harvesting Complexes Interacting with Photosystem II Subunit S. *Plant Physiology* **168**(4): 1747–1761.
- Gilbert, I. R., Jarvis, P. G., and Smith, H.** (2001). Proximity signal and shade avoidance differences between early and late successional trees. *Nature* **411**(6839): 792–795.
- Gilmore, A. M. and Yamamoto, H. Y.** (1992). Dark induction of zeaxanthin-dependent nonphotochemical fluorescence quenching mediated by ATP. *Proceedings of the National Academy of Sciences* **89**(5): 1899–1903.
- Gilmore, A. M., Mohanty, N., and Yamamoto, H. Y.** (1994). Epoxidation of zeaxanthin and antheraxanthin reverses non-photochemical quenching of photosystem II chlorophyll a fluorescence in the presence of trans-thylakoid Δ pH. *FEBS Letters* **350**(2-3): 271–274.
- Gilmore, A. M., Hazlett, T. L., and Govindjee** (1995). Xanthophyll cycle-dependent quenching of photosystem II chlorophyll a fluorescence: formation of a quenching complex with a short fluorescence lifetime. *Proceedings of the National Academy of Sciences* **92**(6): 2273–2277.
- Giovagnetti, V., Ware, M. A., and Ruban, A. V.** (2015). Assessment of the impact of photosystem I chlorophyll fluorescence on the pulse-amplitude modulated quenching analysis in leaves of *Arabidopsis thaliana*. *Photosynthesis Research* **125**(1-2): 179–189.
- Giovagnetti, V. and Ruban, A. V.** (2017). Detachment of the fucoxanthin chlorophyll a/c binding protein (FCP) antenna is not involved in the acclimative regulation of photoprotection in the pennate diatom *Phaeodactylum tricornutum*. *Biochimica et Biophysica Acta (BBA) - Bioenergetics* **1858**(3): 218–230.
- Giovagnetti, V. and Ruban, A. V.** (2018). The evolution of the photoprotective antenna proteins in oxygenic photosynthetic eukaryotes. *Biochemical Society Transactions* **46**(5): 1263–1277.

- Głowacka, K., Kromdijk, J., Kucera, K., Xie, J., Cavanagh, A. P., Leonelli, L., Leahey, A. D. B., Ort, D. R., Niyogi, K. K., and Long, S. P.** (2018). Photosystem II Subunit S overexpression increases the efficiency of water use in a field-grown crop. *Nature Communications* **9**(1): 868.
- Goral, T. K., Johnson, M. P., Duffy, C. D. P., Brain, A. P. R., Ruban, A. V., and Mullineaux, C. W.** (2012). Light-harvesting antenna composition controls the macrostructure and dynamics of thylakoid membranes in *Arabidopsis*. *Plant Journal* **69**(2): 289–301.
- Goss, R. and Lepetit, B.** (2015). Biodiversity of NPQ. *Journal of Plant Physiology* **172**: 13–32.
- Gradinaru, C. C., van Stokkum, I. H. M., Pascal, A. a., van Grondelle, R., and van Amerongen, H.** (2000). Identifying the Pathways of Energy Transfer between Carotenoids and Chlorophylls in LHCII and CP29. A Multicolor, Femtosecond PumpProbe Study. *The Journal of Physical Chemistry B* **104**(39): 9330–9342.
- Gradinaru, C. C., Kennis, J. T., Papagiannakis, E., Van Stokkum, I. H., Cogdell, R. J., Fleming, G. R., Niederman, R. A., and Van Grondelle, R.** (2001). An unusual pathway of excitation energy deactivation in carotenoids: Singlet-to-triplet conversion on an ultrafast timescale in a photosynthetic antenna. *Proceedings of the National Academy of Sciences of the United States of America* **98**(5): 2364–2369.
- Hager, A. and Holocher, K.** (1994). Localization of the xanthophyll-cycle enzyme violaxanthin de-epoxidase within the thylakoid lumen and abolition of its mobility by a (light-dependent) pH decrease. *Planta* **192**(4): 581–589.
- Havaux, M. and Niyogi, K. K.** (1999). The violaxanthin cycle protects plants from photooxidative damage by more than one mechanism. *Proceedings of the National Academy of Sciences* **96**(15): 8762–8767.
- Havaux, M., Dall'Osto, L., and Bassi, R.** (2007). Zeaxanthin has enhanced antioxidant capacity with respect to all other xanthophylls in *arabidopsis* leaves

- and functions independent of binding to PSII antennae. *Plant Physiology* **145**(4): 1506–1520.
- Heber, U.** (1969). Conformational changes of chloroplasts induced by illumination of leaves in vivo. *Biochimica et Biophysica Acta (BBA) - Bioenergetics* **180**(2): 302–319.
- Holleboom, C. P., Gacek, D. A., Liao, P. N., Negretti, M., Croce, R., and Walla, P. J.** (2015). Carotenoid-chlorophyll coupling and fluorescence quenching in aggregated minor PSII proteins CP24 and CP29. *Photosynthesis Research* **124**(2): 171–180.
- Holt, N. E., Zigmantas, D., Valkunas, L., Li, X. P., Niyogi, K. K., and Fleming, G. R.** (2005). Carotenoid cation formation and the regulation of photosynthetic light harvesting. *Science* **307**(5708): 433–436.
- Holzwarth, A. R.**, Time-resolved fluorescence spectroscopy. In *Methods in Enzymology*, vol. 246, 334–362 (Elsevier Inc., 1995).
- Holzwarth, A. R., Miloslavina, Y., Nilkens, M., and Jahns, P.** (2009). Identification of two quenching sites active in the regulation of photosynthetic light-harvesting studied by time-resolved fluorescence. *Chemical Physics Letters* **483**(4-6): 262–267.
- Hontani, Y., Kloz, M., Polívka, T., Shukla, M. K., Sobotka, R., and Kennis, J. T.** (2018). Molecular Origin of Photoprotection in Cyanobacteria Probed by Watermarked Femtosecond Stimulated Raman Spectroscopy. *Journal of Physical Chemistry Letters* **9**(7): 1788–1792.
- Horton, P. and Black, M. T.** (1980). Activation of adenosine 5 triphosphate-induced quenching of chlorophyll fluorescence by reduced plastoquinone: The basis of state Istate II transitions in chloroplasts. *FEBS Letters* **119**(1): 141–144.
- Horton, P., Allen, J. F., Black, M. T., and Bennett, J.** (1981). Regulation of phosphorylation of chloroplast membrane polypeptides by the redox state of plastoquinone. *FEBS Letters* **125**(2): 193–196.

- Horton, P. and Hague, A.** (1988). Studies on the induction of chlorophyll fluorescence in isolated barley protoplasts. IV. Resolution of non-photochemical quenching. *Biochimica et Biophysica Acta (BBA) - Bioenergetics* **932**(C): 107–115.
- Horton, P., Ruban, A. V., Rees, D., Pascal, A. A., Noctor, G., and Young, A. J.** (1991). Control of the light-harvesting function of chloroplast membranes by aggregation of the LHCII chlorophyll-protein complex. *FEBS Letters* **292**(1-2): 1–4.
- Horton, P. and Ruban, A. V.** (1992). Regulation of Photosystem II. *Photosynthesis Research* **34**(3): 375–385.
- Horton, P., Ruban, A. V., and Walters, R. G.** (1996). Regulation of light harvesting in green plants. *Annual Review of Plant Physiology and Plant Molecular Biology* **47**(1): 655–684.
- Horton, P., Ruban, A. V., and Wentworth, M.** (2000). Allosteric regulation of the light-harvesting system of photosystem II. *Philosophical Transactions of the Royal Society B: Biological Sciences* **355**(1402): 1361–1370.
- Horton, P., Wentworth, M., and Ruban, A.** (2005). Control of the light harvesting function of chloroplast membranes: The LHCII-aggregation model for non-photochemical quenching. *FEBS Letters* **579**(20): 4201–4206.
- Hubbart, S., Smillie, I. R. A., Heatley, M., Swarup, R., Foo, C. C., Zhao, L., and Murchie, E. H.** (2018). Enhanced thylakoid photoprotection can increase yield and canopy radiation use efficiency in rice. *Communications Biology* **1**(1): 1–12.
- Hurry, V., Anderson, J. M., Badger, M. R., and Price, G. D.** (1996). Reduced levels of cytochrome b 6/f in transgenic tobacco increases the excitation pressure on Photosystem II without increasing sensitivity to photoinhibition in vivo. *Photosynthesis Research* **50**(2): 159–169.
- Ilioaia, C., Johnson, M. P., Horton, P., and Ruban, A. V.** (2008). Induction of Efficient Energy Dissipation in the Isolated Light-harvesting

- Complex of Photosystem II in the Absence of Protein Aggregation. *Journal of Biological Chemistry* **283**(43): 29505–29512.
- Ilioaia, C., Johnson, M. P., Duffy, C. D. P., Pascal, A. A., van Grondelle, R., Robert, B., and Ruban, A. V.** (2011a). Origin of Absorption Changes Associated with Photoprotective Energy Dissipation in the Absence of Zeaxanthin. *Journal of Biological Chemistry* **286**(1): 91–98.
- Ilioaia, C., Johnson, M. P., Liao, P.-N., Pascal, A. A., van Grondelle, R., Walla, P. J., Ruban, A. V., and Robert, B.** (2011b). Photoprotection in Plants Involves a Change in Lutein 1 Binding Domain in the Major Light-harvesting Complex of Photosystem II. *Journal of Biological Chemistry* **286**(31): 27247–27254.
- Ioannidis, N. E., Papadatos, S., and Daskalakis, V.** (2016). Energizing the light harvesting antenna: Insight from CP29. *Biochimica et Biophysica Acta - Bioenergetics* **1857**(10): 1643–1650.
- Iwai, M., Takahashi, Y., and Minagawa, J.** (2008). Molecular Remodeling of Photosystem II during State Transitions in *Chlamydomonas reinhardtii*. *The Plant Cell* **20**(8): 2177–2189.
- Jahns, P., Polle, A., and Junge, W.** (1988). The photosynthetic water oxidase: its proton pumping activity is short-circuited within the protein by DCCD. *The EMBO journal* **7**(3): 589–94.
- Jahns, P. and Junge, W.** (1989). The protonic shortcircuit by DCCD in photosystem II A common feature of all redox transitions of water oxidation. *FEBS Letters* **253**(1-2): 33–37.
- Jahns, P. and Junge, W.** (1990). Dicyclohexylcarbodiimide-binding proteins related to the short circuit of the proton-pumping activity of photosystem II. Identified as light-harvesting chlorophyll-a/b-binding proteins. *European Journal of Biochemistry* **193**(3): 731–736.

- Jahns, P. and Junge, W.** (1992). Thylakoids from Pea Seedlings Grown under Intermittent Light : Biochemical and Flash-Spectrophotometric Properties. *Biochemistry* **31**(32): 7390–7397.
- Jahns, P., Wehner, A., Paulsen, H., and Hobe, S.** (2001). De-epoxidation of Violaxanthin after Reconstitution into Different Carotenoid Binding Sites of Light-harvesting Complex II. *Journal of Biological Chemistry* **276**(25): 22154–22159.
- Jahns, P., Latowski, D., and Strzalka, K.** (2009). Mechanism and regulation of the violaxanthin cycle: The role of antenna proteins and membrane lipids. *Biochimica et Biophysica Acta (BBA) - Bioenergetics* **1787**(1): 3–14.
- Jansson, S.** (1994). The light-harvesting chlorophyll ab-binding proteins. *Biochimica et Biophysica Acta (BBA) - Bioenergetics* **1184**(1): 1–19.
- Jansson, S.** (1999). A guide to the Lhc genes and their relatives in Arabidopsis. *Trends in Plant Science* **4**(6): 236–240.
- Jhutti, C. S., Jávorfí, T., Merzlyak, M. N., and Naqvi, K. R.,** Triplet-Triplet Absorption Spectra and Extinction Coefficients of Lutein, Neoxanthin And Violaxanthin. In *Photosynthesis: Mechanisms and Effects*, 491–494 (Springer Netherlands, 1998).
- Johnson, G. N., Young, A. J., Scholes, J. D., and Horton, P.** (1993). The dissipation of excess excitation energy in British plant species. *Plant, Cell and Environment* **16**(6): 673–679.
- Johnson, M. P., Havaux, M., Triantaphylidès, C., Ksas, B., Pascal, A. A., Robert, B., Davison, P. A., Ruban, A. V., and Horton, P.** (2007). Elevated Zeaxanthin Bound to Oligomeric LHCII Enhances the Resistance of Arabidopsis to Photooxidative Stress by a Lipid-protective, Antioxidant Mechanism. *Journal of Biological Chemistry* **282**(31): 22605–22618.
- Johnson, M. P. and Ruban, A. V.** (2009). Photoprotective energy dissipation in higher plants involves alteration of the excited state energy of the emitting

- chlorophyll(s) in the light harvesting antenna II (LHCII). *Journal of Biological Chemistry* **284**(35): 23592–23601.
- Johnson, M. P., Pérez-Bueno, M. L., Zia, A., Horton, P., and Ruban, A. V.** (2009). The Zeaxanthin-Independent and Zeaxanthin-Dependent qE Components of Nonphotochemical Quenching Involve Common Conformational Changes within the Photosystem II Antenna in Arabidopsis. *Plant Physiology* **149**(2): 1061–1075.
- Johnson, M. P. and Ruban, A. V.** (2010). Arabidopsis plants lacking PsbS protein possess photoprotective energy dissipation. *Plant Journal* **61**(2): 283–289.
- Johnson, M. P., Zia, A., Horton, P., and Ruban, A. V.** (2010). Effect of xanthophyll composition on the chlorophyll excited state lifetime in plant leaves and isolated LHCII. *Chemical Physics* **373**(1-2): 23–32.
- Johnson, M. P., Brain, A. P. R., and Ruban, A. V.** (2011a). Changes in thylakoid membrane thickness associated with the reorganization of photosystem II light harvesting complexes during photoprotective energy dissipation. *Plant Signaling & Behavior* **6**(9): 1386–1390.
- Johnson, M. P., Goral, T. K., Duffy, C. D., Brain, A. P., Mullineaux, C. W., and Ruban, A. V.** (2011b). Photoprotective Energy Dissipation Involves the Reorganization of Photosystem II Light-Harvesting Complexes in the Grana Membranes of Spinach Chloroplasts. *The Plant Cell* **23**(4): 1468–1479.
- Johnson, M. P. and Ruban, A. V.** (2011). Restoration of rapidly reversible photoprotective energy dissipation in the absence of PsbS protein by enhanced ΔpH . *Journal of Biological Chemistry* **286**(22): 19973–19981.
- Johnson, M. P., Zia, A., and Ruban, A. V.** (2012). Elevated ΔpH restores rapidly reversible photoprotective energy dissipation in Arabidopsis chloroplasts deficient in lutein and xanthophyll cycle activity. *Planta* **235**(1): 193–204.

- Johnson, M. P. and Ruban, A. V.** (2014). Rethinking the existence of a steady-state $\Delta\psi$ component of the proton motive force across plant thylakoid membranes. *Photosynthesis Research* **119**(1-2): 233–242.
- Kana, R., Kotabová, E., Kopečná, J., Trsková, E., Belgio, E., Sobotka, R., and Ruban, A. V.** (2016). Violaxanthin inhibits nonphotochemical quenching in light-harvesting antenna of *Chromera velia*. *FEBS Letters* **590**(8): 1076–1085.
- Kantola, I. B., Masters, M. D., Beerling, D. J., Long, S. P., and DeLucia, E. H.** (2017). Potential of global croplands and bioenergy crops for climate change mitigation through deployment for enhanced weathering. *Biology Letters* **13**(4).
- Khoroshyy, P., Bína, D., Gardian, Z., Litvín, R., Alster, J., and Pšenčík, J.** (2018). Quenching of chlorophyll triplet states by carotenoids in algal light-harvesting complexes related to fucoxanthin-chlorophyll protein. *Photosynthesis Research* **135**(1-3): 213–225.
- Killian, J.** (1998). Hydrophobic mismatch between proteins and lipids in membranes. *Biochimica et Biophysica Acta (BBA) - Reviews on Biomembranes* **1376**(3): 401–416.
- Kirchhoff, H., Haferkamp, S., Allen, J. F., Epstein, D. B., and Mullineaux, C. W.** (2008). Protein Diffusion and Macromolecular Crowding in Thylakoid Membranes. *Plant Physiology* **146**(4): 1571–1578.
- Kirchhoff, H.** (2014). Diffusion of molecules and macromolecules in thylakoid membranes. *Biochimica et Biophysica Acta (BBA) - Bioenergetics* **1837**(4): 495–502.
- Kiss, A. Z., Ruban, A. V., and Horton, P.** (2008). The PsbS protein controls the organization of the photosystem II antenna in higher plant thylakoid membranes. *Journal of Biological Chemistry* **283**(7): 3972–3978.

- Kondo, T., Chen, W. J., and Schlau-Cohen, G. S.** (2017). Single-molecule fluorescence spectroscopy of photosynthetic systems. *Chemical Reviews* **117**(2): 860–898.
- Kouřil, R., Wientjes, E., Bultema, J. B., Croce, R., and Boekema, E. J.** (2013). High-light vs. low-light: Effect of light acclimation on photosystem II composition and organization in *Arabidopsis thaliana*. *Biochimica et Biophysica Acta (BBA) - Bioenergetics* **1827**(3): 411–419.
- Kovács, L., Damkjær, J., Kereïche, S., Iliaia, C., Ruban, A. V., Boekema, E. J., Jansson, S., and Horton, P.** (2006). Lack of the Light-Harvesting Complex CP24 Affects the Structure and Function of the Grana Membranes of Higher Plant Chloroplasts. *The Plant Cell* **18**(11): 3106–3120.
- Krah, N. M. and Logan, B. A.** (2010). Loss of psbS expression reduces vegetative growth, reproductive output, and light-limited, but not light-saturated, photosynthesis in *Arabidopsis thaliana* (Brassicaceae) grown in temperate light environments. *American Journal of Botany* **97**(4): 644–649.
- Kramer, D. M., Sacksteder, C. A., and Cruz, J. A.** (1999). How acidic is the lumen? *Photosynthesis Research* **60**(2-3): 151–163.
- Krause, G.** (1973). The high-energy state of the thylakoid system as indicated by chlorophyll fluorescence and chloroplast shrinkage. *Biochimica et Biophysica Acta (BBA) - Bioenergetics* **292**(3): 715–728.
- Krause, G.** (1991). Chlorophyll Fluorescence And Photosynthesis: The Basics. *Annual Review of Plant Physiology and Plant Molecular Biology* **42**(1): 313–349.
- Krause, G. H. and Behrend, U.** (1986). Δ pH-dependent chlorophyll fluorescence quenching indicating a mechanism of protection against photoinhibition of chloroplasts. *FEBS Letters* **200**(2): 298–302.
- Krieger, A., Moya, I., and Weis, E.** (1992). Energy-dependent quenching of chlorophyll a fluorescence: effect of pH on stationary fluorescence and picosecond-relaxation kinetics in thylakoid membranes and Photosystem II

- preparations. *Biochimica et Biophysica Acta (BBA) - Bioenergetics* **1102**(2): 167–176.
- Krieger, A. and Weis, E.** (1993). The role of calcium in the pH-dependent control of Photosystem II. *Photosynthesis Research* **37**(2): 117–130.
- Krieger-Liszkay, A., Kienzler, K., and Johnson, G. N.** (2000). Inhibition of electron transport at the cytochrome b6f complex protects photosystem II from photoinhibition. *FEBS Letters* **486**(3): 191–194.
- Kromdijk, J., Głowacka, K., Leonelli, L., Gabilly, S. T., Iwai, M., Niyogi, K. K., and Long, S. P.** (2016). Improving photosynthesis and crop productivity by accelerating recovery from photoprotection. *Science* **354**(6314): 857–861.
- Krüger, T. P. J., Novoderezhkin, V. I., Iliaia, C., and Van Grondelle, R.** (2010). Fluorescence spectral dynamics of single LHCII trimers. *Biophysical Journal* **98**(12): 3093–3101.
- Krüger, T. P. J., Wientjes, E., Croce, R., and van Grondelle, R.** (2011a). Conformational switching explains the intrinsic multifunctionality of plant light-harvesting complexes. *Proceedings of the National Academy of Sciences* **108**(33): 13516–13521.
- Krüger, T. P. J., Iliaia, C., Valkunas, L., and van Grondelle, R.** (2011b). Fluorescence Intermittency from the Main Plant Light-Harvesting Complex: Sensitivity to the Local Environment. *The Journal of Physical Chemistry B* **115**(18): 5083–5095.
- Krüger, T. P. J., Iliaia, C., Johnson, M. P., Ruban, A. V., Papagiannakis, E., Horton, P., and Van Grondelle, R.** (2012). Controlled disorder in plant light-harvesting complex II explains its photoprotective role. *Biophysical Journal* **102**(11): 2669–2676.
- Krüger, T. P. J., Iliaia, C., Johnson, M. P., Belgio, E., Horton, P., Ruban, A. V., and Van Grondelle, R.** (2013). The specificity of controlled

- protein disorder in the photoprotection of plants. *Biophysical Journal* **105**(4): 1018–1026.
- Krüger, T. P. J., Iliaia, C., Johnson, M. P., Ruban, A. V., and van Grondelle, R.** (2014). Disentangling the low-energy states of the major light-harvesting complex of plants and their role in photoprotection. *Biochimica et Biophysica Acta (BBA) - Bioenergetics* **1837**(7): 1027–1038.
- Krüger, T. P. J. and van Grondelle, R.** (2017). The role of energy losses in photosynthetic light harvesting. *Journal of Physics B: Atomic, Molecular and Optical Physics* **50**(13): 132001.
- Kühlbrandt, W. and Wang, D. N.** (1991). Three-dimensional structure of plant light-harvesting complex determined by electron crystallography. *Nature* **350**(6314): 130–134.
- Külheim, C., Ågren, J., and Jansson, S.** (2002). Rapid regulation of light harvesting and plant fitness in the field. *Science* **297**(5578): 91–93.
- Lampoura, S. S., Barzda, V., Owen, G. M., Hoff, A. J., and Van Amerongen, H.** (2002). Aggregation of LHCII leads to a redistribution of the triplets over the central xanthophylls in LHCII. *Biochemistry* **41**(29): 9139–9144.
- Larkum, A. W. D.**, The Evolution of Chlorophylls and Photosynthesis. In **Grimm, B., Porra, R. J., Rüdiger, W., and Scheer, H.** (editors), *Chlorophylls and Bacteriochlorophylls*, vol. 25 of *Advances in Photosynthesis and Respiration*, 261–282 (Springer Netherlands, Dordrecht, 2006).
- Lemeille, S. and Rochaix, J. D.** (2010). State transitions at the crossroad of thylakoid signalling pathways. *Photosynthesis Research* **106**(1-2): 33–46.
- Li, L., Aro, E.-M., and Millar, A. H.** (2018). Mechanisms of Photodamage and Protein Turnover in Photoinhibition. *Trends in Plant Science* **23**(8): 667–676.

- Li, X. P., Björkman, O., Shih, C., Grossman, A. R., Rosenquist, M., Jansson, S., and Niyogi, K. K.** (2000). A pigment-binding protein essential for regulation of photosynthetic light harvesting. *Nature* **403**(6768): 391–395.
- Li, X. P., Muller-Moule, P., Gilmore, A. M., and Niyogi, K. K.** (2002). PsbS-dependent enhancement of feedback de-excitation protects photosystem II from photoinhibition. *Proceedings of the National Academy of Sciences* **99**(23): 15222–15227.
- Li, X. P., Gilmore, A. M., Caffarri, S., Bassi, R., Golan, T., Kramer, D., and Niyogi, K. K.** (2004). Regulation of photosynthetic light harvesting involves intrathylakoid lumen pH sensing by the PsbS protein. *Journal of Biological Chemistry* **279**(22): 22866–22874.
- Li, Z., Ahn, T. K., Avenson, T. J., Ballottari, M., Cruz, J. A., Kramer, D. M., Bassi, R., Fleming, G. R., Keasling, J. D., and Niyogi, K. K.** (2009). Lutein Accumulation in the Absence of Zeaxanthin Restores Nonphotochemical Quenching in the Arabidopsis thaliana npq1 Mutant. *The Plant Cell* **21**(6): 1798–1812.
- Liguori, N., Periole, X., Marrink, S. J., and Croce, R.** (2015). From light-harvesting to photoprotection: structural basis of the dynamic switch of the major antenna complex of plants (LHCII). *Scientific Reports* **5**(1): 15661.
- Liguori, N., Xu, P., van Stokkum, I. H., van Oort, B., Lu, Y., Karcher, D., Bock, R., and Croce, R.** (2017). Different carotenoid conformations have distinct functions in light-harvesting regulation in plants. *Nature Communications* **8**(1): 1994.
- Liguori, N., Campos, S. R., Baptista, A. M., and Croce, R.** (2019). Molecular Anatomy of Plant Photoprotective Switches: The Sensitivity of PsbS to the Environment, Residue by Residue. *Journal of Physical Chemistry Letters* **10**(8): 1737–1742.
- Liu, Z., Yan, H., Wang, K., Kuang, T., Zhang, J., Gui, L., An, X., and Chang, W.** (2004). Crystal structure of spinach major light-harvesting complex at 2.72 Å resolution. *Nature* **428**(6980): 287–292.

- Llansola-Portoles, M. J., Sobotka, R., Kish, E., Shukla, M. K., Pascal, A. A., Polívka, T., and Robert, B.** (2017). Twisting a β -Carotene, an Adaptive Trick from Nature for Dissipating Energy during Photoprotection. *Journal of Biological Chemistry* **292**(4): 1396–1403.
- Long, S. P. and Ort, D. R.** (2010). More than taking the heat: Crops and global change. *Current Opinion in Plant Biology* **13**(3): 240–247.
- Ma, Y. Z., Holt, N. E., Li, X. P., Niyogi, K. K., and Fleming, G. R.** (2003). Evidence for direct carotenoid involvement in the regulation of photosynthetic light harvesting. *Proceedings of the National Academy of Sciences of the United States of America* **100**: 4377–4382.
- Malkin, S., Armond, P. A., Mooney, H. A., and Fork, D. C.** (1981). Photosystem II Photosynthetic Unit Sizes from Fluorescence Induction in Leaves. *Plant Physiology* **67**(3): 570–579.
- Malý, P. and Van Grondelle, R.** (2018). Interplay of disorder and delocalization in photosynthetic light harvesting. *Current Opinion in Chemical Biology* **47**: 1–6.
- Martin-Fernandez, M. L., Tynan, C. J., and Webb, S. E.** (2013). A ‘pocket guide’ to total internal reflection fluorescence. *Journal of Microscopy* **252**(1): 16–22.
- Mascoli, V., Liguori, N., Xu, P., Roy, L. M., van Stokkum, I. H., and Croce, R.** (2019). Capturing the Quenching Mechanism of Light-Harvesting Complexes of Plants by Zooming in on the Ensemble. *Chem* **5**(11): 2900–2912.
- Mazor, Y., Borovikova, A., and Nelson, N.** (2015). The structure of plant photosystem I super-complex at 2.8 Å resolution. *eLife* **4**: 1–18.
- Mazor, Y., Borovikova, A., Caspy, I., and Nelson, N.** (2017). Structure of the plant photosystem I supercomplex at 2.6 Å resolution. *Nature Plants* **3**(3): 17014.

- Mehler, E. L., Fuxreiter, M., Simon, I., and Garcia-Moreno E, B.** (2002). The role of hydrophobic microenvironments in modulating pKa shifts in proteins. *Proteins: Structure, Function and Genetics* **48**(2): 283–292.
- Mendes-Pinto, M. M., Sansiaume, E., Hashimoto, H., Pascal, A. A., Gall, A., and Robert, B.** (2013). Electronic absorption and ground state structure of carotenoid molecules. *Journal of Physical Chemistry B* **117**(38): 11015–11021.
- Miloslavina, Y., Wehner, A., Lambrev, P. H., Wientjes, E., Reus, M., Garab, G., Croce, R., and Holzwarth, A. R.** (2008). Far-red fluorescence: A direct spectroscopic marker for LHCII oligomer formation in non-photochemical quenching. *FEBS Letters* **582**(25-26): 3625–3631.
- Miloslavina, Y., De Bianchi, S., Dall’Osto, L., Bassi, R., and Holzwarth, A. R.** (2011). Quenching in Arabidopsis thaliana mutants lacking monomeric antenna proteins of photosystem II. *Journal of Biological Chemistry* **286**(42): 36830–36840.
- Monod, J.**, *Chance and necessity: An essay on the natural philosophy of modern biology* (Alfred A. Knopf, Inc, New York, NY, 1971).
- Moya, I., Silvestri, M., Vallon, O., Cinque, G., and Bassi, R.** (2001). Time-resolved fluorescence analysis of the photosystem II antenna proteins in detergent micelles and liposomes. *Biochemistry* **40**(42): 12552–12561.
- Mozzo, M., Dall’Osto, L., Hienerwadel, R., Bassi, R., and Croce, R.** (2008). Photoprotection in the antenna complexes of photosystem II: Role of individual xanthophylls in chlorophyll triplet quenching. *Journal of Biological Chemistry* **283**(10): 6184–6192.
- Müh, F., Madjet, M. E. A., and Renger, T.** (2010). Structure-based identification of energy sinks in plant light-harvesting complex II. *Journal of Physical Chemistry B* **114**(42): 13517–13535.
- Müller, M. G., Lambrev, P., Reus, M., Wientjes, E., Croce, R., and Holzwarth, A. R.** (2010). Singlet energy dissipation in the photosystem II

- light-harvesting complex does not involve energy transfer to carotenoids. *ChemPhysChem* **11**(6): 1289–1296.
- Mullineaux, C. W., Pascal, A. A., Horton, P., and Holzwarth, A. R.** (1993). Excitation-energy quenching in aggregates of the LHC II chlorophyll-protein complex: a time-resolved fluorescence study. *Biochimica et Biophysica Acta (BBA) - Bioenergetics* **1141**(1): 23–28.
- Mullineaux, C. W., Ruban, A. V., and Horton, P.** (1994). Prompt heat release associated with Δ pH-dependent quenching in spinach thylakoid membranes. *Biochimica et Biophysica Acta (BBA) - Bioenergetics* **1185**(1): 119–123.
- Murakami, S. and Packer, L.** (1970). Protonation and chloroplast membrane structure. *Journal of Cell Biology* **47**(2): 332–351.
- Murata, N.** (1969). Control of excitation transfer in photosynthesis I. Light-induced change of chlorophyll a fluorescence in *Porphyridium cruentum*. *Biochimica et Biophysica Acta (BBA) - Bioenergetics* **172**(2): 242–251.
- Murata, N., Takahashi, S., Nishiyama, Y., and Allakhverdiev, S. I.** (2007). Photoinhibition of photosystem II under environmental stress. *Biochimica et Biophysica Acta (BBA) - Bioenergetics* **1767**(6): 414–421.
- Murchie, E. H., Chen, Y. Z., Hubbart, S., Peng, S., and Horton, P.** (1999). Interactions between senescence and leaf orientation determine in situ patterns of photosynthesis and photoinhibition in field-grown rice. *Plant Physiology* **119**(2): 553–563.
- Murchie, E. H. and Lawson, T.** (2013). Chlorophyll fluorescence analysis: A guide to good practice and understanding some new applications. *Journal of Experimental Botany* **64**(13): 3983–3998.
- Murchie, E. H. and Ruban, A. V.** (2019). Dynamic nonphotochemical quenching in plants: from molecular mechanism to productivity. *The Plant Journal* in press.

- Nagao, R., Kato, K., Suzuki, T., Ifuku, K., Uchiyama, I., Kashino, Y., Dohmae, N., Akimoto, S., Shen, J.-R., Miyazaki, N., and Akita, F.** (2019). Structural basis for energy harvesting and dissipation in a diatom PSII-FCPII supercomplex. *Nature Plants* **5**(8): 890–901.
- Naqvi, K., Melø, T., Raju, B., Jávorfí, T., Simidjiev, I., and Garab, G.** (1997). Quenching of chlorophyll a singlets and triplets by carotenoids in light-harvesting complex of photosystem II: comparison of aggregates with trimers. *Spectrochimica Acta Part A: Molecular and Biomolecular Spectroscopy* **53**(14): 2659–2667.
- Natali, A., Gruber, J. M., Dietzel, L., Stuart, M. C., Van Grondelle, R., and Croce, R.** (2016). Light-harvesting Complexes (LHCs) cluster spontaneously in membrane environment leading to shortening of their excited state lifetimes. *Journal of Biological Chemistry* **291**(32): 16730–16739.
- Nawrocki, W. J., Santabarbara, S., Mosebach, L., Wollman, F. A., and Rappaport, F.** (2016). State transitions redistribute rather than dissipate energy between the two photosystems in *Chlamydomonas*. *Nature Plants* **2**(4): 1–7.
- Nechushtai, R., Thornber, J. P., Patterson, L. K., Fessenden, R. W., and Levanon, H.** (1988). Photosensitization of triplet carotenoid in photosynthetic light-harvesting complex of photosystem II. *Journal of Physical Chemistry* **92**(5): 1165–1168.
- Nematov, S., Casazza, A. P., Remelli, W., Khuvondikov, V., and Santabarbara, S.** (2017). Spectral dependence of irreversible light-induced fluorescence quenching: Chlorophyll forms with maximal emission at 700702 and 705710 nm as spectroscopic markers of conformational changes in the core complex. *Biochimica et Biophysica Acta (BBA) - Bioenergetics* **1858**(7): 529–543.
- Neubauer, C. and Schreiber, U.** (1987). The polyphasic rise of chlorophyll fluorescence upon onset of strong continuous illumination: I. saturation characteristics and partial control by the photosystem II acceptor side.

- Zeitschrift fur Naturforschung - Section C Journal of Biosciences* **42**(11-12): 1246–1254.
- Nicol, L., Nawrocki, W. J., and Croce, R.** (2019). Disentangling the sites of non-photochemical quenching in vascular plants. *Nature Plants* **5**(11): 1177–1183.
- Niedzwiedzki, D. M., Sullivan, J. O., Polívka, T., Birge, R. R., and Frank, H. A.** (2006). Femtosecond time-resolved transient absorption spectroscopy of xanthophylls. *Journal of Physical Chemistry B* **110**(45): 22872–22885.
- Nield, J., Funk, C., Barber, J., Hideg, E., Heber, U., Asada, K., and Allen, J. F.** (2000). Supermolecular structure of photosystem II and location of the PsbS protein. *Philosophical Transactions of the Royal Society B: Biological Sciences* **355**(1402): 1337–1344.
- Nishimura, M. and Akazawa, T.** (1975). Photosynthetic Activities of Spinach Leaf Protoplasts. *Plant Physiology* **55**(4): 712–716.
- Niyogi, K., Shih, C., Soon, C., Pogson, B., Dellapenna, D., and Björkman, O.** (2001). Photoprotection in a zeaxanthin- and lutein-deficient double mutant of Arabidopsis. *Photosynthesis research* **67**(1-2): 139–145.
- Niyogi, K. K., Grossman, A. R., and Björkman, O.** (1998). Arabidopsis Mutants Define a Central Role for the Xanthophyll Cycle in the Regulation of Photosynthetic Energy Conversion. *The Plant Cell* **10**(7): 1121–1134.
- Niyogi, K. K., Li, X. P., Rosenberg, V., and Jung, H. S.** (2005). Is PsbS the site of non-photochemical quenching in photosynthesis? *Journal of Experimental Botany* **56**(411): 375–382.
- Niyogi, K. K. and Truong, T. B.** (2013). Evolution of flexible non-photochemical quenching mechanisms that regulate light harvesting in oxygenic photosynthesis. *Current Opinion in Plant Biology* **16**(3): 307–314.

- Noctor, G., Rees, D., Young, A., and Horton, P. (1991). The relationship between zeaxanthin, energy-dependent quenching of chlorophyll fluorescence, and trans-thylakoid pH gradient in isolated chloroplasts. *Biochimica et Biophysica Acta (BBA) - Bioenergetics* **1057**(3): 320–330.
- Noctor, G., Ruban, A. V., and Horton, P. (1993). Modulation of Δ pH-dependent nonphotochemical quenching of chlorophyll fluorescence in spinach chloroplasts. *Biochimica et Biophysica Acta (BBA) - Bioenergetics* **1183**(2): 339–344.
- Nosek, L., Semchonok, D., Boekema, E. J., Ilík, P., and Kouřil, R. (2017). Structural variability of plant photosystem II megacomplexes in thylakoid membranes. *The Plant Journal* **89**(1): 104–111.
- Novoderezhkin, V. I., Palacios, M. A., Van Amerongen, H., and Van Grondelle, R. (2005). Excitation dynamics in the LHCII complex of higher plants: Modeling based on the 2.72 Å crystal structure. *Journal of Physical Chemistry B* **109**(20): 10493–10504.
- Nürnberg, D. J., Morton, J., Santabarbara, S., Telfer, A., Joliot, P., Antonaru, L. A., Ruban, A. V., Cardona, T., Krausz, E., Boussac, A., Fantuzzi, A., and Rutherford, A. W. (2018). Photochemistry beyond the red limit in chlorophyll containing photosystems. *Science* **360**(6394): 1210–1213.
- Ocampo-Alvarez, H., García-Mendoza, E., and Govindjee (2013). Antagonist effect between violaxanthin and de-epoxidated pigments in nonphotochemical quenching induction in the qE deficient brown alga *Macrocystis pyrifera*. *Biochimica et Biophysica Acta (BBA) - Bioenergetics* **1827**(3): 427–437.
- Ort, D. R., Merchant, S. S., Alric, J., Barkan, A., Blankenship, R. E., Bock, R., Croce, R., Hanson, M. R., Hibberd, J. M., Long, S. P., Moore, T. A., Moroney, J., Niyogi, K. K., Parry, M. A. J., Peralta-Yahya, P. P., Prince, R. C., Redding, K. E., Spalding, M. H., van Wijk, K. J., Vermaas, W. F. J., von Caemmerer, S., Weber, A.

- P. M., Yeates, T. O., Yuan, J. S., and Zhu, X. G.** (2015). Redesigning photosynthesis to sustainably meet global food and bioenergy demand. *Proceedings of the National Academy of Sciences* **112**(28): 1–8.
- Owens, T.**, Excitation energy transfer between chlorophylls and carotenoids. A proposed molecular mechanism for non-photochemical quenching. In **Baker, N. R. and Boyer, J. R.** (editors), *Photoinhibition of Photosynthesis: From Molecular Mechanisms to the Field*, 95–109 (Bios Scientific, Oxford, 1994).
- Owens, T. G., Shreve, A. P., and Albrecht, A. C.**, Dynamics and mechanism of singlet energy transfer between carotenoids and chlorophylls: light harvesting and nonphotochemical fluorescence quenching. In **Murata, N.** (editor), *Research In Photosynthesis, Vol. 1; IXth International Congress On Photosynthesis*, 179–186 (Kluwer Academic Publishers, 1992).
- Pagliano, C., Barera, S., Chimirri, F., Saracco, G., and Barber, J.** (2012). Comparison of the α and β isomeric forms of the detergent n-dodecyl-D-maltoside for solubilizing photosynthetic complexes from pea thylakoid membranes. *Biochimica et Biophysica Acta (BBA) - Bioenergetics* **1817**(8): 1506–1515.
- Pagliano, C., Nield, J., Marsano, F., Pape, T., Barera, S., Saracco, G., and Barber, J.** (2014). Proteomic characterization and three-dimensional electron microscopy study of PSII-LHCII supercomplexes from higher plants. *Biochimica et Biophysica Acta - Bioenergetics* **1837**(9): 1454–1462.
- Pan, X., Li, M., Wan, T., Wang, L., Jia, C., Hou, Z., Zhao, X., Zhang, J., and Chang, W.** (2011). Structural insights into energy regulation of light-harvesting complex CP29 from spinach. *Nature Structural & Molecular Biology* **18**(3): 309–315.
- Pan, X., Ma, J., Su, X., Cao, P., Chang, W., Liu, Z., Zhang, X., and Li, M.** (2018). Structure of the maize photosystem I supercomplex with light-harvesting complexes I and II. *Science* **360**(6393): 1109–1113.

- Papageorgiou, G. and Govindjee** (1968). Light-Induced Changes in the Fluorescence Yield of Chlorophyll a In Vivo. *Biophysical Journal* **8**(11): 1316–1328.
- Park, S., Fischer, A. L., Li, Z., Bassi, R., Niyogi, K. K., and Fleming, G. R.** (2017). Snapshot Transient Absorption Spectroscopy of Carotenoid Radical Cations in High-Light-Acclimating Thylakoid Membranes. *The Journal of Physical Chemistry Letters* **8**(22): 5548–5554.
- Park, S., Fischer, A. L., Steen, C. J., Iwai, M., Morris, J. M., Walla, P. J., Niyogi, K. K., and Fleming, G. R.** (2018). Chlorophyll-Carotenoid Excitation Energy Transfer in High-Light-Exposed Thylakoid Membranes Investigated by Snapshot Transient Absorption Spectroscopy. *Journal of the American Chemical Society* **140**(38): 11965–11973.
- Park, S., Steen, C. J., Lyska, D., Fischer, A. L., Endelman, B., Iwai, M., Niyogi, K. K., and Fleming, G. R.** (2019). Chlorophyllcarotenoid excitation energy transfer and charge transfer in *Nannochloropsis oceanica* for the regulation of photosynthesis . *Proceedings of the National Academy of Sciences* **116**(9): 3385–3390.
- Pascal, A. A., Liu, Z., Broess, K., Van Oort, B., Van Amerongen, H., Wang, C., Horton, P., Robert, B., Chang, W., and Ruban, A.** (2005). Molecular basis of photoprotection and control of photosynthetic light-harvesting. *Nature* **436**(7047): 134–137.
- Peter, G. F. and Thornber, J. P.** (1991). Biochemical composition and organization of higher plant photosystem II light-harvesting pigment-proteins. *The Journal of Biological Chemistry* **266**(25): 16745–16754.
- Peterman, E., Dukker, F., van Grondelle, R., and van Amerongen, H.** (1995). Chlorophyll a and carotenoid triplet states in light-harvesting complex II of higher plants. *Biophysical Journal* **69**(6): 2670–2678.
- Peterman, E. J. G., Gradinaru, C. C., Calkoen, F., Borst, J. C., van Grondelle, R., and van Amerongen, H.** (1997). Xanthophylls in

- Light-Harvesting Complex II of Higher Plants: Light Harvesting and Triplet Quenching. *Biochemistry* **36**(40): 12208–12215.
- Petrou, K., Belgio, E., and Ruban, A. V.** (2014). PH sensitivity of chlorophyll fluorescence quenching is determined by the detergent/protein ratio and the state of LHCII aggregation. *Biochimica et Biophysica Acta - Bioenergetics* **1837**(9): 1533–1539.
- Pfundel, E. E. and Dilley, R. A.** (1993). The pH Dependence of Violaxanthin Deepoxidation in Isolated Pea Chloroplasts. *Plant Physiology* **101**(1): 65–71.
- Phillip, D., Ruban, A. V., Horton, P., Asato, A., and Young, A. J.** (1996). Quenching of chlorophyll fluorescence in the major light-harvesting complex of photosystem II: a systematic study of the effect of carotenoid structure. *Proceedings of the National Academy of Sciences* **93**(4): 1492–1497.
- Pietrzykowska, M., Suorsa, M., Semchonok, D. A., Tikkanen, M., Boekema, E. J., Aro, E. M., and Jansson, S.** (2014). The light-harvesting chlorophyll a/b binding proteins Lhcb1 and Lhcb2 play complementary roles during state transitions in Arabidopsis. *Plant Cell* **26**(9): 3646–3660.
- Pinnola, A., Staleva-Musto, H., Capaldi, S., Ballottari, M., Bassi, R., and Polívka, T.** (2016). Electron transfer between carotenoid and chlorophyll contributes to quenching in the LHCSR1 protein from *Physcomitrella patens*. *Biochimica et Biophysica Acta (BBA) - Bioenergetics* **1857**(12): 1870–1878.
- Pinnola, A. and Bassi, R.** (2018). Molecular mechanisms involved in plant photoprotection. *Biochemical Society Transactions* **46**(2): 467–482.
- Pogson, B. J., Niyogi, K. K., Bjorkman, O., and DellaPenna, D.** (1998). Altered xanthophyll compositions adversely affect chlorophyll accumulation and nonphotochemical quenching in Arabidopsis mutants. *Proceedings of the National Academy of Sciences* **95**(22): 13324–13329.
- Polívka, T., Herek, J. L., Zigmantas, D., Åkerlund, H. E., and Sundström, V.** (1999). Direct observation of the (forbidden) S1 state in

- carotenoids. *Proceedings of the National Academy of Sciences of the United States of America* **96**(9): 4914–4917.
- Polívka, T., Zigmantas, D., Sundström, V., Formaggio, E., Cinque, G., and Bassi, R.** (2002). Carotenoid S1 state in a recombinant light-harvesting complex of photosystem II. *Biochemistry* **41**(2): 439–450.
- Polívka, T. and Sundström, V.** (2004). Ultrafast dynamics of carotenoid excited states—from solution to natural and artificial systems. *Chemical Reviews* **104**(4): 2021–2071.
- Polívka, T. and Sundström, V.** (2009). Dark excited states of carotenoids: Consensus and controversy. *Chemical Physics Letters* **477**(1-3): 1–11.
- Polívka, T. and Frank, H. A.** (2010). Molecular factors controlling photosynthetic light harvesting by carotenoids. *Accounts of Chemical Research* **43**(8): 1125–1134.
- Porra, R., Thompson, W., and Kriedemann, P.** (1989). Determination of accurate extinction coefficients and simultaneous equations for assaying chlorophylls a and b extracted with four different solvents: verification of the concentration of chlorophyll standards by atomic absorption spectroscopy. *Biochimica et Biophysica Acta (BBA) - Bioenergetics* **975**(3): 384–394.
- Powles, S. B.** (1984). Photoinhibition of Photosynthesis Induced by Visible Light. *Annual Review of Plant Physiology* **35**(1): 15–44.
- Premvardhan, L., Robert, B., Beer, A., and Büchel, C.** (2010). Pigment organization in fucoxanthin chlorophyll a/c2 proteins (FCP) based on resonance Raman spectroscopy and sequence analysis. *Biochimica et Biophysica Acta (BBA) - Bioenergetics* **1797**(9): 1647–1656.
- Quemeneur, F., Sigurdsson, J. K., Renner, M., Atzberger, P. J., Bassereau, P., and Lacoste, D.** (2014). Shape matters in protein mobility within membranes. *Proceedings of the National Academy of Sciences of the United States of America* **111**(14): 5083–5087.

- Ramanan, C., Gruber, J. M., Malý, P., Negretti, M., Novoderezhkin, V., Krüger, T. P., Mančal, T., Croce, R., and Van Grondelle, R.** (2015). The Role of exciton delocalization in the major photosynthetic light-harvesting antenna of plants. *Biophysical Journal* **108**(5): 1047–1056.
- Raven, J. A.** (1989). Flight or flight: the Economics of Repair and Avoidance of Photoinhibition of Photosynthesis. *Functional Ecology* **3**(1): 5–19.
- Rees, D., Young, A., Noctor, G., Britton, G., and Horton, P.** (1989). Enhancement of the ΔpH -dependent dissipation of excitation energy in spinach chloroplasts by light-activation: correlation with the synthesis of zeaxanthin. *FEBS Letters* **256**(1-2): 85–90.
- Rees, D., Noctor, G., Ruban, A. V., Crofts, J., Young, A., and Horton, P.** (1992). pH dependent chlorophyll fluorescence quenching in spinach thylakoids from light treated or dark adapted leaves. *Photosynthesis Research* **31**(1): 11–19.
- Reinhold, C., Niczyporuk, S., Beran, K. C., and Jahns, P.** (2008). Short-term down-regulation of zeaxanthin epoxidation in *Arabidopsis thaliana* in response to photo-oxidative stress conditions. *Biochimica et Biophysica Acta (BBA) - Bioenergetics* **1777**(5): 462–469.
- Robert, B., Horton, P., Pascal, A. A., and Ruban, A. V.** (2004). Insights into the molecular dynamics of plant light-harvesting proteins in vivo. *Trends in Plant Science* **9**(8): 385–390.
- Roy, R., Hohng, S., and Ha, T.** (2008). A practical guide to single-molecule FRET. *Nature Methods* **5**(6): 507–516.
- Ruban, A., Rees, D., Noctor, G., Young, A., and Horton, P.** (1991). Long-wavelength chlorophyll species are associated with amplification of high-energy-state excitation quenching in higher plants. *Biochimica et Biophysica Acta (BBA) - Bioenergetics* **1059**(3): 355–360.
- Ruban, A. and Horton, P.** (1992). Mechanism of ΔpH -dependent dissipation of absorbed excitation energy by photosynthetic membranes. I. Spectroscopic

BIBLIOGRAPHY

- analysis of isolated light-harvesting complexes. *Biochimica et Biophysica Acta (BBA) - Bioenergetics* **1102**(1): 30–38.
- Ruban, A., Walters, R., and Horton, P.** (1992). The molecular mechanism of the control of excitation energy dissipation in chloroplast membranes Inhibition of Δ pH-dependent quenching of chlorophyll fluorescence by dicyclohexylcarbodiimide. *FEBS Letters* **309**(2): 175–179.
- Ruban, A., Calkoen, F., Kwa, S., van Grondelle, R., Horton, P., and Dekker, J.** (1997a). Characterisation of LHC II in the aggregated state by linear and circular dichroism spectroscopy. *Biochimica et Biophysica Acta (BBA) - Bioenergetics* **1321**(1): 61–70.
- Ruban, A. V., Horton, P., and Young, A. J.** (1993a). Aggregation of higher plant xanthophylls: Differences in absorption spectra and in the dependency on solvent polarity. *Journal of Photochemistry and Photobiology, B: Biology* **21**(2-3): 229–234.
- Ruban, A. V., Young, A. J., and Horton, P.** (1993b). Induction of Nonphotochemical Energy Dissipation and Absorbance Changes in Leaves (Evidence for Changes in the State of the Light-Harvesting System of Photosystem II in Vivo). *Plant Physiology* **102**(3): 741–750.
- Ruban, A. V., Young, A., and Horton, P.** (1994a). Modulation of chlorophyll fluorescence quenching in isolated light harvesting complex of Photosystem II. *Biochimica et Biophysica Acta (BBA) - Bioenergetics* **1186**(1-2): 123–127.
- Ruban, A. V. and Horton, P.** (1994). Spectroscopy of non-photochemical and photochemical quenching of chlorophyll fluorescence in leaves; evidence for a role of the light harvesting complex of Photosystem II in the regulation of energy dissipation. *Photosynthesis Research* **40**(2): 181–190.
- Ruban, A. V., Young, A. J., Pascal, A. A., and Horton, P.** (1994b). The Effects of Illumination on the Xanthophyll Composition of the Photosystem II Light-Harvesting Complexes of Spinach Thylakoid Membranes. *Plant Physiology* **104**(1): 227–234.

- Ruban, A. V. and Horton, P.** (1995). An Investigation of the Sustained Component of Nonphotochemical Quenching of Chlorophyll Fluorescence in Isolated Chloroplasts and Leaves of Spinach'. *Plant Physiology* **108**(2): 721–726.
- Ruban, A. V., Horton, P., and Robert, B.** (1995a). Resonance Raman Spectroscopy of the Photosystem II Light-Harvesting Complex of Green Plants: A Comparison of Trimeric and Aggregated States. *Biochemistry* **34**(7): 2333–2337.
- Ruban, A. V., Dekker, J. P., Horton, P., and van Grondelle, R.** (1995b). Temperature Dependence of Chlorophyll Fluorescence From the Light Harvesting Complex II of Higher Plants. *Photochemistry and Photobiology* **61**(2): 216–221.
- Ruban, A. V., Young, A. J., and Horton, P.** (1996). Dynamic properties of the minor chlorophyll a/b binding proteins of photosystem II, an in vitro model for photoprotective energy dissipation in the photosynthetic membrane of green plants. *Biochemistry* **35**(3): 674–678.
- Ruban, A. V., Phillip, D., Young, A. J., and Horton, P.** (1997b). Carotenoid-Dependent Oligomerization of the Major Chlorophyll a/b Light Harvesting Complex of Photosystem II of Plants. *Biochemistry* **36**(25): 7855–7859.
- Ruban, A. V., Phillip, D., Young, A. J., and Horton, P.** (1998a). Excited-State Energy Level Does Not Determine the Differential Effect of Violaxanthin and Zeaxanthin on Chlorophyll Fluorescence Quenching in the Isolated Light-Harvesting Complex of Photosystem II. *Photochemistry and Photobiology* **68**(6): 829–834.
- Ruban, A. V., Pesaresi, P., Wacker, U., Irrgang, K.-D. J., Bassi, R., and Horton, P.** (1998b). The Relationship between the Binding of Dicyclohexylcarbodiimide and Quenching of Chlorophyll Fluorescence in the Light-Harvesting Proteins of Photosystem II. *Biochemistry* **37**(33): 11586–11591.

- Ruban, A. V., Lee, P. J., Wentworth, M., Young, A. J., and Horton, P.** (1999). Determination of the Stoichiometry and Strength of Binding of Xanthophylls to the Photosystem II Light Harvesting Complexes. *Journal of Biological Chemistry* **274**(15): 10458–10465.
- Ruban, A. V. and Horton, P.** (1999). The Xanthophyll Cycle Modulates the Kinetics of Nonphotochemical Energy Dissipation in Isolated Light-Harvesting Complexes, Intact Chloroplasts, and Leaves of Spinach. *Plant Physiology* **119**(2): 531–542.
- Ruban, A. V., Pascal, A. A., and Robert, B.** (2000). Xanthophylls of the major photosynthetic light-harvesting complex of plants: Identification, conformation and dynamics. *FEBS Letters* **477**(3): 181–185.
- Ruban, A. V., Pascal, A. A., Robert, B., and Horton, P.** (2001). Configuration and Dynamics of Xanthophylls in Light-harvesting Antennae of Higher Plants. *Journal of Biological Chemistry* **276**(27): 24862–24870.
- Ruban, A. V., Wentworth, M., Yakushevskaya, A. E., Andersson, J., Lee, P. J., Keegstra, W., Dekker, J. P., Boekema, E. J., Jansson, S., and Horton, P.** (2003). Plants lacking the main light-harvesting complex retain photosystem II macro-organization. *Nature* **421**(6923): 648–652.
- Ruban, A. V., Solovieva, S., Lee, P. J., Iliaia, C., Wentworth, M., Ganeteg, U., Klimmek, F., Chow, W. S., Anderson, J. M., Jansson, S., and Horton, P.** (2006). Plasticity in the Composition of the Light Harvesting Antenna of Higher Plants Preserves Structural Integrity and Biological Function. *Journal of Biological Chemistry* **281**(21): 14981–14990.
- Ruban, A. V., Berera, R., Iliaia, C., van Stokkum, I. H., Kennis, J. T. M., Pascal, A. a., van Amerongen, H., Robert, B., Horton, P., and van Grondelle, R.** (2007). Identification of a mechanism of photoprotective energy dissipation in higher plants. *Nature* **450**(7169): 575–578.
- Ruban, A. V. and Johnson, M. P.** (2009). Dynamics of higher plant photosystem cross-section associated with state transitions. *Photosynthesis Research* **99**(3): 173–183.

- Ruban, A. V.**, Identification of Carotenoids in Photosynthetic Proteins: Xanthophylls of the Light Harvesting Antenna. In **Landrum, J. T.** (editor), *Carotenoids: Physical, Chemical, and Biological Functions and Properties*, 113–136 (CRC Press, 2009a).
- Ruban, A. V.** (2009b). Plants in light. *Communicative & Integrative Biology* **2**(1): 50–55.
- Ruban, A. V. and Johnson, M. P.** (2010). Xanthophylls as modulators of membrane protein function. *Archives of Biochemistry and Biophysics* **504**(1): 78–85.
- Ruban, A. V. and Murchie, E. H.** (2012). Assessing the photoprotective effectiveness of non-photochemical chlorophyll fluorescence quenching: A new approach. *Biochimica et Biophysica Acta (BBA) - Bioenergetics* **1817**(7): 977–982.
- Ruban, A. V., Johnson, M. P., and Duffy, C. D.** (2012). The photoprotective molecular switch in the photosystem II antenna. *Biochimica et Biophysica Acta (BBA) - Bioenergetics* **1817**(1): 167–181.
- Ruban, A. V.**, *The Photosynthetic Membrane* (John Wiley & Sons, Ltd, Chichester, UK, 2012).
- Ruban, A. V. and Belgio, E.** (2014). The relationship between maximum tolerated light intensity and photoprotective energy dissipation in the photosynthetic antenna: chloroplast gains and losses. *Philosophical Transactions of the Royal Society B: Biological Sciences* **369**(1640): 20130222.
- Ruban, A. V. and Johnson, M. P.** (2015). Visualizing the dynamic structure of the plant photosynthetic membrane. *Nature Plants* **1**(11): 15161.
- Ruban, A. V.** (2016). Nonphotochemical Chlorophyll Fluorescence Quenching: Mechanism and Effectiveness in Protecting Plants from Photodamage. *Plant Physiology* **170**(4): 1903–1916.
- Ruban, A. V.** (2017). Crops on the fast track for light. *Nature* **541**(7635): 36–37.

- Ruban, A. V.** (2018). Light harvesting control in plants. *FEBS Letters* **592**(18): 3030–3039.
- Ruban, A. V.** (2019). The Mechanism of Nonphotochemical Quenching: The End of the Ongoing Debate. *Plant physiology* **181**(2): 383–384.
- Rungrat, T., Almonte, A. A., Cheng, R., Gollan, P. J., Stuart, T., Aro, E. M., Borevitz, J. O., Pogson, B., and Wilson, P. B.** (2019). A Genome-Wide Association Study of Non-Photochemical Quenching in response to local seasonal climates in *Arabidopsis thaliana*. *Plant Direct* **3**(5): 1–13.
- Rutkauskas, D., Chmeliov, J., Johnson, M., Ruban, A., and Valkunas, L.** (2012). Exciton annihilation as a probe of the light-harvesting antenna transition into the photoprotective mode. *Chemical Physics* **404**: 123–128.
- Sabine, C. L.** (2004). The Oceanic Sink for Anthropogenic CO₂. *Science* **305**(5682): 367–371.
- Saccon, F., Durchan, M., Kana, R., Prášil, O., Ruban, A. V., and Polívka, T.** (2019). Spectroscopic Properties of Violaxanthin and Lutein Triplet States in LHCII are Independent of Carotenoid Composition. *The Journal of Physical Chemistry B* **123**(44): 9312–9320.
- Sacharz, J., Giovagnetti, V., Ungerer, P., Mastroianni, G., and Ruban, A. V.** (2017). The xanthophyll cycle affects reversible interactions between PsbS and light-harvesting complex II to control non-photochemical quenching. *Nature Plants* **3**(2): 16225.
- Sakurai, I., Hagio, M., Gombos, Z., Tyystjärvi, T., Paakkarinen, V., Aro, E. M., and Wada, H.** (2003). Requirement of Phosphatidylglycerol for Maintenance of Photosynthetic Machinery. *Plant Physiology* **133**(3): 1376–1384.
- Salvadori, E., Di Valentin, M., Kay, C. W., Pedone, A., Barone, V., and Carbonera, D.** (2012). The electronic structure of the lutein triplet state in plant light-harvesting complex II. *Physical Chemistry Chemical Physics* **14**(35): 12238–12251.

- Santabarbara, S., Barbato, R., Zucchelli, G., Garlaschi, F. M., and Jennings, R. C.** (2001). The quenching of photosystem II fluorescence does not protect the D1 protein against light induced degradation in thylakoids. *FEBS Letters* **505**(1): 159–162.
- Santabarbara, S., Bordignon, E., Jennings, R. C., and Carbonera, D.** (2002). Chlorophyll triplet states associated with Photosystem II of thylakoids. *Biochemistry* **41**(25): 8184–8194.
- Santabarbara, S., Agostini, G., Heathcote, P., and Carbonera, D.** (2005). A fluorescence detected magnetic resonance investigation of the carotenoid triplet states associated with photosystem II of isolated spinach thylakoid membranes. *Photosynthesis Research* **86**(1-2): 283–296.
- Santabarbara, S., Horton, P., and Ruban, A. V.** (2009). Comparison of the thermodynamic landscapes of unfolding and formation of the energy dissipative state in the isolated light harvesting complex II. *Biophysical Journal* **97**(4): 1188–1197.
- Sapozhnikov, D., Krasovskaya, T., and Mayeskaya, A.** (1957). Changes in the Ratio of Main Carotenoids in Green Leaf Plastids under Light Action. *Dokl. Akad. Nauk SSSR* -(113): 465–467.
- Schaller, S., Latowski, D., Jemiola-Rzemińska, M., Dawood, A., Wilhelm, C., Strzałka, K., and Goss, R.** (2011). Regulation of LHCII aggregation by different thylakoid membrane lipids. *Biochimica et Biophysica Acta (BBA) - Bioenergetics* **1807**(3): 326–335.
- Schlau-Cohen, G. S., Yang, H. Y., Krüger, T. P., Xu, P., Gwizdala, M., Van Grondelle, R., Croce, R., and Moerner, W. E.** (2015). Single-molecule identification of quenched and unquenched states of LHCII. *Journal of Physical Chemistry Letters* **6**(5): 860–867.
- Schödel, R., Irrgang, K. D., Voigt, J., and Renger, G.** (1998). Rate of carotenoid triplet formation in solubilized light-harvesting complex II (LHCII) from spinach. *Biophysical Journal* **75**(6): 3143–3153.

- Schoenlein, R., Peteanu, L., Mathies, R., and Shank, C.** (1991). The first step in vision: femtosecond isomerization of rhodopsin. *Science* **254**(5030): 412–415.
- Scholes, G. D., Curutchet, C., Mennucci, B., Cammi, R., and Tomasi, J.** (2007). How solvent controls electronic energy transfer and light harvesting. *Journal of Physical Chemistry B* **111**(25): 6978–6982.
- Scholes, G. D., Fleming, G. R., Olaya-Castro, A., and Van Grondelle, R.** (2011). Lessons from nature about solar light harvesting. *Nature Chemistry* **3**(10): 763–774.
- Schönknecht, G., Neimanis, S., Katona, E., Gerst, U., and Heber, U.** (1995). Relationship between photosynthetic electron transport and pH gradient across the thylakoid membrane in intact leaves. *Proceedings of the National Academy of Sciences of the United States of America* **92**(26): 12185–12189.
- Schreiber, U., Schliwa, U., and Bilger, W.** (1986). Continuous recording of photochemical and non-photochemical chlorophyll fluorescence quenching with a new type of modulation fluorometer. *Photosynthesis Research* **10**(1-2): 51–62.
- Schreiber, U. and Neubauer, C.** (1990). O₂-dependent electron flow, membrane energization and the mechanism of non-photochemical quenching of chlorophyll fluorescence. *Photosynthesis Research* **25**(3): 279–293.
- Schrödinger, E.**, *What is Life? The Physical Aspect of the Living Cell* (Cambridge University Press, Cambridge, 1944).
- Schuldiner, S., Rottenberg, H., and Avron, M.** (1972). Determination of ΔpH in Chloroplasts. 2. Fluorescent Amines as a Probe for the Determination of ΔpH in Chloroplasts. *European Journal of Biochemistry* **25**(1): 64–70.
- Schulten, K. and Karplus, M.** (1972). On the origin of a low-lying forbidden transition in polyenes and related molecules. *Chemical Physics Letters* **14**(3): 305–309.
- Scopes, R. K.**, *Protein Purification* (Springer New York, 1987).

- Seiwert, D., Witt, H., Janshoff, A., and Paulsen, H.** (2017). The non-bilayer lipid MGDG stabilizes the major light-harvesting complex (LHCII) against unfolding. *Scientific Reports* **7**(1): 1–10.
- Shapiguzov, A., Ingelsson, B., Samol, I., Andres, C., Kessler, F., Rochaix, J. D., Vener, A. V., and Goldschmidt-Clermont, M.** (2010). The PPH1 phosphatase is specifically involved in LHCII dephosphorylation and state transitions in Arabidopsis. *Proceedings of the National Academy of Sciences of the United States of America* **107**(10): 4782–4787.
- Shen, J.** (2015). The Structure of Photosystem II and the Mechanism of Water Oxidation in Photosynthesis. *Annual Review of Plant Biology* **66**(1): 23–48.
- Shuvalov, V. A. and Parson, W. W.** (1981). Triplet states of monomeric bacteriochlorophyll in vitro and of bacteriochlorophyll dimers in antenna and reaction center complexes. *Biochimica et Biophysica Acta (BBA) - Bioenergetics* **638**(1): 50–59.
- Siefermann, D. and Yamamoto, H. Y.** (1975). Properties of NADPH and oxygen-dependent zeaxanthin epoxidation in isolated chloroplasts. A transmembrane model for the violaxanthin cycle. *Archives of Biochemistry and Biophysics* **171**(1): 70–77.
- Siefermann-Harms, D.** (1987). The light-harvesting and protective functions of carotenoids in photosynthetic membranes. *Physiologia Plantarum* **69**(3): 561–568.
- Sistrom, W. R., Griffiths, M., and Stanier, R. Y.** (1956). The biology of a photosynthetic bacterium which lacks colored carotenoids. *Journal of Cellular and Comparative Physiology* **48**(3): 473–515.
- Spetea, C., Hideg, ., and Vass, I.** (1997). Low pH accelerates light-induced damage of photosystem II by enhancing the probability of the donor-side mechanism of photoinhibition. *Biochimica et Biophysica Acta - Bioenergetics* **1318**(1-2): 275–283.

- Staleva, H., Komenda, J., Shukla, M. K., Šlouf, V., Kanâ, R., Polívka, T., and Sobotka, R.** (2015). Mechanism of photoprotection in the cyanobacterial ancestor of plant antenna proteins. *Nature Chemical Biology* **11**(4): 287–291.
- Steffen, W., Rockström, J., Richardson, K., Lenton, T. M., Folke, C., Liverman, D., Summerhayes, C. P., Barnosky, A. D., Cornell, S. E., Crucifix, M., Donges, J. F., Fetzer, I., Lade, S. J., Scheffer, M., Winkelmann, R., and Schellnhuber, H. J.** (2018). Trajectories of the Earth System in the Anthropocene. *Proceedings of the National Academy of Sciences of the United States of America* **115**(33): 8252–8259.
- Stirbet, A. and Govindjee** (2011). On the relation between the Kautsky effect (chlorophyll a fluorescence induction) and Photosystem II: Basics and applications of the OJIP fluorescence transient. *Journal of Photochemistry and Photobiology B: Biology* **104**(1-2): 236–257.
- Strasser, R. J. and Govindjee** (1991). The F0 and the O-J-I-P fluorescence rise in higher plants and algae. *Regulation of chloroplast biogenesis* 423–426.
- Strasser, R. J. and Srivastava, A.** (1995). Polyphasic Chlorophyll a Fluorescence Transient in Plants and Cyanobacteria. *Photochemistry and Photobiology* **61**(1): 32–42.
- Su, X., Ma, J., Wei, X., Cao, P., Zhu, D., Chang, W., Liu, Z., Zhang, X., and Li, M.** (2017). Structure and assembly mechanism of plant C2S2M2-type PSII-LHCII supercomplex. *Science* **357**(6353): 815–820.
- Sylak-Glassman, E. J., Malnoë, A., De Re, E., Brooks, M. D., Fischer, A. L., Niyogi, K. K., and Fleming, G. R.** (2014). Distinct roles of the photosystem II protein PsbS and zeaxanthin in the regulation of light harvesting in plants revealed by fluorescence lifetime snapshots. *Proceedings of the National Academy of Sciences* **111**(49): 17498–17503.
- Taylor, S. H. and Long, S. P.** (2017). Slow induction of photosynthesis on shade to sun transitions in wheat may cost at least 21% of productivity.

- Philosophical Transactions of the Royal Society B: Biological Sciences* **372**(1730).
- Teardo, E., de Laureto, P. P., Bergantino, E., Dalla Vecchia, F., Rigoni, F., Szabò, I., and Giacometti, G. M.** (2007). Evidences for interaction of PsbS with photosynthetic complexes in maize thylakoids. *Biochimica et Biophysica Acta (BBA) - Bioenergetics* **1767**(6): 703–711.
- Tebaldi, C., Hayhoe, K., Arblaster, J. M., and Meehl, G. A.** (2006). Going to the extremes: An intercomparison of model-simulated historical and future changes in extreme events. *Climatic Change* **79**(3-4): 185–211.
- Thallmair, S., Vainikka, P. A., and Marrink, S. J.** (2019). Lipid Fingerprints and Cofactor Dynamics of Light-Harvesting Complex II in Different Membranes. *Biophysical Journal* **116**(8): 1446–1455.
- Tikkanen, M., Nurmi, M., Suorsa, M., Danielsson, R., Mamedov, F., Styring, S., and Aro, E.-M.** (2008). Phosphorylation-dependent regulation of excitation energy distribution between the two photosystems in higher plants. *Biochimica et Biophysica Acta (BBA) - Bioenergetics* **1777**(5): 425–432.
- Tikkanen, M. and Aro, E.-M.** (2014). Integrative regulatory network of plant thylakoid energy transduction. *Trends in Plant Science* **19**(1): 10–17.
- Tikkanen, M., Mekala, N. R., and Aro, E.-M.** (2014). Photosystem II photoinhibition-repair cycle protects Photosystem I from irreversible damage. *Biochimica et Biophysica Acta (BBA) - Bioenergetics* **1837**(1): 210–215.
- Townsend, A. J., Ware, M. A., and Ruban, A. V.** (2018a). Dynamic interplay between photodamage and photoprotection in photosystem II. *Plant, Cell & Environment* **41**(5): 1098–1112.
- Townsend, A. J., Saccon, F., Giovagnetti, V., Wilson, S., Ungerer, P., and Ruban, A. V.** (2018b). The causes of altered chlorophyll fluorescence quenching induction in the Arabidopsis mutant lacking all minor antenna complexes. *Biochimica et Biophysica Acta (BBA) - Bioenergetics* **1859**(9): 666–675.

- Treves, H., Raanan, H., Kedem, I., Murik, O., Keren, N., Zer, H., Berkowicz, S. M., Giordano, M., Norici, A., Shotland, Y., Ohad, I., and Kaplan, A. (2016). The mechanisms whereby the green alga *Chlorella ohadii*, isolated from desert soil crust, exhibits unparalleled photodamage resistance. *New Phytologist* **210**(4): 1229–1243.
- Tutkus, M., Chmeliov, J., Rutkauskas, D., Ruban, A. V., and Valkunas, L. (2017). Influence of the Carotenoid Composition on the Conformational Dynamics of Photosynthetic Light-Harvesting Complexes. *The Journal of Physical Chemistry Letters* **8**(23): 5898–5906.
- Tutkus, M., Saccon, F., Chmeliov, J., Venckus, O., Ciplys, I., Ruban, A. V., and Valkunas, L. (2019). Single-molecule microscopy studies of LHCII enriched in Vio or Zea. *Biochimica et Biophysica Acta (BBA) - Bioenergetics* **1860**(6): 499–507.
- Ünlü, C., Drop, B., Croce, R., and van Amerongen, H. (2014). State transitions in *Chlamydomonas reinhardtii* strongly modulate the functional size of photosystem II but not of photosystem I. *Proceedings of the National Academy of Sciences* **111**(9): 3460–3465.
- Vallon, O., Bulte, L., Dainese, P., Olive, J., Bassi, R., and Wollman, F. A. (1991). Lateral redistribution of cytochrome b6/f complexes along thylakoid membranes upon state transitions. *Proceedings of the National Academy of Sciences of the United States of America* **88**(18): 8262–8266.
- van Amerongen, H. and van Grondelle, R., Transient absorption spectroscopy in study of processes and dynamics in biology. In Sauer, K. (editor), *Methods in Enzymology*, vol. 246, 201–226 (Elsevier Inc., 1995).
- van Amerongen, H., van Grondelle, R., and Valkunas, L., *Photosynthetic Excitons* (World Scientific, 2000).
- van Amerongen, H. and van Grondelle, R. (2001). Understanding the Energy Transfer Function of LHCII, the Major Light-Harvesting Complex of Green Plants. *The Journal of Physical Chemistry B* **105**(3): 604–617.

- van Amerongen, H. and Chmeliov, J.** (2019). Instantaneous switching between different modes of non-photochemical quenching in plants. Consequences for increasing biomass production. *Biochimica et Biophysica Acta (BBA) - Bioenergetics* in press.
- van Bezouwen, L. S., Caffarri, S., Kale, R. S., Kouřil, R., Thunnissen, A.-M. W. H., Oostergetel, G. T., and Boekema, E. J.** (2017). Subunit and chlorophyll organization of the plant photosystem II supercomplex. *Nature Plants* **3**(7): 17080.
- van der Vos, R., Carbonera, D., and Hoff, A. J.** (1991). Microwave and optical spectroscopy of carotenoid triplets in light-harvesting complex LHC II of spinach by absorbance-detected magnetic resonance. *Applied Magnetic Resonance* **2**(2): 179–202.
- van Grondelle, R.** (1985). Excitation energy transfer, trapping and annihilation in photosynthetic systems. *Biochimica et Biophysica Acta (BBA) - Reviews on Bioenergetics* **811**(2): 147–195.
- van Grondelle, R., Dekker, J. P., Gillbro, T., and Sundstrom, V.** (1994). Energy transfer and trapping in photosynthesis. *Biochimica et Biophysica Acta (BBA) - Bioenergetics* **1187**(1): 1–65.
- van Oort, B., van Hoek, A., Ruban, A. V., and van Amerongen, H.** (2007). Equilibrium between Quenched and Nonquenched Conformations of the Major Plant Light-Harvesting Complex Studied with High-Pressure Time-Resolved Fluorescence. *The Journal of Physical Chemistry B* **111**(26): 7631–7637.
- van Oort, B., Alberts, M., de Bianchi, S., Dall’Osto, L., Bassi, R., Trinkunas, G., Croce, R., and van Amerongen, H.** (2010). Effect of Antenna-Depletion in Photosystem II on Excitation Energy Transfer in *Arabidopsis thaliana*. *Biophysical Journal* **98**(5): 922–931.
- van Oort, B., Roy, L. M., Xu, P., Lu, Y., Karcher, D., Bock, R., and Croce, R.** (2018). Revisiting the Role of Xanthophylls in Nonphotochemical Quenching. *The Journal of Physical Chemistry Letters* **9**(2): 346–352.

- Van Roon, H., Van Breemen, J. F. L., De Weerd, F. L., Dekker, J. P., and Boekema, E. J.** (2000). Solubilization of green plant thylakoid membranes with n-dodecyl- α ,D-maltoside. Implications for the structural organization of the Photosystem II, Photosystem I, ATP synthase and cytochrome b6f complexes. *Photosynthesis Research* **64**(2-3): 155–166.
- Varotto, C., Pesaresi, P., Jahns, P., Leßnick, A., Tizzano, M., Schiavon, F., Salamini, F., and Leister, D.** (2002). Single and Double Knockouts of the Genes for Photosystem I Subunits G, K, and H of Arabidopsis. Effects on Photosystem I Composition, Photosynthetic Electron Flow, and State Transitions. *Plant Physiology* **129**(2): 616–624.
- Wahadoszamen, M., Berera, R., Ara, A. M., Romero, E., and van Grondelle, R.** (2012). Identification of two emitting sites in the dissipative state of the major light harvesting antenna. *Phys. Chem. Chem. Phys.* **14**(2): 759–766.
- Wahadoszamen, M., Margalit, I., Ara, A. M., van Grondelle, R., and Noy, D.** (2014). The role of charge-transfer states in energy transfer and dissipation within natural and artificial bacteriochlorophyll proteins. *Nature Communications* **5**(1): 5287.
- Wahadoszamen, M., Belgio, E., Rahman, M. A., Ara, A. M., Ruban, A. V., and van Grondelle, R.** (2016). Identification and characterization of multiple emissive species in aggregated minor antenna complexes. *Biochimica et Biophysica Acta (BBA) - Bioenergetics* **1857**(12): 1917–1924.
- Walters, R. G. and Horton, P.** (1994). Acclimation of Arabidopsis thaliana to the light environment: Changes in composition of the photosynthetic apparatus. *Planta* **195**(2): 248–256.
- Walters, R. G., Ruban, A. V., and Horton, P.** (1994). Higher plant light-harvesting complexes LHCIIa and LHCIIc are bound by dicyclohexylcarbodiimide during inhibition of energy dissipation. *European Journal of Biochemistry* **226**(3): 1063–1069.

- Walters, R. G., Ruban, a. V., and Horton, P.** (1996). Identification of proton-active residues in a higher plant light-harvesting complex. *Proceedings of the National Academy of Sciences of the United States of America* **93**(24): 14204–14209.
- Walters, R. G., Rogers, J. J., Shephard, F., and Horton, P.** (1999). Acclimation of *Arabidopsis thaliana* to the light environment: The role of photoreceptors. *Planta* **209**(4): 517–527.
- Walters, R. G.** (2005). Towards an understanding of photosynthetic acclimation. *Journal of Experimental Botany* **56**(411): 435–447.
- Ware, M. A., Belgio, E., and Ruban, A. V.** (2015a). Comparison of the protective effectiveness of NPQ in *Arabidopsis* plants deficient in PsbS protein and zeaxanthin. *Journal of Experimental Botany* **66**(5): 1259–1270.
- Ware, M. A., Giovagnetti, V., Belgio, E., and Ruban, A. V.** (2015b). PsbS protein modulates non-photochemical chlorophyll fluorescence quenching in membranes depleted of photosystems. *Journal of Photochemistry and Photobiology B: Biology* **152**: 301–307.
- Ware, M. A., Dall'Osto, L., and Ruban, A. V.** (2016). An In Vivo Quantitative Comparison of Photoprotection in *Arabidopsis* Xanthophyll Mutants. *Frontiers in Plant Science* **7**: 841.
- Wehner, A., Grasses, T., and Jahns, P.** (2006). De-epoxidation of violaxanthin in the minor antenna proteins of photosystem II, LHCB4, LHCB5, and LHCB6. *Journal of Biological Chemistry* **281**(31): 21924–21933.
- Wei, X., Su, X., Cao, P., Liu, X., Chang, W., Li, M., Zhang, X., and Liu, Z.** (2016). Structure of spinach photosystem II-LHCII supercomplex at 3.2 Å resolution. *Nature* **534**(7605): 69–74.
- Weis, E.** (1984). Short Term Acclimation of Spinach to High Temperatures. *Plant Physiology* **74**(2): 402–407.

- Weis, E. and Berry, J. A.** (1987). Quantum efficiency of Photosystem II in relation to energy-dependent quenching of chlorophyll fluorescence. *Biochimica et Biophysica Acta (BBA) - Bioenergetics* **894**(2): 198–208.
- Wentworth, M., Ruban, A. V., and Horton, P.** (2001). Kinetic analysis of nonphotochemical quenching of chlorophyll fluorescence. 2. Isolated light-harvesting complexes. *Biochemistry* **40**(33): 9902–9908.
- Wentworth, M., Ruban, A. V., and Horton, P.** (2003). Thermodynamic investigation into the mechanism of the chlorophyll fluorescence quenching in isolated photosystem II light-harvesting complexes. *Journal of Biological Chemistry* **278**(24): 21845–21850.
- Wentworth, M., Ruban, A. V., and Horton, P.** (2004). The Functional Significance of the Monomeric and Trimeric States of the Photosystem II Light Harvesting Complexes. *Biochemistry* **43**(2): 501–509.
- Wietrzynski, W., Schaffer, M., Tegunov, D., Albert, S., Kanazawa, A., Plitzko, J. M., Baumeister, W., and Engel, B. D.** (2019). Charting the native architecture of thylakoid membranes with single-molecule precision. *bioRxiv* .
- Wilk, L., Grunwald, M., Liao, P.-N., Walla, P. J., and Kuhlbrandt, W.** (2013). Direct interaction of the major light-harvesting complex II and PsbS in nonphotochemical quenching. *Proceedings of the National Academy of Sciences* **110**(14): 5452–5456.
- Wilson, S. and Ruban, A. V.** (2019). Enhanced NPQ affects long-term acclimation in the spring ephemeral *Berteroa incana*. *Biochimica et Biophysica Acta (BBA) - Bioenergetics* in press.
- Wraight, C. A. and Crofts, A. R.** (1970). EnergyDependent Quenching of Chlorophyll a Fluorescence in Isolated Chloroplasts. *European Journal of Biochemistry* **17**(2): 319–327.
- Xu, P., Tian, L., Klotz, M., and Croce, R.** (2015). Molecular insights into Zeaxanthin-dependent quenching in higher plants. *Scientific reports* **5**: 13679.

- Yamamoto, H. Y.** (1979). Biochemistry of the violaxanthin cycle in higher plants. *Pure and Applied Chemistry* **51**(3): 639–648.
- Yan, H., Zhang, P., Wang, C., Liu, Z., and Chang, W.** (2007). Two lutein molecules in LHCII have different conformations and functions: Insights into the molecular mechanism of thermal dissipation in plants. *Biochemical and Biophysical Research Communications* **355**(2): 457–463.
- Yin, Z. H. and Johnson, G. N.** (2000). Photosynthetic acclimation of higher plants to growth in fluctuating light environments. *Photosynthesis Research* **63**(1): 97–107.
- Yoo, S. D., Cho, Y. H., and Sheen, J.** (2007). Arabidopsis mesophyll protoplasts: A versatile cell system for transient gene expression analysis. *Nature Protocols* **2**(7): 1565–1572.
- Zewail, A. H.** (2000). Femtochemistry. Past, present, and future. *Pure and Applied Chemistry* **72**(12): 2219–2231.
- Zhu, X. G., Ort, D. R., Whitmarsh, J., and Long, S. P.** (2004). The slow reversibility of photosystem II thermal energy dissipation on transfer from high to low light may cause large losses in carbon gain by crop canopies: A theoretical analysis. *Journal of Experimental Botany* **55**(400): 1167–1175.
- Zhu, X.-G., Long, S. P., and Ort, D. R.** (2010). Improving Photosynthetic Efficiency for Greater Yield. *Annual Review of Plant Biology* **61**(1): 235–261.